Development of Novel polysaccharides-based cryogels for drug delivery applications

Hamideh Gholizadeh

2021

School of Science

A thesis submitted to

Auckland University of Technology

in (partial) fulfilment of the requirements for the degree of

Doctor of Philosophy

Abstract

The rate of intranasal disorders is globally increasing due to local or systemic causes such as trauma, climate change, exposure to pollutants and chemicals, haematological disorders, and some body system dysfunctions. Epistaxis, commonly known as nose bleeding, is a common intranasal condition with more than 50% of the world population experiencing it at least once in their life. Although it is generally self-manageable, some cases require medical attention. In addition to epistaxis, sinusitis and nasal septum deviation are the two other common intranasal disorders that require surgical interventions, endoscopic sinus surgery (ESS) and septoplasty, in many patients.

Nasal packing has been generally practiced in epistaxis to cease bleeding by mechanically facilitating blood clot formation. In addition, this medical device is placed in the nasal cavity during and after some intranasal surgeries for several days to weeks to enhance wound healing and reduce risk of post-operative complications.

A literature review was conducted focusing on the composition of current nasal packs, their applications and clinical outcomes in terms of effectiveness, patients' satisfaction and complications associated with their use. The review indicated that the current nasal packs do not fulfil the expectations of clinicians and patients and there is a demand for development of new products. Also, it was found that in conjunction with packing, some drugs – mainly prophylactic– are systemically administrated to facilitate blood clotting, wound healing and minimise infection. In addition, several attempts were reported by some researchers in locally delivering these drugs utilising nasal packs as drug carriers, however the erratic results indicated further investigation in feasibility of this method. Therefore, it was realised that there is a need for development of ready to use drug-eluting nasal packs with customised controlled release property for fast and slow-release functions.

Hence, it was attempted to design, formulate and develop a prototype of an erodible nasal pack using abundant biopolymers and lyophilisation technique. The prototype composed of κ-carrageenan hydrogel was developed and its capability in hosting and releasing some therapeutic model drugs was tested in vitro. The results of the in vitro

studies indicated that the developed prototype is suitable for the matrix of nasal pack and meets some requirements of this medical device in terms of hosting the drugs, swelling, fluid absorption and releasing the drugs. The prototype acts as a regular nasal pack and drug carrier and can host hydrophilic and hydrophobic drugs with minor alterations in formulation. However, in vivo studies are required to investigate the behaviour of the developed nasal pack in real conditions.

Contents

List of Figures

List of Tables

Attestation of Authorship

I hereby declare that this submission is my own work and that, to the best of my knowledge and belief, it contains no material previously published or written by another person (except where explicitly defined in the acknowledgements), nor material which to a substantial extent has been submitted for the award of any other degree or diploma of a university or other institution of higher learning.

Hamideh Gholizadeh

_____ 03 Oct 2021

Signature Date

Acknowledgements

Creating a PhD thesis is not an individual experience. It takes place in a social context that includes several individuals whom I would like to thank. First, I would like to express my deep gratitude to my primary research supervisor, Professor Owen Young, and my co-supervisor, Associate Professor Dr Ali Seyfoddin for giving me the opportunity to do this research and providing invaluable guidance throughout this research. Their dynamism, vision, sincerity, and motivation have deeply inspired me. Dr Seyfoddin ignited the love for research in drug delivery in me by involving me in a drug delivery project and his professional guidance and support motivated me in doing this research. Professor Young has taught me the methodology to carry out the research and to present the research results as clearly as possible. It was a privilege and honour to work and study under his guidance. I would also like to thank my supervisors for spending many hours on reading my chapter drafts and making valuable suggestions.

Also, thanks go to the AUT for facilitating this opportunity by awarding me the AUT Doctoral Fees Scholarship and continuous support of the Graduate Research School during the duration of my study. I acknowledge Maurice and Phyllis Paykel Trust, Dick and Mary Earl and Freemasons New Zealand; their generous scholarship enabled me achieving my dreams.

Thanks also go to AUT laboratory technicians in the School of Science, Saeedeh Saraby, Meie Zou, Adrian Owens, Yan Wang, and laboratory manager, Tim Layt. Their support in accessing laboratory equipment and facilities is greatly appreciated.

I specifically appreciate the help of Tony Chen, the senior instrument technician in AUT, for his help in developing methods for quantitative analysis of drug release using LCMS. Also, special thanks go to Dr Ashveen Nand for his time and guidance in collection and interpretation of FTIR data.

In addition, I would like to express my appreciation to my friends and colleagues Dr Eileen Kitundu, Dr Abbey Long, and French intern student Lena Garino for their

helpful suggestions in setting up experiments and collecting data. I also thank Sue Knox for her incredible service in the final formatting of my thesis.

Finally, I am extremely grateful to my parents for their love, prayers, caring and sacrifices for educating and preparing me for my future. I am very thankful to my husband Alireza Memar Bashi and my son Matin for their love, understanding and continuous support to complete this research work. Likewise, I express my thanks to my mother-in-law and father-in-law for their support and prayers. Family love and faith in me constantly inspired me to strive towards my goal and made me who I am today.

Chapter 1 General introduction

1.1 Introduction

In the past several decades, intranasal drug delivery has attracted pharmaceutical scientists and clinicians. The nasal cavity is a promising and potentially versatile route of drug administration due to its large surface area, high vasculature, convenient accessibility, high drug permeability and by passing the hepatic- first pass metabolism (Ghori, Mahdi Aljeboury, Smith, & Conway, 2015).

A range of intranasal drug delivery systems have been developed to utilise this route for local and systemic delivery of drugs. Topical nasal delivery of drugs has been practiced for many years to treat congestion, rhinitis, related allergic conditions and sinusitis. However, systemic delivery of drugs through this route has received increasing investigation in the recent years. Despite of the extensive research on intranasal drug delivery, only a small number of drug delivery systems are currently in the market. These systems are in the form of nasal drops, nasal sprays, nasal gel pumps and nasal inhalers. Also, the applications of these systems are limited to treatment of migraine, acute pain relief, vitamin B12 deficiency, osteoporosis and smoking cessation (Alagusundaram et al., 2010).

This review aims to explore the most common intranasal drug delivery systems with the focus on treatment of common nasal disorders. It presents a brief overview of nasal anatomy and physiology and most common nasal ailments and their associated treatments. Then, factors influencing drug permeation and absorption are described. Finally, most common conventional forms of intranasal drug delivery systems are reviewed.

1.2 Nasal anatomy and physiology

The human nose is generally composed of nostrils and nasal cavity. A median septum made of bone and cartilage divides the nasal cavity into two symmetrical halves. The septum provides structure and support to the nasal construction. The nasal cavity is composed of three main regions: nasal vestibule, the respiratory region and the olfactory region (Figure 1). Nasal vestibule is the dilated area at the opening of nostrils and contains nasal hair and squamous epithelial cells spanning over 0.6 cm^2 of the nasal cavity (Keller, Merkel, & Popp, 2021).

Air enters into the vestibule and travels through the respiratory region into the respiratory system (Keller et al., 2021). The respiratory region represents the largest surface area of the nasal cavity (150 cm^2 of the lateral wall) and is covered with folded epithelium known as nasal mucosa (Dahl & Mygind, 1998). This folded structure makes up superior, median and inferior turbinates (Figure 1). These turbinates create turbulence in the inhaled air causing a swirl that increases the contact time between the air and nasal mucosa. The nasal mucosa is covered with numerous microvilli that further extend the large surface area for air and drug absorption and transport.

The mucosa that covers the respiratory region consists of goblet cells that secret mucus, ciliated and non-ciliated columnar cells and basal cells (Keller et al., 2021). The secreted mucus and high blood supply under the epithelium condition the inhaled air by warming and moistening it. The mucus acts as a physical barrier to trap foreign particles and prevent them entering the respiratory system. It also regulates immune response if the physical barrier fails in filtration of pathogens (A. K. Singh, Singh, & Madhav, 2012).

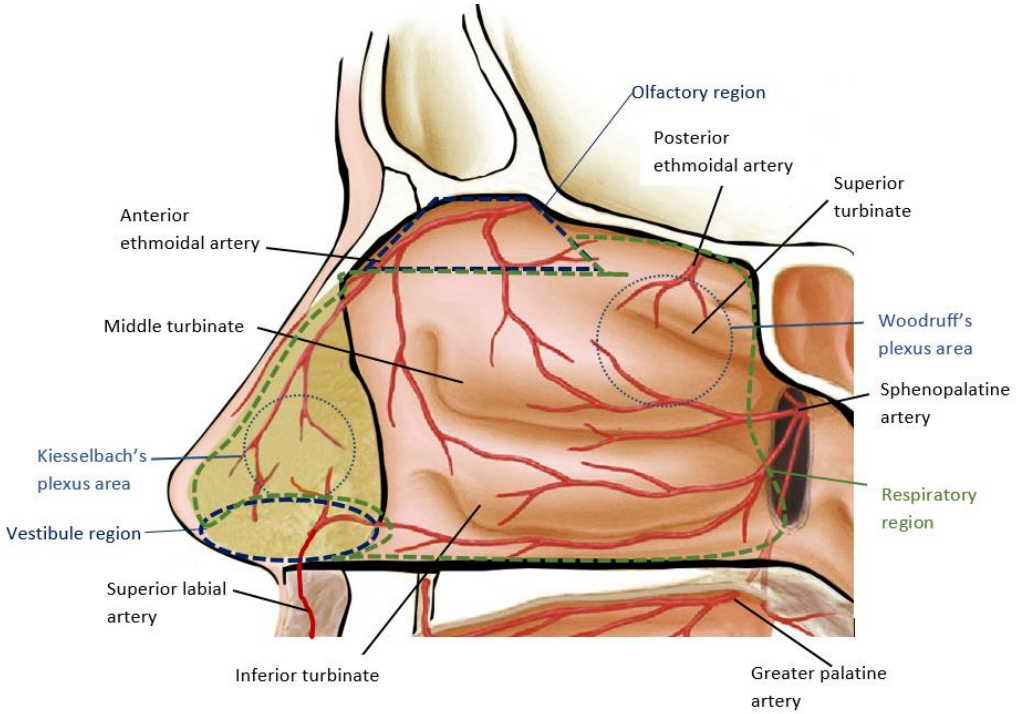

Figure 1. Nasal cavity regions and its blood supply

The olfactory region is located at the superior part of the nasal cavity occupying 10 cm^2 of its area (Crisler, Johnston, Sivula, & Budelsky, 2020). This region houses basal cells of olfactory neurons and their supporting cells, and tubular Bowman's glands that secret mucus (Keller et al., 2021).

It is known that external and internal carotid artery systems supply the nasal blood. The external carotid system provides the blood via the internal maxillary artery and facial artery (MacArthur & McGarry, 2017). The facial artery forms the superior labial artery that supplies blood to the septum and nasal alae. Internal maxillary artery branches into five arteries named as sphenopalatine, pharyngeal, greater palatine, infraorbital and superior alveolar artery, but mainly sphenopalatine and greater palatine arteries supply the nasal cavity (Figure 1). Sphenopalatine artery supplies the septum, middle turbinate and inferior turbinate area of the nasal cavity, while greater palatine supplies anterior part of the septum (Fatakia, Winters, & Amedee, 2010). Internal carotid supplies the nasal cavity by the terminal branches of ophthalmic artery and ethmoidal artery (Figure 1) and provide blood for the nasal septum and lateral nasal walls. Woodruff area and Kiesselbach's plexus are the two areas forming anastomoses of two arteries that often provide a source of nose bleeding known as epistaxis (Fatakia et al., 2010).

1.3 Paranasal sinuses

Paranasal sinuses are the hollow spaces with air-filled cavities in the skull and facial bones around the nose (Nuñez-Castruita, López-Serna, & Guzmán-López, 2012) There are four pairs of paranasal sinuses in human face and skull: Maxillary, frontal, ethmoidal and sphenoid sinuses (Figure 2). Nasal cavity is extended to the paranasal sinuses and the mucosa that covers the sinuses drains mucus into the nasal cavity to keep it moist and purify inhaled air (Lafci Fahrioglu, VanKampen, & Andaloro, 2020). In addition, the sinuses protect head against trauma, impact vocal resonance, enhance facial aesthetics and play role in immune surveillance (Sobol, 2007).

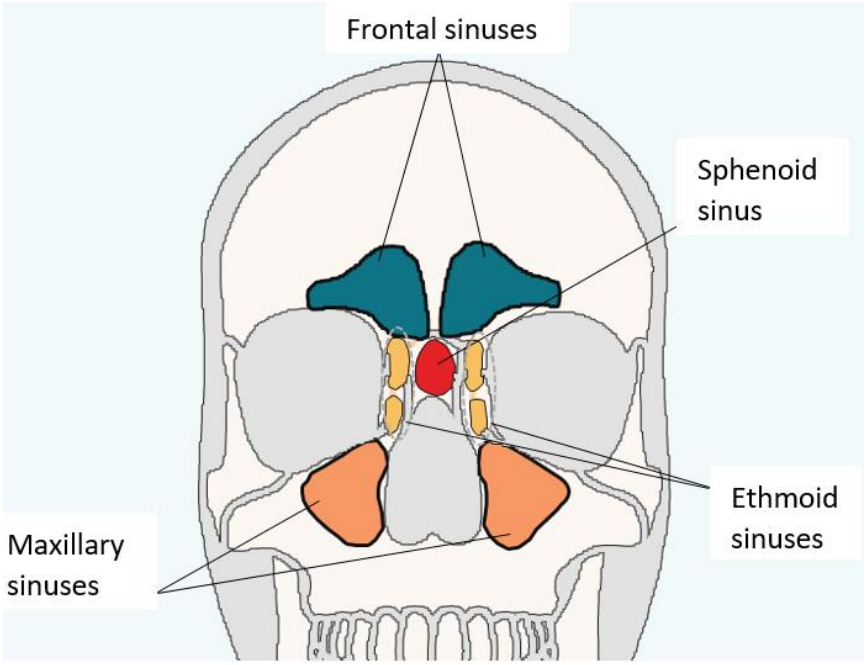

Figure 2. Location of paranasal sinuses in skull and facial bones of human

1.4 Common nasal ailments and their treatments

The prominent position of the nose makes it vulnerable to injuries and infection. Nasal mucosa and paranasal sinuses are prone to infection and inflammation due to their function. Nasal disorders are a collection of diseases primarily appear at the nose or paranasal sinuses as a limited disease or part of systemic involvement as a result of a primary disease (Sachse & Stoll, 2010). Epistaxis, rhinosinusitis and septal deviation are the most common nasal ailments requiring specialised treatment.

1.4.1 Epistaxis and treatment

Epistaxis (nose bleeding) is a common problem appearing in 60% of the general population (Kucik & Clenney, 2005) with most cases occurring in the children under 10 and adults over 45 years of age (Cho & Kim, 2012). Epistaxis can be initiated by both local and systemic factors. Mucosal inflammation, infection, trauma, anatomical deviation, exposure to chemicals and pollutants and digital manipulation are reported as local causes of bleeding (Kucik & Clenney, 2005). Coagulopathy due to haematological disorders, cardiovascular diseases, liver and renal dysfunctions and use of anticoagulant drugs are the main systemic causes of epistaxis (Parajuli, 2015).

Most cases of epistaxis are manageable with conventional procedures but occasionally the condition can present as a life-threatening problem. Cauterisation,

nasal packing, arterial ligation and embolisation of the bleeding vessels are the common practices in treatment of persistent or severe epistaxis (Logan & Pantle, 2016; Weber, 2009). Nasal packing is the second line of epistaxis treatment and it is available if cauterisation is unsuccessful or the point of bleeding is unidentified (Yau, 2015). In this case, the nasal cavity is packed with a biocompatible absorbent material to cease bleeding by applying mechanical pressure on the bleeding site and facilitating blood clot formation. Local administration of some drugs may be prescribed to enhance the procedure and accelerate haemostasis (Zahed, Mousavi Jazayeri, Naderi, Naderpour, & Saeedi, 2017).

1.4.2 Rhinosinusitis

The epithelial lining of the paranasal sinuses is continuous with the nasal cavity, therefore any infection initiated in the nasal lining can spread to the sinuses (Henson, Drake, & Edens, 2020). Rhinosinusitis is defined as inflammation and infection of lining of paranasal sinuses and intranasal mucosa (Almutairi et al., 2017). Viral and bacterial upper respiratory infection are the most frequent cause of this disease. Common symptoms are rhinosinusitis are stuffy nose with thick yellowish discharge, facial pain and pain in the upper teeth (Lemiengre et al., 2018). Acute rhinosinusitis is the progression of these symptoms for 4 to 12 weeks and the sinus mucosa normalises by appropriate treatments such as administration of local and systemic anti-inflammatory and antibiotics, and nasal irrigation. However, chronic rhinosinusitis (CRS) is diagnosed when acute rhinosinusitis is unresolved or the symptoms persevere beyond 12 weeks (Ah-See & Evans, 2007). The global prevalence of chronic sinusitis varies from 5 to 12% (Dietz de Loos et al., 2019). Medical treatment options of CRS start with topical nasal steroids, oral steroids or antibiotics, but rhinosinusitis surgery (generally endoscopic sinus surgery) will be considered if maximal drug treatment has failed or further complications are suspected (Almutairi et al., 2017). In some cases, nasal packing after endoscopic sinus surgery is practiced to control postoperative bleeding, enhance the wound healing process, and prevent lateralization of the middle turbinate, but it may cause insufficient ventilation (Kang, Kim, Shin, Park, & Lee, 2017).

1.4.3 Nasal obstruction

Nasal obstruction (septal deviation) is misalignment of the septum from the midline causing compression of the middle turbinate and reduction of volume and air flow into the nasal cavity (Cappello, Minutello, & Dublin, 2020; Codari et al., 2016). Deviated septum can be severe and result in nasal blockage, sleep apnoea, nasal polyposis and some other complications. Some medication such as nasal dilators or anti-inflammatory drugs may reduce the associated symptoms, but severe deviated septum must be corrected by a surgery known as septoplasty (Ozkececi et al., 2016).

1.5 Nasal cavity as the drug delivery route

The nasal anatomy and physiology indicates the nasal cavity is a potential route for practical administration of topical and systemic therapeutics, especially in treatment of common nasal disorders. The reasons for this claim are the large surface raea of mucosa and the rich vascular system underneath this layer that facilitate drug absorption (Pires, Fortuna, Alves, & Falcão, 2009).

To intranasally administer a drug, the drug contacts the mucus membrane of the nasal cavity and passes through this layer to be absorbed to the mucosa. There are several mechanisms of absorption through mucosa, but only two mechanisms are dominant. In the first mechanism, paracellular process, small hydrophilic drugs simply diffuse across the membrane in a passive and slow process (Muthumanickam et al., 2010). The second mechanism, known as transcellular process, transports lipophilic drugs through the mucosa. In this mechanism, active transport of drugs across the cell membrane is facilitated by carrier-mediated cells through openings of tight junctions (Arora, Sharma, & Garg, 2002).

Administration through the intranasal route improves drug bioavailability and may reduce effective dosage and associated side effects of the drugs. Moreover, the theraputic can be self-administered by the patient in a rapid oneset of non-invasive action (A. K. Singh et al., 2012).

1.6 Factors influencing intranasal drug absorption

The rate of drug diffusion and absorption can be affected by many factors including nasal factors and drug properties. Some of these important factors and their effects on drug deposition and absorption are described below.

1.6.1 Anatomical and physiological properties of the nasal cavity

Large surface area of nasal mucosa, abundance of blood vessels under the mucosa, easy access for drug administration and the ability of mucosa in absorption of deposited drugs makes it an attractive potential route for drug delivery, but delivery via this route is restricted by the structure and condition of nasal mucosa.

1.6.1.1 Membrane permeability

Drugs can cross the mucosa membrane by diffusion or active transport, but limitation of membrane permeability affects drug bioavailability and absorption. Polarity and molecular weight of the drugs limit their permeation and absorption. Permeability of polar drugs is generally low and it becomes lower with increase in molecular weight. Small (less than 300 Da) non-polar drugs can passively cross the membrane by diffusion while polar drugs with molecular weight of higher than 1k Da, such as insulin and calcitonin, barely pass the membrane via active transport (McMartin, Hutchinson, Hyde, & Peters, 1987). Although the tight junctions of the membrane are flexible, the mean size of their openings is less than 0.001 µm, therefore transport of large molecules via these junctions is restricted (Inagaki, Sakakura, Itoh, Ukai, & Miyoshi, 1985). Endocytotic process may facilitate transport of large molecules such as peptides and protein across the membrane in a low level, but addition of absorption enhancing agents, such as surfactants, bile salts, or phospholipids, to the formulation can improve drug permeability (Davis & Illum, 2003; Illum, 2000).

1.6.1.2 Mucocilliary clearance

A mucus layer covers the nasal membrane to protect the respiratory system by trapping the inhaled substances. Nasal mucocilliary clearance system transports the mucus to the nasopharynx by ciliary beating to be swallowed into the stomach (Merkus, Verhoef, Schipper, & Marttin, 1998). The generally rapid clearance of mucus lowers membrane transport of the drugs, especially when the drugs are not easily absorbed across the membrane (Muthumanickam et al., 2010). The half-life of

mucocilliary clearance for non-mucoadhesive formulations is 15 to 20 minutes and the rate of clearance at the posterior part of nasal cavity is higher than the less-ciliated anterior (Illum, 2000). To improve membrane transport of the drugs, deposition of the drug into the anterior part of nasal cavity (Harris, Nilsson, G-.Wagner, & Alkner, 1986) or addition of mucoadhesive carriers or excipients to the drug formulation (Belgamwar et al., 2011; Soane, Hinchcliffe, Davis, & Illum, 2001) is suggested.

1.6.1.3 Enzymatic activity of nasal mucosa

The epithelial layer of nasal cavity contains exo-peptidase enzymes that are able to cleave peptides/protein drugs and degrade them (Alagusundaram et al., 2010). Addition of proteolytic enzyme inhibitors to the drug formulation is one of the approaches to overcome this issue (Romeo et al., 1998). However, presence of the enzyme inhibitors in the formulation may negatively affect the normal body metabolism of the patient, resulting in serious side effects (Duan & Mao, 2010). Also, inclusion of the enzyme does not improve permeability or residence time of the drug on the nasal mucosa. Enzymatic degradation of the drugs is not applicable for non-peptide/protein drugs.

1.6.2 Physicochemical properties of the drugs

In order to achieve effective treatment via intranasal route, physicochemical properties of the drugs play key role in deposition and absorption of the drugs. Molecular size of the drug, its degree of lipophilicity and mucoadhesion property are the most significant factors considered in design and development of intranasal drug delivery systems.

1.6.2.1 Molecular weight and particle size of the drug

There is an inverse correlation between the molecular weight of hydrophilic drugs and their absorption to nasal mucosa when the molecular weight is less than 300 Da (Fisher, Illum, Davis, & Schacht, 1992). These small molecules are able to cross the mucosa through aqueous channels of the membrane (Morita, Yamamoto, Hashida, & Sezaki, 1991). However, increase in molecular weight of drugs significantly decreases absorption to the point that the drugs with molecular weights higher that 1000 Da are unable to be absorbed in absence of permeability enhancers in the

formulation (Davis & Illum, 2003). In terms of lipophilic drugs, there is a direct correlation between the drug molecular weight and drug absorption (Alagusundaram et al., 2010).

The particle size also influences drug permeation and absorption. The drug particles greater than 10 µm in size deposit in the nasal cavity, while the particles of 2 to 10 µm retain in lungs and less than 1 µm particles are exhaled (A. K. Singh et al., 2012).

1.6.2.2 Lipophilicity-hydrophilicity balance

The nasal mucosa is naturally lipophilic and increase in lipophilicity of the drugs enhances their permeability and absorption. Lipophilic drugs can readily cross the mucosa membrane via the transcellular mechanism that enables them to partition into lipid of the phospholipid bilayer membrane and diffuse into the cells.

1.6.2.3 Drug solubility

Drug solubility is a prerequisite for bioavailability and absorption of the drug in a dosage form. The deposited drug on the nasal mucosa must be dissolved in mucus and saturate it prior absorption. Therefore, rate of solubility and saturation determines extent of drug absorbed by nasal mucosa (N. Jones, 2001).

1.7 Intranasal drug delivery formulations: Liquid and gel forms

Intranasal drug delivery has been practised for treatmant of nasal disorders to administer topical nasal treatments such as antihistamins and anti-inflammatory drugs (corticosoids) to treat nasal infection, congestion and allergy (Kovacs, Adappa, & Kuan, 2021; A. K. Singh et al., 2012).

In addition to anatomy and physiology of nasal cavity and physicochemical properties of drugs that were described in the previous sections, introduction of drugs into a suitable delivery vehicle system is also important. The delivery vehicle must provide drug stability and ideal dispensing characteristics, therefore, careful consideration on selection of the vehicles for specific pharmaceutical compounds are required (Marx, Williams, & Birkhoff, 2015).

The most common intranasal drug delivery systems for locally or systemic acting drugs are generally in form of liquid (such as solutions, suspensions or emulsions) and

gel. Selection of dosage form depends on the type of drug, its function, population of users, number of doses required for treatment, and convenience of administration (Ghori et al., 2015). These forms of dosage require a suitable delivery vehicle to ensure administration of accurate dosage, safety and patient compliance.

1.7.1 Liquid form dosage

Liquid form is the most popular form of dosage in intranasal drug delivery. Liquid formulations are commonly administered via nasal sprays or aerosol pumps. These water based systems administer drugs by compressed air nebulisers, squeezed nasal bottles and metered-dose pump sprays.

Compressed air nebuliser is a device that is loaded with a drug suspension or solution upon use. The air pressure or ultrasonic power breaks up the liquid formulation into small aerosols to be directly inhaled through the mouth piece of the nebuliser (Alagusundaram et al., 2010). This system is used for administration of corticosoids and bronchodilators and effectively delivers the drug into the respiratory tract (Muthumanickam et al., 2010).

Decongestants are mainly delivered via the squeezed bottle devices. This device delivers the drug suspension or solution by squeezing the plastic bottle to press out the air inside the container to the nozzle and atomise a certain volume of the liquid. Although use of this device is convenient and patient can self-administer the drug, dose accuracy depends on the mode of administration. Also, microbial contamination of the nozzle and suction of nasal secretion into the bottle are the disadvantages of this system (Washington, Washington, & Wilson, 2000).

Metered-dose spray pumps are the most popular intranasal delivery systems used in delivering solution, suspension or emulsion forms of pharmaceutical compunds to treat nasal congestions and allergy symptoms. This self-administration device is a cost effective, convenient hand operated tool and function by spraying a certain volume of fine mist into the nasal cavity through nostrils (50 to 100 µL into each nostril) (Marx et al., 2015). Size of aerosols generated by the spray pumps is in the range of 40 to 100 µm and deposit well on the nasal cavity and find their way into the lower part of the respiratory tract (Stuart, 1984). The sprayed liquid deposits on the anterior part of nasal cavity and spreads over the mucosa by mucociliary clearance action of nasal

cavity. However, this mucocilliuary action may reduce residence time of the drug resulting in poor deposition and absorption.

In spite of many advantages of spray pumps, some drawbacks limit their applications. The pump sprays usually deliver an accurate dose, but the viscosity of the compound may slightly reduce dose accuracy (Djupesland, 2013). Also, the pump systems do not have any measures to prevent microbial contamination, thereofre preservatives are added to improve shelf life and in-use stability (Marx et al., 2015).

1.7.2 Gel form dosage

Nasal gels are solutions or suspensions of drugs that are thickened by combining with a biocompatible, water soluble gelling polymer generally called hydrogel. Hydrogel is a three dimensional configuration of a hydrophilic polymer which swells in water and show high volume transition in response to various stimuli such as pH, temperature, ionic stimuli and electric or magnetic field (Gupta, Vermani, & Garg, 2002). Hydrogel systems are formulated in various physical forms such as films, slabs, in situ gels, microparticles, nanoparticles and nanogels (Sosnik & Seremeta, 2017).

Hydrogel viscosity plays a crucial role in drug bioavailability and absorption. Incorporation of hydrogel to the drug increases viscosity of the system and reduces post-nasal drip and anterior leakage after administration. However, high viscosity of the hydrogel limits spreadability and distribution of the drug throughout the mucosa (R. M. Singh, Kumar, & Pathak, 2013).

In the past, most of nasal hydrogel formulations were fabricated prior administration, known as preformed gels. The preformed gels are simply viscous solutions (semi-solid) or solid materials in forms of film, particles and monoliths that undergo sol-gel transition outside the body and their rheological and mechanical properties do not change after administration. Some of these systems require invasive to minimally invasive procedures of administration (Sosnik & Seremeta, 2017). Hydrogel-based nasal inserts are good examples of this system. These solid formulations are crosslinked hydrogels that transform into soft gel after placement into nasal cavity (Luppi, Bigucci, Cerchiara, & Zecchi, 2010). Solid inserts can be obtained by drying of hydrogels using drying techniques such as freeze drying and supercritical CO_2 drying. Several works reported development of nasal inserts by employing hydroxypropyl

methylcellulose and chitosan (Bertram & Bodmeier, 2006; McInnes et al., 2005). Applications of these type of hydrogel formulations are restricted to treatment of ailments on posterior part of nasal cavity and wound healing.

More recently, a number of drug delivery systems are developed that are injected or sprayed into the nasal cavity in form of liquid or semi-solid and undergo in situ sol-gel transition under physiological conditions (Kouchak, 2014). To form in situ gel, sol-gel transition must be triggered by internal stimuli such as Temperature, pH, presence of ions, or external stimuli, e.g., photo-initiation and polymerisation, presence of a magnetic or an electric field (Vigani et al., 2020). In situ nasal gelling system is a very appealing strategy to attain patient's compliant and comfort.

Although nasal gel formulations are simple and effective, their stability, shelf life and dispensing into nasal cavity are elements of concern.

1.8 Hydrogel-based intranasal drug delivery systems

The growth of hydrogel technology is due to biocompatibility, hydrophilicity, bioadhesion and capability of simply crosslinking the polymers to obtain various compositions. Degree of crosslinking influences water absorption and swelling, mechanical strength, mucoadhesion and degradation rate. The hydrogel forming polymers must be capable of adhering to mucus membrane through attractive and repulsive molecular interactions (Lynch et al., 2020). A mucoadhesive hydrogel spreads over the mucosa and adheres to it to increase surface contact and residence time and enhance drug deposition and bioavailability (Ghori et al., 2015).

The intranasal route is naturally suitable for topical administration of drugs for treatment of local disorders that affect nose and paranasal sinuses such as acute and chronic rhinitis, rhinosinusitis and nasal polyps (Pires et al., 2009). Numerous research groups have confirmed unique benefits of hydrogel systems in topical delivery of anti-inflammatory and antibiotic drugs through the nasal cavity. Chitosan, poloxamers, carbopols, pectin, gelatine and cellulose-derived polymers are the widely used hydrogel-forming polymers in field of intranasal hydrogel delivery systems.

As mentioned above, in situ gels systems require internal stimuli (presence of reacting ions, temperature change, pH difference) or external stimuli (magnetic or electric fields) to form gels. A nanoparticle hydrogel system composed of alginate and pectin was fabricated by Dukovski et al. (2017) to treat inflammation caused by chronic rhinosinusitis. The drug (dexamethasone) was loaded to alginate nanoparticles and dispersed in pectin solution to be easily sprayed on the inflammation site and form gel upon contact with the Ca^{2+} present in nasal mucus. The in vitro studies indicated that presence of pectin in the formulation hindered drug release and achieved extended anti-inflammatory effect in comparison to dexamethasone solution. Another in situ gelling system was prepared by Nižić et al. (2019) to investigate effects of concentration of two gelling agents (pectin and gellan gum) in spray-ability and deposition of the fluticasone (an anti-inflammatory drug) on the nasal turbinates. Pectin and gellan gum formed gel upon interaction with nasal mucosa and reaction with Ca^{2+} present on the mucus. Sodium hyaluronate was used as the bioactive ingredient facilitating wound healing. In vitro studies of Nižić and colleagues demonstrated that the sprayable suspension instantly formed a viscous gel and deposited on nasal mucosa. Also, they stressed that concentration of gellan gum plays crucial role in spray ability and adhesion force to mucosa. However, drug release and therapeutic effect was not investigated in this study.

The use of thermos-sensitive polymers in formulation of in situ hydrogel delivery systems has also been explored by some researchers. Altuntaş and Yener (2017) exploited an in situ gelling system composed of poloxamer 407 and carbopol 974P to formulate a prolonged release momentasone furate delivery system for treatment of allergic rhinitis. They were able to reduce the sol-gel transition temperature to 30˚C by increasing the concentration of poloxamer 407 to rapidly form an in situ well-structured gel capable of releasing accurate drug doses. Gholizadeh et al. (2019) developed a thermos-sensitive sprayable chitosan hydrogel loaded with tranexamic acid to treat nasal bleeding and wounds. In this formulation β-glycerophosphate was added to the formulation to enable sol-gel transition of chitosan at 32˚C in less than five minutes. The formulation revealed itself suitable for intranasal drug delivery system and showed six times faster wound healing compared to control TXA solution.

In general, in situ gelling systems proved to be useful due to ease of drug administration, increasing drug bioavailability, minimising dose frequency and drug toxicity, biocompatibility and degradation. However, high level of fluid, low stability of the solution, limitation of small dosage and low mechanical strength of the gel are disadvantages of in situ nasal gelling systems. Low mechanical strength may result in premature dissolution of the formulation or dislocation of the formulation from the local target site (Mohanty, Bakshi, Simharaju, Haque, & Sahoo, 2018). Also, in situ gels cannot be administered when nasal bleeding is uncontrolled or nasal mucosa is infected.

1.9 Conclusion

Intranasal drug delivery is a technology with an interesting past and a fascinating future. This fast emerging technology circumvents drug bioavailability and enable development of controlled, extended release formulations. Intranasal local drug delivery formulations are limited to conventional drops and sprays that deliver drugs in forms of solution, suspension and emulsion. In situ nasal gelling systems have been proposed as valid candidates in treatment of intranasal disorders. Review of the literature indicated lack of recent research in preformed hydrogel nasal delivery systems. These semi-solid and solid formulations allow intimate contact with surface of mucosa, prolong residence time of the formulation and improve bioavailability with respect to solution form. Higher drug loading capacity and great physical and chemical stability of the formulations during product distribution and storage are the other advantages of semi-solid and solid formulations over the in situ gel products. There is high scope for research work on preformed gel systems in order to utilise advance hydrogel fabrication techniques to develop novel intranasal drug delivery systems.

Novel controlled release delivery systems can provide numerous advantages over conventional systems. Exploitation of preformed nasal gels can be considered for extended controlled-release of drugs in treatment of intranasal disorders to improve effectiveness of the treatment and reduce dosage and repeating of the treatment.

Chapter 2 Literature review and thesis framework

2.1 Introduction

Epistaxis (nose bleeding) is a condition characterised by nose bleeding. It is a common condition occurring at some point in life in about 60% of the population (Kucik & Clenney, 2005), with incidence peaking in children under 10 and adults older than 50 years (Cho & Kim, 2012).

The nasal blood vessels, located immediately under mucosa, are easy to damage. The common causes of damage are local causes (e.g., trauma, mucosal dehydration, inflammation, tumours, and aneurysms); and systemic causes such as age fragility, hypertension, coagulopathy, medications that interfere with normal blood clotting, and systemic fibrovascular dysplasia. Additionally, epistaxis may occur during and after intranasal operations such as septoplasty and sinus surgery. Most cases of epistaxis are easy to manage; however, severe epistaxis can be life threatening and requires prompt treatment (Cho & Kim, 2012).

Epistaxis is commonly classified as anterior or posterior, based on the location of bleeding in the nose. Anterior epistaxis is the most common with about 90% of cases. Blood flows from nostrils. Posterior epistaxis occurs at the back of the nasal cavity from branches of the sphenopalatine artery. Blood flows down the throat (Kucik & Clenney, 2005).

Nasal packs are the primary devices generally used to control bleeding in severe anterior and posterior epistaxis. Nasal packs induce haemostasis by filling the nasal cavity, exerting pressure on the wound site, and creating a moist environment to facilitate wound healing (Weber, Keerl, Hochapfel, Draf, & Toffel, 2001). According to the International Journal of Otolaryngology, the number of epistaxis incidents and prevalence of nasal diseases and disorders due to hypertension, and air pollution is annually increasing and driving the high demand for nasal packing devices (Traboulsi, Alam, & Hadi, 2015). Nasal packs are also used as a post-operative intervention devices during and after intranasal surgeries such as endoscopic sinus surgery (ESS) (Weber & Hosemann, 2015) and septoplasty (Banglawala et al., 2014). Nasal packing after endoscopic sinus surgery is used to control postoperative bleeding, enhance the wound healing process, and prevent lateralization of the middle turbinate, which causes insufficient ventilation (Kang, Kim, Shin, Park, & Lee, 2017). Generally, these

devices facilitate haemostasis by absorbing the wound fluid, applying gentle pressure on the operated site and provide a site for blood to clot. Nasal packs also support the cartilaginous and bony nasal structure or mucosa (Weber, 2009), reduce the risk of tissue adhesion between the freshly operated tissues and minimise risk of hematoma formation between the two re-sectioned membranes supporting their firm union after septoplasty (Eski, Guvenc, Hizal, & Yilmaz, 2014).The aims of this review are to assess commercial nasal packs in terms of composition and physical structure, then to review advantages and disadvantages of these products in clinical studies. Topical intranasal drug delivery systems using hydrocolloids will also be reviewed. This will identify candidates for formulation and development of new generation of drug-eluting nasal packs for treatment of epistaxis and intranasal postoperative complications.

2.2 Application of nasal packs in treatment of epistaxis and intranasal postoperative complications

There is no standard for the materials used in fabrication of nasal packs, nor when packs should be used, nor how long they should be in situ at the bleeding site, although typical residence times are between 48 to 120 hours. Nasal packs must have the following characteristics: biocompatibility, hydrophilicity, a porous structure but with a smooth surface, high fluid absorbency and expansion to exert gentle pressure on the nasal mucosa.

Traditional clinically-prepared anterior and posterior packs are made of a cotton gauze or lubricated with petroleum jelly, a vasoconstrictor and an antibiotic, and are inserted into the nose (Bertrand et al., 2005). There is also a range of commercially available nasal packs.

2.3 Commercial nasal packs

Commercial nasal packs are available in pharmaceutical markets in the form of non-erodible and in situ-erodible materials. Non-erodible nasal packs require physical removal at the end of treatment period. Erodible nasal packs gradually break down and absorb or simply drain from the nasal cavity during the treatment period and so do not require withdrawal.

2.4 Non-erodible nasal packs

Non- erodible nasal products (examples in *Figure 3*) are mainly used in emergency departments of hospitals, nursing homes and home care settings or are inserted into the nasal cavity during or after sinus surgery. These sterile products, with shapes to fit the nasal cavity, are commonly made of polyvinyl alcohol (PVA), polyvinyl acetate or other synthetic biocompatible materials. All require withdrawal after treatment ceases.

Ivalon (Fabco, UK), Merocel (Medtronic, USA) and AbsorbENT (Innovia Medical, USA) are biocompatible spongy packs made from cross-linked PVA where the chemical links are undescribed. The hydrophilic property of PVA sponges is due to their abundant hydroxy groups. Merocel and AbsorbENT swell in the nasal cavity by absorbing fluid from intranasal tissues and stop bleeding by exerting mechanical pressure over the wound. Both products are designed in several shapes and lengths with a typical thickness of 15 mm after swelling. Some packs have an internal silicon airway tube or a drawstring for easy removal (Medtronic, 2012; Summitmedical, 2017). Some are surface coated with polyethylene (Merocel 2000) or oxidised cellulose to aid insertion and removal (Merocel Hemox) (Massey & Singh, 2017). Similarly, Telfa (The Kendall Company, USA) is non-erodible, but made of cotton fleece coated with non-adherent polyethylene terephthalate.

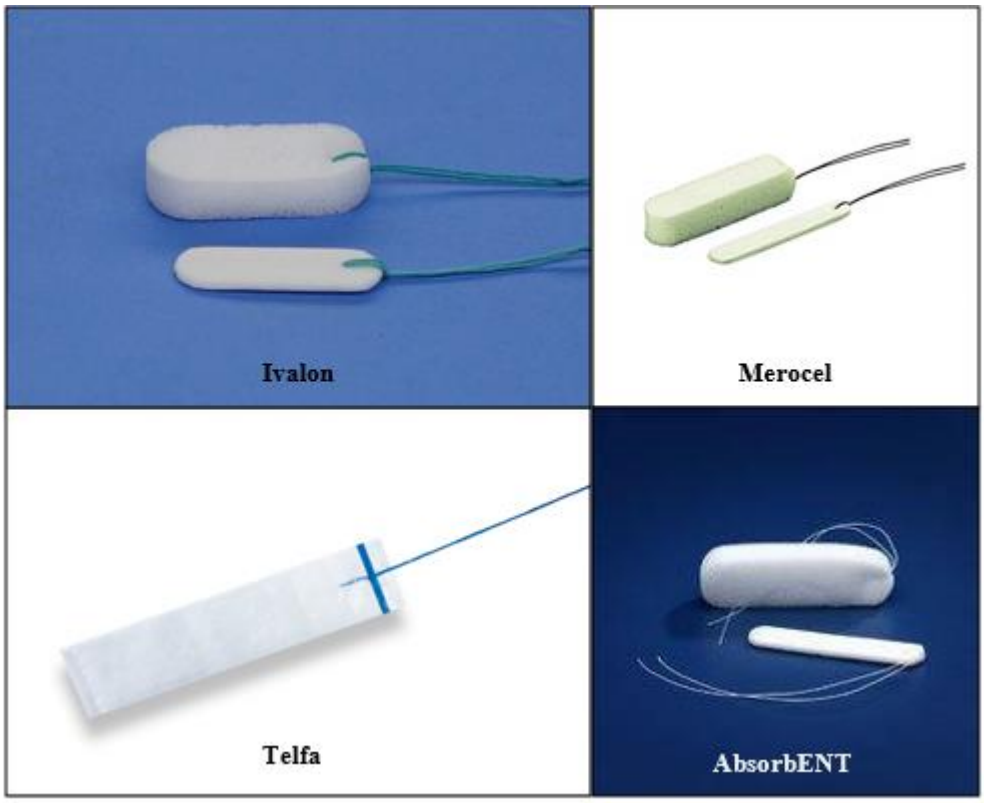

Figure 3. Common non-erodible commercial nasal packing products. All the packs are made of absorbent materials to absorb wound exudate and provide a moist environment.

2.4.1 Erodible nasal packs

Erodible nasal packs (examples in Figure 4) are composed of materials that can be fragmented or biologically resorbed in the nasal cavity. Erosion of these packs eliminates the need for sometimes painful removal so there is a trend toward use of erodible nasal packs.

Current commercial erodible nasal packs are composed of hyaluronic acid (a mucopolysaccharide), polyurethane (PU), gelatine and chitosan. Physicochemical (e.g., water solubility, gelation and hydrophilicity) and biological (e.g., biocompatibility, biodegradability, anti-inflammatory and antioxidant) characteristics of these biopolymers make them attractive in formulation of nasal packs.

MeroGel (Medtronic, USA) is a highly absorbent woven fleece of esterified hyaluronic acid where all the carboxylic groups of glucuronic acid are esterified with benzyl alcohol, termed HYAFF®. The fleece becomes a mucoadhesive gel in less than 48 hours and slowly disperses over two weeks. It is generally used for intranasal postoperative treatments. A related product, MeroPak (Medtronic), is a sponge comprised 80%

HYAFF® and 20% collagen, designed for postoperative haemostasis and wound healing. This biopolymer nasal pack similarly disperses within two weeks.

MeroGel Injectable (Medtronic, USA) is a space-occupying gel and used after nasal trauma or surgery and comprises unspecified cross-linked polymers of hyaluronic acid. The gel is injected into the nasal cavity through a catheter.

Rapid Rhino NASASTENT (Smith & Nephew, USA) is a CMC-coated fabric sponge (image not shown in Figure 3) and claimed to absorb up to 16 times its dry weight while conforming to nasal anatomy, then later fragmenting into pieces that drain from the nasal cavity. But some residues may remain, requiring physical removal (Smith & Nephew, 2015).

NasoPore **(**Stryker, Canada) is a fragmentable nasal pack produced from polyurethane by freeze-drying. This pack can absorb up to 25 times its weight of fluid. During the critical healing period (36 to 48 hours after insertion), it begins to degrade into CO_2, H_2O and O_2, while still providing sufficient support without swelling. Fragmented NasoPore drains from the nasal cavity via natural pathways and additional saline spray accelerates its fragmentation (Easmed, 2014).

Novashield (Medtronic, USA) is an injectable chitosan-based fragmentable gel positioned in the sinus or nasal cavities after surgery to prevent bleeding, tissue adhesion and infection. The gel breaks up to small fragments, which are claimed to be easy and painless to remove.

Figure 4. Common erodible commercial nasal packing products. These products are solid gels or injectable sols that conform to gel when absorbing fluid. They resorb through mucosa or fragment into pieces drained or recovered from nasal pathways.

Cutanplast (Mascia Brunelli, Italy) and Gelfoam (Pharmacia and Upjohn, USA) are gelatine-based dressings with suitable physical characteristics and haemostatic effect in postoperative treatment after nasal surgery. Cutanplast can absorb fluid and blood up to 50 times its dry weight and becomes completely absorbed within several weeks when left in situ. Gelatine at the surface activates an enzymatic cascade, encouraging blood clotting (Yan et al., 2014). Gelfoam, a similar haemostatic nasal dressing, liquefies in two to five days, presumably by a similar hydrolytic mechanism.

RapidRhino Stammberger Sinu-Foam (Medtronic, USA), made of CMC, actively promotes platelet aggregation upon blood contact and is claimed to be an ideal packing treatment after surgery (Yan et al., 2014). This product is initially a dry powder enclosed in a syringe and forms a viscous gel when hydrated with water. The gel conforms to the nasal and sinus cavities and provides a moist hydrocolloid barrier that disperses over several days.

2.4.2 Complications associated with non-erodible nasal packs

Despite the claimed utility of the non-erodable nasal packs, there are complications associated with insertion of such packs such as vascular collapse, laceration of soft palette tissue (damage to nares) and failure to control bleeding (Fairbanks, 1986).

Also, pain experienced on placement and removal are the most common complaints of patients using these products. Pain and rebleeding during removal can be due to growth of the new tissue into the pack or adhesion of the pack to the mucosal tissue (Deniz, Çiftçi, Işık, Demirel, & Gültekin, 2014). The pressure applied by nasal packs may also damage the endonasal tissue septal cartilage or septum bone (Kucik & Clenney, 2005).

In addition, breathing difficulties due to closure of the nasal airway may cause hypoxia, associated hypercapnia (Bertrand et al., 2005), obstructive sleep apnoea (Weber, 2009) and neurogenic fainting during insertion (Fairbanks, 1986). Other complications may include foreign body reaction (Weber, 2009), dislocation and disorientation of the pack (Fairbanks, 1986), allergic response to the pack material (Weber, 2009) and temporary ostachian tube dysfunction with negative middle ear pressure (Bertrand et al., 2005; Weber, 2009). Also, prolonged residence of nasal packing may cause toxic shock syndrome due to staphylococcus infection (Bertrand et al., 2005; Weber, 2009).

2.4.3 Complications associated with erodible nasal packs

The problems associated with nasal packs requiring physical removal have led to development of erodible materials. The majority of the studies agree that the erodible products can improve the patient's experience and reduce discomfort, in respect to in situ pain and re-bleeding (Burduk, Wierzchowska, Grześkowiak, Kaźmierczak, & Wawrzyniak, 2016; J. Wang, Cai, & Wang, 2014). However, the outcomes in terms of nasal blockage, mucosal healing, tissue adhesion, mucosal edema, and long term nasal healing have been erratic. Some studies showed that erodible nasal packs (MeroGel and Gelfilm) reduced nasal obstruction and tissue adhesion (Catalano & Roffman, 2003; Yan et al., 2014), but Maccabee, Trune, and Hwang (2003) found that MeroGel and Floseal impair mucosal healing by growth of regenerated tissue in the pack and loss of surface epithelium and mucocillary blanket due to fibrosis of basal lamina. They also found that remnants of Merocel and floseal fibers were incorporated into regenerated epithelium. With respect to re-epithelization, Y. P. Wang et al. (2011) found that polyurethane-based Nasopore increased formation of granulated tissue growing into the pack during early stages of wound healing, while Berlucchi, Castelnuovo, Vincenzi, Morra, and Pasquini (2009)

and G. Xu, Chen, Wen, and Li (2003) found that normal re-epithelization improved with hyaluronic acid-based MeroGel.

Thus, although the current erodible products such as NovaShield and Merogel are useful, they do not necessarily fulfill the entire surgical expectations in terms of effectiveness and patient comfort (Berlucchi et al., 2009; Weber, 2009). One study suggested MeroGel may potentially cause osteogenesis (Jacob, Faddis, & Chole, 2002) and NasoPore may cause tissue granulation (Y. P. Wang et al., 2011). Also, collagen in MeroPack may increase synechiae and tissue granulation (Tom, Palasti, Potsic, Handler, & Wetmore, 1997). In addition, the consituents of the packs derived from animal products like gelatine can elicit an antibody formation and may be a source of zoonoses[1] (Antisdel, Matijasec, Ting, & Sindwani, 2011). Therefore, it appears that complications of erodible nasal packs depend on the chemical matrix.

However, infection and perforation still occur with use of both non-erodible and erodible products. In spite of the complications of nasal packing and debate over their functionality, nasal packing is still the most common treatment of anterior and posterior epistaxis and postoperative intranasal care.

2.4.4 Improvements to nasal packs

The results of these clinical studies highlight the need for improvement of current nasal packs or development of new products. In general, a constructive nasal pack expected to:

i. be made of biocompatible, non-allergenic and non-toxic materials in applied dosages
ii. have high fluid absorption capacity and keep the wound site moist.
iii. show some degree of swelling to apply gentle pressure on the wound site and faciliate haemostasis.
iv. show mechanical strength to withstand the physical pressures applied to the bulk during placemant and residence time in nasal cavity.
v. be sufficiently adhesive to mucosa and cohesive to maintain its form for the desired period.

[1] Infectious diseases of animals that can be transmitted to humans.

vi. erode during the treatment period to avoid a new wound caused by removal.

Along with nasal packing, systemic administration of anti-fibrinolytic, anti-inflammatory and antibiotics may be prescribed during and after intranasal surgeries to facilitate wound healing and prevent infection. However, local administration of these drugs is usually preferred. To improve the functionality of nasal packs in terms of stopping bleeding and local administration of drugs, researchers attempted to incorporate drugs into nasal packs. Chang, Alandejani, Akbari, Ostry, and Javer (2011) investigated the effects of inserting Merocel impregnated with budesonide or gentamicin on tissue inflammation, wound healing and pain on pack removal. They found no difference in outcomes compared to the non-medicated Merocel as control. Similarly, Rudmik, Mace, and Mechor (2012) evaluated the effects of Rapid Rhino sinu-foam impregnated with dexamethasone but found no clinical differences due to the drug.

In contrast, Côté and Wright (2010) found that impregnating Nasopore packs with the triamcinolone, an anti-inflammatory drug, reduced inflammation on the wound site and accelerated haemostasis and wound healing. Thus, development of a drug-eluting erodible nasal pack capable of effective localdrug delivery would be a huge advantage.

2.4.5 Novel medicated nasal packs: materials and techniques

As mentioned in the sections above, in addition to biocompatibility, fluid absorption capacity, swelling ability to fill nasal cavity and erosion, the novel nasal packs must be able to act as the drug carrier. They are expected to confine the drug within their matrix structure and make it available to the nasal mucosa when needed.

Literature review of intranasal drug delivery systems suggests that hydrogel systems are therapeutically suitable systems for sustained and controlled release of drugs. They are popular in drug delivery because of showing the following properties: hydrophilicity, biocompatibility, the ability to confine large amounts of water soluble drug and the ability to control their drug release in physiological environments by structural changes in the hydrogel during manufacturing process (Jianyu Li & Mooney, 2016; Sun, Song, Wang, Hu, & Wu, 2020). The polymer network formed during processing of hydrogels can be matched with the application by modifying its

physical and chemical structure using various methods such as blending with other polymers and crosslinking (Jianyu Li & Mooney, 2016) . The sustainable biopolymers used in fabrication of hydrogels are abundant in nature and widely used in food and pharmaceutical industries such as: alginate, carrageenan and agar extracted from seaweeds, locust bean gum and gellan gum, and starch.

Regarding the drying techniques for hydrogels, supercritical drying (Manzocco et al., 2017; Plazzotta, Calligaris, & Manzocco, 2019) and lyophilisation (Grenier et al., 2019; Nakagawa, Sowasod, Charinpanitkul, Soottitantawat, & Tanthapanichakoon, 2011) are suggested in the literature. The principle involved in the supercritical drying is displacement of water in the hydrogel using a supercritical fluid such as ethanol, and removal of alcohol/water mixture using supercritical CO_2 dryer (Brown, Fryer, Norton, & Bridson, 2010; Nita, Ghilan, Rusu, Neamtu, & Chiriac, 2020) and the product is called aerogel. This drying method can protect the gel structure with smaller pore size (nano scale) and high specific surface but it is time consuming and require significant quantities of solvents and supercritical gas making this method is expensive and less-environmentally friendly (Long, Weng, & Wang, 2018)

Freeze drying (lyophilisation) technique involves cooling of liquid solvent (water) and convert it into ice crystals followed by sublimation of the ice under vacuum conditions and its evaporation, producing cryogel (Adams, 2007). In comparison to supercritical drying, freeze drying is quicker, more cost effective and environmentally friendly, however cryogels perform larger pore size (micro scale), lower surface area, and more degree of shrinkage (Long et al., 2018; Nita et al., 2020).

Freeze-drying is a suitable technique for fabrication of novel nasal packs due to the requirement for micro pore size for fast absorption of wound exudate and reduce the risk regenerated tissue growing into the pack. However, release of drugs from this microstructure may be very fast and require processes that extend release of the drug such as blending with other biopolymers or crosslinking.

2.5 Biopolymers in development of erodible wound healing and drug delivery systems

In the past decades many researchers have explored biocompatible polysaccharide polymers from marine and land plants to develop novel wound healing products and

drug delivery systems for topical drug administration. These polymers, commonly called hydrocolloids, have been successfully used as superabsorbent materials due to the presence of hydrophilic groups such as hydroxy (-OH), carboxylic (-COOH), amidic (-CONH-) and sulphonic (-SO_3H) within their polymer chain backbone or side chains (Ganji, Vasheghani Farahani, & Vasheghani-Farahani, 2010). Biocompatibility, water retention, swelling and drug diffusibility, erosion and bioadhesion are major characteristics of hydrocolloids suitable for fabrication of advanced drug delivery systems (Bajpai, Daheriya, Ahuja, & Gupta, 2016; Boateng, Pawar, & Tetteh, 2013; Fan et al., 2011; Nair, Raman, & Doble, 2016).

Marine-based hydrocolloids are predominantly extracted from marine macroalgae. Carrageenan, alginate, fucoidan and agar are dominant examples. They exhibit a range of useful bioactivities of which at least two may be clinically useful in nasal packs: antioxidant activity (Barahona, Chandía, Encinas, Matsuhiro, & Zúñiga, 2011), and anti-inflammatory activity (Cumashi et al., 2007).

2.5.1 Carrageenan

Carrageenan is a high molecular weight linear polysaccharide (400 to 600 kDa) with repeating disaccharide units comprised of 1,3-linked β-D-galactose 4-sulphate and 1,4-linked 3,6-anhydro-α-D-galactose (Figure 5). This water dispersible polysaccharide is extracted from species of red seaweed (Rhodophyceae) and is widely used in food, cosmetic and pharmaceutical industries as thickening, gelling and stabilising agents (Campo, Kawano, Silva, & Carvalho, 2009).

Based on the number and position of sulphate groups, three main types of carrageenan are identified: iota (ί), kappa (κ) and lambda (λ) carrageenan (Figure 5).

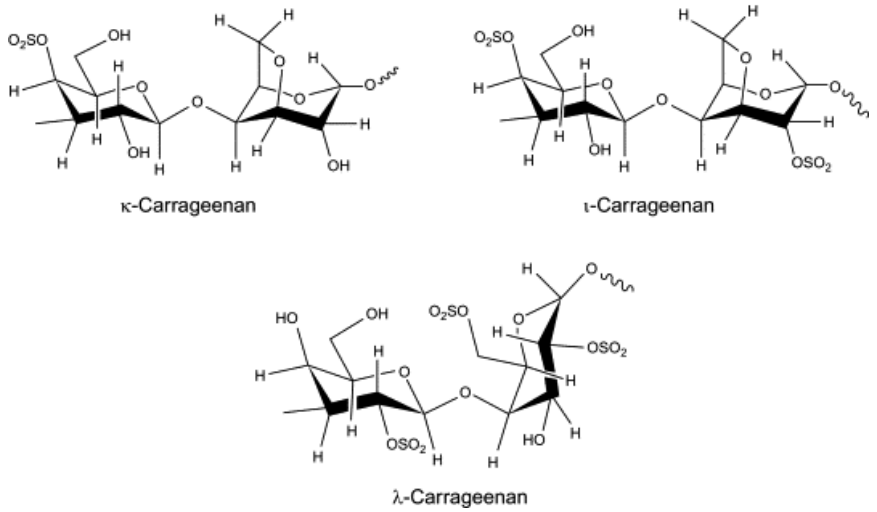

Figure 5. Representative chemical structures of the three carrageenans. All are based on galactose but differ in their degree of sulphation and other chemical features (Cunha & Grenha, 2016).

All the three types disperse in hot water, but only kappa and iota undergo sol-gel transition upon cooling in presence of counter ions such as K^+ and Ca^{2+}.

These two carrageenans produce thermoreversible sol-gels by formation of random coil structures in the sol stage, followed by double helix structure during cooling due to a twist in galactose sequences present in the carrageenan chains (Kianfar, 2011). Of the three carrageenans , κ-carrageenan (κ-Car) has been most used in development of pharmaceutical formulations. At concentrations higher than 1% (w/w) κ-Car produces a transparent, firm and brittle gel upon cooling (Garcia-Gonzalez, 2011) and a highly viscous sol at lower concentrations.

κ-Car has been used in wound dressing and healing materials due to its biocompatibility and degradability (T. H. Silva et al., 2012), and controlled drug release properties (Boateng et al., 2013; Eouani, Piccerelle, Prinderre, Bourret, & Joachim, 2001; Fan et al., 2011; Kianfar, 2011; Nair et al., 2016; Vigani et al., 2019). Due to its abundant hydroxy and sulphate groups κ-Car can bind to mucus membrane and thus impart bioadhesive properties to the formulation (Kianfar, 2011).

Among wound healing and dressing materials, films are favoured due to their simplicity and creation of a moist wound environment that promotes healing (Boateng et al., 2013). However, films are usually mechanically weak with poor water vapour barrier properties. For these reasons biopolymers are usually combined with

other biological or synthetic polymers or are chemically cross-linked to improve their properties (Khalil et al., 2017). For example, Boateng et al. (2013) fabricated a drug-loaded transparent film with high elasticity and controlled release of the drugs for 72 hours, using a combination of κ-Car and polyethylene oxide polymer. Bajpai and Daheriya (2014) produced κ-Car and polyvinyl alcohol films crosslinked with gluteraldehyde and loaded with an antibiotic.

Other studies have reported wound healing κ-Car products. For example, Fan et al. (2011) formulated a powder with inherent antibacterial activity by carboxymethylation of κ-Car using hydrogen peroxide. Compacts and compacted granules were made using κ-Car and chitosan by Sánchez-Sánchez et al. (2015). Lokhande et al. (2018) nanoengineered injectable hydrogel comprised of κ-Car and nanosilicates crosslinked by K^+ to accelerate blood clotting and promote wound healing. C. Li et al. (2014) created a thermosensitive hydrogel system by combining κ-Car and a polypropylene glycol polymer to enhance bioavailability of a model drug. Erosion of this combination depended on the concentration of potassium ion in the medium and the temperature of the release environment. These studies indicate that κ-Car is a suitable candidate in formulation of topical drug delivery systems, so it can be used in development of drug eluting nasal packs.

2.5.2 Alginates

Alginates are salts of alginic acid extracted from brown and red seaweeds, and are widely used as stabilising, gelling and thickening agents in the food industry. These high molecular mass (32,000 to 400,000 g mol^{-1}) linear polysaccharides comprise 1,4-linked β-D-mannuronic acid and its carbon 5 epimer 1,4-linked α-L-guluronic acid (Figure 6) in various distributions, giving them varying properties (Lahaye, 2001). Alginic acid disperses in water to form viscous sols either as the free acid or carboxyl group ionically bound to Na^+ or K^+.

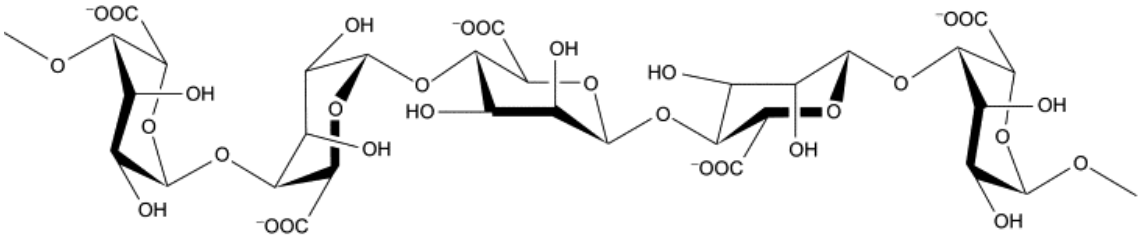

Figure 6. Chemical structure of alginate (alginic acid) where each uronic acid can and does repeat in regions of variable length. This image shows three guluronic and two mannuronic residues (Hillier & Rakkar, 2007).

Importantly, alginic acid demonstrates a marked affinity for divalent cations such as Mg^{2+}, Ca^{2+} and Sr^{2+}. These behave as crosslinkers to form an egg box model by bonding to guluronate blocks of alginate in one chain and the guluronate blocks of adjacent chains resulting in a gel structure (Grant, Morris, Rees, Smith, & Thom, 1973). The gels are particularly firm with long sequences of adjacent guluronic acid residues. Alginate gel properties can also be controlled in other ways including covalent crosslinking using polyethyleneglycol (Eiselt, Lee, & Mooney, 1999; K. Y. Lee et al., 2000).

The most common divalent cation used in ionic crosslinking is Ca^{2+}. However these gels have low stability in physiological environments due to ion exchange reactions with physiological Na^{+} and K^{+}. This feature can be useful in development of wound healing products, because the released Ca^{2+} may promote haemostasis when the gel provides a matrix for aggregation of platelets and erythrocytes (Suzuki et al., 1998).

Commercial calcium alginate wound dressings are considered biocompatible and noncytotoxic. They absorb wound exudate, maintain a moist wound environment, and promote haemostasis and healthy tissue granulation (Johnson et al., 2020) as discussed by Suzuki et al. (1998). Several studies have explored improvement of alginate wound dressings in forms of scaffolds and films. Johnson et al. (2020) fabricated a porous calcium alginate scaffold impregnated with ibuprofen, and showed it to accelerate burn healing by supressing inflammation and faclitating healthy tissue granulation. A porous alginate-gelatin scaffold was developed by Afjoul, Shamloo, and Kamali (2020), which absorbed fluid up to 8 times of its weight, had acceptable tensile strength and degradated within 12 days. In another example, W. S. Tan et al. (2020) and X. Zhao et al. (2020) incorporated vicenin 2 (an anti-

inflammatory drug) and hydrogen sulphide, respectively, to their hydrogel films and investigated mechanical proprties of the films and release of the loaded drugs. They found that the uniform and flexible films were able to release the drugs sustainably and facilitate wound healing in in vitro studies.

These results suggest that alginate can be useful in development of wound healing and dressing products, but there is no reference to using alginate for nasal packs in the literature.

2.5.3 Fucoidan

Fucoidan (Figure 7), extracted from marine brown algae, is a negatively charged sulphated polysaccharide composed of α-L-fucose units (deoxygalactose) as the sugar backbone, where the sulphate groups usually occur on carbon 2 and 4. However, the location of sulphate groups varies between species and residues of mannose, galactose, xylose and mannuronic acid may be present as side chains (Cunha & Grenha, 2016) making this polysaccharide significantly heterogeneous (Ale, Mikkelsen, & Meyer, 2011).

Fucoidan is highly hygroscopic and is soluble in water and acid solutions, but these are not viscous so fucoidan has not industrial uses as a thickening or gelling agent. It is non-toxic, biocompatible and FDA approved as a food ingredient in functional foods due to its antioxidant activity at the maximum level of 250 mg day^{-1} (Adams-S. & Keefe, GRAS notice: No.GRN 000661).

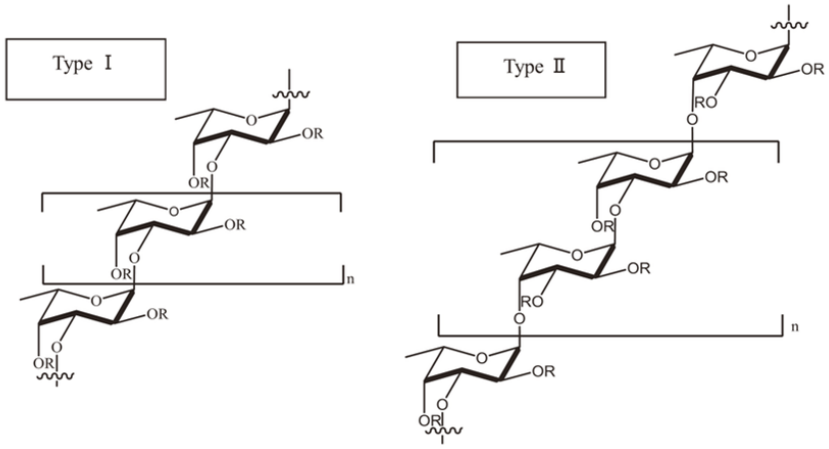

Figure 7. Common chemical structures of fucoidan. Type I and type II are common backbone chains and R can be fucopyranose, glucuronic acid and sulphate groups. The location of other sugars such as glucose, galactose, mannose and xylose in seaweed species may be different (Luthuli et al., 2019).

Fucoidan has gained especial interest due to its antioxidant (Thangapandi, Ajith Kumar, Shanmugaasokan, & Devi, 2014), anti-tumour (Malyarenko & Ermakova, 2017) and anti-coagulant (Kuznetsova et al., 2003; Ushakova et al., 2009) activities and its activity in regulating metabolism of glucose and cholesterol (Yokota, Nomura, Nagashima, & Kamimura, 2016). Fucoidan, by itself or combination with other polymers, plays an important role in pharmaceutical technology and design of various dosage forms, especially hydrogels (Murakami, Aoki, et al., 2010), films (Murakami, Ishihara, et al., 2010), and nano- and micro-particles (Y.-C. Huang, Chen, Lam, & Chen, 2014; Pawar et al., 2019). It can form polyelectrolyte complexes serving as carriers of drugs, growth factors (Y. C. Huang & Yang, 2016), proteins (Sezer & Akbuğa, 2006) and genes (Sezer & Akbuğa, 2009).

The unique anti-inflammatory and anticoagulant properties of fucoidan makes it a suitable biopolymer in formulation of hydrogels combined with positively charged chitosan applied in treatment of wounds and burns. Sezer et al. (2008b) prepared a poly-ion complex of chitosan and fucoidan microspheres and evaluated its treatment efficiency on dermal burns. In vitro and in vivo studies revealed that fucoidan in the formulation significantly improved bioadhesion of the hydrogel to the burn area followed by fast and effective regeneration and re-epithelisation of skin leading to shorter treatment period.

Murakami, Aoki, et al. (2010) blended fucoidan with chitin, chitosan, and alginate powders to produce a composite hydrogel film as a wound dressing. The film provided a moist environment on the healing-impaired wound and demonstrated easy application and removal, good adherence to the skin and significant stimulated wound repair in rats. Similarly, another study used low molecular weight fucoidan alone to formulate a transparent film for wound dressing to treat full thickness wounds in a rat model (Park et al., 2017). The results suggested that antioxidant and anti-inflammatory properties of fucoidan and its ability to interact with growth factors promotes dermal wound healing. In reviewing the literature, no study was found on use of fucoidan in development of nasal packs.

2.5.4 Agar

Agar, a water-dispersible polysaccharide extracted from certain red algae, comprises agarose and agaropectin with agarose dominating. Agarose, which dominates agar, can form gels but agaropectin cannot. Agarose is typically composed of repeating alternate units of β-1,3-linked-D-galactose and α-1,4-linked-3,6-anhydro-L-galactose (Figure 8).

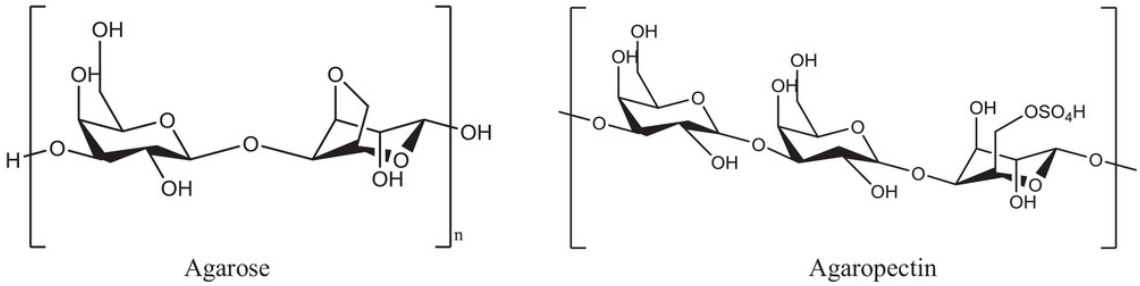

Figure 8. Chemical structure of agarose and agaropectin). Agarose comprises chains of repeating alternate units of β-1,3-linked-D-galactose and α-1,4-linked 3,6-anhydro-L-galactose. Agaropectin is composed of agarose and varying percentages of ester sulphate, D-glucuronic acid and small amounts of pyruvic acid. The proportion of these two polymers varies according to the species of seaweed. Agarose normally represents at least 70% of the natural agar (Tanna & Mishra, 2019).

Agar disperses as a hydrocolloid in water at around 90ºC and forms a hydrogel upon cooling to 40ºC (Tyeb, Kumar, Kumar, & Verma, 2018). Agar is extensively used in food industry as a gelling agent and in microbiology as a solid support in growth media.

Agar is an attractive medium for wound dressing and wound healing scaffolds due to its biocompatibility and biodegradability (Awadhiya, Kumar, & Verma, 2016). Shanmugarajan, Selvan, and Uppuluri (2020) developed a squalene oil-loaded agar scaffold using lecithin as an emulsifier to successfully treat full-thickness burns in a rat model. Similarly, an agar and PVA hydrogel loaded with icariin (a model antibiotic drug) showed good physical properties as a wound healing scaffold and drug release profile (Uppuluri & Shanmugarajan, 2019).

Tyeb et al. (2018) fabricated a sericin-loaded agar hydrogel film as a novel dressing for chronic wounds. The authors reported that the film exhibited adequate tensile strength, satisfactory swelling behavior and improved collagen production on the wound site. Basha et al. (2020) used agar to develop silver nitrate nanoparticles loaded with fumaric acid. The biodegradable nanoparticles maintained a moist environment while and the silver ions and fumaric acid respectively reduced risk of infection and facilitated desirable angiogenesis.

Together, these studies indicate that agar can be used as the basis of a wound healing product and a drug carrier, absorbing the wound exudate, and releasing a drug in kinetically useful way, restoring homeostasis, and eroding by the end of treatment.

2.6 Concluding remarks

Recent successes in wound healing and drug delivery products highlight the need for continuing research with the seaweed-derived polysaccharides, carrageenan, alginate, fucoidan and agar. However, a literature review on nasal packs shows that these polysaccharides have been largely neglected in novel intranasal wound healing products. Extrapolating from topical wound healing and drug delivery experience suggests these polysaccharides are candidates for development of novel nasal pack matrices. Their useful characteristics are their sustainability, likely low fabrication costs, biocompatibility, degradability, high absorption capacity resulting in swelling, and capability of blending with other polymers to achieve modified properties. In addition, they can entrap drugs within their network without destructive chemical interaction or other chemical changes to a drug and release the drug in a kinetically useful way.

2.1 Thesis Aims and structure

The overall aim of this research is design, formulation and development of a prototype in form of erodible monolithic cryogel capable of hosting therapeutics and releasing them in desired controlled manners. The prototype must meet the requirements of a regular nasal pack in terms of filling the nasal cavity, swelling and fluid absorption. The cryogel matrix acts as the drug carrier and should not chemically intervene with the loaded drugs. The capability of the prototype for customisation of the formulation for hosting hydrophilic and hydrophobic drugs with minor alterations is considered in its design.

The specific objectives of this thesis are:

i. To explore the feasibility of fabricating a porous solid structure using κ-carrageenan (κ-Car) biopolymer by lyophilisation technique to serve as a basic erodible nasal pack.

ii. To characterise the κ-Car prototypes in terms of physical and mechanical properties to evaluate their fitness for nasal packing application.

iii. To evaluate the capability of the developed prototype for drug delivery purpose by confinement of tranexamic acid (TXA), an antifibrinolytic drug used in management of epistaxis, and investigate the suitability of the formulations for immediate release of TXA.

iv. To modify the TXA- prototype formulation with combining κ-Car and locust bean gum or gelatine to investigate the effects of the combination on physical, mechanical and release profile of TXA for immediate release purpose.

v. To explore the suitability of the drug carriers developed for TXA in formulation of dexamethasone phosphate (DEX)-loaded nasal packs, an anti-inflammatory drug in reducing mucosa inflammation in intranasal operations, and investigate the effect of DEX on physical, mechanical and release profile of DEX for extended sustainable drug delivery.

vi. To formulate an antibiotic-loaded nasal pack, gatifloxacin (GFX) as the drug model, using κ-Car as the main matrix composition for prolonging sustainable release

of GFX and investigate the effects of blending κ-Car with agar on physical and mechanical properties and drug release profile of the formulations.

2.2 Thesis structure

This thesis consists of a general introduction (Chapter1), a literature review (Chapter 2), four experimental chapters (Chapter 3 to 6), a final thesis discussion and conclusion (Chapter 7) and a comprehensive reference list.

2.2.1 Chapter contents and rationales

2.2.1.1 Chapter 2- Literature review: Nasal packs: Applications, characteristics, limitations, and potential biopolymers in development of a new generation of nasal packs

Nasal packs are primary devices in treatment of epistaxis and extensively used as post-operative intervention of intranasal surgeries. This literature review introduced nasal packs, their applications in intranasal complications and divided them into two groups of non-erodible and erodible products. Common nasal packs in these groups were reviewed in terms of their composition, structure and complications associated with their use. This review indicated a need for development of novel erodible nasal packs as drug delivery systems to locally administer drugs when the pack is in situ.

The potential materials in development of nasal packs were studied and with the focus on sustainability and biocompatibility, seaweed extracted polysaccharides were studied in detail.

2.2.1.2 Chapter 3- Research chapter: Development of κ-carrageenan (κ-Car) cryogel for nasal packing and intranasal drug delivery

After summarising the literature of polysaccharides in pharmaceutical area, κ-Car was selected to examine its feasibility in fabrication of a plain nasal pack using freeze-drying technology. Therefore, a prototype of the biopolymer was developed. In this study, three concentrations of κ-Car hydrogel (1.2, 2 and 2.5% w/v) were prepared and subsequently dried using freeze-drying technique. These cryogels were characterised to assess their potential as a plain nasal pack. The microstructure, swelling and porosity studies exhibited microporous structure with high degree of swelling. Also, a degree of bioadhesion was observed and the cryogels were eroded in physiological environment (pH 7.4 and temperature 35˚C). This work demonstrates

the feasibility of using κ-Car and freeze-drying for manufacturing of customised nasal packs as drug delivery systems.

However, as a prototype, some limitations were noticed: i) increase in concentration of the biopolymer enhances bioadhesion and delays erosion but negatively affects porosity and swelling ability of the cryogel as important factors in nasal packs, ii) Reflecting the short erosion profile, this device may not be suitable for long term drug release. Considering these limitations, the prototype was used in development of drug loaded nasal packs as the basic matrix to investigate the effect of the drugs loaded into this matrix and the effects of blending this matrix with other biopolymers based on release profile requirements.

2.2.1.3 Chapter 4- Research chapter: Tranexamic acid-eluting nasal pack: a fast release local delivery system

Tranexamic acid (TXA) is an antifibrinolytic drug used to accelerate formation of blood clot and stop bleeding. In the case of epistaxis, fast release of this drug is required to act immediately. In the other hand, in intranasal mid and post-operative treatments, initial fast release can stop bleeding followed by continuous release to prevent re-bleeding.

This study investigated the effects of loading TXA in κ-Car matrix and the blend of this biopolymer with two other biopolymers (locust bean gum or gelatine) in bioadhesion, release and erosion profile of the device. Locust bean gum and gelatine were chosen in this study to evaluate their effects on drug release and erosion profile of their formulations. It was predicted that addition of locust bean gum will extend the release profile of the drug, but the results indicated inconsiderable change compared to the κ-Car formulation. When gelatine was used, the release was consistent within the first 4 hours period of the study, then considerably slowed down after this time point by more than 50% compared to the κ-Car formulation.

Therefore, the formulations composed of κ-Car (single polymer) and κ-Car with locust bean gum (two polymers) are fast release and suitable for immediate treatment of epistaxis, while the formulations containing gelatine are suitable for controlled extended-release of tranexamic acid in intranasal post-operative treatments.

2.2.1.4 Chapter 5- Research chapter: Dexamethasone-eluting nasal pack: an extended-release drug delivery system

In this study, the matrices developed in chapter 4 (containing κ-Car only and combined with locust bean gum or gelatine) were used to be loaded with DEX (an anti-inflammatory drug) and the physical characteristics and release profile of the formulations were investigated. The cylindrical formulations showed various microstructures depending on their compositions. Bioadhesion was generally improved in DEX formulations, showing the mucoadhesion property of the drug. In situ drug release study demonstrated that all the formulations actively released the drug within 33 hours with less than 50% released in the first 8 hours. It indicated that the type of drug can significantly affect properties of the nasal pack, particularly its release profile. It shows that the cryogel matrices are suitable carriers for extended release of DEX.

2.2.1.5 Chapter 6- Research chapter: Gatifloxacin-eluting nasal pack: a system for local administration of antibiotic

In prolong post-operative treatments by nasal packs systemic or local administration of antibiotics is prescribed to reduce the chance of infection, especially toxic shock syndrome. Current local antibiotic delivery systems are not very effective and high drug dosage is typically required. Also, mucucilliary clearance of nasal cavity promotes clearance of the antibiotic drugs resulted in deficient drug absorption and poor effectivity. To overcome this issue, this study focused on modification of the nasal pack matrices developed in Chapter 3 with the aim of extending release period of the drug. Gatifloxacin (GFX) was used as a model drug and agar was combined to κ-Car in various concentration to enhance stability of the nasal pack and prolong the release period. The results of this study showed active release of GFX for 48 hours and significant extension in erosion time.

Chapter 3 Development of κ-carrageenan cryogel for nasal packing and intranasal drug delivery

3.1 Introduction

Carrageenan is a high molecular mass sulphated linear polysaccharide extracted from edible red algae (Rhodophyta). Carrageenan exists in nominally three forms, with repeating units of 1,3-linked β-D-galacose and 1,4-linked 3,6-anhydro α-D-galactose units variously substituted with sulphate on hydroxy groups. Differences are based on source and extraction conditions and can be classed in three main types that differ in their degree of sulphation. κ-Car has one sulphate group per disaccharide, iota-carrageenan (ι-Car) two, and lambda-carrageenan (λ) three. κ-Car is also characterised by a 3,6-anhydro ring structure (Figure 9) (Paşcalău et al., 2012). Like all carrageenans, κ-Car is strongly hydrophilic due to the presence of hydroxyl and ester sulphate groups in its chemical structure. In common with ι-car, κ-car forms gels with several mono or divalent cations. κ-Car gels are the firmer.

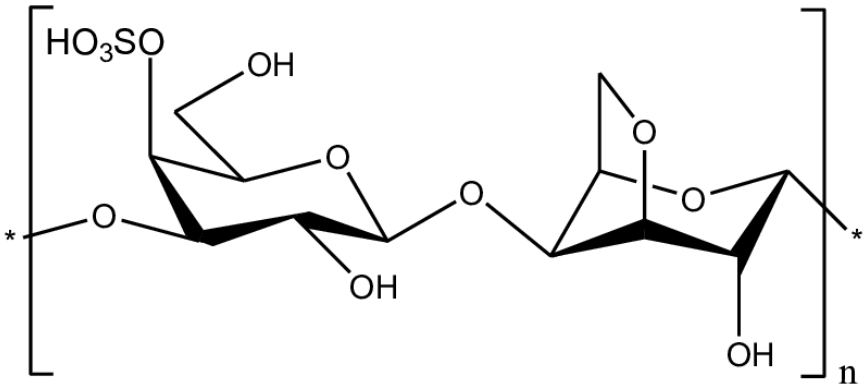

Figure 9. Chemical structure of k-carrageenan. This linear polysaccharide polymer consists of alternating 3-linked-β-D-galactose and 4-linked-α-D-galactose units.

κ-Car fully disperses in water above about 70°C. When fully dispersed it adopts a random coil conformation that transforms to rigid double helices on cooling. Gel formation is due to physical crosslinking through helix formation, association of helices and formation of junction zones (Funami et al., 2007). The resulting hydrogel is transparent, brittle and stable at pH 7 and above, but will undergo hydrolysis in an acid environment (BeMiller, 2019).

The strength of κ-Car gel is prominently influenced by its concentration and type of cations present in the reacting environment. Two studies have systematically investigated the effect of Na^+, K^+, Ca^{2+} and Ba^{2+}, and found that an adequate concentration of each cation independently improves gel strength by enhancing

conformational ordering and subsequent aggregation of helical structure (Lai, Wong, & Lii, 2000; Thrimawithana, Young, Dunstan, & Alany, 2010).

As a family of hydrocolloids, κ-Car is biocompatible, biodegradable, non-toxic and generally recognized as safe (GRAS) by the United States Food and Drug Administration under the United States Code of Federal Regulations (21 CFR 182.7255) and is approved as a food additive (21 CFR 172.620) (Weiner, 1991). Systemic administration of high dosage of this natural polymer may cause a variety of health effects particularly on the immune system, but there is no report on pertinent effect of its oral and topical administration (Cohen & Ito, 2002).

Due to its gelling ability, κ-Car is widely used in food and pharmaceutical industries. In the food industry κ-Car is generally used as a gelling, emulsifying, stabilising and thickening agent. A number of studies have utilised this polysaccharide for enhancement of texture in dairy products (Shchipunov & Chesnokov, 2003), puddings (Verbeken, Thas, & Dewettinck, 2004), salad dressings and sauces (Saha & Bhattacharya, 2010). It is also utilised in the production of low-fat sausages (Garcia, Yamashita, Youssef, Prudencio, & Shimokomaki, 2013) and patties.

In pharmaceutical studies, κ-Car has been used in the development of wound dressings (Boateng et al., 2013). κ-Car backbone composition of sulphated polysaccharides resembles glycosaminoglycans, which are natural components of connective tissues (Y. Zhang et al., 2015). Also, the ability to absorb body fluid and but retain moisture at the wound site compatibility with human cells, high mechanical strength and viscoelastic properties of its hydrogel makes it a great candidate for this application (Zia et al., 2017).

A number of trials have used κ-Car in combination with other biopolymers or cross-linking agents in form of hydrogel films for wound dressing (Bajpai et al., 2016; Boateng et al., 2013; Lokhande et al., 2018), tissue regeneration composites (Cielecka et al., 2018; Mihaila et al., 2013; Rode et al., 2018), and as a nasal insert cryogel for migraine treatment (Alavi & Mortazavi, 2018). These trials have confirmed the suitability of κ-Car for these purposes due to its biocompatibility, non-toxicity, hydrophilicity, porosity and suitable erosion profile at body temperature.

In the applications above, the polymers were in the form of conventionally dried hydrogels. In a departure from this approach Ganesan and Ratke (2014) reported on the development of a monopolymeric and monolithic κ-Car aerogel by drying with supercritical CO_2. The cylindrical aerogel obtained with 1 to 3% (w/v) κ-Car exhibited low envelope density, high porosity (with meso- and macro-porous structure), a high specific surface area and low volume shrinkage. The authors suggested that this porous material would be capable of hosting chemicals for many applications. Recently, Rege et al. (2018) investigated this aerogel in terms of texture and mechanical characteristics and developed a constitutive predictive model of its mechanical behaviour; however no indications of further uses of this aerogel in pharmaceutical applications have been found to date. More attention has focused on formulation of κ-Car and combination of it with other polymers in the form of films and beads (Y. Zhang & Zhang, 2012), and injectable hydrogels (Rasool, Ata, Islam, & Khan, 2019). Applications of κ-Car as a monopolymeric and monolithic cryogel have yet to be exploited.

Referring to Literature Review of this thesis (Chapter 2), nasal packs are used to treat severe epistaxis by applying physical force on the bleeding site and thus facilitating haemostasis. The desired characteristics of nasal packs in stopping epistaxis include a highly porous structure, hydrophilicity, and high fluid absorbency and related expansion, and harmless degradation at the end of clinical treatment. Based on these criteria and the results of Ganesan and Ratke (2014) κ-Car may be a suitable biopolymer candidate for development of a novel nasal pack capable of intranasal drug delivery. The aims of this study were:

i. to explore the feasibility of fabricating cryogel by freeze dying technique.
ii. to evaluate the effect of κ-Car concentration on the physicochemical properties of κ-Car cryogels.
iii. to characterise the cryogels in terms of morphology, porosity, swelling, mechanical strength and degradation attributes.
iv. to evaluate bioadhesive capability of the cryogels intended for intranasal drug delivery device.

3.2 Materials and Methods

3.2.1 Materials

Food-grade κ-Car (Gelcarin® GP 911) was kindly donated by Hawkins Watt Ltd. (Auckland, New Zealand). As received the κ-car was an off-white powder with potassium and calcium as cations comprising 3.8% and 2.5% by weight, respectively. Ultrapure water was used for preparation of hydrogels. The reagents were analytical grade from a variety of suppliers. Drugs were not included in this phase of research.

3.2.2 Methods

3.2.2.1 Hydrogel preparation

Dispersions of 1.5, 2 and 2.5% (w/v) κ-Car in ultrapure water were prepared by heating to 85˚C on the hot plate under constant stirring at 300 rpm until a transparent colloidal suspension was obtained. Hydrosols were then immediately (temperature at 85˚C) poured into vertical polyethylene syringe barrels (30 mm long x 14 mm diameter) where the Luer lock end had been machined off. The retracted piston plugged the barrel. The assemblies were kept at room temperature for 1 hour then stored overnight at 4˚C.

3.2.2.2 Cryogel preparation

To obtain the cryogels, the following drying conditions were investigated and applied:

a) Rapid freezing by immersion in liquid nitrogen (-195˚C) with subsequent freeze drying.
b) Slow freezing at -4˚C (using conventional freezer) with subsequent freeze drying.
c) Faster freezing at -80˚C (using an ultracold freezer) with subsequent freeze drying.

In all cases freeze drying was with an AdVantage Pro bench top freeze dryer (SP Scientific, USA).

3.2.3 Characterisation

The hydrogels and cryogels were characterised for their physicochemical and mechanical characteristics using the following methods:

3.2.3.1 pH

The pH of the 1.5, 2 and 2.5% of nascent κ-Car hydrogels was measured using a calibrated pH-meter (pH Bench-top Meter. PL-700PC, Interlab, NZ) at 40˚C prior to formation of the firm gel.

3.2.3.2 Dimensions and mass of hydrogels and cryogels

The diameters, lengths, and masses of the hydrogel and cryogel formulations (n=3) were measured with a calliper and electronic balance.

3.2.3.3 Microstructure analysis by scanning electron microscopy

Surface and cryo-fractured cross-sectional images of the κ-Car cryogels were obtained using a Schottky field emission scanning electron microscope (SU-70, Hitachi, UK) under an accelerating voltage of 3 kV for the surface and 15 kV for internal cross-sectional area. Prior to examination, samples were placed on metallic stubs and coated for imaging with platinum under vacuum for 60 seconds using an ion sputter coater (E-1045, Hitachi, UK). The schematic diagram in

Figure 10 shows the cross-sectional, longitudinal and surface view of the cryogels cylinders used in this research to clarify the view directions.

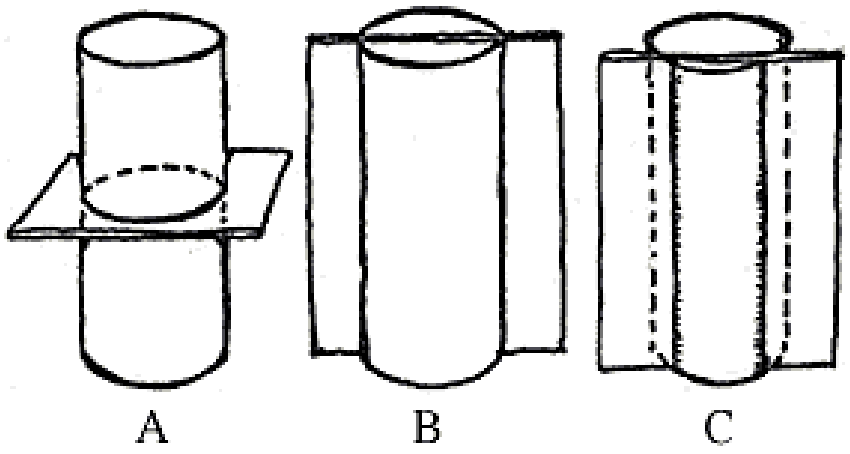

Figure 10. Schematic diagrams of cross-sectional or transverse (A), longitudinal or mid-sagittal (B) and surface view of the cryogels.

3.2.3.4 Mechanical properties of cryogels

Texture profile analysis to derived hardness, springiness and cohesiveness was evaluated using a TA-XT plus texture analyser (Stable Micro System, England) as reported by (D. S. Jones, Woolfson, & Brown, 1997; Thrimawithana et al., 2010).

Cryogels were prepared and stored in sealed plastic bags to prevent moisture absorption, maintained at ambient temperature (ca. 22˚C) in a desiccator prior analysis. Each cryogel sample was horizontally located on the stage of the texture analyser and an analytical probe (50 mm diameter) was compressed twice to a depth of 8 mm at speed test of 0.5 mm s^{-1}, allowing a relaxation period of 5 s between compression cycles (n= 4). The data were analysed with TA-XT Exponent software to derive hardness, springiness and cohesiveness.

3.2.3.5 Porosity measurement

The porosity of κ-Car cryogels were determined by a solvent replacement method (Nanda, Sood, Reddy, & Markandeywar, 2013). Cryogel samples (n=3) were weighed and immersed in cyclohexane at room temperature overnight to ensure the porous structures are filled to equilibrium with the solvent. The samples were blotted with tissue paper to remove the excess cyclohexane and immediately weighed. The porosity was calculated using the following equation:

$$\text{Porosity (\%)} = (W_{after} - W_{before} / \rho V) \times 100$$

where W_{after} is the weight of cryogel after soaking in cyclohexane, W_{before} is the weight of cryogel before soaking, ρ is the density of cyclohexane and V is the volume of the cryogel.

3.2.3.6 Swelling ratio determined by cryogel wet weight

The swelling ratio of κ-Car cryogels in phosphate buffered saline (PBS) (pH 7.4) was determined at 35 ± 2˚C in water bath using a gravimetric method (Khurma, Rohindra, & Nand, 2006). Cylindrical cryogels (n=3 in each formulation) were weighed and placed in stainless steel mesh containers to prevent floating and submerged in the PBS shaken at 100 rpm on a benchtop shaker (SK-300, Lab Companion, Korea). The cryogels were removed and restored at intervals, blotted and weighed to determine equilibrium weight. The swelling ratio at equilibrium was calculated:

$$\text{Swelling ratio} = [(W_{equil} - W_{dry}) / W_{dry})]$$

where W_{equil} is wet weight of the cryogel at equilibrium and W_{dry} is weight of the original dry cryogel. Equilibrium point is when the cryogel is saturated with the PBS and has reached constant weight.

3.2.3.7 Swelling ratio determined by diameter expansion

The diameter of formulations submerged in PBS for the swelling study were similarly measured by calliper up to and at constant diameter (Bajpai et al., 2016):

$$\text{Expansion ratio} = D_{equil} / D_{dry}$$

where D_{equil} is diameter of the wet cryogel at equilibrium and D_{dry} is diameter of the dry cryogel.

3.2.3.8 Matrix erosion determined by cryogel dried weight

Erosion of κ-Car cryogels was determined as described by Roy and Rohera (2002). Cryogels (n=3 in each treatment) were weighed and contained in the mesh containers submerged in 100 mL of PBS (pH 7.4) at 35±2˚C shaken at 100 rpm on a benchtop shaker (SK-300, Lab Companion, Korea). At set intervals, the cryogels were removed from the dissolution medium and dried to constant weight in conventional oven at 60˚C. The percentage matrix erosion at a given time was calculated:

$$\text{Percent matrix erosion} = [(W_{dry} - W_{eroded}) / W_{dry})] \times 100$$

where W_{dry} is initial weight of the cryogel and W_{eroded} is the weight of dry eroded formulation at a given time.

3.2.3.9 In vitro bioadhesion studies

The main aim of this research was development of a medicated nasal insert intended for intranasal drug delivery. Bioadhesion in drug delivery is defined as adherence of a drug carrier system to a specific biological location. In the case of attachment to a mucus coated tissue (e.g. intranasal mucus membrane) it is defined as mucoadhesion (Shaikh, Raj Singh, Garland, Woolfson, & Donnelly, 2011). Due to the importance of this factor in intranasal drug delivery, the bioadhesiveness of the formulations were assessed based on the force required to detach a mucin-moistened cryogel from a mucin-coated membrane. For this purpose, bioadhesion measurements to mucin were performed using the TA-XT analyser adapting the method employed by Şenyiğit Zeynep et al. (2014). The texture analyser was equipped with 500 N load cell and a cylindrical probe 50 mm in diameter.

κ-Car cryogel discs of 35 mm in diameter and 8 mm high were prepared for this experiment (n=4). A mucin dispersion (5% w/v, pH 6.4) from porcine stomach Type II (bound sialic acid, ≤ 1.2%, Sigma Aldrich, NZ) was used as biological adhesion medium.

A small petri dish containing solid agar was overlaid with a cellulose filter membrane on its surface mimicking the intranasal tissue surface. The petri dish was fixed to the texture analyser's stage by double-sided tape. The cellulose membrane and cryogel disc were each moistened with 1 mL of mucin dispersion and the cryogel disc was attached to the probe by double-sided tape (See Figure 11 for the set up).

The cryogel sample and mucin were held in contact for 60 seconds, and then the probe was then raised at 0.5 mm s^{-1} to separate the two mucin-coated surfaces. The maximum detachment force was recorded as a function of displacement at an ambient temperature (24˚C).

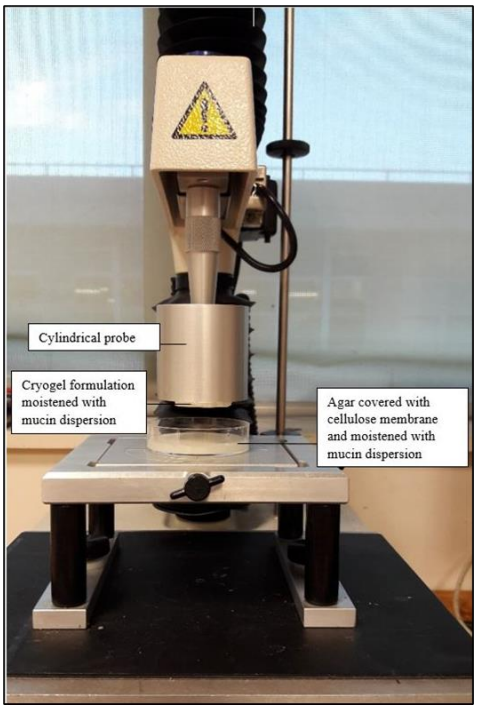

Figure 11. Set up of the texture analyser for bioadhesion test. The cryogel formulation is attached to the cylindrical probe by a double - sided tape and moistened with porcine mucin dispersion. The surface of the solid agar in the plate is also covered with a cellulose membrane and moistened with porcine mucin dispersion. The plate is attached to the stage of the texture analyser using the double-sided tape.

3.3 Statistical analysis

Data were marshalled using Excel then analysed for one-way variance using the ANOVA routine in XLSTAT (Addinsoft) with Tukey's multiple range test.

3.4 Results and discussion

3.4.1 Cryogel preparation

Freeze-drying was used to create the cryogel. It was used because of its simplicity, low labour cost, energy efficiency, and the absence of solvents required for supercritical drying.

In freeze drying the water in frozen hydrogel is sublimated (D. Zhang, Zhang, Xie, & Zhou, 2012). Several studies have reported that this technology can produce a well-maintained aligned pore structure with minimal shrinkage (Alavi & Mortazavi, 2018; Plazzotta et al., 2019).

Prior to freeze-drying hydrogels are typically frozen. Intuitively it was thought that rapid freezing in liquid nitrogen (or in isopentane liquid cooled to liquid nitrogen temperature) would give superior freezing. In the event, the frozen hydrogels cracked and disintegrated immediately after contact with liquid nitrogen. Subsequently, slow freezing at -4°C and fast freezing at -80°C were tried but resulted in expansion and deformation of the cylindrical hydrogels. Failure to get a frozen well-maintained cylindrical shape showed these methods did not work.

As a further possibility, hydrogels stored at 4 ˚C were horizontally laid on polystyrene trays and freeze dried under these conditions: shelf temperature, 2°C; temperature on freeze dryer shelf, -70°C; and vacuum pressure, 120 mbar. The resultant cylindrical cryogels maintained their shape but showed a degree of expansion and deep longitudinal fissure on the edge contacting the tray (Figure 12 a).

To get an even and smooth surface, the hydrogels were placed vertically on the polystyrene tray and freeze-dried under the same conditions (Figure 12 c). The resulting dried cylinders had shrivelled surface but barely visible superficial cracks with a hump at the centre top end (Figure 12 b). At higher κ-Car concentrations – 2.0

and 2.5% rather than 1.5% – more superficial wrinkles and surface pores were observed but with a smaller hump.

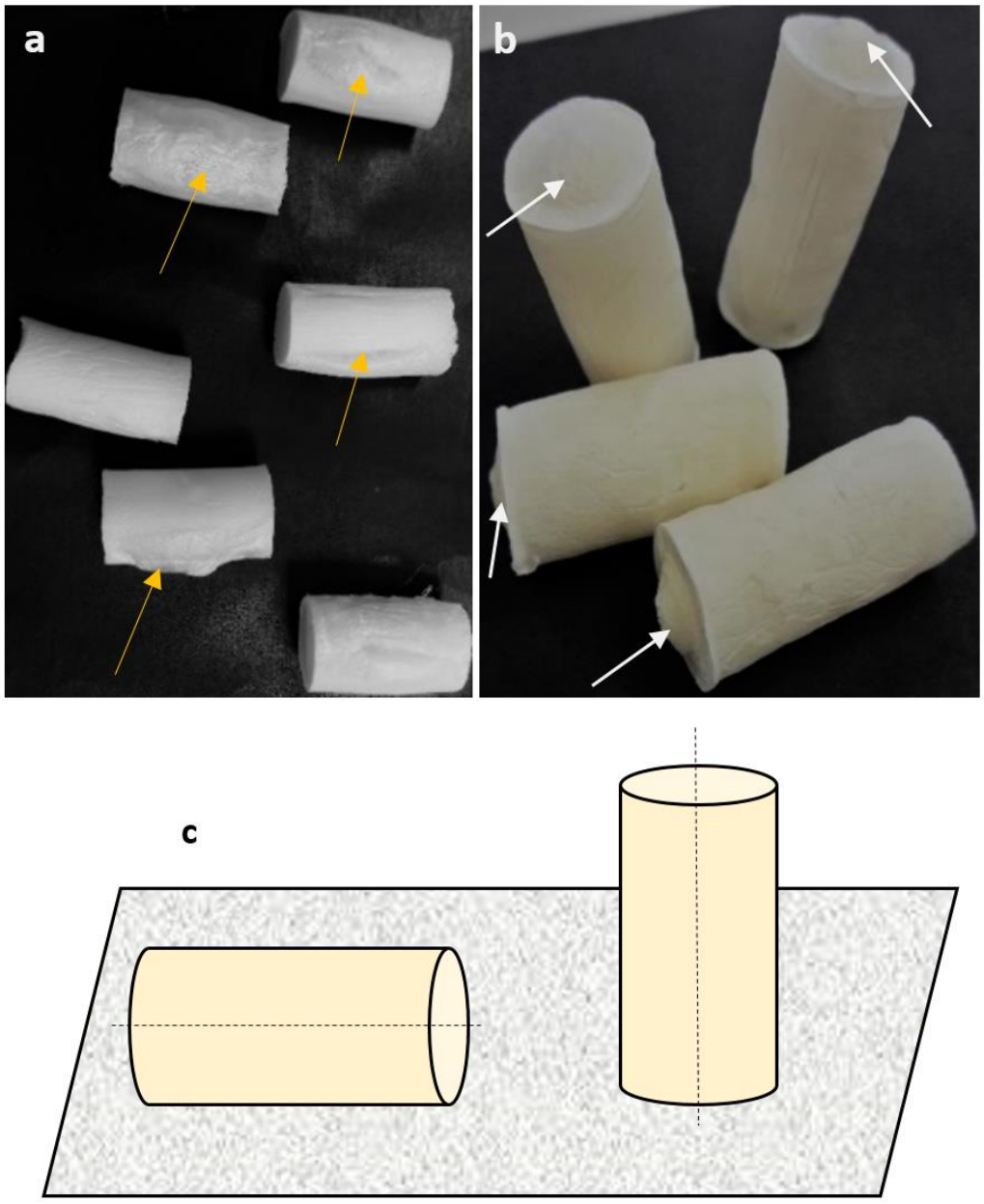

Figure 12. Photographs of κ-Car cryogels: (a) dried horizontally, (b) dried vertically. A longitudinal crack (yellow arrows) developed on the cryogels dried horizontally (a), while vertically dried samples developed a top hump (white arrows), but with no longitudinal crack (b). The difference in colour is due to the lighting used during the photography. Figure c shows vertical direction (left) and horizontal direction (right) of placing hydrgels into the tray for drying (this figure is for clarification puepose).

Working with a gelcast ceramic, Tian et al. (2015) suggested that cracks can be controlled by increasing the shelf temperature and pressure of the drying chamber. Therefore, different settings were chosen to explore outcomes, where it was found

that increasing the shelf temperature from 2 to 4°C reduced wrinkle occurrence. Considering these limited optimisation results, it is expected there is further scope to improve freeze-dried morphology but beyond the goals this thesis.

3.4.2 pH

The measured pH of the 1.5, 2 and 2.5% hydrosols were 7.71, 7.80 and 8.03 respectively at ambient temperature (22˚C), indicating that the κ-Car was slightly alkaline. The process to extract carrageenan uses NaOH, suggesting that residues remain. However, with sulphate residues common in carrageenan, the κ-Car would have no pH buffering capacity.

3.4.3 Dimensions and mass of hydrogels and cryogels κ-Car

Physical dimensions of κ-Car formulations before and after freeze-drying are tabulated in Table 1. Comparison of weight of the 1.5, 2 and 2.5% κ-Car hydrogels and their corresponding cryogels indicated significant difference in weight loss of hydrogels with lowest weight loss of 87% in the 2.5% κ-Car and 92% in the 1.5% κ-Car formulation ($p<0.001$).

Table 1. Weight, height and diameters of κ-Car hydrogels and their corresponding cryogels. Data are means ± SD (n=3), and superscripts indicate significant differences between formulations. Means with different letters are significantly different (p<0.001).

Formulation	**Hydrogel dimensions**			**Percent loss on cryogel formation**		
	Weight (g)	Height (mm)	Diameter (mm)	Weight loss (%)	Height shrinkage (%)	Diameter shrinkage (%)
1.5% κ-Car	5.20 ± 0.02	30.17 ± 0.29	14 ± 0.0	92 ± 0.56 [a]	10 ± 0.76 [a]	13.0 ± 1.8 [a]
2.0% κ-Car	5.12 ± 0.01	30.07 ± 0.03	14 ± 0.0	90 ± 0.08 [b]	13 ± 0.24 [ab]	13.0 ± 0.7 [ab]
2.5% κ-Car	5.26 ± 0.05	30.07 ± 0.08	14 ± 0.0	87 ± 0.12 [c]	15 ± 0.71 [b]	20.0 ± 0.8 [b]

The major weight loss of virtually 90% in cryogel indicates evaporation of the solvent from the hydrogel during the freeze drying process. Among the cryogel formulations, the height and diameter of 1.5% κ-Car and 2.5% κ-Car cryogels were also significantly reduced ($p<0.0001$ and $p<0.001$, respectively) following an increase in concentration

of κ-Car, showing the highest reduction in the 2.5% κ-Car formulation. The 2% κ-Car experienced a degree of height and diameter shrinkage, although it was not significantly different form 1.5% κ-Car and 2.0% κ-Car cryogels.

3.4.4 Microstructure analysis by scanning electron microscopy

Scanning electron microscopy (SEM) was used to explore the effect of κ-Car concentration on the morphology of prepared cryogels at external and cryo-fractured cross-sectinal surfaces (Figure 13). At this magnification κ-Car the cryogel surface exhibited a smooth non-porous (in 1.5% κ-Car) or wrinkled surface with scattered pores (in 2.0 and 2.5% κ-Car), while the interior resembled a macroscopic honeycomb tubular structure. Similarly, Thrimawithana et al. (2010) and Dunstan et al. (2001) reported the tubular honeycomb structure of a 0.4% (w/v) and 1% κ-Car cryogels, respectively. An increase in concentration of κ-Car resulted in an increase in density of smaller pores of various shapes and sizes and replacement of the tubular structures by the spongy porous structure in 2.5% κ-Car (Figure 13).

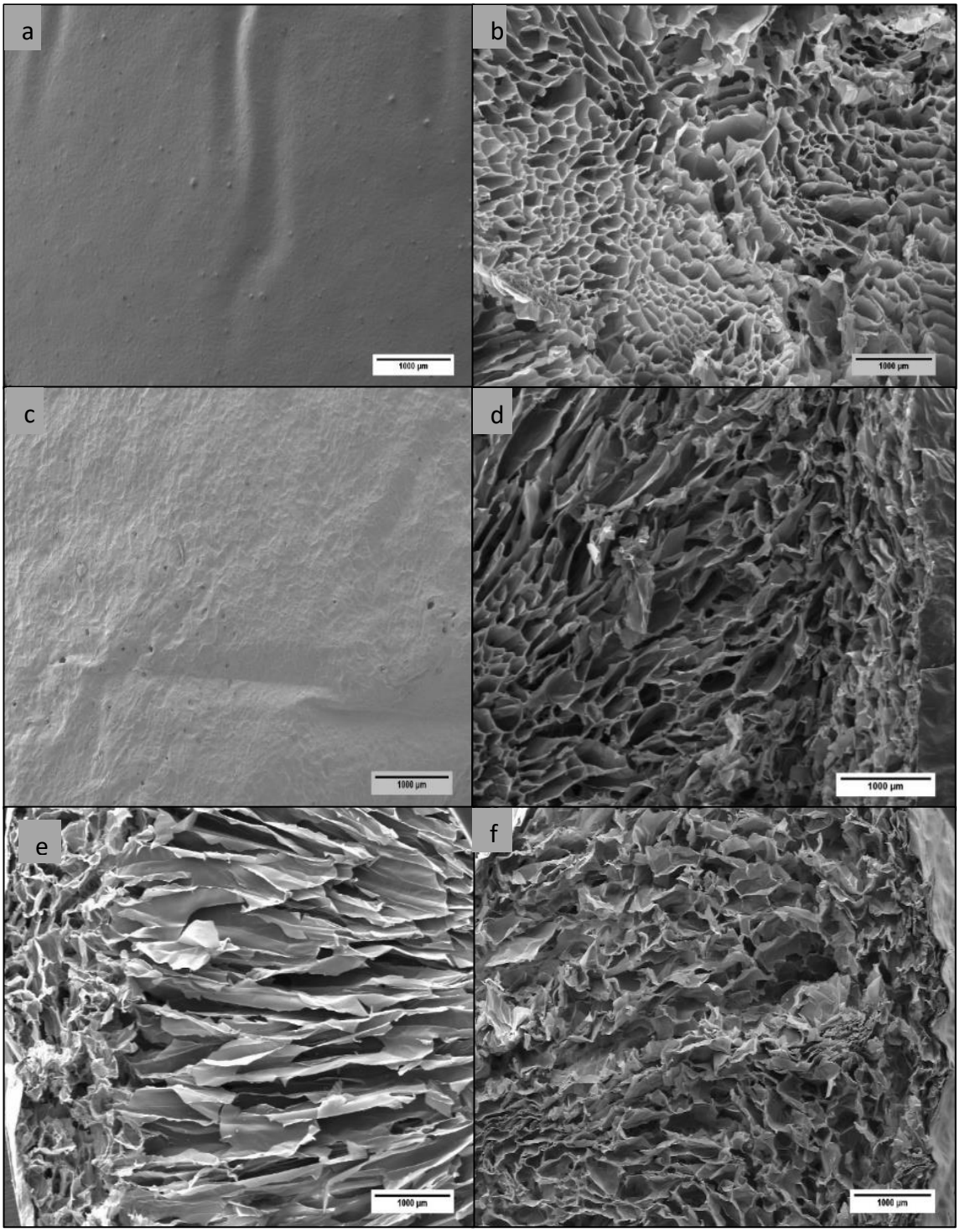

Figure 13. SEM images of an external surface (a) and transverse cryo-fractured surface of a 1.5% k-Car cryogel (b). Equivalent surfaces of a 2.0% k-car cryogel (c and d). Longitudinal cryo-fractured surface of a 1.5% k-Car cryogel (e) and cross sectional cryo-fractured surface of 2.5% k-Car cryogel (f).

3.4.5 Mechanical characteristics

Texture profile analysis (TPA) is a rapid and popular analytical technique with extensive applications in the food industry and elsewhere. The mechanical properties of the κ-Car formulations in terms of hardness, springiness and cohesiveness were derived from the force versus time plots adapted from Jones et al. (1997) (Table 2). 'Hardness' is defined as the peak force required to deform the cryogel; 'springiness', is the ability of a material to recover its original shape after compression, and 'cohesiveness' means the ability of a material to hold together as a unit. An increase in κ-Car concentration from 1.5 to 2.5% significantly altered the mechanical properties. However, the mechanical properties of these two formulations were not significantly different from the 2.0% κ-Car formulation.

Table 2. Mechanical characteristics of cryogel formulations. Different superscripts letters within columns show significant Tukey differences ($p<0.05$).

Formulation	Hardness (N)	Springiness (%)	Cohesiveness
1.5% κ-Car	11.4 ± 1.1 ^{a}	86.8 ± 2.8 ^{a}	0.50 ± 0.04 ^{a}
2.0% κ-Car	17.6 ± 1.0 ^{ab}	74.1 ± 5.3 ^{ab}	0.44 ± 0.03 ^{ab}
2.5% κ-Car	27.4 ± 2.1 ^{b}	53.1 ± 3.9 ^{b}	0.34 ± 0.01 ^{b}

The results revealed the highest deformation force of 27.4 N for the 2.5% κ-Car formulation, while 1.5% κ-Car required a much lower 11.44 N to deform. In contrast, 1.5% κ-Car demonstrated the highest springiness of 86.8% and cohesiveness of 0.50 among the samples. Thus, hardness was inversely related to springiness and cohesiveness.

Overall, these results indicated that increase in concentration of κ-Car polymer led to higher stiffness of the cryogels. The results agreed with the constitutive predictive model for κ-Car established by Rege et al. (2018), which revealed that increase in concentration of κ-Car reduced density and pore size distribution due to denser network of micropores, but increased stability of the network against mechanical force applied to the cryogel. The SEM images indicated that at lower concentration of κ-Car, the pores containing air are larger and accommodate a higher air volume. Presence of a large volume of air and the failure of the air pockets to withstand the

compressive load during testing results in lower strength and springiness of the cryogels (Sachithanadam & Joshi, 2014).

3.4.6 Porosity measurement

Porosity, the volume of pores in the dry matrix, is shown in Figure 14. The high porosity of the freeze-dried samples is due to retention of the overall volume after which is well-preserved during subsequent water sublimation (Racheva et al., 2013).

The porosity of cryogel samples showed a decreasing trend with the increasing concentration of κ-Car – a result consistent with SEM images in Figure 3.3 d, e and f – from 65% with 1.5% κ-Car to 58% with 2% κ-Car and finally to 45% in 2.5% κ-Car samples ($p<0.05$). A similar trend in porosity was reported by Rege et al. (2018) in κ-Car aerogels of 1 to 3% prepared with potassium thiocyanate as cross-linker. They found that an increase in fibril diameter and density of the microcell network of the aerogel caused reduced porosity.

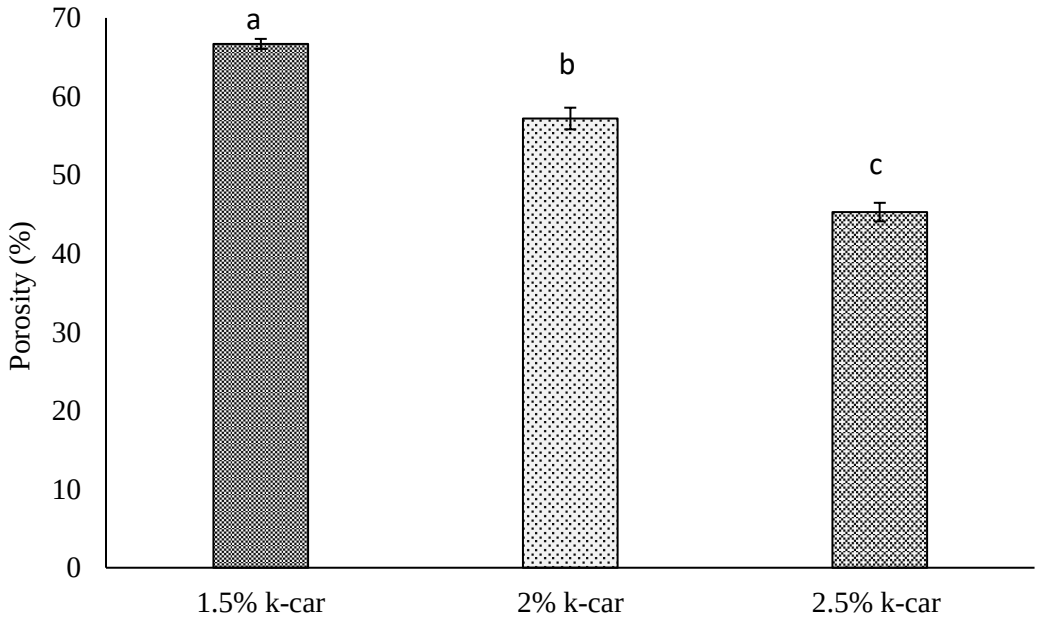

Figure 14. Porosity in κ-Car cryogel formulations. Data are means (n=3) ± SD.

Whereas the inverse relationship between pore size (Figure 13) and porosity (

Figure 14) was to be expected, the porosity values – none of which exceeded 67% – were far lower than might be expected from the percent loss of weight due to water on freeze drying (Table 1). Thus, the percent weight loss on drying values were

respectively 98.5, 98.1 and 97.7% for 1.5, 2.0 and 2.5% κ-Car. This suggests that the cyclohexane could not intimately penetrate very small micro pores of the cryogel due to hydrophobicity of the cyclohexane compared with hydrophilicity of the Carrageenan and water.

3.4.7 Swelling ratio determined by cryogel wet weight

Time dependent swelling in PBS (pH 7.4) of κ-Car cryogel formulations as a function of κ-Car concentration are shown in Figure 15. All cryogels were highly absorbent being able to uptake PBS various times their dry weight by swelling and reaching an equilibrium state in about 6 hours. Absorption of PBS by cryogel is due to the hydrophilicity of κ-Car cryogel to interact with water molecules forming hydrogen bonds.

Higher concentrations of κ-Car decreased the swelling response in the formulations. The maximum equilibrium swelling ratio of 93.1% was obtained at around 8 hours with lowest concentration of κ-Car (1.5%). This lowest concentration also swelled the fastest. After this time point, the 1.5% κ-Car samples started to disintegrate; therefore, swelling kinetics after this time may not be accurately known. Formulations of 2.0 and 2.5% κ-Car exhibited a relatively low equilibrium swelling ratio to a maximum 45% at around 8 hours and slower swelling rate compared with the 1.5% κ-Car formulation. It can be seen from Figure 13 that increase in concentration of κ-Car modulated the morphology and pore size of cryogels and strongly affected the swelling properties of matrices.

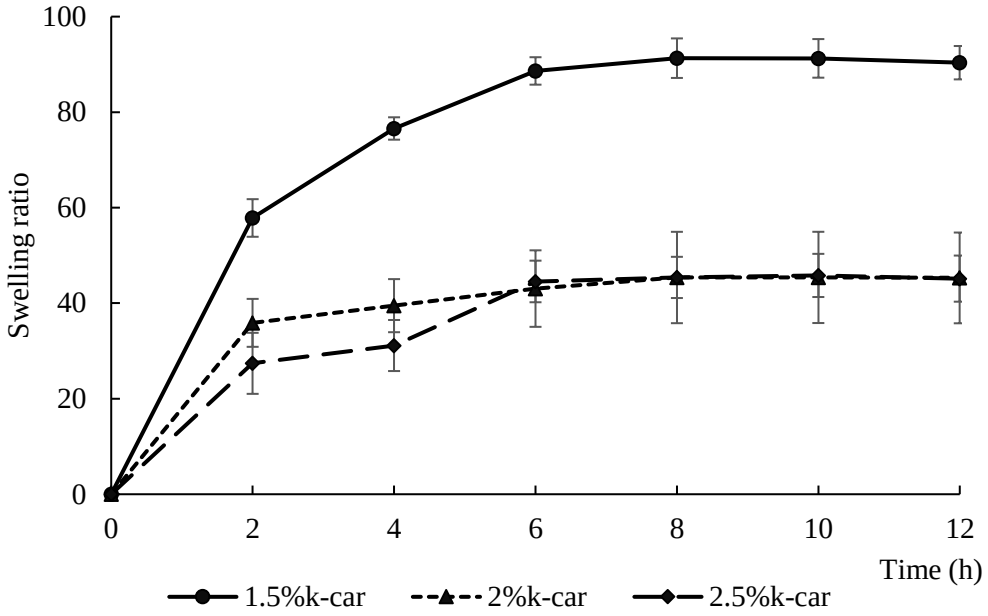

Figure 15. Swelling kinetics of κ-Car cryogels at 35 ± 2˚C in PBS buffer with increasing concentration of κ-Car. Values are means ± SD (n=3).

The high swelling ratio of 1.5% κ-Car was probably due to its larger void structure and high pore volume, as discussed earlier. The results is consistent with a study by Lefnaoui and Moulai-Mostefa (2011) where an increase in concentration of κ-Car from 0.55 to 0.70 % reduced the swelling ratio.

3.4.8 Swelling ratio determined by diameter expansion

Time dependent diameter expansion of κ-Car cryogels during swelling was also measured (Figure 16). The swelling 1.5% κ-Car cryogels reached their maximum diameter of 21% after about 6 hours, and after about 7 hours for the other two formulations, both 17%. Erosion in PBS after 6 hours, was visible in all formulations, but more so in 1.5% cryogels than the other two formulations. In terms of diameter expansion, the 1.5% κ-Car showed significantly faster and greater expansion compared with the two other formulations ($p<0.05$). The results obtained from swelling, pore volume and analysis of SEM images suggested that the higher diameter expansion in 1.5% κ-Car is due to presence of loose large void structure allowing fluid absorption, flexibility and expansion of the thin walls.

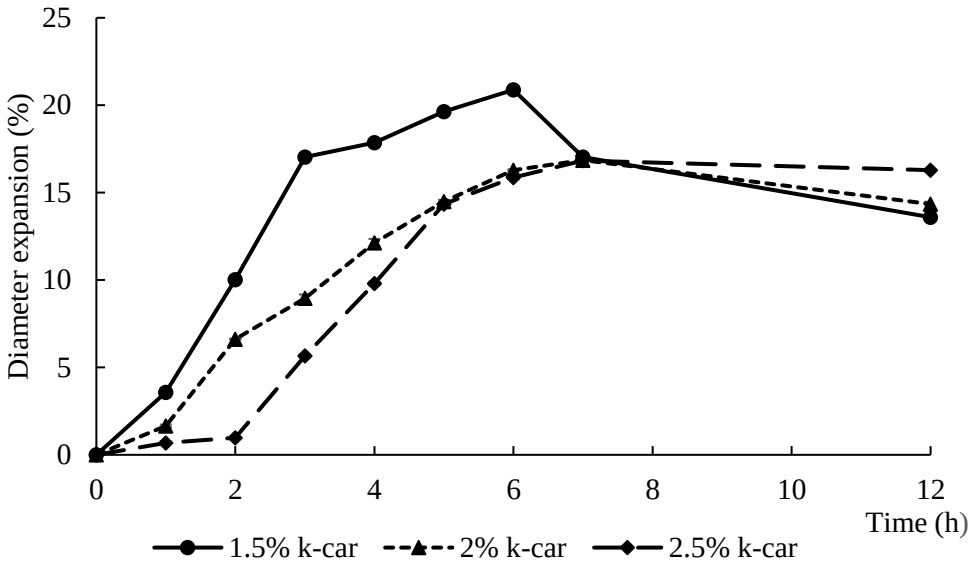

Figure 16. Diameter expansion ratio of κ-Car cryogels at 35 ± 2˚ C in PBS buffer with increasing concentration of κ-Car

3.4.9 Matrix erosion determined by cryogel dry weight

The polymer erosion was also confirmed by loss of mass into PBS at 35°C. In Figure 17, the concentration of κ-Car affected the rate of hydrogel erosion showing the highest rate of erosion in 1.5% κ-Car formulation. However, all formulations retained their physical structure inside the first 4 hours of exposure to PBS. Cryogels with 1.5% κ-Car started losing κ-Car between 4 and 6 hours, however, the structure was appeared intact in that period. The gel was 100% degraded by 12 hours. Based on the results of Lefnaoui and Moulai-Mostefa (2011) and Sánchez-Sánchez et al. (2015), the rapid rate of erosion for 1.5% κ-Car can be attributed to a rapid rate of PBS diffusion into the loose network, causing an over-expansion and collapse of the network. The other two formulations showed a maximum of 25% degradation at 12 hours, continuing steadily to 32 hours and probably beyond. Using various concentrations of κ-Car combined with starch, Lefnaoui and Moulai-Mostefa (2011), confirmed that an increase in amount of κ-Car concentration improved network stability and erosion resistance due to the denser porous structure. Despite of different erosion rates between the formulations, they all showed bulk erosion because the diffusion process – penetration of water through the material – occurred before significant erosion on the surface of the cylindrical gels (Figure 17).

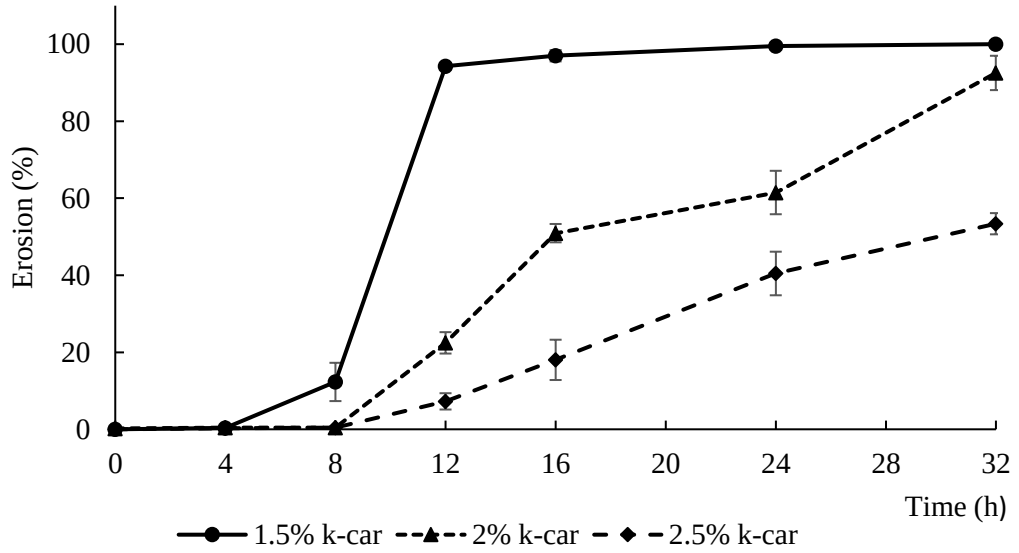

Figure 17. Erosion profile of κ-Car cryogels in PBS medium (pH 7.4) at 35 ± 2˚C. Values are means ± SD (n=3).

3.4.10 In vitro bioadhesion studies

The in vitro bioadhesive behaviour of κ-Car cryogels is shown in Figure 18. All formulations demonstrated a degree of adhesion to the mucin covered membrane. An increase in κ-Car concentration from 1.5 to 2.5% numerically increased the maximum detachment force of cryogel formulations, but the difference was not significant (p>0.05).

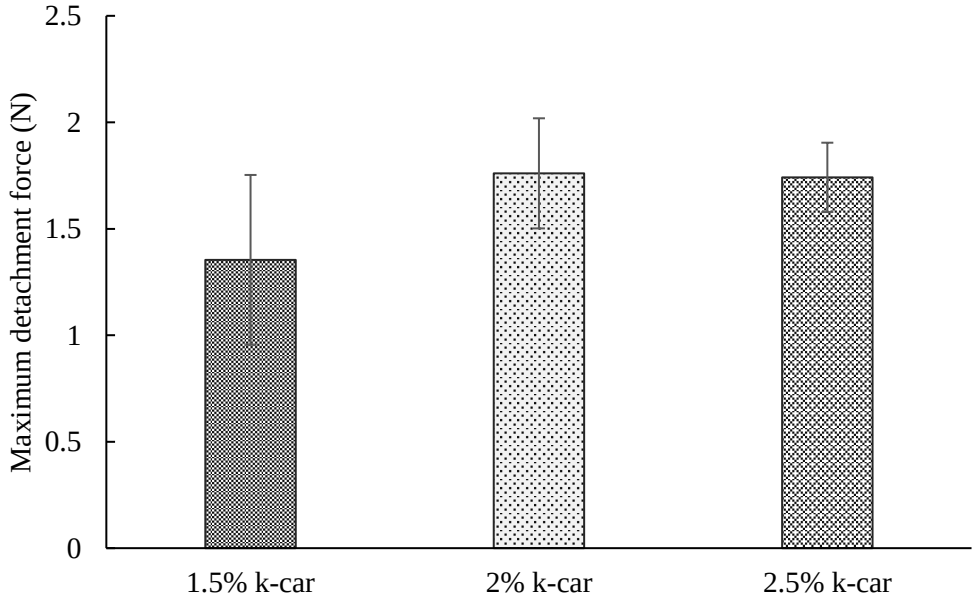

Figure 18. Bioadhesion behaviour of κ-Car cryogels shown as maximum detachment force. Data are means ± SD (n=4).

Vigani et al. (2019) reported maximum detachment force of 1.6 N for 0.4 and 0.6% κ-Car hydrogel formulations with no significant difference ($p>0.05$), which is close to the figure of 1.4 N obtained for 1.5% κ-Car in this study. In addition, Lefnaoui and Moulai-Mostefa (2011) found that maximum adhesion of κ-Car hydrogel occurs with the concentration of 0.5%, and beyond this concentration adhesion values may fall. The latter authors believed that higher concentration of κ-Car produced a rigid gel, which was less adhesive. The bioadhesion property of κ-Car to mucin may be attributed to hydrophilicity of κ-Car to absorb mucin, interpenetration of the polymer into the biological substrate (mucin) followed by formation of secondary non-covalent bonding, mainly hydrogen bonds, between the κ-Car and mucin (Lefnaoui & Moulai-Mostefa, 2011). Formation of these hydrogen bonds is due to presence of negatively charged sulphate ($-OSO_3^-$) in κ-Car which maintains overall negative charge and is responsible for mucoadhesive properties (Riley et al., 2001).

3.5 Conclusion

A κ-Car cryogel system has been synthesised with different concentrations of κ-Car without addition of a cross-linker. An increase in the concentration of κ-Car in the formulation showed reduced porosity, swelling behaviour and diameter expansion. Conversely, a higher concentration of κ-Car enhanced the stability of the cryogel against mechanical compression force and rate of degradation in PBS. The ability of κ-Car cryogel to behave differently at various concentrations suggested that this polymer could be a suitable drug carrier in development of fast and controlled-release drug delivery systems. The 1.5% κ-Car formulation may be a suitable candidate for fast release eroding drug delivery system due to its high swelling and fast erosion rate, while the two other formulations may be more suitable for extended release systems with lower erosion rate.

In principle, the present work confirms the potential and feasibility of the κ-Car cryogel as a nasal pack matrix and intranasal drug release system due to its high fluid absorption capacity, swelling behaviour, mechanical properties and eventual degradability. In the following chapters, the ability of this matrix to carry and deliver drugs by means of in vitro studies has been investigated.

Chapter 4 Tranexamic acid-eluting nasal pack: a local delivery system in treatment of epistaxis

4.1 Introduction

Epistaxis is defined as bleeding from nasal mucosa that covers nasal cavity and is considered as a common condition occurring in 60% of the general population (Gambhir, 2001). It appears to be a bimodal age distribution, mostly occurring in children under age of 10 and adults above the age of 45 (Alter, 2011). In addition, epistaxis can occur following the intranasal surgeries such as endoscopic sinus surgery, chronic rhinosinusitis, septal deviation (septoplasty) and inferior turbinate hypertrophy (Yan et al., 2014). It is reported that annually in the United States, approximately 450,000 emergency department visits are for epistaxis (Logan & Pantle, 2016) and more than 400,000 endoscopic sinus surgery are performed (Antisdel et al., 2011), which may require epistaxis treatment.

About 90% of the epistaxis cases are anterior arising from Kiesselbach's plexus area through bleeding from anterior and posterior ethmoid arteries. It can be commonly controlled by first-line treatment such as applying brief direct pressure on the nostrils, administration of topical vasoconstrictors, or by cautery. In contrast, posterior epistaxis occurs at the back of the nasal cavity bleeding from the sphenopalatine artery. Such bleeding is usually difficult to localise due to bleeding from both nostrils and is mostly resistant to standard interventions. In cases where primary interventions fail for both anterior and posterior bleeding, more invasive treatments such as nasal packing, administration of blood products to reverse coagulopathies or arterial ligation and embolization are applied (Logan & Pantle, 2016).

Nasal packing was first introduced in the ortorhinolarynogological literature in 1951 (Valentine, Wormald, & Sindwani, 2009). Removable nasal packs have been designed and used to stop bleeding by their tamponade effect and acting as barrier for tissue adhesion, e.g. (Vaseline-covered gauze, and proprietary products like Merocel, Ivalon and RapidRhino nasastant). However, clinical studies have shown that removable nasal packs variously cause considerable discomfort and complications for patients in terms of pain, failure in control of bleeding (Fairbanks, 1986), septal perforation (Kucik & Clenney, 2005), pack dislocation (Fairbanks, 1986), toxic shock syndrome (Bertrand et al., 2005; Weber, 2009), aspiration and obstructive sleep apnoea(Weber, 2009).

In more recent past decades, the limitations of removable nasal packs have led to development and application of numerous erodible nasal packs. The use of erodible biomaterials in nasal packs began in 1969 (Valentine et al., 2009). These nasal packs resorb, fragment, or biologically degrade during the treatment period and reduce the complications of subsequent pack removal while providing support for the middle turbinate, facilitating haemostasis, and promoting wound healing. Some of these erodible nasal packs provide clotting factors (e.g., Floseal) or a substrate to stimulate blood clotting (e.g., RapidRhino Stammberger Sinu-Foam).

Despite advantages of current non-erodible and erodible nasal packs, they may not be sufficient for treatment of severe or persistent epistaxis, especially in patients with hereditary haemorrhage or hypertension. In these cases, thrombin containing products such as Surgiflo (Ethicon, USA) and Floseal (Baxter, USA) (Buiret, Pavic, Pignat, & Pasquet, 2013; Murray et al., 2018) have been applied, demonstrating comfort and effectiveness compared with traditional packing. Alternatively, topical application of antifibrinolytic and therefore haemostatic drugs such as tranexamic acid (TXA) have been tried (Athanasiadis, Beule, & Wormald, 2007; Logan & Pantle, 2016; Zahed, Moharamzadeh, AlizadehArasi, Ghasemi, & Saeedi, 2013; Zahed, Mousavi Jazayeri, Naderi, Naderpour, & Saeedi, 2017).

Tranexamic acid (trans-4-aminomethyl-cyclohexanecarboxylic acid) (TXA) is an FDA and WHO approved synthetic amino acid which is a cheap, readily available, and useful medicine in emergency departments. This efficacious antifibrinolytic drug is widely used to treat various bleeding disorders (Coetzee, 2007; Jahadi Hosseini, Khalili, & Motallebi, 2014; Kaewpradub, Apipan, & Rummasak, 2011; J. Liang et al., 2016; Zahed et al., 2013; Zahed et al., 2017).

TXA facilitates clot formation by reversibly binding to plasminogen, inhibiting its interaction with fibrin and preventing dissolution of fibrin clots (Logan & Pantle, 2016). The drug is pharmaceutically available in forms of oral rinse (4.8%), intravenous solution (IV) for injection (100 mg mL^{-1}), and oral tablet (650 mg) for patients with hereditary angioneurotic oedema and menorrhagia, plus for reduction of postoperative blood loss.

Local administration of TXA through nasal route for treatment of epistaxis has been reported in several studies. Tibbelin et al. (1995) conducted a clinical study to compare the efficacy of 10% TXA gel (1500 mg TXA) and a placebo gel for treatment of mild to severe epistaxis and recurrent bleeding. The results showed that the time of bleeding cessation in patients receiving the TXA gel into their nasal cavity did not significantly differ from the patients treated with placebo gel. The gel formulation was not described in that study. In contrast, the following three clinical studies indicated effectiveness of TXA in nasal packing. Jahanshahi et al. (2014) investigated the effects of topical administration of TXA in bleeding and quality of surgical field during functional endoscopic sinus surgery using cotton pledgets soaked in a TXA solution and found that the drug reduced bleeding and improved quality of surgical field. Topical effectiveness of injectable form of TXA was compared with anterior nasal packing in patients with idiopathic anterior epistaxis in two studies (Zahed et al., 2013; Zahed et al., 2017) and the outcomes indicated success of TXA in terms of blood arrest, recurrence of bleeding and overall patient's satisfaction.

Similarly, a recent study by Whitworth, Johnson, Wisniewski, and Schrader (2020) demonstrated that local administration of aerosolised TXA solution in the bleeding nostril followed by direct pressure on the nostril was more effective than local application of oxymetazoline[2] in terms of achieving haemostasis and reducing the chance of re-bleeding.

The effectiveness of TXA or other haemostatic drug in nasal applications depends on its bioavailability that is affected by the mucociliary clearance mechanism that limits drug absorption within the nasal cavity, and absorption through mucosal membrane of nasal cavity, especially when bleeding. In that cotton pledget study described above, the pledget increased drug absorption by making it available for a longer time and played the role of a sustained drug releaser, but in an uncontrolled manner. Another recent study indicated that chitosan gel spray loaded with TXA was most effective than TXA solution spray in nasal wound healing (Gholizadeh et al., 2019). Therefore, a drug carrier capable of binding to the nasal mucosal membrane and controlling the release of TXA can improve efficacy of the treatment. In addition, an ideal carrier must absorb fluids resulted from injury and bleeding, have a degree of

[2] Oxymetazoline shrinks blood vessels in the nasal passages.

expansion to fill the nasal cavity and facilitate haemostasis, and erode (self-destruct) late in the treatment period to eliminate the need for removal and thus associated complications.

From Chapter 3 of this thesis, κ-carrageenan (κ-Car) was identified as a suitable candidate for this application. This polymer developed in form of cryogel demonstrated fluid absorbing ability of more than 100 times of its weight, and expansion of about 20%, a degree of bioadhesion, and erosion in less than 48 hours at 35°C. These characteristics makes this polymer a promising excipient of TXA for nasal drug delivery.

The requisites of this novel nasal pack are fast release of TXA to promptly arrest bleeding and subsequent sustained release of TXA for the therapeutic period to minimise re-bleeding. In addition, the pack must be able to absorb the blood and start eroding after exercising the desired therapeutic effect. As for its physical properties, it must withstand the exerted pressure of insertion into the nasal cavity and to be rigid enough to be squeezed into nostrils. A degree of mucoadhesion is also required to enhance topical TXA absorption process. To optimise these characteristics locust bean gum and fish skin gelatine were also added independently to κ-Car to investigate their effects on some physicochemical characteristics of the basic κ-Car cryogel nasal pack formulations.

The present study was designed to:

1. Explore the feasibility of a κ-Car cryogel as TXA carrier intended for nasal insertion.
2. Characterise the formulation in terms of morphology, swelling and porosity, mechanical properties, bioadhesion, drug release and degradation.
3. Evaluate the effect of addition of locust bean gum (LBG) or cold-water fish skin gelatine as second biopolymers to κ-Car on the physicochemical, drug release and degradation profiles of the formulations to optimise the formulation for the intended use.

4.2 Materials

Food-grade carrageenan powder (κ-Car) (Gelcarin® GP 911) containing 3.8% potassium and 2.5% calcium cations was donated by Hawkins Watt Ltd., Auckland, New Zealand as was locust bean gum powder (LBG). Gelatine powder from cold water fish skin (Gel) and tranexamic acid (trans-4-(aminomethyl)cyclohexanecarboxylic acid) (TXA) were from Sigma Aldrich (Auckland, New Zealand). Mucin from porcine stomach (type III, bound sialic acid 0.5-1.5%) was purchased from Sigma Aldrich (Auckland, New Zealand). Ultrapure water was used for preparation of hydrogels. All reagents were analytical grade.

4.3 Methods

4.3.1 Preparation of TXA-loaded cryogels

Five formulations were prepared for this study as shown in Table 3. The κ-Car formulation was made by adding 1.5 g κ-Car to 90 mL of water and heating at 85˚C under constant magnetic stirring at 300 rpm until a transparent hydrosol was obtained. TXA solution was prepared by dissolving 100 mg of the drug powder in 10 mL of stirring water. The drug solution was added to the transparent κ-Car hydrosol to obtain a concentration of 1% w/v. The mixture was stirred at the same temperature for 10 minutes to ensure even distribution of the drug. The four other formulations (LBG1, LBG2, Gel1 and Gel2) were comprised of two biopolymers. Their preparation process paralleled that of TXA κ-Car, except that κ-Car was dispersed in 70 mL of water while LBG or Gel were dispersed in 25 mL of water, and TXA was dissolved in 5 mL of water in all cases maintaining a final volume of 100 mL. LBG and Gel were separately dispersed in stirred water at 95˚C before addition to the κ-Car hydrosol followed by stirring at 85˚C and 300 rpm. Finally, the TXA solution was added, and the mixtures stirred for a further 10 minutes.

The drug-loaded hydrosols were cast in cylindrical polyethylene syringe barrels (30 mm long x 14 mm diameter) where the Luer lock end had been machined off and the piston retracted into the barrel. The assemblies were kept vertical at room temperature for 1 hour then stored overnight at 4°C. The hydrogels were then extruded from the barrels, placed vertically on polystyrene trays, and freeze dried under the following conditions: shelf temperature, 2°C; temperature on freeze dryer

shelf, -70°C; and pressure, 120 mbar (AdVantage Pro freeze dryer, SP Scientific, USA). The prepared nasal packs were stored in sealed plastic bags in a desiccator, maintained at ambient temperature (24˚C) to prevent moisture absorption.

Table 3. *Composition of TXA loaded formulations*

Formulation	κ-Car (g)	LBG (g)	Gel (g)	TXA (mg)
TXA κ-Car	1.5	0.0	0	100
TXA LBG1	1.5	0.1	0	100
TXA LBG2	1.5	0.2	0	100
TXA Gel1	1.5	0.0	1	100
TXA Gel2	1.5	0.0	2	100

4.3.2 Characterisation

The TXA loaded formulations were characterised for their physicochemical, mechanical and drug release characteristics using the following methods.

4.3.2.1 Microstructure analysis by scanning electron microscopy

Surface and cryo-fractured cross-sectional (transverse section) images of the cryogel formulations were acquired using a Schottky field emission scanning electron microscope (SU-70, Hitachi, UK) under an accelerating voltage of 5 kV. Prior to examination, samples were mounted on metallic stubs and coated for imaging with platinum with 25 mA under vacuum for 40 seconds using an ion sputter coater (E-1045, Hitachi, UK) at room temperature.

4.3.2.2 Mechanical properties of cryogels

Texture profile analysis to derived hardness, springiness and cohesiveness was evaluated using a TA.XT Plus texture analyser (Stable Micro System, UK) as reported by D. S. Jones et al. (1997) and Thrimawithana et al. (2010). Each cryogel sample was horizontally located on the heavy-duty platform and an analytical probe (50 mm diameter) was compressed twice to a depth of 8 mm at speed test of 0.5 mm s^{-1}, allowing a relaxation period of 5 s between the two compression cycles. The data were analysed with TA.XT Exponent software to derive hardness, springiness and cohesiveness values.

4.3.2.3 Porosity measurement

The porosity of the cryogel formulations were determined by a solvent replacement method (Nanda et al., 2013) as more fully described in Chapter 3. It is a measure of the proportion of the cryogel that is airspace. In outline, cryogels were immersed in cyclohexane at room temperature overnight to achieve an equilibrium solvent absorption. The weight of cyclohexane absorbed, the density of cyclohexane (ρ) and the volume of the original hydrogel (V) were used to calculate percent porosity.

4.3.2.4 Swelling study determined by cryogel wet weight

The swelling study of the cryogel formulations in phosphate buffered saline (pH 7.4) was determined at 35 ± 2°C using a gravimetric method (Khurma et al., 2006) as fully described in section 3.2.3 of Chapter 3. It is a unitless measure of the saline that can be absorbed by a cryogel. It is the equilibrium weight of absorbed saline expressed as a fraction of the dry cryogel weight.

4.3.2.5 pH

The pH of the TXA-loaded hydrosol formulations was measured by meter (pH Benchtop Meter, PL-700PC, Interlab, NZ) at 40°C a temperature at which the mixtures were sols.

4.3.2.6 In vitro bioadhesion studies

Bioadhesion measurements to mucin were performed using the TA.XT analyser adapting the method employed by Boateng et al. (2013) and Şenyiğit Zeynep et al. (2014). The method is fully described in Chapter 3. In outline the texture analyser is used in tension mode to measure the adhesion of dry cryogel discs to a fixed filter paper base where both surfaces were moistened with mucin dispersion (5% w/v, pH 6.4) from porcine stomach (Sigma Aldrich, NZ). After the moist surfaces were in contact for 60 seconds, the probe carrying the cryogel disc was raised at 0.5 mm s^{-1} to separate the two mucin-coated surfaces. The maximum detachment force was recorded as a function of displacement at an ambient 24˚C ± 2˚C.

4.3.2.7 Fourier transform infrared (FTIR) spectroscopy

To characterise the presence of specific chemical groups in the TXA-loaded cryogel formulations, FTIR spectra were obtained using a Nicolet iS10 FTIR

spectrophotometer (Thermos Scientific, USA) in attenuated total reflectance (ATR) mode using a diamond reflectance crystal. A thin slice of each formulation was placed on the ATR crystal and maximum pressure was applied by using the pressure clamp accessory of the instrument to get intimate contact of sample and crystal. Similarly, the pure ingredients (TXA powder, and κ-Car, gelatine and LBG powders) and drug free cryogel formulations were examined as controls. The spectra of the samples were recorded in the range of 400-4000 cm^{-1} with an average of 32 scans at a resolution of 4 cm^{-1} using the proprietary OMNIC® software. The absorbance of each sample was obtained by background subtraction of the ATR crystal spectrum.

4.3.2.8 Total TXA content and in vitro drug release studies

The content of TXA successfully loaded in cryogel formulations was determined before performing the drug dissolution studies. It was measured by soaking the cryogel formulations in PBS (pH 7.4) at 35˚C with stirring and left overnight to completely disperse. The drug dissolutions were centrifuged at 2,250 rcf for 15 minutes at 4 ˚C (Eppendorf 5804R Benchtop Refrigerated Centrifuge) and filtered through a 0.2 µm syringe filter (Whatman uniflow syringe filter, Sigma Aldrich) to remove any gel particles present and obtain the transparent solution.

The determination of TXA was initially explored with five ultraviolet colorimetric methods exemplified by Ansari, Raza, and Rehman (2005) and Rind et al. (2009). After many attempts to get a reproducible method, these were all rejected in favour of a Liquid chromatography-mass spectrometry (LC-MS) that had to be fully developed, as described in the third paragraph of this section.

In vitro TXA release from the cryogel formulations was studied in PBS buffer (pH 7.4) under sink conditions. A pH of 7.4 was chosen to represent the pH of blood and nasal mucosal discharge in rhinitis (England, Homer, Knight, & Ell, 1999). A degenerated cellulose dialysis membrane (SnakeSkin™ Dialysis Tubing, 3.5K MWCO, 16 mm) was used to confine the formulation and minimise passage of the polymer particles into the dissolution medium during the release period.

The samples were placed into a dialysis membrane with 5 mL PBS buffer added to the membrane tube, tightly secured at both ends. The sealed tube was placed in a 50 mL screwed centrifuge tube containing 45 mL of PBS and incubated at 35°C while shaking

at 1.67 Hz on a benchtop shaker. At intervals, 1 mL of the release medium from each sample was recovered and an equal amount of fresh PBS was added to each release system to maintain the original volume and sink condition.

The concentration of TXA in the release medium was determined by LC-MS after derivatisation with accutag (6-aminoquinolyl-N-hydroxysuccinimidyl carbamate) (adapted from Salazar, Armenta, and Shulaev (2012)) using an Agilent 1260 Infinity Quaternary LC-MS System (Agilent, USA). A Waters XSelect CSH C18 column (2.1 x 100 mm, 3 µm) was used for this analysis. The mobile phases were water with 0.1 % (v/v) formic acid, and acetonitrile with 0.1% (v/v) formic acid. Authentic TXA was used as the external standard and drug free cryogel formulations were used as controls. This method is described in TXA determination by LC–MS in the Results and discussion section.

4.3.2.9 TXA determination by LC-MS

TXA determination by LC–MS analyses were conducted using an Agilent 1260 Infinity Quaternary LC System (Santa Clara, CA 95051 USA). The system consisted of the following components: 1260 quaternary pump (model number: G1311B), 1260 infinity ALS sampler (model number: G1329B), 1260 infinity TCC column component (model number: G1316A), 1260 infinity diode array detector (DAD) (model number: G4212B), connected to a 6420 triple quadrupole LC/MS system with multimode ionisation source (model number: G1978B).

The MS ionisation source conditions were as follows: capillary voltage of 2 kV, drying gas temperature of 325 °C, drying gas flow of 6 L/min, vaporiser temperature of 200 °C and nebuliser pressure of 60 psi. The positive electrospray ionisation (ESI) mode was performed with multiple reaction monitoring (MRM) for quantitative analysis. The precursor-to-product ion transition used for derivatised tranexamic acid was [M+H] + m/z 328.2 -> 171.1 with fragmentor voltage of 100 v and collision energy of 20 eV. Derivatised d4-alanine [M+H] + m/z 264.1 -> 171.1 with fragmentor voltage of 100 V and collision energy of 20 eV was used as internal standard.

Waters XSelect CSH C18 (2.1 x 100mm, 3µm) was used for this analysis. The mobile phases were composed of water containing 0.1%(v/v) formic acid (A) and acetonitrile containing 0.1% (v/v) formic acid (B)with flow rate of 0.4 mL min^{-1}. The initial gradient

condition was 97:3 (A:B). From 0 to 3.5 min the B was increased to 30%, from 3.5 to 4.5 min the B was increased to 80% and from 4.5 to 6 min B was decreased to 3%. The total run time was 10 min. The injection volume was 1 µL and the retention time of derivatised tranexamic acid was 5.15 min (Figure 19).

A series of calibration standard solutions of 1 to 100 µg.mL^{-1} TXA were injected (1µL) and a calibration curve was obtained based on the peak areas and concentrations of the standard solutions (Figure 20).

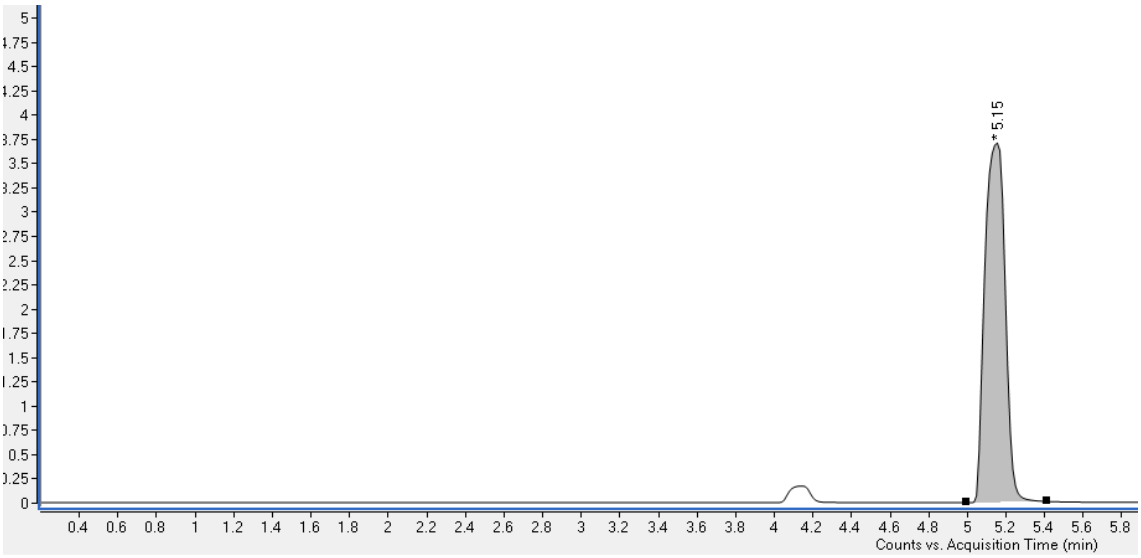

Figure 19. Representative chromatogram for TXA (retention time: 5.15 min)

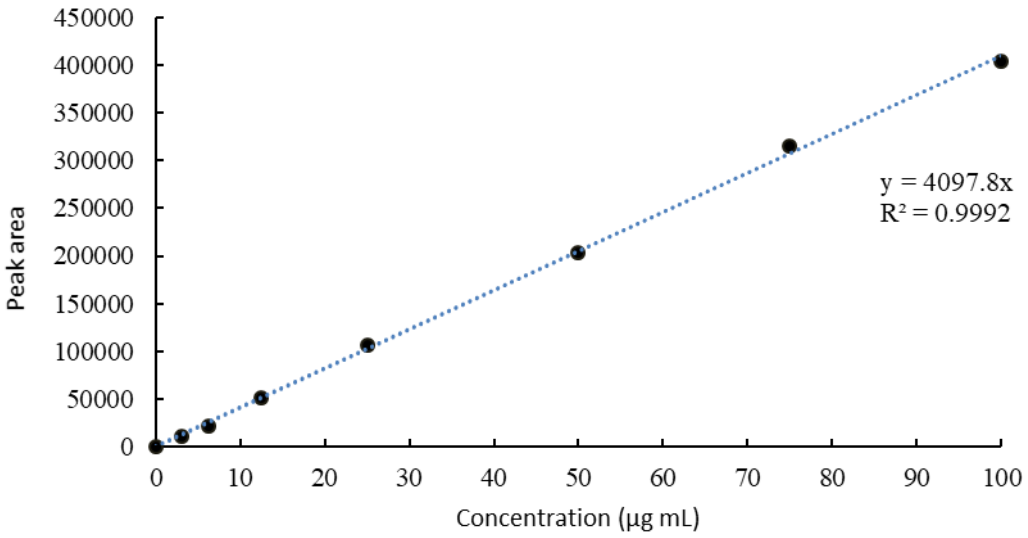

Figure 20. Calibration curve of derivatised TXA (Plot of peak areas versus concentrations)

4.3.2.10 Matrix erosion determined by cryogel dried weight

Erosion of TXA-loaded cryogels was determined as described by Roy and Rohera (2002), and detailed in Chapter 3. In summary cryogels were weighed dry, submerged

and shaken in PBS at 1.67 Hz and 35°C. At intervals, the cryogels were removed from the dissolution medium and dried to constant weight. The percent matrix erosion was calculated:

$$\text{Percent matrix erosion} = [(W_{dry} - W_{eroded})/ W_{dry})] *100$$

where W_{dry} was initial weight of the cryogel and W_{eroded} was the weight of dried eroded formulation at a given time.

4.4 Statistical analysis

Data were subjected to one-way analysis of variant (ANOVA) and Tukey's comparison test using XLSTAT software.

4.5 Results and discussion

4.5.1 Preparation of TXA-loaded cryogels

All TXA-loaded hydrogel formulations were completely dry after freeze drying process. All were pale white. TXA LBG1 and TXA LBG2 experienced diameter shrinkage, while TXA κ-Car and TXA Gel1 showed diameter expansion at mid height, but the expansion did not cause a fracture on the external surface. The longitudinal cracks observed on the surface of the basic cryogels in Chapter 3 was no longer evident in any TXA-loaded cryogel. The cryogel formulations exhibited porous and variably rough external textures, all rougher than the drug free cryogels reported in Chapter 3. The roughest formulation was TXA LBG2, but the surface of TXA Gel1 and TXA Gel2 formulations were comparatively smooth and less porous than the other three formulations.

4.5.2 Macro and microstructure by inspection and scanning electron microscopy

The macrostructure of the TXA-loaded cryogel formulations were observed with unaided eyes and photographed. Inspection revealed smoother external surface in TXA κ-Car and TXA Gel formulations compared with TXA LBG formulations (Figure 21 a). Observation of internal macrostructure of the formulations (transverse and mid-sagittal sections) showed very similar structure in all the formulations. The transverse section (Figure 21 b) showed radial structure initiated from the central

point of the cylinder. A central axis was observed inFigure 21 c indicating the dense area at the centre of the cylinder. On this macro scale, no noticeable difference was found between the formulations.

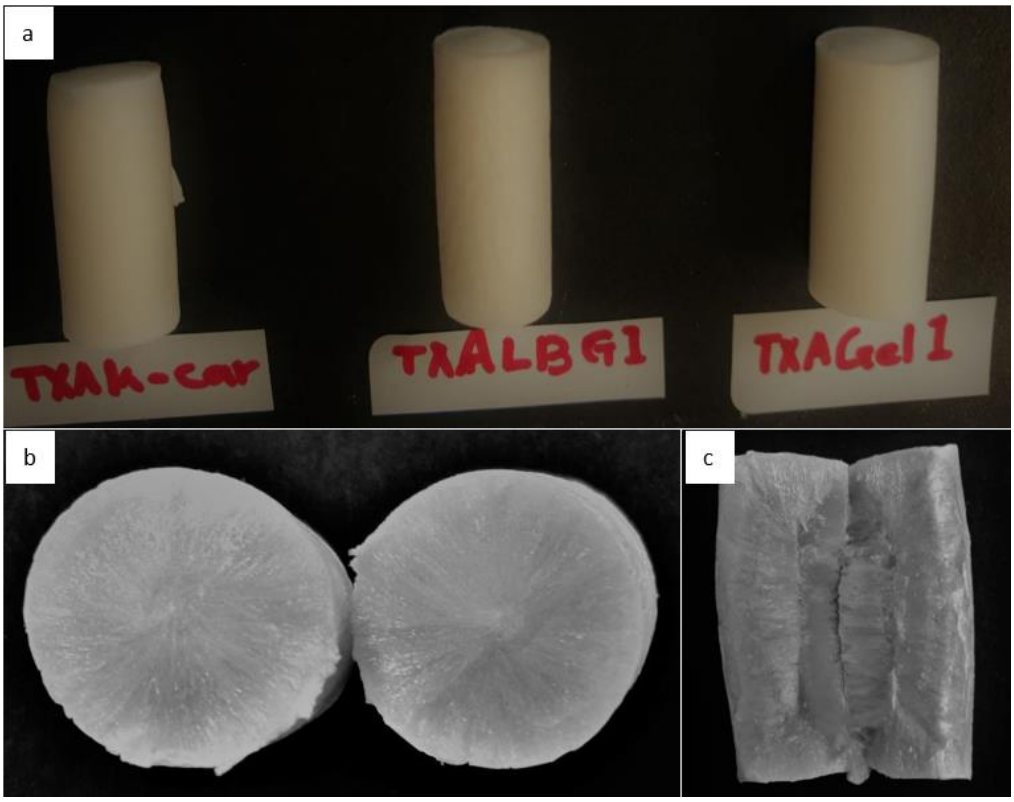

Figure 21. Macrographs of TXA κ-Car, TXA LBG1 and TXA Gel1 formulations (a), transverse section of TXA LBG2 (b) and mid-sagittal section of TXA LBG2 (c). The same macro internal structure was observed in all the five formulations.

The microstructure of cross sectional cryo-fractured surface of the TXA-loaded formulations are shown in Figure 22. A broad pore size distribution was observed in these images in a predominantly macropore range, wider than 50 nm). The pore size increased in with inclusion of LBG (Figure 22 b and c) but was unaffected by addition of Gel (Figure 22 d). However, the presence of 1 and 2% Gel in the formulations resulted in development of hair-like fibres inside the tubular pores, visible only at higher magnifications (not shown). Fibre formation was reported by Dunstan et al. (2001) in formulation of hydrogels using 1% κ-Car and 1% LBG with the ratio of 8:2, however, they were not observed in current microscopic images of TXA LBG1 and TXA LBG2, which may be due to low proportion of LBG to κ-Car.

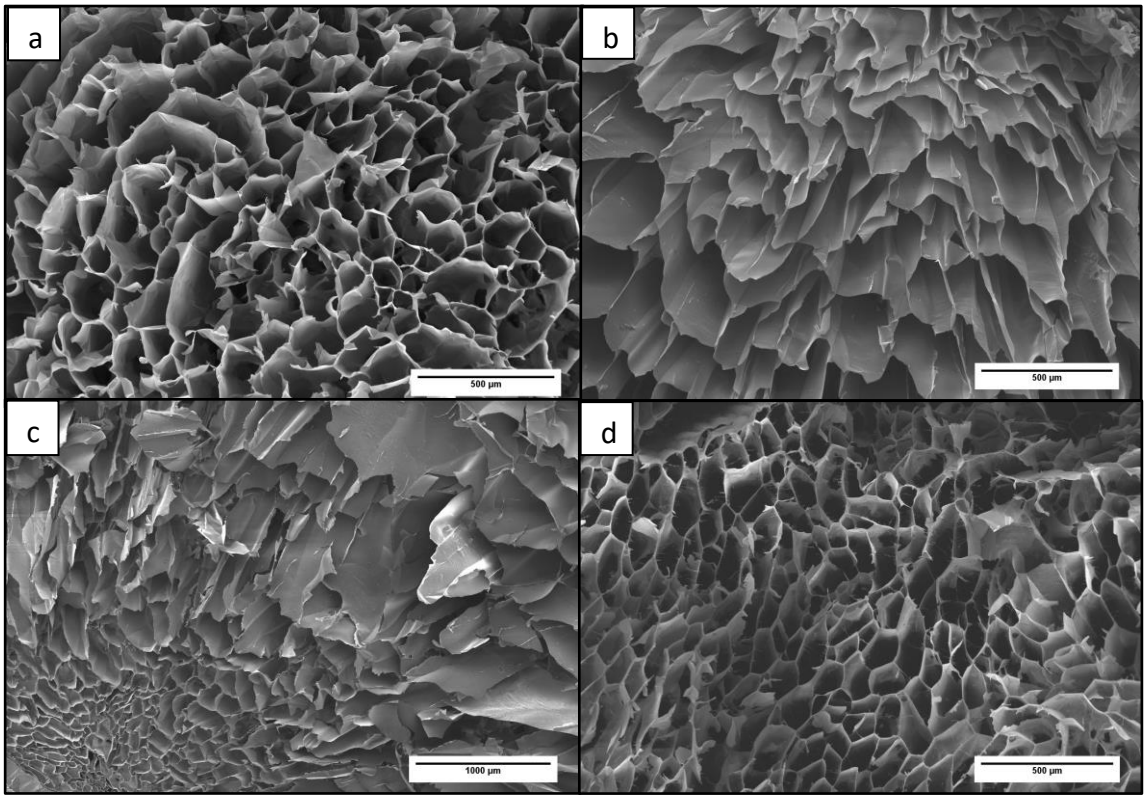

Figure 22. SEM images of cross sectional cryo-fractured surfaces of a TXA k-Car formulation (a), a TXA LBG1 formulation (b), a TXA LBG2 formulation (c) and a TXA Gel1 formulation (d). Note the scale difference in image (c).

The image morphologies indicated that κ-Car is the dominant structural component and that incorporation of LBG, Gel and TXA did not qualitatively affect the cryogel internal structure compared with simple 1.5% κ-Car cryogels reported in Chapter 3 (Figure 13). The surfaces of internal tubular structures were smooth and there was no sign of drug crystal formation on them. It appears that the drug was well-distributed within the delivery matrix with drug particle sizes below the resolution limits of these micrographs at these magnifications (X. Zhang & Cresswell, 2016).

4.5.3 Mechanical characteristics

The mechanical properties of nasal packs play a significant role in establishment of their fitness for the purpose. The mechanical properties, hardness, cohesiveness, and springiness of the formulated cryogels, are shown in Table 4. These features are important for the topical drug delivery purpose in the nasal cavity because a suitable formulation should offer a reasonable resistant microgel network against mechanical pressures during insertion to the nostrils and its residence period in the nasal cavity where fluid absorption, expansion, and drug release takes place.

Table 4. Mechanical characteristics of TXA-loaded cryogel formulations. Different superscript letters within columns show significant Tukey differences (p<0.0001).

Formulation	Hardness (N)	Cohesiveness	Springiness (%)
TXA κ-Car	30.5 ± 1.8 [a]	0.43 ± 0.01 [a]	80.4 ± 1.5 [a]
TXA LBG1	24.7 ± 0.6 [b]	0.37 ± 0.00 [b]	55.7 ± 0.8 [b]
TXA LBG2	29.1 ± 0.5 [c]	0.27 ± 0.01 [c]	51.5 ± 2.4 [bc]
TXA Gel1	41.8 ± 2.3 [d]	0.28 ± 0.02 [cd]	50.0 ± 1.3 [c]
TXA Gel2	30.8 ± 1.8 [a]	0.25 ± 0.01 [d]	43.2 ± 2.2 [d]

Addition of a second polymer caused complex effects on hardness. TXA Gel1 required the highest force of 41.8 N to deform while TXA κ-Car and TXA Gel2 were deformed by 30 N. In the TLBG formulations, doubling the concentration of LBG significantly augmented hardness, but a doubling of Gel markedly reduced the hardness of TXA Gel formulations ($p<0.0001$).

Cohesiveness, the ability of the cryogel to hold together as a unit, was measured because to its importance in topical nasal drug delivery system. The formulation should be able to maintain its structural network in the nasal cavity while absorbing blood and wound fluid and releasing the drug during its therapeutic phase. Fast disintegration of the nasal pack could potentially release a drug too rapidly. In addition, the disintegrated particles may dislocate to the nasopharynx or be expelled through nostrils. TXA κ-Car had the highest cohesiveness (Table 4). Inclusion of LBG or Gel in two different concentrations significantly reduced cohesion of the formulations ($p<0.001$). Springiness was also reduced by inclusion of LBG or Gel, and in contrast to the complex relationships with hardness; there was a direct positive correlation between cohesiveness and springiness for the five formulations (graph not shown). It appears that addition of LBG to the TXA κ-Car network increased the void size and central density (denser part at the centre) of the LBG formulations seen in related scanning micrograph images (Figure 22 b and c). The presence of TXA may interrupt electrostatic or hydrogen bonds that are believed to form between the two polymers lowering the cohesion of the cryogel formulations.

Incorporation of Gel to TXA κ-Car reduced the cohesion and springiness at both 1 and 2% concentrations but increased hardness at 1% inclusion. There are changes in morphology at 1% Gel at least, notably defect voids and thinner walls with large size variation (see incomplete cell walls in Figure 22 d). However, there is nothing obvious in the micrograph that can point to increased hardness and lower cohesion and springiness. According to (Panyukov, 2019), an incomplete void wall structures can be due to formation of gelatine 'loops', caused when the gelatine folded and bind to themselves instead of binding to κ-Car chains. The presence of these loops weakens the structure and reduces hardness, cohesiveness, and springiness of the formulation. These loops can be reduced by slower addition of gelatine solution to the κ-Car hydrogel (Trafton, 2012).

4.5.4 Porosity measurement

The percent porosity of the TXA-loaded formulations was measured by cyclohexane uptake (Figure 23). The pores in the cryogels were created by evaporation of the liquid phase (water) from the gel during freeze-drying resulting in a tubular morphology with high potential for absorbing fluids. TXA κ-Car and TXA LBG1 showed highest porosity, more than 75%, nominally higher than the porosity of 1.5% κ-Car cryogel (67%) reported in Chapter 3 (Figure 14). A doubling of the LBG concentration significantly lowered the porosity of the formulation ($p<0.0001$); its porosity was insignificantly higher than that of TXA Gel1. TXA Gel2 had the lowest porosity. Clearly, porosity was reduced by incorporation of a second polymer in all the formulations. These results for TXA κ-Car and TXA LBG1 are consistent with the micrographs in Figure 23, however, inconsistent for TXA Gel1 and TXA Gel2. Morphology alone was not a good guide to porosity. The results of swelling test in the following section explain the reduction in porosity.

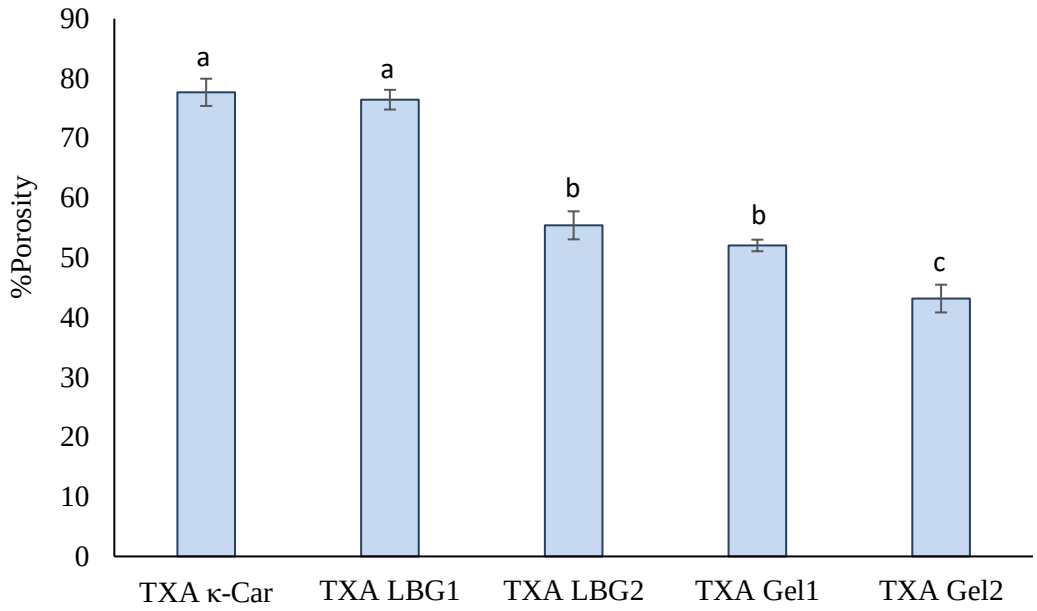

Figure 23. Porosity of TXA-loaded formulations. Data are means (n=3) ± SD

4.5.5 Swelling studies

The swelling conditions of PBS at pH 7.4 and 35˚C for 6 hours were selected to simulate the nasal cavity experiencing epistaxis (pH of blood 7.4). Different formulations reached their maximum swelling ratio at different times, the most rapid being TXA κ-Car within or at 1 hour to achieve a ratio of 34 (Figure 24). The subsequent fall in weight of TXA κ-Car after this time was presumably due to polymer erosion in the PBS medium. Comparison of swelling of 1.5% κ-Car cryogel (Figure 15 in Chapter 3) and TXA κ-Car – also 1.5% carrageenan (Table 3) – showed that 0.5% (w/v) TXA in the gel resulted in much reduced swelling. Thus, the maximum ratio was 34 here but 93 for the unloaded cryogel – but with values subject to unquantified erosion[3]. The TXA κ-Car formulation comprises a relatively weak and macroporous internal structure with large voids (reference to the micrograph) which probably results in high initial expansion due to PBS, but subsequent fast erosion as described later.

Addition of 0.1% (w/v) LBG did not affect the maximum swelling degree of the formulation compared with TXA κ-Car, but it improved physical stability of the

[3] It is tempting to ascribe a downturn in swelling as erosion that occurs only after peak swelling. However, there is scant evidence for this. Erosion might be occurring within minutes of immersion, with the kinetic pattern merely showing the balance between swelling and unquantified erosion.

formulation in PBS with no obvious indication of erosion within 6 hours. Incorporation of 0.2% (w/v) LBG in TXA LBG2 had the same effect in its physical stability; but halved its extent of swelling. Reduced swelling can be due to formation of intermolecular interactions between κ-Car and LBG (Damodaran, Parkin, & Fennema, 2008) perhaps resulting in a decrease in pore size and pore distribution of the cryogel and tighter internal wall structures, as observed in Figure 22 c (Pushpamalar, Langford, Ahmad, Hashim, & Lim, 2013).

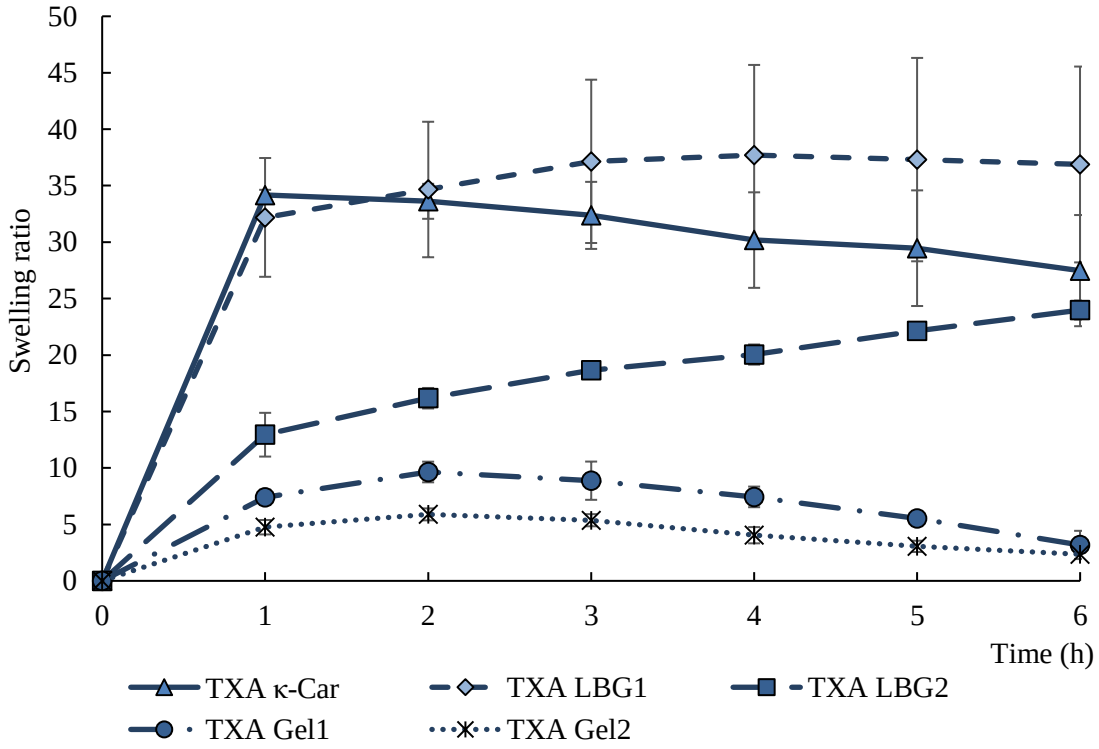

Figure 24. Swelling ratio of TXA-loaded formulations at 35 ± 2˚C in PBS buffer at pH 7.4. Values are means ± SD (n=3)

TXA Gel1 and TXA Gel2 showed the least swelling, peaking at 9 and 5 respectively after two hours. Thus, addition of the gelatine significantly dropped the swelling ratio and the gel structures probably started to lose their structural integrity after one hour of submersion in PBS due to solubilisation of the cryogel. This high weight loss suggests that the polymer networks formed in the cryogel are weak or there are small portions of the polymers tangled in the connected network that can easily separate from it (Pinkas & Zilberman, 2014).

4.5.6 pH

The pH of the TXA-loaded hydrosols was measured before freeze-drying and was in the range 6.9 to 7.9 (Table 5). The marked fall in pH of the hydrosol formulations compared with the TXA κ-Car formulation can be due to presence of LBG (pH 6.9 in 0.1g LBG and pH 6.8 in 0.2 g LBG dispersed in 25 mL of water at 40 ºC) or fish gelatine (pH of 1g and 2g gelatine dispersed in 25 mL of water was 5.4 and 5.2, respectively, at 40 ºC). The lowest pH was recorded for TXA Gel2.

Table 5. pH of TXA-loaded formulations at 40˚C

Formulation	pH
TXA κ-Car	7.9
TXA LBG1	7.7
TXA LBG2	7.2
TXA Gel1	7.0
TXA Gel2	6.9

The normal nasal mucosal pH is slightly acidic within the range of 5.5 - 6.5. The pH values of some hydrogel-based intranasal drug delivery formulations were reported within the range of 4.5 to 6.5 (Galgatte, Kumbhar, & Chaudhari, 2014; Sherafudeen & Vasantha, 2015; Y. Wang, Jiang, Wang, & Bie, 2017). Although the pH value of the TXA-loaded formulations (6.9 -7.9) are higher than these studies, irritation of nasal mucosa is not expected due to compatibility with the nasal pH. However, to achieve deposition of the drug in the nasal mucosa, the pH of these nasal formulations must be maintained in the range of 4.5 to 6.5 (Arora et al., 2002). Therefore, lowering the pH of the formulations during preparation is recommended.

4.5.7 In vitro bioadhesion studies

In vitro bioadhesion measurements were performed on the five formulations using a TA.XT plus texture analyser and the maximum force required to detach the formulation from the model surface mucosal membrane determined the adhesive strength of each formulation (Figure 25). TXA LBG2 required the greatest force of 1.42 N to separate from the mucin coated membrane, while TXA κ-Car required the

least, 1.19 N. However, inspection of the plots shows differences were not marked and were statistically insignificant ($p>0.05$).

Compared to the bioadhesion 1.5% κ-Car cryogel (Figure 18, Chapter 3), TXA κ-Car exhibited a reduced maximum detachment of 1.35 N to 1.19 N.

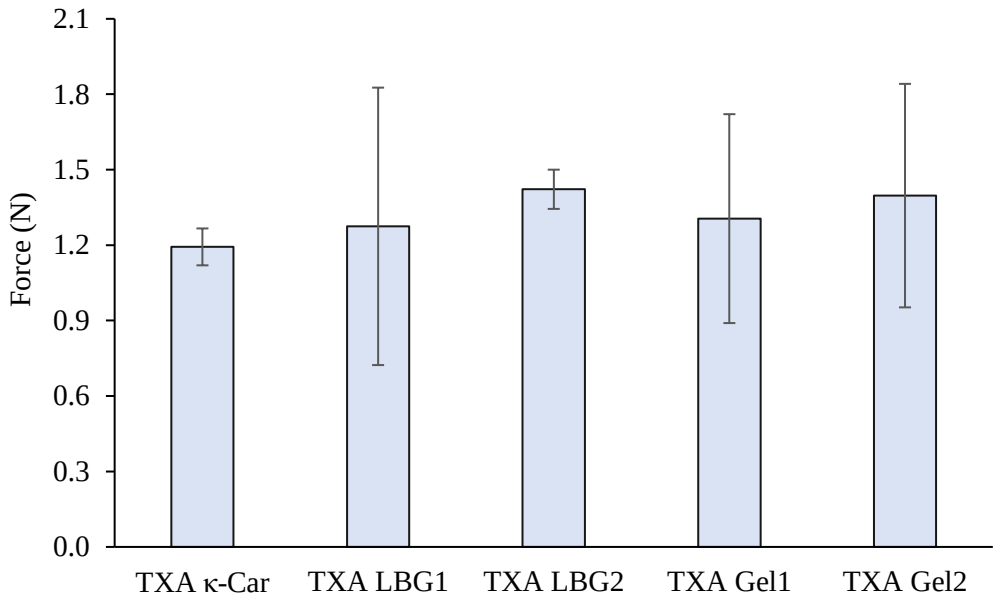

Figure 25. Bioadhesion behaviour of TXA loaded formulations shown as maximum detachment force. Data are means ± SD (n=4)

Bioadhesion of a drug delivery system improves therapeutic performance of the drug by prolonging the residence time of the drug at the mucosal surface and facilitates intimate contact and absorption of the drug to the mucosal lining (Prajapati et al., 2014). Like the unloaded κ-Car cryogel in Chapter 3, the TXA κ-Car showed bioadhesion due to its negatively charged sulphate groups in κ-Car interacted with the mucin layer through hydrogen bonding between sialic acid and the sulphate groups in addition to physical entanglement with the hydrated flexible polymer (Menchicchi et al., 2015).

LBG has been used in several drug delivery studies to improve bioadhesion in developing drug delivery systems (Harikrishnan, Madhusudhan, & Santhiagu, 2015; Prajapati et al., 2014; Vijayaraghavan, Vasanthakumar, & Ramakrishnan, 2008). In this study, LBG combined with 1.5% κ-Car numerically enhanced bioadhesion but the

effect was insignificant due to low concentrations of LBG. A study conducted by Prajapati et al. (2014) on drug loaded LBG-alginate gels reported significant enhancement in bioadhesion of the gels after increasing the LBG content of 0.1 to 0.2 and 0.3 g followed by reducing the κ-Car ratio by the added amount of LBG. The greater bioadhesive property of TXA LBG formulations can be due to presence of non-ionisable hydroxyl groups that form a strong gel network with the glycoprotein of the mucin through hydrogen bonding (Prajapati et al., 2014). However, ever-increasing concentrations of LBG may usefully increase bioadhesion of the formulations, but may negatively affect the other properties, swelling ratio, mechanical properties, and the all-important TXA release profile.

Higher bioadhesion by addition of Gel was found by Sonawane and Patil (2017) in formulation of Gel κ-Car extended release palettes. However, in this study the higher bioadhesion in TXA Gel formulations may be due to their higher total biopolymer content of 2.5 and 3.5% compared with 1.5% in TXA κ-Car formulation.

4.5.8 Fourier transform infrared (FTIR) spectroscopy

FTIR analysis can be useful to identify chemical interactions or modifications of the drugs and polymers that may occur during fabrication. FTIR spectra of TXA, drug-free cryogel and drug loaded cryogels are shown in Figure 26. In the FTIR spectrum of TXA powder, the carbonyl group of carboxylic acid (C=O) was detected at 1542 cm^{-1}.

In the 1.5% κ-Car cryogel, used as the drug carrier, the small peak at 848 cm^{-1} indicates the D-galactose-4-sulfate group, the band at 928 cm^{-1} indicates 3,6-anhydride-galactose (Fan et al., 2011) and 1263 cm^{-1} indicated an ester sulphate group, and the bands around 3100 to 3600 cm^{-1} indicated the O-H stretching modes and vibration of hydroxyl groups of κ-Car (Bajpai & Daheriya, 2014; Derkach et al., 2018) (Figure 27). Inclusion of TXA to the carrier matrices (κ-Car, LBG and Gel) was confirmed by the appearance of a small peak depicted for C=O stretching band at 1540 cm^{-1} attributed to the carbonyl group of carboxylic acid group of TXA (Figure 27). An equivalent peak was also observed in the Gel spectra but with lower intensity. This peak represents carbonyl groups of amino acids present in the gelatine chemical structure, possibly aspartic and glutamic acid residues. In all formulations containing TXA, the low intensity of the peak is probably due to the low concentration of TXA in the

formulations compared with pure TXA as no new bands which could be attributed to such interactions were evident in FTIR spectra.

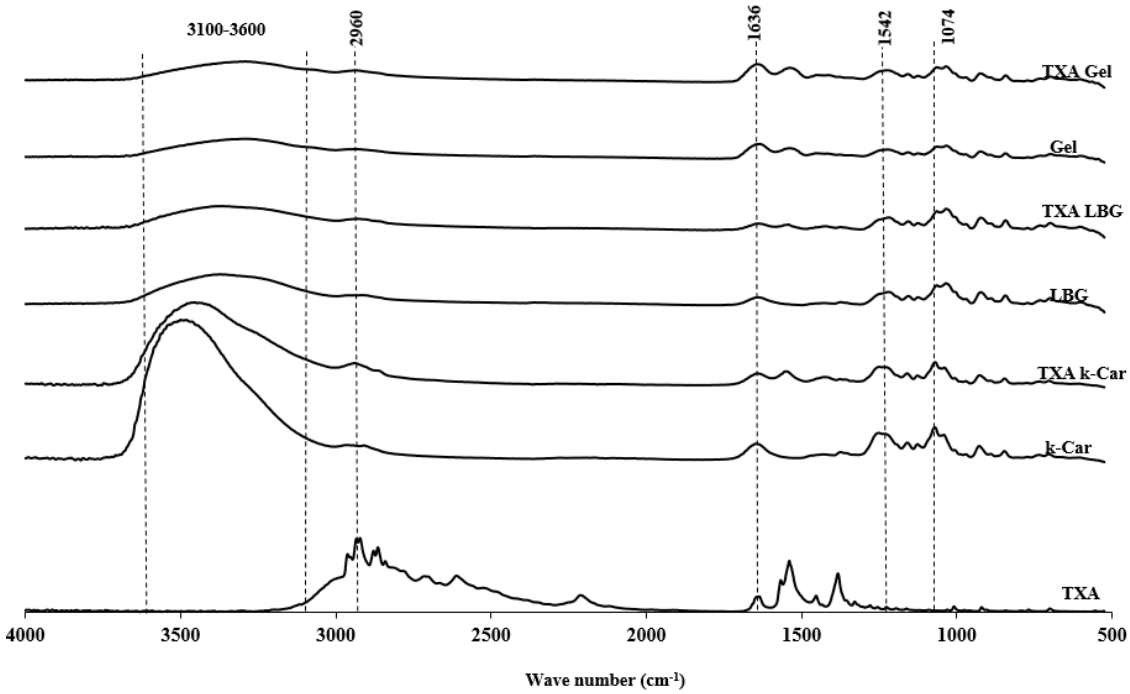

Figure 26. FTIR spectra of pure TXA powder (TXA), drug free formulations (k-Car, LBG and Gel) and TXA loaded formulations (TXA k-Car, TXA LBG and TXA Gel).

However, significant low swelling (Figure 23) and retarded TXA release in TXA Gel1 and TXA Gel2 formulations as described in the next section – suggested possible chemical interactions between the κ-Car and Gel. To explore this possibility, the FTIR spectra of individual κ-Car and gelatine polymers were compared with spectra of combined κ-Car and gelatine cryogel (Gel1). The FTIR spectra of pure gelatine showed characteristic bands at 1539 cm^{-1} (Amide II, N-H and C-N vibration), 1654 cm^{-1} (Amide I, stretching vibrations of C=O and C-N group) and a wide band at 3300 cm^{-1} indicating vibration of the N-H group (Derkach et al., 2018; Segtnan & Isaksson, 2004). As seen in Figure 27, addition of κ-Car to Gel, led to the shift of Amide II band from 1539 cm^{-1} to 1541 cm^{-1}. In addition, the Amide I band shifted from 1654 cm^{-1} to 1657 cm^{-1} in Gel1. In addition, shift of wave number due to sulphate ester in κ-Car from 1263 to 1238 cm^{-1} was observed.

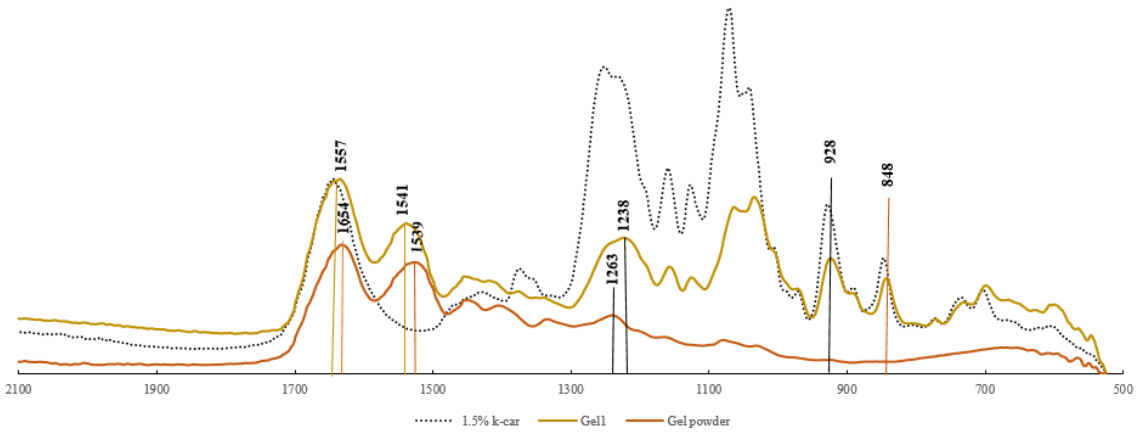

Figure 27. FTIR analysis of 1.5% k-Car cryogel, Gel(atine) powder, and k-Car and gelatine cryogel formulation (Gel1). A shift in Amide I band from 1238 in Gel powder to 1263 cm-1 in Gel 1 and Amide II band from 1539 in Gel powder to 1541 cm-1 in Gel1 can be seen in the mixture of k-Car and Gel (Gel1) spectrum.

These observed shifts were also reported by Derkach et al. (2018). They suggested that interaction between negatively charged sulphate groups of κ-Car and positively charged amide groups of gelatine leads to formation of polyelectrolyte complexes. Also, the shifts observed for amide band in Gel formulation may change the conformation state of gelatine macromolecules, increasing their ordered structure and polyelectrolyte complex formation. These events can cause an increase in intermolecular contacts and physical strength of the formulations (Derkach et al., 2018). The increase in hardness was observed in TXA Gel1, but not in TXA Gel2. Therefore, low swelling and slow drug release in TXA Gel formulations may be due to these intermolecular interactions causing slow rate of PBS penetration, but a rapid rate of erosion – to be shown soon.

4.5.9 Total TXA content and in vitro drug release studies

The TXA content of each cryogel formulation was measured by LC-MS after derivatisation with accutag. The calculated drug content of each nasal pack based on the syringe dimensions of 14 mm diameter × 30 mm height (volume of 4.62 mL) was expected to be 4.62 mg. After complete dispersion in PBS, the measured contents of TXA were as reported in Table 6, each less than 4.62 mg but rather consistent. The difference could be due to a systematic variation in size of the extruded hydrogel cylinders and/or systematic errors in recovery, derivatisation and analysis.

Table 6. Measured total TXA content of loaded formulations

Formulation	Total TXA content (mg)
TXA κ-Car	4.13 ± 0.44
TXA LBG1	4.08 ± 0.09
TXA LBG2	4.14 ± 0.13
TXA Gel1	4.01 ± 0.03
TXA Gel2	4.00 ± 0.03

In vitro TXA release from the five formulations was observed for four hours (Figure 28). A burst release of the drug from TXA κ-Car and TXA LBG formulations occurred by first hour of exposure to PBS, releasing more than 50% of their total drug content. They subsequently released TXA but at a decelerated rate. TXA LBG1 and TXA LBG2 showed a maximum release of 85% of their theoretical drug content within 4 hours compared with the release of 85% in TXA κ-Car. Release from Gel formulations was more restrained reaching 35% in TXA Gel1 and Gel2 formulations at 4 hours.

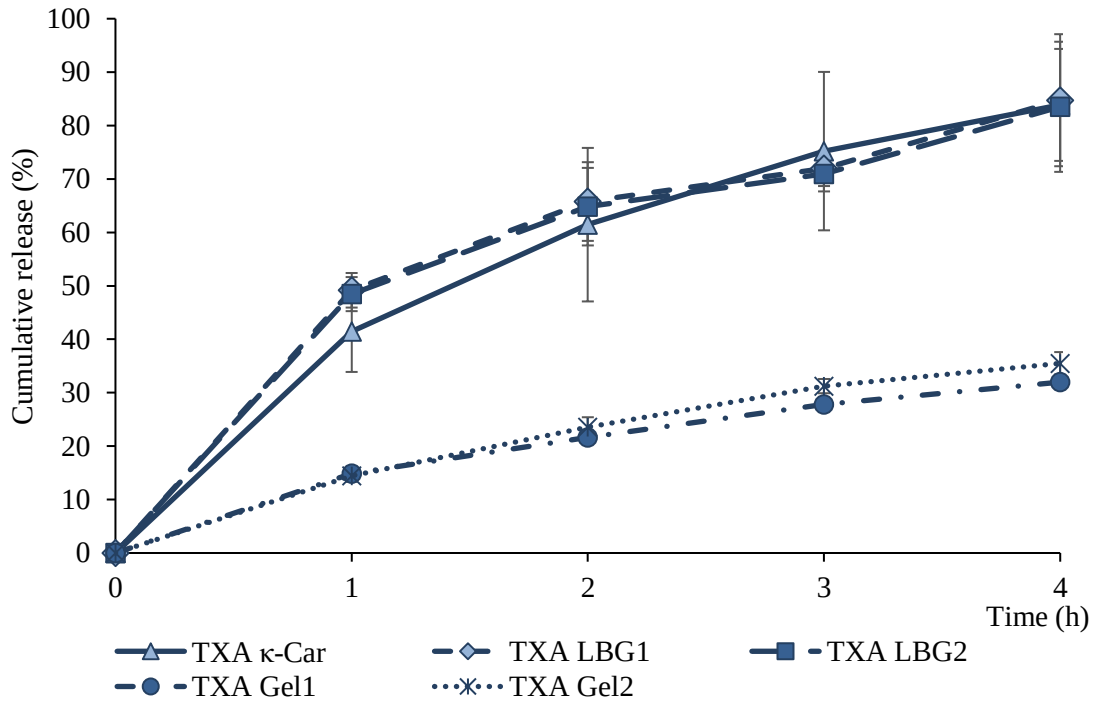

Figure 28. Cumulative release of TXA in drug loaded formulations, Data are means ± SD (n=3)

TXA release was later measured for 7 hours but the release after 4 hours in TXA κ-Car and TXA LBG formulations were negligible. TXA Gel formulations continued their very slow release even after 7 hours (not shown).

It remains to explain these release phenomena in physicochemical terms. The following model is proposed for the rapid release group (TXA κ-Car and TXA LBG formulations). The rapid TXA release in the first hour is due to the combined hydrophilicity of the drug and polymers, and high surface areas of the cryogels causing immediate hydration and diffusion of PBS into the cryogel network. This results in fast swelling of the matrix (Figure 24) and reciprocal diffusion of the water soluble TXA into the PBS initially from the external surface and large voids. However, after rapid initial swelling the remaining drug was released at a slower rate, associated with the slower rate of fluid absorption into smaller voids and slower reciprocal TXA release.

A model proposed for the slower and more sustained TXA is that Gel formulations represents its smaller voids (Figure 22) and electrostatic interactions between the positively charged amine groups in polypeptide chains of gelatine and negative sulphate groups of κ-Car lead to conformation changes of the gelatine macromolecules (Derkach et al., 2018) that may trap TXA. This combination results in lower PBS absorption and reciprocal drug diffusion into the PBS.

These two models are just that – models, and confirmation of them is beyond the scope of this thesis. The empirical results are more important: release kinetics from TXA κ-Car and TXA LBG1 and 2 are likely to be more useful in treatment of epistaxis.

4.5.10 Matrix erosion determined by cryogel dry weight

Erosion of the nasal pack formulations is required to eliminate physical removal and its resulting complications. Erosion of TXA-loaded formulations in PBS at 35°C are reported in Figure 29 by measuring dry weight of the formulations at 8, 24 and 32 hours.

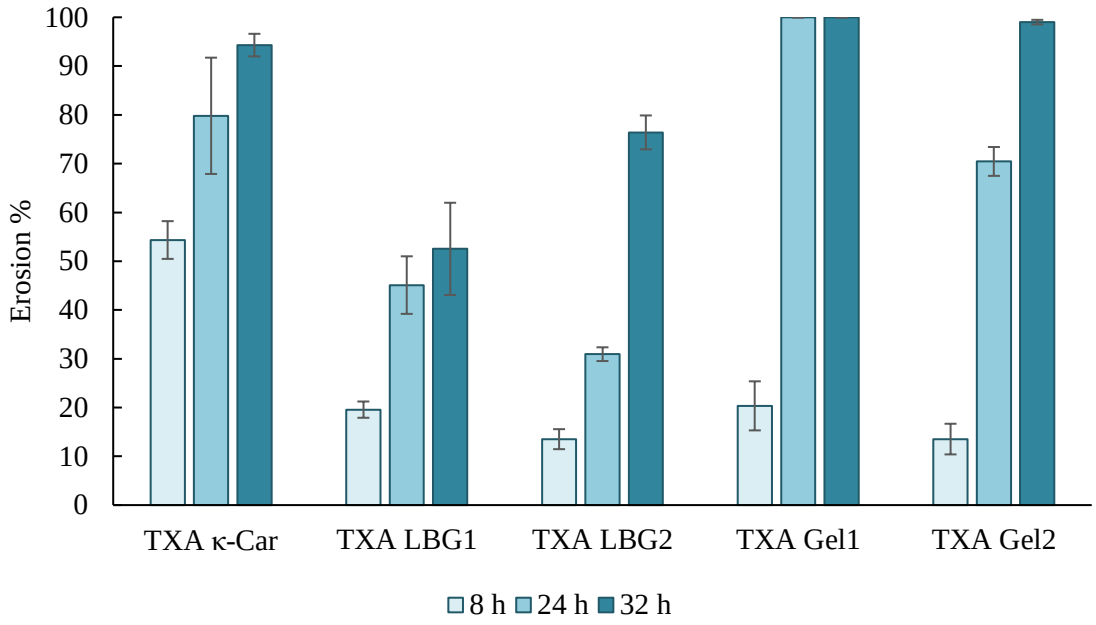

Figure 29. Erosion profile of TXA-loaded formulations in PBS medium (pH 7.4) at 35 ± 2˚C. Values are means ± SD (n=3)

The TXA κ-Car formulation showed highest erosion, more than 50% in the first 8 hours followed by TXA Gel1, TXA LBG1, TXA Gel2 and TXA LBG2, in that order. All the latter eroded less than 23% in that time. Lower erosion rate in TXA LBG and TXA Gel formulations in the first 8 hours must be due to the presence of a second biopolymer (LBG or Gel) in addition to κ-Car, resulting in increase in total polymer concentration and a difference in degree of fluid absorption, swelling, expansion and erosion. In TXA Gel1 and TXA Gel2, erosion accelerated between 8 and 24 hours resulting in complete (100%) and 75% weight loss at 24 hours, respectively. Similar findings were reported by Piluso, Lendlein, and Neffe (2017) explaining the event as the following: during erosion, the Gel amide bonds randomly split and form an increasing number of dangling chains resulting in a swollen loose hydrogel network. At this stage low mass loss from the hydrogel is observed (first 8 hours). Subsequently scission of more amide bonds leads to breakage of the chains into small fragments releasing from the hydrogel matrix resulting in great mass loss and finally disintegration of the hydrogel network in 24 hours (Piluso et al., 2017). TXA LBG formulations showed the lowest total degree of erosion among the formulations in 32 hours due to the synergistic effect between κ-Car and LBG and formation of a stronger network with higher pore density. Similarly, a study conducted by Ngwuluka et al. (2015) showed that addition

of LBG to a cellulose hydrogel increased stability of the hydrogel in the aqueous medium and decreased its erosion rate.

4.6 Summary and conclusion

In chapter three of this thesis, a κ-Car cryogel was developed using 1.5, 2 and 2.5% κ-Car biopolymer and its fluid absorption capacity, swelling, and erosion properties indicated that it can be a suitable carrier for a drug eluting nasal pack. This chapter aimed to develop and characterise a TXA-loaded κ-Car formulation for intranasal drug delivery as an alternative to a TXA gel product and cotton pledgets soaked in TXA solution, as discussed in the Introduction section of this chapter.

TXA is commonly used in treatment of severe epistaxis for immediate effect, therefore an immediate release dosage formulation is required to instantaneously release the drug and disintegrate to make the drug available for action. The outcomes of characterisation and comparison of the κ-Car formulations developed in Chapter 3 indicated that 1.5%κ-Car is the preferred matrix due to its fastest and highest swelling and erosion rate, and highest expansion to fill the nasal cavity. However, the bioadhesion of this formulation was the least. To enhance bioadhesion, incorporation of a bioadhesive polymer to κ-Car was suggested. LBG and Gel were selected biopolymers to be individually added to the κ-Car hydrogel.

LBG is a non-ionic galactomannan consisting of a mannan backbone of β-(1 → 4)-d-mannose with α-D-galactose at carbon 6. Several researchers have reported synergistic effect of κ-Car with this biopolymer in fabrication of κ-Car hydrogels (Chronakis, Borgström, & Piculell, 1999; Dunstan et al., 2001) and films (Martins et al., 2012). At the same time, the bioadhesive properties of LBG in combination with other biopolymers has been reported in development of mucoadhesive drug delivery systems (Cazorla-Luna et al., 2019). However, far too little attention has been paid to the effect of LBG combined with κ-Car in physicochemical, mechanical, swelling and bioadhesion properties of its cryogel formulations.

This study investigated the effect of LBG in 0.1 and 0.2% concentrations and compared the resulting TXA-loaded cryogel formulations with the TXA κ-Car formulation focusing on their mechanical, bioadhesive, swelling and drug release

profile. According to the obtained results, LBG significantly increased strength of the cryogels, insignificantly improved bioadhesion, reduced swelling and facilitated burst release of TXA in the used concentrations of 0.1 and 0.2%, making LBG a likely candidate for inclusion in a viable epistaxis treatment.

On the other hand, gelatine is a water-soluble biopolymer derived from collagen and an extensively investigated material for tissue adhesive formulations. This material and its physically cross-linked hydrogels perform weak mechanical strength, by chemical cross-linking or a suitable polymer additive can enhance its mechanical strength. In this study, fish gelatine was added in 1 and 2% concentrations to enhance bioadhesion of the TXA κ-Car formulation and facilitate fast erosion. Surprisingly, addition of gelatine did not significantly improve bioadhesion of the formulation. The drop in bioadhesion force observed in the TXA κ-Car compared with the TXA free 1.5% κ-Car in Chapter 3 suggested that presence of TXA may interrupt the hydrogen bonding or electrostatic bonding between the mucus covered membrane and the cryogel due to its conjugation with the κ-Car and gelatine polymers (Pinkas & Zilberman, 2014). However, addition of gelatine dramatically increased erosion rate, making it a prospective candidate for fast eroding nasal pack formulations. However, rate of drug release in the formulations containing Gel must be considered.

To conclude, this study designed and developed TXA-loaded cryogel formulations for nasal packing applications. The TXA κ-Car cryogel formulation showed good physical integrity, flexibility and porosity. In the swelling and drug release assessment, this formulation showed the ability to absorb fluid and release the drug in the desired manner. The FTIR results indicated least degree of interaction between the drug and the polymer making the TXA release hassle free. All these properties indicate that the TXA κ-Car cryogel formulation could be used as a suitable candidate for a TXA-eluting nasal pack and could open the opportunity for developing a new generation of drug eluting nasal packs in epistaxis managements.

Chapter 5 Dexamethasone-eluting nasal pack: a local intranasal delivery system for treatment of postoperative inflammation

5.1 Introduction

The paranasal sinuses and nose form a dynamic system that humidify, filter and warm the air we breathe. They are empty spaces extended outward from the main nasal passage, connected by narrow tube-like structures, forming frontal and maxillary sinuses perpendicularly to the airflow (Siu, Shrestha, Inthavong, Shang, & Douglas, 2020). Ethmoid sinuses and sphenoid sinuses are located between the eyes (Figure 30).

Chronic rhinosinusitis (CRS) occurs when a persistent inflammatory condition of the paranasal sinuses lasts for over 12 weeks and can occur with or without polyps. According to Stevens, Lee, Schleimer, and Cohen (2015) approximately 15% of the general population in United States are affected by CRS at any stage of their life. This condition is characterized by clinical symptoms that include a blocked nasal airway, nasal discharge, facial pain, headaches and anosmia (Bachert et al., 2014).

To manage the symptoms of CRS in the patients not responding to medications, functional endoscopic sinus surgery (FESS) is a standard approach effective in 90% of the patients (Welch & Stankiewicz, 2009). FESS principally aims to reinstate ventilation of the paranasal sinuses and return their functionality to normal state by widening of the natural drainage pathways between the sinuses and the nose, and removal of the inflamed tissue (polyp) (T. C. Wang & Hsu, 2017).

Although FESS is a common practice in treatment of CRS, the outcomes of the treatment can be compromised by bleeding, inflammation, polyp reformation and adhesion of nasal mucosal lining (Soler, Mace, & Smith, 2008). To overcome these complications and attain optimal long-term outcomes, a variety of nasal spacers such as nasal packs (El Maraghy, Younis, Dawood, & Mohammed, 2019; T. C. Wang & Hsu, 2017) and nasal stents (Marple et al., 2012; Stefan, Rabie, Sobhy, & Maarouf, 2019) are commonly used. The functions of nasal packs and their importance in control of post-operative bleeding, prevention of tissue adhesion and middle turbinate lateralisation and facilitating wound healing were explained in Chapter 2 (Literature Review) of this thesis.

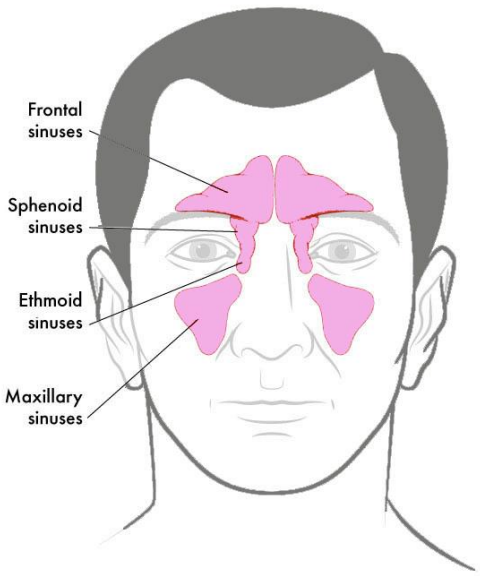

Figure 30. Location of four sinuses in human face. Frontal sinuses are a pair of cavities located in the forehead, maxillary sinuses are on the buccal bone, and ethmoid and sphenoid sinuses are between the eyes.

In addition, the merits and disadvantages of using nasal packs were discussed in that chapter. Based on the literature review and despite of the professional conflicts over use of non-degradable and degradable nasal packs, these products are still commonly used by many surgeons as an intervention in CRS due to some advantages over discomfort and complications.

During the wound healing process, inflammatory cells immediately proliferate in the wound and increase the expression of metalloproteinase (MMP-9) in the extracellular matrix of the cells. Uncontrolled increase in MMP-9 may lead to poor wound healing (Watelet et al., 2005). Therefore, along with the intra-operative nasal packing, medical treatment with topical or systemic anti-inflammatory drugs are postoperatively used to control inflammation. A systematic review by Pundir et al. (2016) showed that pre-, intra- and postoperative use of systemic and topical corticosteroids significantly reduces postoperative pain and improves wound healing after FESS, however, limited studies investigated the effects of intraoperative use of these drugs.

Although preparations containing corticosteroids are typically prescribed for local administration after FESS (Dawson, Gutteridge, Cervin, & Robinson, 2018; Rowe-Jones, Medcalf, Durham, Richards, & Mackay, 2005), tissue inflammation limits

accessibility of the drugs to the target area and thus reduces their efficacy. Therefore, an effective drug delivery system with sustainable local drug absorption, extended residence time and minimal depletion is needed (Albu, 2012). Nasal packs, space-filling gels and structured nasal stents are the typical devices used to keep the middle meatus open and minimise tissue adhesion. Among these devices, nasal packs and stents have been used to deliver drugs to the wound, while achieving their main function as spacers (Sabarinath, Harish, & Divakaran, 2017; Stefan et al., 2019).

However, as discussed in the Introduction of Chapter 4, drug impregnated nasal packs tend to release medication in uncontrolled and inconsistent ways causing erratic treatment outcomes (Pundir et al., 2016; Sabarinath et al., 2017). Moreover, drug-eluting stents are expensive and unaffordable for many patients. Drug-loaded nasal packs capable of prolong and sustainable release of anti-inflammatory drugs would be useful.

Outcomes reported in Chapter 4 indicated that a freeze-dried matrix of carrageenan was a suitable carrier for fast release of TXA, but that favorable property may not extend to other drugs with different physicochemical properties.

Dexamethasone, momantasonfurate, fluticasone propionate and betamethasone are anti-inflammatory drugs and their administration for FESS has been reported by several researchers (Dawson et al., 2018; Khalmuratova, Kim, & Jeon, 2011; Rowe-Jones et al., 2005; Sabarinath et al., 2017; Stefan et al., 2019). This study has investigated the effect of loading a corticosteroid drug on subsequent physicochemical characteristics and importantly the release profile of the drug. Dexamethasone phosphate (DEX) was arbitrarily chosen as the model drug.

The requisites of this novel nasal pack are prolonged release of DEX to supress excessive inflammation but using low concentrations of DEX to avoid suppression of natural inflammatory response and sustained release of DEX for the therapeutic period. In addition, the pack must be able to absorb the wound exudate and start eroding during or after exercising the therapeutic effect. To optimise these characteristics, locust bean gum and fish skin gelatine were blended independently to κ-Car to investigate their effects on some physicochemical characteristics of the basic κ-Car cryogel nasal pack formulations.

The present study was designed to:

1. Explore the feasibility of a κ-Car cryogel as a DEX carrier intended as an anti-inflammatory drug-eluting nasal insert.
2. Characterise the formulation in terms of morphology, swelling and porosity, mechanical properties, bioadhesion, drug release and degradation.
3. Evaluate the effect of addition of locust bean gum (LBG) or cold water fish skin gelatine (Gel) as second biopolymers to κ-Car on the above properties.
4. Compare the physical properties and drug release profile of DEX loaded formulations with TXA loaded formulations investigated in Chapter 4.

It was hypothesized that presence of DEX and blend of κ-Car and LBG or Gel in the drug carrier formulation would alter the physical characteristics and drug release profile of the system compared with the TXA equivalent and would be a suitable matrix for extended drug release.

5.2 Materials

Food-grade κ-Car powder (Gelcarin® GP 911) containing 3.8% potassium and 2.5% calcium cations was kindly donated by Hawkins Watt Ltd. (Auckland, New Zealand). Locust bean gum (LBG) powder was also donated by Hawkins Watt Ltd. Gelatine powder from cold water fish skin (Gel) was purchased from Sigma Aldrich (Auckland, New Zealand). Dexamethasone phosphate (DEX) (log P=1.83) was purchased from Flem Pharma (Shanghai, China). Mucin from porcine stomach (type III, bound sialic acid 0.5-1.5%) was purchased from Sigma Aldrich (Auckland, New Zealand). Mucin from porcine stomach (type III, bound sialic acid 0.5-1.5%) was purchased from Sigma Aldrich (Auckland, New Zealand). Ultrapure water was used for preparation of hydrogels. All the reagents were analytical grade.

5.3 Methods

5.3.1 Preparation of DEX-loaded cryogels

Five formulations were prepared for this study (Table 7). The DEX κ-Car1 and DEX κ-Car2 formulations were made by addition of 1.5 and 2 g κ-Car to 90 mL of water heated to 85˚C with constant magnetic stirring until a transparent hydrosol was obtained. DEX solution was prepared by similarly dissolving 150 mg of the drug

powder in 10 mL of water. The drug solution was added to the transparent κ-Car hydrosol. The mixture was further stirred at same temperature for 10 minutes to ensure even distribution of the drug. Other formulations (DEX LBG1, DEX LBG2, DEX Gel1 and DEX Gel2) were comprised of two biopolymers, all containing κ-Car. Preparation of these formulations was as described for κ-Car, except that κ-Car was dispersed in 70 mL of water and LBG or Gel were added to 25 mL of water and DEX was dissolved in 5 mL of water to maintain the final volume of water at 100 mL. LBG and Gel were separately dissolved in water heating at 95˚C under constant stirring to obtain a clear dispersion. Subsequently, they were added to the κ-Car hydrosol and stirred for 10 minutes at 95˚C. Finally, the DEX solutions were added and stirred for another 10 minutes.

The drug-loaded hydrosols were then cast in cylindrical polyethylene syringe barrels (30 mm long x 14 mm diameter) as explained in Chapter 4. The assemblies were kept at room temperature for 1 hour then stored overnight at 4°C to obtain hydrogels. The hydrogels were then removed from the casts, vertically placed in polystyrene trays and freeze dried under the following conditions: shelf temperature, 2°C; temperature on freeze dryer shelf, -70°C; and vacuum 120 mbar (AdVantage Pro bench top freeze dryer, SP Scientific, USA).

Table 7. Composition of DEX-loaded formulations

Formulation	κ-Car (g)	LBG (g)	Gel (g)	DEX (mg)
DEX κ-Car1	1.5	0	0	150
DEX κ-Car2	2.0	0	0	150
DEX LBG1	1.5	0.1	0	150
DEX LBG2	1.5	0.2	0	150
DEX Gel1	1.5	0	0.1	150
DEX Gel2	1.5	0	0.2	150

5.3.2 Characterisation

The DEX loaded formulations were characterised for their physicochemical and drug release characteristics using the following methods:

5.3.2.1 Microstructure analysis by scanning electron microscopy

Surface and cryo-fractured cross-sectional images of the DEX loaded nascent nasal inserts were obtained using a Schottky field emission scanning electron microscope (SU-70, Hitachi, UK) as explained in Methods section of Chapter 3.

5.3.2.2 Mechanical properties of cryogels

Texture profile analysis of hardness, springiness and cohesiveness was evaluated using a TA.XT plus texture analyser (Stable Micro System) as described by D. S. Jones et al. (1997) and Thirawong, Nunthanid, Puttipipatkhachorn, and Sriamornsak (2007) following the fully explained procedure in Methods section of Chapter 4.

5.3.2.3 Porosity measurement

The porosity of DEX loaded nascent nasal inserts (cryogels) were determined by a solvent replacement method (Nanda et al., 2013) as explained in Methods section of Chapter 3.

5.3.2.4 Swelling ratio determined by cryogel wet weight

The swelling ratio of DEX loaded nasal cryogels inserts in phosphate buffered saline (pH 7.4) was determined at 35 ± 2˚C in water bath using a gravimetric method (Khurma et al., 2006) following the procedure in section 3.2.3 of Chapter 3.

5.3.2.5 pH

The pH of the DEX loaded hydrosol formulations was measured at 40˚C using a calibrated pH-meter (pH Bench-top Meter. PL-700PC, Interlab, NZ) at 40˚C prior to formation of the firm gel.

5.3.2.6 In vitro bioadhesion studies

Bioadhesion measurements to mucin were performed using the TA.XT analyser adapting the methods of Boateng et al. (2013) and Şenyiğit Zeynep et al. (2014). The procedure is explained in detail in section 3.2.3 of Chapter 3.

5.3.2.7 Fourier transform infrared (FTIR) spectroscopy

To characterise the presence of specific chemical groups in the DEX-loaded cryogel formulation, FTIR spectra was obtained using a Nicolet iS10 FTIR spectrophotometer

(Thermo Scientific, USA) in attenuated total reflectance mode using a diamond crystal. Details are reported in section 4.2.2 of Chapter 4.

5.3.2.8 Total DEX content and in vitro drug release studies

The content of DEX within the DEX-loaded cryogel formulations was determined before performing the drug dissolution studies. It was measured by soaking the cryogel formulations in PBS (pH 7.4) at 35˚C with overnight stirring in the not unreasonable expectation that the drug would completely dissolve. The solutions were centrifuged and filtered to remove the any remaining gel particles if any. The concentration of DEX in PBS was assayed by LC-MS as described below.

In vitro DEX release from the cryogel formulations was studied in PBS buffer (pH 7.4) under sink conditions following the procedure in Methods of Chapter 4.

The concentration of DEX was determined by LC-MS, using an Agilent 1260 Infinity Quaternary LC-MS System (Santa Clara, USA). A Waters XSelect CSH C18 column (2.1 x 100mm, 3µm) was used for this analysis. The mobile phases were 0.1 % (v/v) formic acid in water and 0.1% (v/v) formic acid in acetonitrile with flow rate of 0.4 mL min^{-1}. Authentic DEX was used as external standard and drug free cryogel formulations were used as controls. This method is described in the following section.

5.3.2.9 DEX determination by LC-MS

DEX determination by LC–MS analysis was conducted using an Agilent 1260 Infinity Quaternary LC System (Santa Clara, CA 95051 USA). The system consisted of the following components: 1260 quaternary pump (model number: G1311B), 1260 infinity ALS sampler (model number: G1329B), 1260 infinity TCC column component (model number: G1316A), 1260 infinity diode array detector (DAD) (model number: G4212B), connected to a 6420 triple quadrupole LC/MS system with multimode ionisation source (model number: G1978B).

The MS ionisation source conditions were as follows: capillary voltage of 1.8 kV, drying gas temperature of 325 °C, drying gas flow of 6 L/min, vaporiser temperature of 200 °C and nebuliser pressure of 60 psi. The positive electrospray ionisation (ESI) mode was performed with multiple reaction monitoring (MRM) for quantitative analysis. The precursor-to-product ion transition used for dexamethasone phosphate

was [M+H] + m/z 473 -> 435 and 473 -> 355 with fragmentor voltage of 87 V and collision energy of 6 and 8 eV, respectively. Dexamethasone phosphate was used as standard.

Waters XSelect CSH C18 (2.1 x 100mm, 3µm) was used for this analysis. The mobile phases were composed of water containing 0.1%(v/v) formic acid (A) and acetonitrile containing 0.1% (v/v) formic acid (B). The initial gradient condition was 75:25 (A:B). From 0 to 3 min the B was increased to 75% and from 3 to 4 min the B was decreased to 3%. The total run time was 8.4 min. The injection volume was 1 µL and the retention time of dexamethasone phosphate (DEX) was 4.67 min (Figure 31).

A series of calibration standard solutions of 1 to 100 µg.mL^{-1} DEX were injected (1µL) and a calibration curve was obtained based on the peak areas and concentrations of the standard solutions (Figure 32).

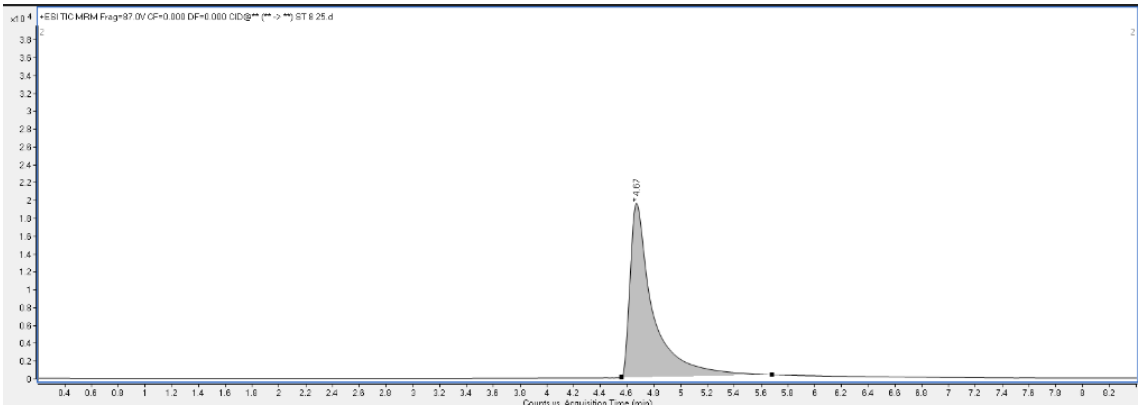

Figure 31. Representative chromatogram for DEX (retention time: 4.67 min)

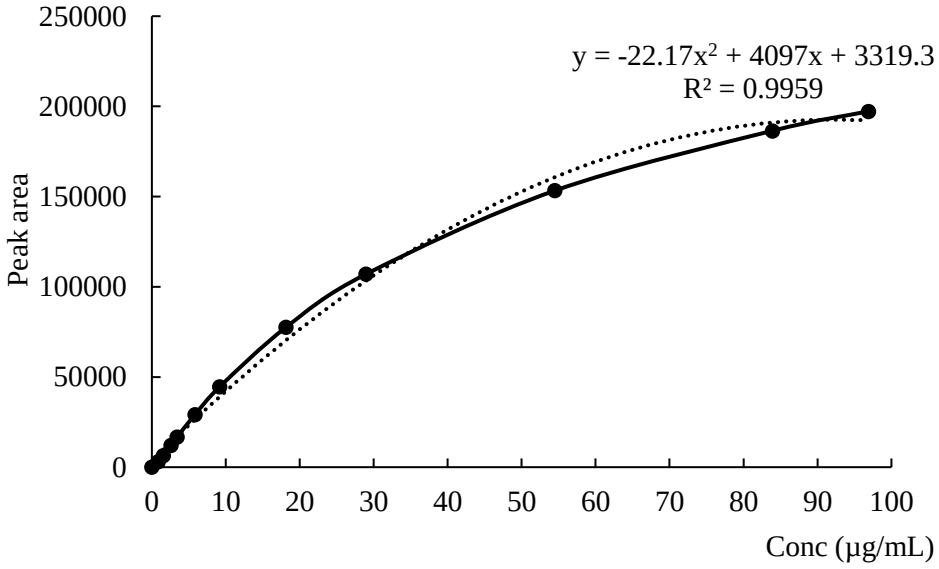

Figure 32. Calibration curve of DEX (Plot of peak areas versus concentrations)

5.3.2.10 Release kinetics

The release kinetics of DEX release from the rehydrated cryogel formulations were fitted to the following models in Table 8 using KinetDS 3.0 software (Mendyk et al., 2012). Where the data fit the model perfectly the R^2 value of the linear plot is 1.00, so the closer to 1.00 the more applicable the plot.

Table 8. Drug release models and descriptions

Model	Description	Comment
Zero order	Cumulative drug release is independent of how much drug remains in the hydrogel with time	Cumulative release versus time is a straight line
First order	Drug release occurs in proportion to the concentration remaining in the hydrogel	Log of the cumulative release versus time is a straight line
Higuchi	Cumulative drug release reduces in proportion to the square root of time	Cumulative drug release versus the square root of time is a straight time
Korsmeyer-Peppas	A refinement of the Higuchi model where the fraction of the drug released is proportional to time in some way but not necessarily the square root	The exponent of time represents diffusion of the drug. Also a straight line
Hixon-Crowell	Describes the release from a system where the surface area and diameter of particles of the matrix changes	The cube root of percent drug remaining versus time is a straight line. The proportionality constant relates surface and volume

Data were fitted to the models and linearly plotted to yield R^2 values.

Zero-order model

This model describes constant rate of drug release that is independent of how much drug remains in the hydrogel (Gouda, Baishya, & Qing, 2017). Thus, the amount of drug released is a straight line from 0 at zero time to an end point equal to the initial drug loading, conveniently expressed as percent of initial drug loading.

$C_t = C_0 + K_0 t$

where C_t is the amount of drug released at time t, C_0 is the initial concentration of drug at time 0, and K_0 is the zero-order rate constant.

First order model

This model states that the rate of drug release is directly proportional to the remaining concentration of the drug in the matrix (Gouda et al., 2017).

$\text{Log } C_t = \log C_0 - K_1 t/2.303$

where K_1 is the first order rate constant (with units of time^{-1}), C_0 is initial concentration of the drug and C_t is the percentage of drug remaining at time t.

Higuchi model

The model describes the release of a drug that involves dissolution and diffusion and is proposed to describe drug release from a porous and non-geometrically shaped matrix (irregular shape or contours) system (Gouda et al., 2017).

$Q = K_H \times t^{1/2}$

where Q is cumulative amount of drug released in time t per unit area and K_H is the Higuchi dissolution constant expressed as units of concentration/time.

Korsmeyer-Peppas model

This model describes drug release from a polymeric system such as hydrogel by finding he relationship between diffusion and dissolution of the drug from the delivery matrix (Gouda et al., 2017).

$Q_t / Q_\infty = K_{KP} t^n$

where Q_t / Q_∞ is a fraction of drug released at time t, K_{KP} is the Korsmeyer release rate constant and n is the diffusional (drug release) exponent.

Hixon-Crowell model

This mode describes the release from a system where the surface area and diameter of particles of the matrix changes (Gouda et al., 2017).

$Q_0^{1/3} - Q_{tr}^{1/3} = K_{HC} t$

Where Q_0 is initial amount of drug in the drug delivery matrix, Q_{tr} is the remaining amount of drug in the matrix at time t and K_{HC} is a constant describing surface-volume relation.

5.3.2.11 Matrix erosion determined by cryogel dried weight

Erosion of DEX-loaded cryogels was determined as described by Roy and Rohera (2002). The procedure was as described in section 4.2.2. of Chapter 4.

5.4 Statistical analysis

Data were marshalled using Excel and one-way analysed for variance (ANOVA) using XLSTAT and Tukey's multiple range test.

5.5 Results and discussion

5.5.1 Macro and microstructure by inspection and scanning electron microscopy

The macrostructure of the DEX–loaded cryogel formulations were observed with unaided eyes and photographed. All DEX–loaded hydrogel formulations became visibly dry after freeze-drying. All were pale white. There were no longitudinal cracks on the surface of the DEX-loaded cryogels. The DEX κ-Car and DEX LBG formulations exhibited variably wrinkled external surfaces (Figure 33 a to d), however, the surface of DEX Gel cryogels was smooth and wrinkle-free (Figure 33 e and f). DEX LBG1 and DEX LBG2 showed the greatest diameter shrinkage, 21% of the original hydrogel diameter governed by syringe internal diameter. This shrinkage was consistent with the development of wrinkles. DEX κ-Car and DEX Gel formulations showed only 7% and 2% shrinkage, respectively.

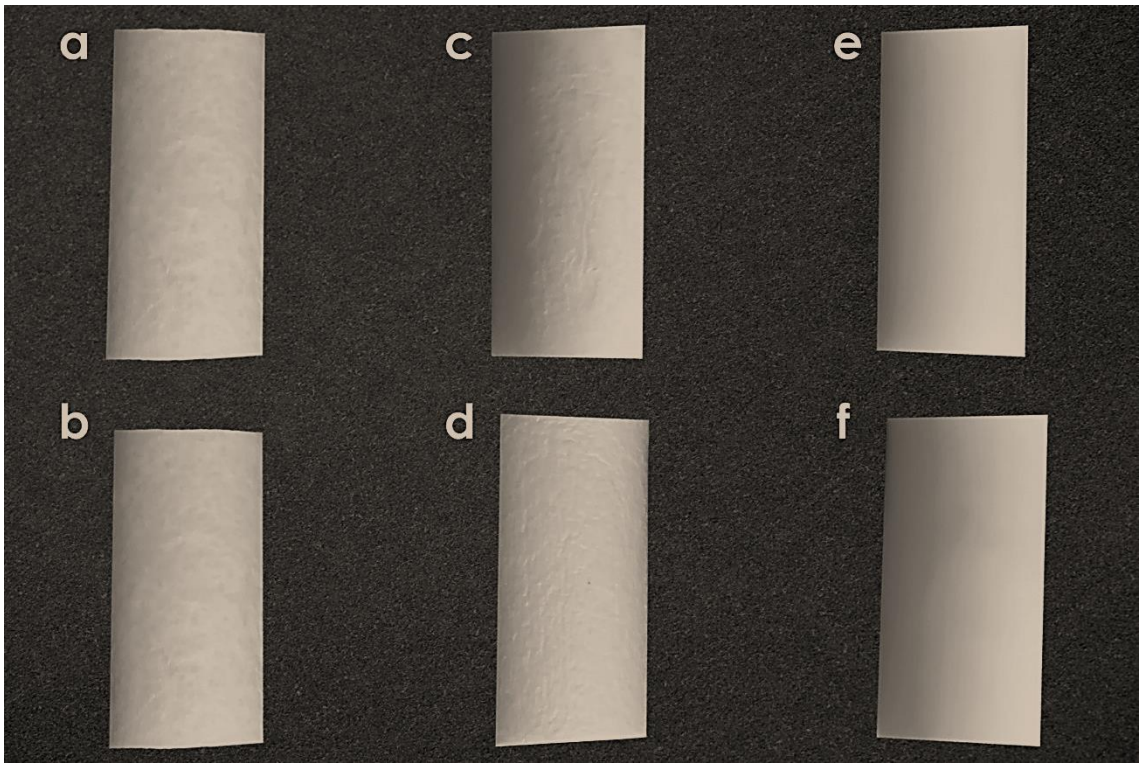

Figure 33. Picture of external surface area. DEX κ-Car1 (a), DEX κ-Car2 (b) DEX LBG1 (c), DEX LBG2 (d), DEX Gel1 (e) and DEX Gel2 (f) formulations.

The internal cross-sectional (transverse) and longitudinal (mid-sagittal) macrostructure of the formulations showed variable morphologies. The transverse section of DEX κ-Car (Figure 34 a and b) DEX LBG1 (Figure 34 c) and DEX Gel (Figure 34 e and f) formulations showed radial structure initiated from the central axis, like the TXA formulations. However, this structure was not evident in DEX LBG2 cryogel (Figure 34 d) and it showed a uniform spongy internal texture with no central axis.

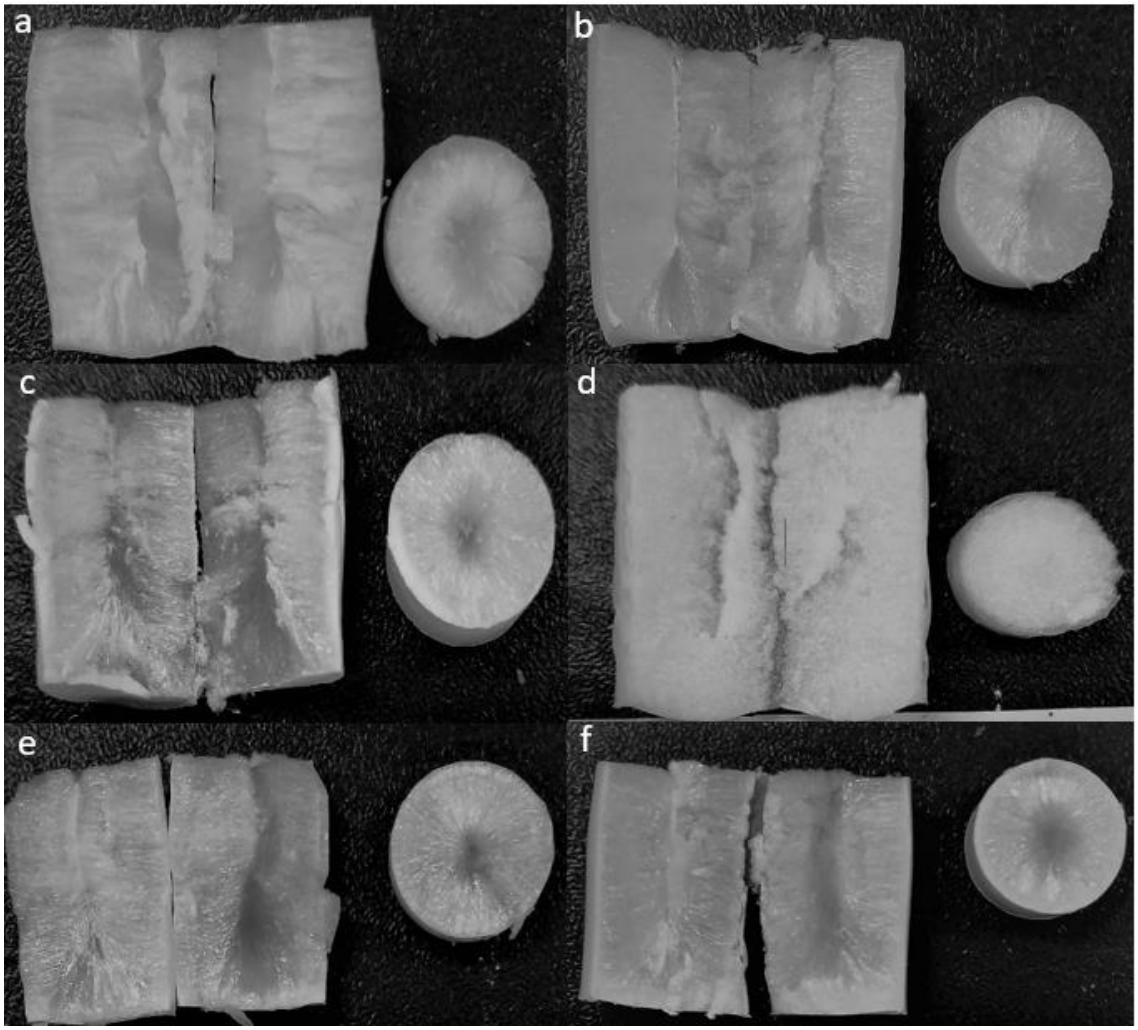

Figure 34. Macrographs of DEX κ-Car1 (a), DEX κ-Car2 (b) DEX LBG1 (c), DEX LBG2 (d), DEX Gel1 (e) and DEX Gel2 (f) formulations in midsagittal and transverse views.

The internal microstructure of cryo-fractured DEX-loaded formulations are shown in Figure 35. A broad pore size distribution was observed in a predominantly macropore range, wider than 50 nm. Duplicates of each formulation from two produced batches were samples and photographed by SEM to ensure consistent observations. In DEX κ-Car1 honeycomb structure with deep voids were observed (Figure 35 a) but increasing to 2.0% κ-Car – DEX κ-Car2 – resulted in a denser structure with thicker cell walls and smaller shallow pores compared with DEX κ-Car1 (Figure 35 b).

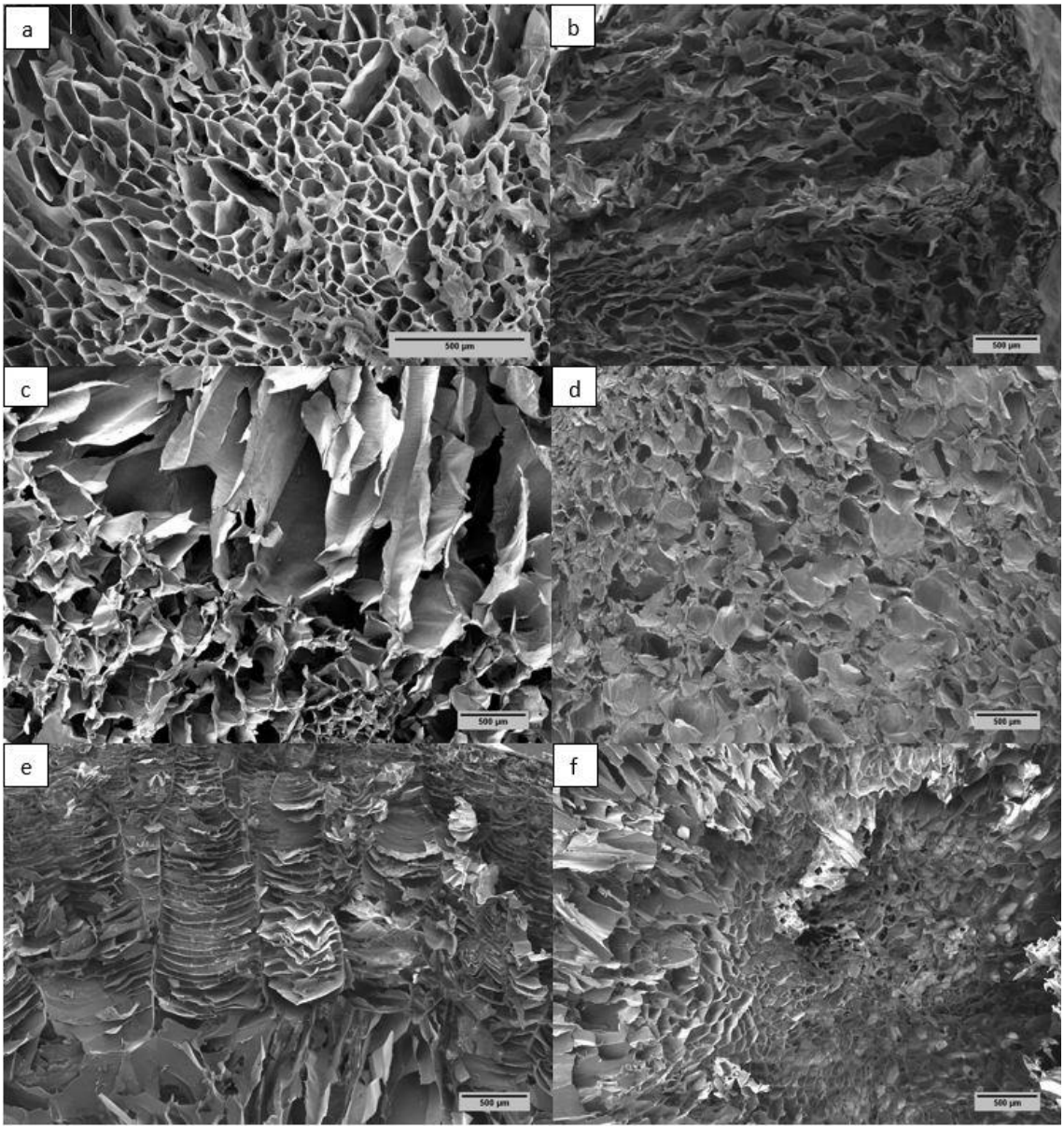

Figure 35. SEM images of cryo-fractured surface of a DEX k-Car1 formulation (a), DEX k-Car2 (b), DEX LBG1 formulation (c), DEX LBG2 formulation (d) and DEX Gel1 formulation (e) and DEX Gel2 (f).

Incorporation of LBG and Gel prominently altered internal structures of DEX LBG and DEX Gel formulations. Addition of LBG and Gel increased pore density and transformed the pore shapes and sizes (Figure 35 c to f). In DEX LBG1, the central part was spongy porous, while the honeycomb structure was evident around the wall of the cryogel, but the honeycomb voids were disappeared in DEX LBG2 showing the most compact spongey structure throughout the cryogel. LBG in DEX LBG1 was insufficient to fully alter the porous structure of DEX LBG1, but 0.2% created a higher

impact on the pore structures by binding to more κ-Car molecules and forming a uniform spongy structure.

The internal microstructure of DEX Gel formulations was also different from other formulations. In DEX Gel1, a dense lamellar structure was observed around the walls with honeycomb voids formed at the central part of the cylinder. In contrast, the lamellar structure was absent in DEX Gel2 and the uniform honeycomb voids, like DEX κ-Car1, were observed but with the denser and smaller voids. The reason for this significant difference is unexplained.

There was no evidence of drug particles in the micrographs suggesting that the drug was dissolved and well-distributed within the delivery matrix. Drug particles will obviously exist, but these will be below the resolution limits at these magnifications (X. Zhang & Cresswell, 2016).

Comparison of the internal structures of TXA (Chapter 4) and DEX formulations indicated that DEX κ-Car1 showed a very similar structure to the TXA formulations with homogenous tubular and highly ordered pore structure and smooth walls. However, the other formulations showed a complex heterogeneous combination of randomly ordered spongy and tubular pore structures.

5.5.2 Mechanical characteristics

The mechanical properties of nasal packs are important in establishment of their suitability for the purpose. They must survive physical insertion into the nasal cavity. The mechanical properties, hardness, cohesiveness, and springiness of the formulated cryogels, are shown in Table 9.

Table 9. Mechanical characteristics of DEX-loaded formulations. Different superscript letters within columns show significant Tukey differences (p<0.0001).

Formulation	Hardness (N)	Cohesiveness	Springiness (%)
DEX κ-Car1	4.53 ± 0.2 [c]	0.45 ± 0.01 [a]	76.0 ± 0.8 [a]
DEX κ-Car2	5.89 ± 0.6 [c]	0.41 ± 0.01 [ab]	71.2 ± 1.5 [ab]
DEX LBG1	27.8 ± 3.6 [b]	0.40 ± 0.02 [b]	67.2 ± 2.3 [b]
DEX LBG2	24.7 ± 1.9 [b]	0.37 ± 0.01 [b]	60.2 ± 2.7 [c]
DEX Gel1	35.0 ± 2.3 [a]	0.31 ± 0.01 [c]	53.6 ± 1.2 [d]
DEX Gel2	30.5 ± 0.6 [ab]	0.28 ± 0.01 [c]	48.1 ± 1.2 [d]

DEX κ-Car formulations required the least force of 4.5 and 5.9 N to rupture. Addition of a second polymer caused 5 and 6-fold increase in hardness. The increase in hardness by addition of LBG is due to the strong synergistic effect interactions between the κ-Car and LBG polymers. The doubling of LBG from 0.1 to 0.2% caused a slight but insignificant reduction in hardness. Likewise doubling the gelatin content insignificantly decreased hardness from the maximum value of 35.0 N in DEX Gel1 to 30.5 N.

In terms of cohesion, DEX κ-Car formulations had the highest cohesiveness values (Table 9) indicating inclusion of LBG or Gels significantly reduced cohesion of the formulations ($p<0.0001$).

Incorporation of Gel to DEX κ-Car reduced the cohesion and springiness at both 1 and 2% concentrations but increased hardness at 1% inclusion. There are changes in morphology at 1% Gel, notably defect voids and compact structure internally around the wall of the cryogels (see the compact area in Figure 35 e).

Springiness was also reduced by inclusion of LBG or Gel and there was a direct positive correlation between cohesiveness and springiness for the six formulations ($r = 0.991$). It appears that addition of LBG to the DEX κ-Car network produced complex heterogeneous structures and reduced cohesion and flexibility of the network. The differences can be seen in related scanning micrograph images (Figure 35 c and d). Moreover, the presence of DEX may interfere electrostatic or hydrogen bonds that

are believed to form between the two polymers, so lowering the cohesion of the cryogel formulations.

5.5.3 Porosity measurement

The percent porosity of the DEX-loaded formulations was measured by cyclohexane uptake (Figure 36). The pores in the cryogels were created by evaporation of the liquid phase (water) from the gel during freeze-drying resulting in various pore shapes and sizes with high potential for absorbing fluids. DEX κ-Car1 showed highest porosity of 67%, matching the high porosity of 1.5% κ-Car cryogel (67%) reported in Chapter 3 (Figure 14). The percentage porosity in DEX κ-Car2 was numerically lower than DEX κ-Car1, but statistically insignificantly different. Addition of LBG and increase in its concentration lowered the porosity of the DEX LBG formulations, but its porosity was insignificantly different from DEX κ-Car2. DEX Gel formulations showed the lowest porosity. Clearly, porosity was reduced by incorporation of a second polymer in all the formulations. These results for all the formulations are consistent with the fine structure shown in Figure 34. Decrease in porosity by increasing polymer concentration can be justified by the fact that higher polymer concentration decreases the size of internal pores and the spaces between spherulites[4] resulting in increase in the number of spherulites, higher nucleation density and decrease in bulk porosity (Akbari & Yegani, 2012).

[4] Spherulites are semi-crystalline regions inside the linear polymers and form with crystallisation of polymers.

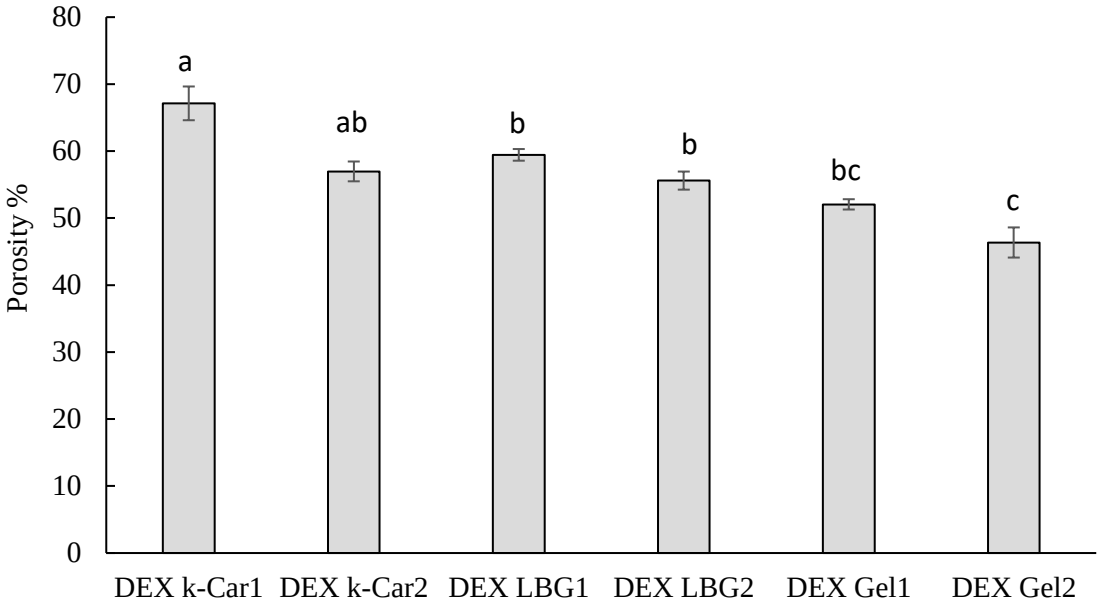

Figure 36. Porosity of DEX-loaded formulations. Data are means (n=3) ± SD. Means with different letters are significantly different (p<0.05).

5.5.4 Swelling studies

Swelling conditions of PBS at pH 7.4 and 35°C for 7 hours were selected to simulate pH of nasal cavity experiencing bleeding. DEX κ-Car and DEX LBG formulations continued swelling up to 7 hours, but DEX Gel1 and DEX Gel2 formulations rapidly reached their maximum swelling ratio of 17 and 19 in under 2 hours (Figure 37). The subsequent apparent fall in the swelling ratio of DEX Gel formulations after this time was presumably due to polymer erosion in the PBS. If true, DEX Gel2 showed the greatest erosion. The erosion profile of the formulations as determined by dry weight is discussed later in this chapter.

Among the other formulations, DEX κ-Car1 and DEX LBG1 stood out with the highest swelling ratios that continued for at least 7 hours, but the swelling ratio of DEX LBG1 was the highest. These two formulations gained weight, despite of the gradual erosion that is described later. DEX κ-Car2 and DEX LBG2 also behaved as a pair with swelling behaviour, but different swelling ratio, to at least 7 hours and DEX κ-Car2 swelled the most of these two.

TXA κ-Car formulation in Chapter 4 and DEX κ-Car1 in here contained the same polymer content and both formulations reached the maximum swelling ratio of about 35%. However, TXA κ-Car reached this level in one hour (Figure 23) while DEX κ-Car1

reached well less than 50% of its eventual swelling in the first hour, Therefore, the drug used in the matrix can alter the swelling behaviour of the formulation.

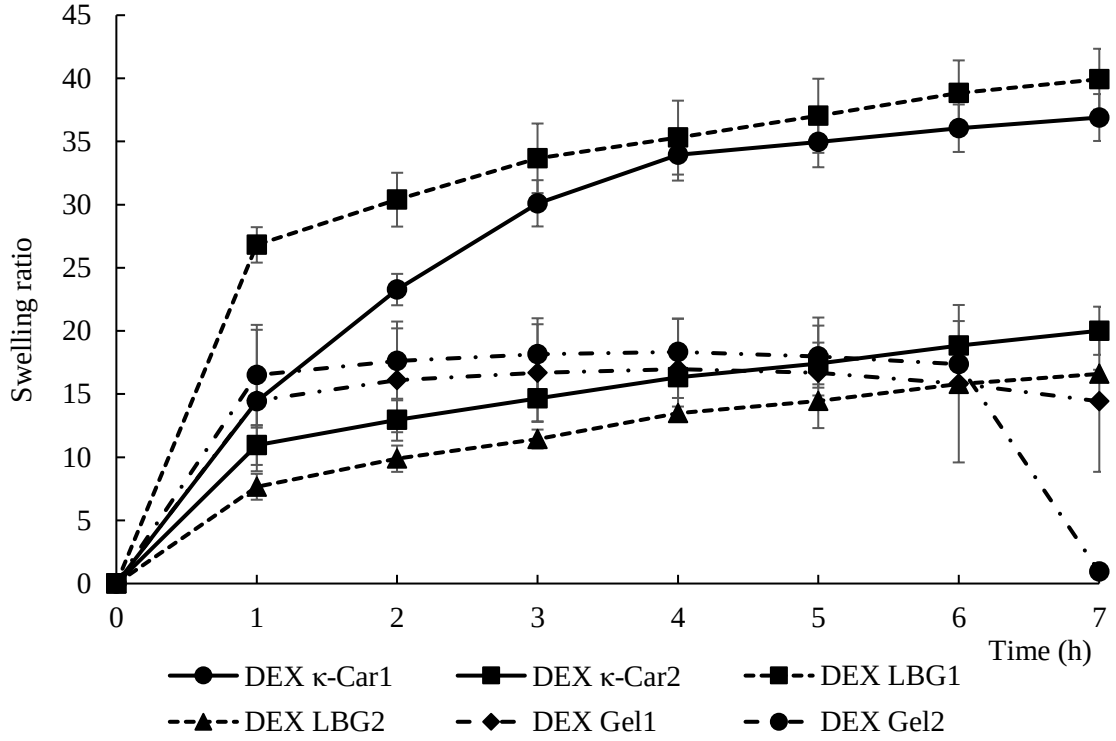

Figure 37. Swelling ratio kinetics of DEX loaded formulations at 35 ± 2˚C in PBS buffer. Values are means ± SD (n=3)

Incorporation of 0.2% LBG to κ-Car significantly dropped swelling degree of the formulation (DEX LBG2). The micrograph of internal structure (Figure 35) shows alteration of pores in size and shape. DEX Gel1 and DEX Gel2 showed significantly less swelling ratio than DEX κ-Car formulations peaking at 17 and 19, respectively, after four hours. Thus, addition of the gelatine significantly dropped the swelling ratio, the gel structures started to lose their structural integrity after one hour of submersion in PBS due to hydrophilicity of the κ-Car, and gelatine polymers and relatively rapid hydrolysis of the cryogel (refer to the erosion section in this chapter). As explained in Chapter 4, this high weight loss can be due to the hydrophilicity of the polymers, weak polymer network of the cryogel and small portions of the gelatine polymers twisted in the connected network causing inconsistency and easy separation from the rest of the network (Pinkas & Zilberman, 2014). It can be concluded that although all the formulations are composed of hydrophilic polymers, the rates of water absorption, water diffusion into the matrix and erosion of matrix play critical roles in swelling

ratio of the formulations. The variations in swelling ratio are due to the type of polymers and their concentrations in the matrix.

5.5.5 pH of DEX-loaded formulations

The pH of the DEX-loaded hydrosols was in the range 6.9 to 7.5 (Table 10). The lowering of pH of the formulations by addition of LBG and gelatine can be traced to the lower pH of those components as pure suspensions in water at 40°C e.g., pH 6.8 for 0.2 g LBG in 25 and pH 5.2 for 2 g of fish gelatine in 25 mL of water. The lowest pH was recorded for DEX Gel2.

Table 10. pH of DEX loaded formulations at 40˚C

Formulation	pH
DEX κ-Car1	7.4
DEX κ-Car2	7.7
DEX LBG1	7.3
DEX LBG2	7.4
DEX Gel1	7.0
DEX Gel2	6.9

The normal nasal pH is slightly acidic within the range of 5.5-6.5 and in patients with CRS is in the range of 5.3 to 7.6. It means that CRS may not disturb the electrolyte environment of the nasal mucosa (Kim et al., 2013). However, the measured pH values three months after surgery exhibited a wider pH range toward the lower pH (range of 3.8 to 7.7) (Kim et al., 2013), but discussing the factors causing reduction in pH during the healing process is beyond the scope of this study. The pH values of some hydrogel-based intranasal drug delivery formulations were reported as 5.6 to 6 for xanthan gum in situ mucoadhesive gel (Sherafudeen & Vasantha, 2015), 4.66 to 5.53 for gellan gum in situ gel (Galgatte et al., 2014) and 4.5 to 6.5 for poloxamer gel (Y. Wang et al., 2017). Although the pH value of the DEX-loaded formulations (6.9-7.7) are higher than these studies, irritation of nasal mucosa is not expected due to compatibility with the nasal pH in CRS patients. However reduction of pH to the range of 5.5 to 6.5 is recommended to enhance drug deposition on the nasal mucosa (Arora et al., 2002).

5.5.6 In vitro bioadhesion studies

Bioadhesion of the polymers used in drug delivery systems requires absorption of mucus and adsorption of the polymer to the mucus membrane. In vitro bioadhesion measurements were performed on the six formulations. The maximum force required to detach the cryogels from the model surface mucosal membrane determined the adhesive strength of each formulation (Figure 38). DEX LBG2 required the greatest force of 3.2 N to separate from the mucin coated membrane, while DEX LBG1 required the least, 1.2 N. The maximum force in DEX κ-Car2 was lower than DEX LBG2 and higher than DEX κ-Car1 but the difference was statistically insignificant.

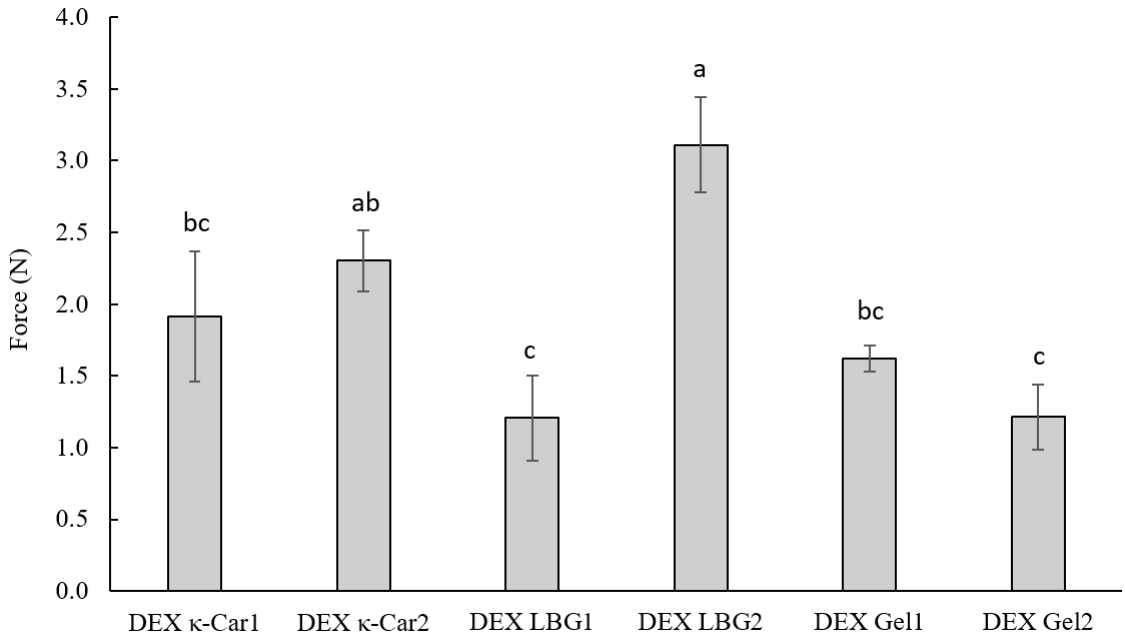

Figure 38. Bioadhesion behaviour of DEX-loaded formulations shown as maximum detachment force. Data are means ± SD (n=4). Means with different letters are significantly different ($p<0.05$).

As noted in Chapters 3 and 4, bioadhesion of κ-Car is due to its negatively charged sulphate groups interacting with the mucin layer through hydrogen bonding between sialic acid and the sulphate groups, in addition to physical entanglement with the hydrated flexible polymer (Menchicchi et al., 2015). Overall, incorporation of DEX enhanced bioadhesion of the cryogels compared with the TXA-loaded formulations (Chapter 4). The increase in maximum detachment force may be due to formation of secondary interactions between the carboxylic groups of mucin, the polymers and

DEX (Szilágyi, Mammadova, Gyarmati, & Szilágyi, 2020). Identification of these interactions require further investigation.

Chen, Yan, Yu, and Wang (2018) claimed that in general, mucoadhesion is limited for a mono-polymeric, hydrophilic drug delivery system such that hydrophilic drugs loaded in this system usually release rapidly in an aqueous environment. Blending polymers is a convenient method to optimise mechanical, bioadhesion and drug release characteristics of the system. In this study, LBG was used to improve bioadhesion of the DEX loaded formulations due to its synergistic effect with κ-Car (Harikrishnan et al., 2015; Prajapati et al., 2014; Vijayaraghavan et al., 2008). Blending 0.2% LBG with 1.5% κ-Car significantly enhanced bioadhesion of DEX LBG2, but 0.1% LBG did not show significant improvement in bioadhesion of DEX LBG1 compared to DEX κ-Car1.

The interactions between mucin and LBG is due to formation of a strong gel network between the non-ionisable hydroxyl groups of LBG form and glycoprotein of the mucin through hydrogen bonding (Prajapati et al., 2014); however, it may be concentration dependent. An increase in ratio of LBG may enhance bioadhesion to a certain level, but the other properties of formulations such as swelling ratio, mechanical properties and DEX release profile will also be altered.

Gel was added to the matrix to improve bioadhesion and facilitate erosion if faster DEX release and erosion were required. However, the 1 and 2% Gel in DEX Gel formulations decreased bioadhesive property of the formulations and undesirably increased erosion rate. Sonawane and Patil (2017) reported that addition of Gel to κ-Car in high concentration improved bioadhesive force of their formulated extended-release palettes, but adversely affected this property in lower concentrations concluding the effect of Gel on bioadhesion depends on the concentrations of both, κ-Car and gel. It is worth to note that these researchers used the minimum total polymer concentration of 20%. Therefore, in case of the current research, Gel is not a suitable polymer for improvement of bioadhesion, but LBG can be a suitable candidate for this purpose.

5.5.7 Fourier transform infrared (FTIR) spectroscopy

The presence of DEX in the biopolymer matrix may cause chemical interactions between the drug and its carrier that might be revealed by FTIR (Figure 39). In the FTIR spectrum of DEX powder, the bond at 848 cm^{-1} indicated the C–F stretching mode of dexamethasone phosphate. The peaks at 980, 1120 and 1650 cm^{-1} were depicted for strong C=C bending, strong C–O stretching and C=O stretching of DEX, respectively (S. Silva, Duarte, Mano, & Reis, 2013). Spectra of cryogel formulations (DF and DEX-loaded) demonstrated the presence of κ-Car in the matrix with peaks of the C–O–SO_3 at 848 cm^{-1} and the band for –CH_2 rocking from 3,6-anhydride-galactose unit at 928 cm^{-1} (Croitoru et al., 2020; Fan et al., 2011). Also, the peak at 1263 cm^{-1} can be assigned to the stretching vibration of ester sulphate group of κ-Car (Bajpai & Daheriya, 2014). The bands at 1539 and 1654 cm^{-1} in DF Gel1 and DEX Gel2 were depicted for N–H and C–N vibration and stretching vibration of C=O and C–N of gelatine (Derkach et al., 2018).

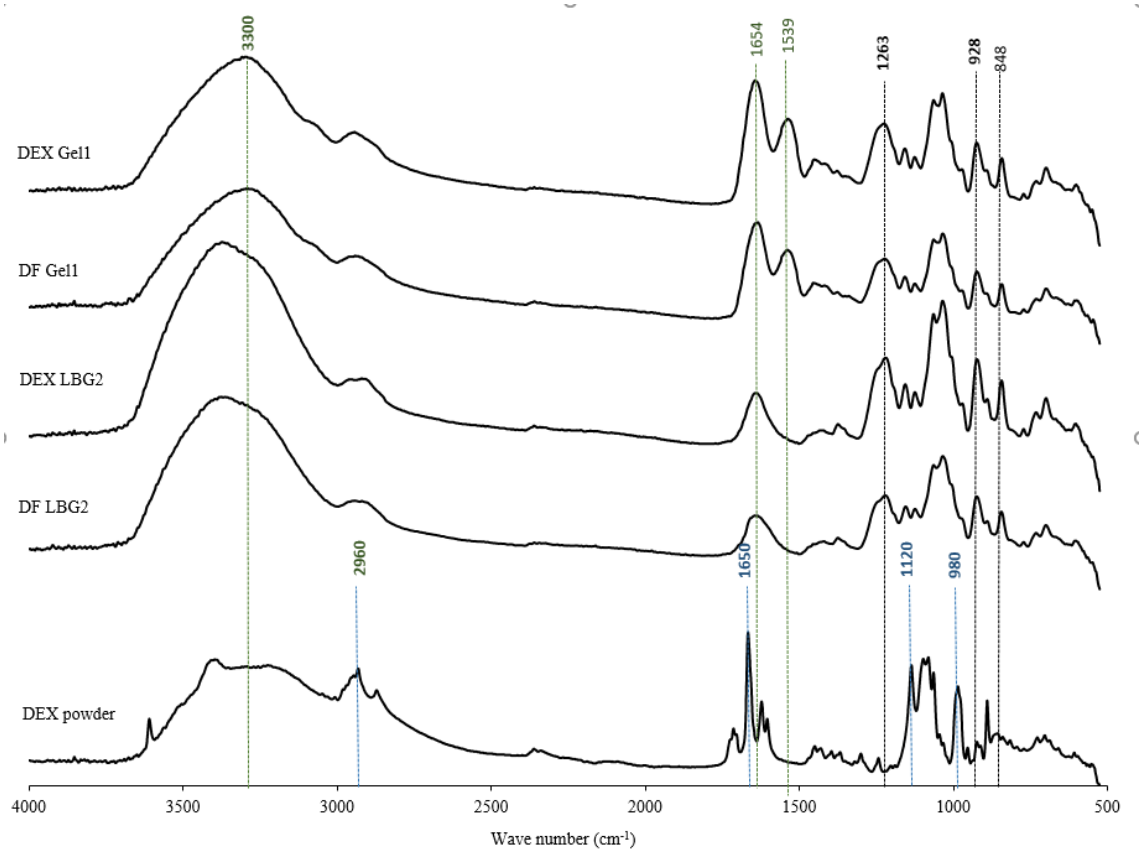

Figure 39. FTIR analysis of Pure DEX powder, DF and DEX loaded formulations

Comparison of FTIR spectra in DF and DEX-loaded formulations showed that there is no evidence of new bands or shift of wave number in DEX-loaded formulations that

could be attributed to chemical interactions between the drug and biopolymers in the carrier matrix, or the peaks were low and masked by the main peaks at the DEX concentration used for this study.

5.5.8 Total DEX content and in vitro drug release studies

The DEX content of each cryogel formulation was measured by LC-MS. The drug content of each nasal pack after complete dispersion in PBS was calculated (Table 11) based on the syringe dimensions of 14 mm diameter × 30 mm height (volume of 4.62 mL). The differences could be due to the polymer concentration, a systematic variation in size of the extruded hydrogel cylinders and/or systematic errors in recovery and analysis.

Table 11. Measured total DEX content of loaded formulations

Formulation	Total TXA content (mg)
DEX κ-Car1	7.36 ± 0.54
DEX κ-Car2	7.28 ± 0.15
DEX LBG1	6.73 ± 0.24
DEX LBG2	7.06 ± 0.25
DEX Gel1	5.80 ± 0.07
DEX Gel2	5.62 ± 0.21

In vitro DEX release from the five formulations was monitored over 33 hours (Figure 40). Release of DEX in all the formulations was sustainable with no burst release suggesting that most DEX was inside the pores or binding to the polymers of the matrix (Pastor, Reguera, Matveeva, & Garcia-Fuentes, 2015). Drug release was controlled and less than 50% of the total drug content was released within the first 8 hours with highest release from DEX κ-Car1, DEX κ-Car2 and DEX Gel2.

The initial release can be attributed to the release of the drug from high surface area of the formulations. The slower release rate of the drug after 8 hours was attributed to the slower diffusion of PBS into the smaller pores and slower counter diffusion of the drug to the PBS (Jie Li et al., 2018).

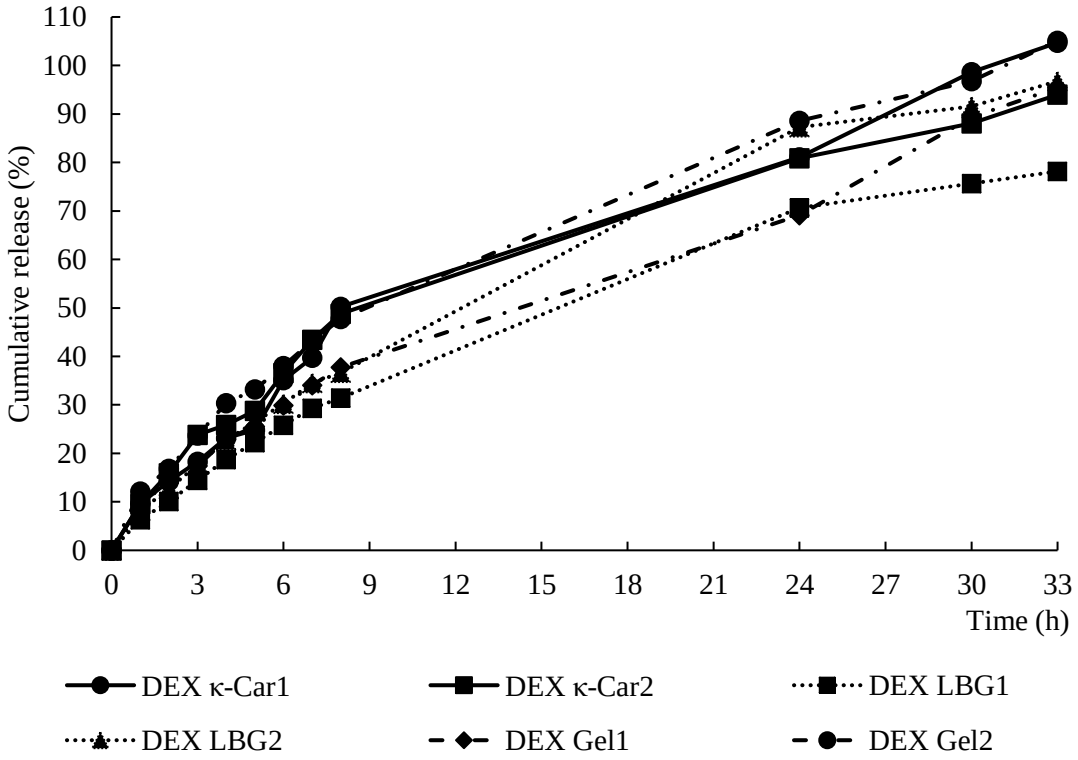

Figure 40. Cumulative release of GFX in drug loaded formulations. Data are means of tripliactes. Standard deviations have been omitted for clarity.

It was expected that an increase in polymer content in formulations would slow the release rate. Contrary to expectations, both DEX LBG1 and DEX Gel1 showed a slower release profile than DEX LBG2 and DEX Gel2. The faster release rate in DEX LBG 2 and DEX Gel2 might possibly be due to higher concentrations of hydrophilic polymers (1.5% κ-Car and 0.2% LBG or 2% Gel) leading to faster absorption of PBS and diffusion of DEX to the dissolution medium, but this model conflicts with the swelling results in Figure 37. DEX LBG1 and DEX LBG2 followed similar release rate in the first 8 hours, however, the release rate from DEX LBG1 slowed after 8 hours. The continuous constant release rate in DEX LBG2 might be due to the homogenous porous structure observed by microscopy (Figure 35 d).

Inspection of internal micrographs of the formulations in Figure 35 showed homogenous pore structures in DEX LBG2 and DEX Gel2, a morphology not observed in DEX LBG1 and DEX Gel1. The presence of large voids towards the edge and smaller voids towards the centre in DEX LBG1 probably explains the slow rate of release after 8 hours. In this scenario in the first 8 hours the drug was released from the surface and lateral large voids but release of the drug after 8 hours from the smaller pores in

the compact central area was slower. In DEX Gel1, the internal compact area with smaller lateral voids caused slow diffusion of DEX into the dissolution medium explaining the slower rate of release than DEX Gel2 in the first 24 hours. It seems possible that pore heterogeneity of DEX LBG1 and DEX Gel1 does not influence swelling rate of the cryogels much, but has a greater effect on the rate of drug diffusion from the matrix (Pastor et al., 2015).

Comparison of TXA release in Chapter 4 and DEX release in this chapter strongly suggests that the type of drug can extensively influence physical characteristics of the formulation and its release profile. TXA is a hydrophilic drug with very low degree of lipophilicity (log P=0.3), while DEX (log P=1.83) has a high degree of lipophilicity. This property of DEX leads to a prolonged release of the drug into the aqueous dissolution medium (PBS) compared to a rapid release of TXA from the same matrices (Sawant, Luu, Ye, & Buchta, 2010). The evidence from that study and the current study confirms that hydrophilic drugs in hydrophilic polymer systems are more suitable for fast release applications and that lipophilic drugs in hydrophilic polymer systems result in prolonged release applications.

Mathematical models of in vitro drug release behaviours are used to define the drug release mechanism is a drug delivery system (Paolino et al., 2019). In general, the drug release from a polymeric system can be described by two phenomena: the swelling phenomenon occurs when the solvent penetrates the polymeric dry matrix to hydrate and swell it by increasing its thickness or diameter. The second phenomenon is disentanglement and erosion of the polymer due to swelling and diffusion of the drug presented in the matrix.

To evaluate DEX release kinetics in the DEX-loaded formulations the in vitro drug release profile of DEX-loaded formulations was fitted into the equations of different mathematical models using Kinet DS 3.0 software (Mendyk et al., 2012) and the R^2 values extracted (Table 12). The highest coefficient determines the most likely mathematical model that follows drug release kinetics (Gouda et al., 2017). Overall, the investigated models were ranked in the following order:

Korsmeyer-Peppas > Zero order > Hixon-Crowell > Higuchi > First order

Based on the comparison of correlation coefficients (R^2), drug release in all the formulations was best fitted in Korsmeyer-Peppas and zero-order models.

In Korsmeyer-Peppas model, the mechanism of release can be analysed by the release exponent (n). When diffusion rate of the release medium (PBS) is slower than the rate of polymer relaxation, n = 0.5 (Fickian diffusion) and the transport is controlled by diffusion rate. When the polymer relaxation (erosion) is slower than the diffusion rate, n = 1 and the diffusion and transport is controlled by rate of polymer relaxation. In the case of 0.5 < n < 1, the transport is controlled by both rates of diffusion and polymer relaxation (Bruschi, 2015; Lisik & Musiał, 2019).

Table 12. R2 values of data fitted to mathematical drug release models. Shaded values show the top values for the best fitted model.

Formulation	Zero-order	First-order	Higuchi	Korsmeyer-Peppas		Hixon-Crowell
	R^2	R^2	R^2	R^2	n	R^2
DEX κ-CAR1	0.964	0.801	0.852	0.982	0.69	0.876
DEX κ-CAR2	0.951	0.757	0.934	0.981	0.64	0.844
DEX LBG1	0.976	0.804	0.825	0.995	0.73	0.890
DEX LBG2	0.980	0.829	0.818	0.998	0.72	0.907
DEX Gel1	0.988	0.855	0.867	0.996	0.66	0.923
DEX Gel2	0.967	0.805	0.942	0.994	0.62	0.880

The Korsmeyer-Peppas model is that release of the drug is the result of simultaneous diffusion of the dissolution medium into the matrix and erosion of the polymer-drug matrix (Kumar, Singh, Prajapati, & Singh, 2012). Observation of DEX-loaded formulations during the release period showed diffusion of PBS into the cryogel matrix and swelling of more than 80% in the first two hours of exposure to PBS leading to DEX release from the surface of the formulations. During this period, the polymer-drug matrix structure became relaxed. Disintegration and erosion of the formulations were observed in all formulations during the entire release period.

Regarding the type of transport, the n values were between 0.62 and 0.73 for all formulations. These values are characteristic of non-Fickian diffusion suggesting that both drug release mechanisms – diffusion and erosion – are involved in release kinetics with diffusion as dominant phenomenon. Comparison of n values within the formulations indicated that addition of gelatine did not change the kinetic release mechanism. This model agrees with the observations and drug release from similar drug-polymer hydrogels (Bacaita, Ciobanu, Popa, Agop, & Desbrieres, 2014; Saidi, Dabbaghi, & Rahmani, 2020; Varshosaz & Hajian, 2004)

5.5.9 Matrix erosion determined by cryogel dry weight

Gradual erosion of the drug-loaded cryogels within the desired therapeutic period is one of the major properties of the novel nasal pack matrix developed in Chapter 3. This property eliminates physical removal of the pack and possible complications after removal. In the other hand, the results of drug release in this current study indicated that this matrix can successfully confine the anti-inflammatory drug, DEX, and release it in a prolong controlled manner. Diffusion and matrix erosion are common mechanisms applied in evaluation of drug release from biopolymeric drug delivery systems. Erosion is physical dissolution of the polymer matrix due to hydrolysis of molecules and bonds in the polymer backbone that results in breakdown of the polymer chains and fragmentation of the matrix (Rabin & Siegel, 2012). Matrix erosion of DEX-loaded formulations were studied and reported in Figure 41.

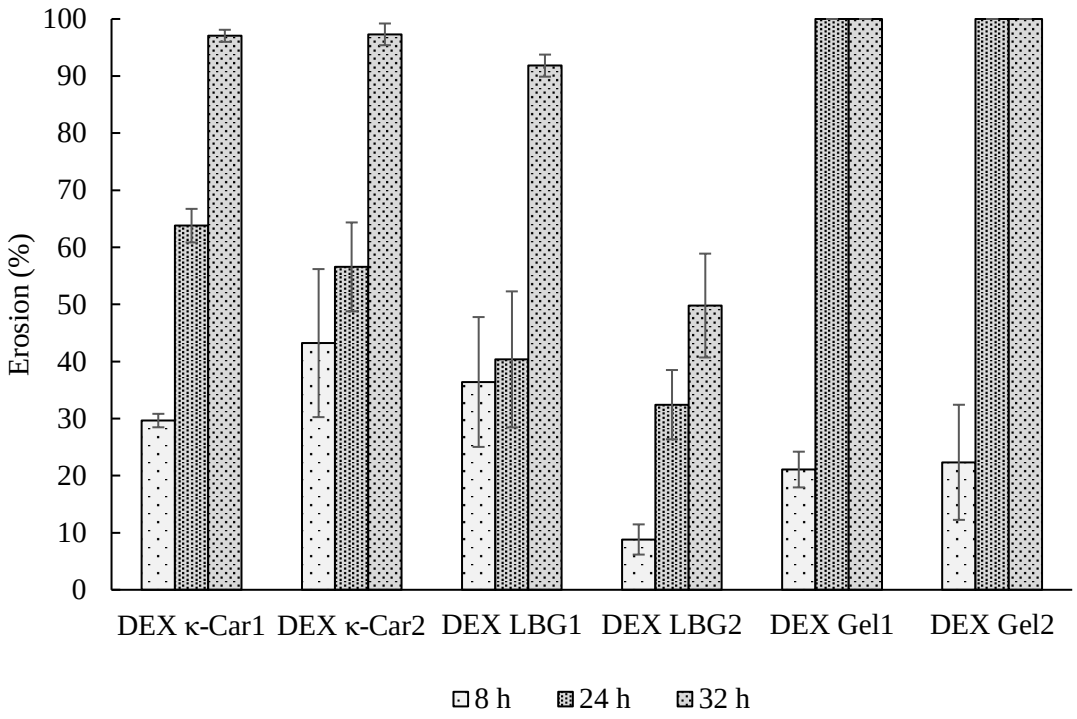

Figure 41. Erosion profile of DEX-loaded formulations in PBS medium (pH 7.4) at 35 ± 2˚C. Values are means ± SD (n=3)

All the formulations experienced various degrees of erosion after 8, 24 and 32 hours. DEX Gel formulations were 100% eroded in 24 hours, while DEX LBG formulations lost less than 40% of their weight in the same period. The sustainable release of DEX in Figure 40 and erosion profile of the formulations in Figure 41 suggests that DEX κ-Car and DEX LBG formulations followed surface erosion mechanism (Rabin & Siegel, 2012) and the drug was progressively released by gradual surface erosion and reduction in size of the cylindrical matrix. Even surface erosion was observed in DEX κ-Car formulations due to their homogenous surface erosion resulted from the single polymer matrix. DEX LBG formulations showed irregular surface erosion that can be due to incorporation of two biopolymers into the matrix resulting in a heterogeneous structure.

The appearance of DEX Gel formulations and weight loss during swelling proposed that these formulations experienced bulk erosion (Rabin & Siegel, 2012) because the cylindrical shape of the matrix was collapsed and fragmented into chunks after 8 hours, then the small fragments were released into the medium causing weight loss. The swelling results (Figure 37) agree with this event.

5.6 Summary and conclusion

In Chapter 4 of this thesis, TXA-loaded formulations were developed and characterised for intranasal drug delivery. The outcomes of this study revealed that the developed matrices are suitable for rapid intranasal delivery of TXA, when excessive bleeding cannot stop by conventional interventions.

In this chapter, feasibility of the cryogel formulations for sustainable extended release of DEX was investigated. The DEX used in this study was water soluble (due to presence of phosphate) and hydrophobic (log P = 1.83). This drug is generally used in postoperative intranasal treatments to reduce inflammation of the mucosa. The outcomes of this study indicated that the hydrophobicity of the drug incorporated into the matrix of hydrophilic biopolymers caused sustainable release of the drug for 33 hours. All the six formulations were able to release the drug within this timeframe, however, DEX κ-Car2 stood out as the most suitable matrix due to its bioadhesion value, rate of release in the first 8 hours eliminate excessive inflammation, and erosion rate by the end of 33 hours. The only deficiency of this formulation was low the swelling ratio, but it did not adversely influence the DEX release compared with the other formulations.

Taken together, these results suggest that the DEX κ-Car formulations are the most suitable carriers for extended sustainable release of DEX. To prolong the release and improve the physical and mechanical properties of the DEX-loaded formulations use of cross-linkers or other excipients can be suggested.

Chapter 6 Gatifloxacin-eluting nasal pack: a system for local drug delivery

6.1 Introduction

Surgical removal of inflamed and infected mucosa from the sinuses is the preferred method of treating chronic sinusitis and enhances delivery of topical medication to the infected mucosa in the nasal and paranasal cavity (Fokkens et al., 2012). However, the need for revision surgery is relatively high due recurrent sinusitis resulting from synechiae formation, turbinate lateralisation or blockage of the opened sinuses (Bugten, Nordgård, Skogvoll, & Steinsvåg, 2006; J. J. Xu, Busato, McKnight, & Lee, 2016). Additionally, persistent local inflammation and infection at the wound site can prolong the healing period and may lead to surgical failure (Grzeskowiak et al., 2019).

As described in the previous chapters of this thesis, a non-erodible or erodible nasal pack is often placed in the middle meatal cavity after endoscopic sinus surgery (ESS) to stop bleeding and prevent synechiae and turbinate lateralisation. However, prolonged treatment with nasal packs may cause overgrowth of bacteria from the infected sinus into and around the pack. It may also cause toxic shock syndrome (TSS) by an exotoxin produced by *Staphylococcus aureus*. Although TSS associated with nasal packing is not very common, its presentation usually appear within 48 hours after packing (Jackman & Fried, 2009) and may lead to recurrence of sinus infection which subsequently delays wound healing or increases the chance of revision surgery (Bhattacharyya, Gopal, & Lee, 2004; Khanna & Sama, 2019; Shikani, 1996). To minimise infection, systemic administration of prophylactic antibiotics is commonly prescribed but not always where nasal packing is applied (Biggs, Nightingale, Patel, & Salib, 2013; Derkay, Hirsch, Johnson, & Wagner, 1989).

Despite debates on the necessity and level of effectiveness of prophylactic antibiotics (Coughlan & Bhandarkar, 2015; Hauser et al., 2016; Ottoline et al., 2013) many clinical studies recommend systemic or topical use of antibiotics as a postoperative intervention. Local administration of antibiotics is preferred due to high local concentration of the drug at the target area and minimisation of side effects from systemic administration (Jonathan Liang & Lane, 2013).

Packing the nasal cavity with nasal packs is a very popular practice after ESS, but local antibiotic therapy during the packing period (when pack is in situ) is difficult or impossible, especially when non-erodible nasal packs are employed. To overcome

this limitation, several clinical studies have reported medication of nasal packs by immersion in an antibiotic solution prior to nasal insertion.

Shikani (1996) investigated the effects of immersing Merocel in a mixed solution of polymyxin, neomycin and the anti-inflammatory hydrocortisone prior to insertion. They showed a decrease in bacterial growth and reduced pain associated with pack removal. A similar study with gentamycin impregnated Merocel showed no significant difference from control Merocel for histopathologic inflammation, pain and discomfort. However, this antibiotic drug is not commonly used for inducing anti-inflammatory effect on the wound but did not cause any adverse effect on infection (Chang et al., 2011).

In contrast, a rodent study on management of chronic rhinosinusitis used ciprofloxacin loaded in an erodible gel (Pluronic F-127) showed negligible systemic and brain exposure to the drug. Moreover, the effective dose of ciprofloxacin was 40-fold less than required for systemic administration (Sousa, Alvesbc, Oliveiraa, Fortuna, & Falcão, 2017). A clinical study investigated the effect of mitomycin C-impregnated Merocel after surgery and observed positive outcomes for discharge, mucosal oedema and maintenance of ostial patency[5](Ramalingam, Parida, Saxena, & Surianarayanan, 2018). Another clinical study compared the effect of ciprofloxacin-soaked Nasopore (an erodible nasal pack) on synechiae formation and crusting after ESS. Observation of the wound site and a patient survey showed significant reduction in synechiae, improvement in wound healing and greater patient comfort (Grzeskowiak et al., 2019).

Although the outcomes of these studies show effectiveness of topical antibiotic delivery via immersion-impregnated nasal packs, this method is deficient in terms of dose control and sustained release, and thus availability of a drug up to treatment completion. Therefore, there is a need for development of controlled-release antibiotic-eluting nasal packs, especially erodible products.

In Chapters 4 and 5 of this thesis, the feasibility of loading and eluting TXA and DEX in the κ-Car cryogel matrix were investigated. These studies revealed that type of the

[5]Ostial patency is a measure of procedure durability for balloon sinus dilation and ESS.

drug and blending κ-Car with locust bean gum (LBG) and gelatine (Gel) can greatly affect physical properties and drug release profile of the nasal packs. In blending κ-Car with LBG, the release profile of TXA did not show a marked change but the swelling ratio increased, and erosion rate declined. In contrast, a blend of κ-Car and Gel reduced the swelling ratio and slowed the release of TXA. In DEX-loaded formulations, a blend of κ-Car with LBG showed similar effects to TXA formulations on drug release and erosion rates. In the other hand, blend of κ-Car with Gel did not affect drug release rates, but significantly accelerated erosion that would be undesirable for extended-release formulations.

Based on these two studies, although blends of κ-Car with LBG or Gel extended the release profile of the formulations, further extension of release was still desired.

To develop an antibiotic-eluting nasal pack, gatifloxacin (GFX) was used as the drug model and κ-Car was retained as the main constituent of the formulation due to its high hydrophilicity, desirable swelling ratio and erosion profile under physiological conditions.

To extend the drug release and matrix erosion of the formulations loaded with GFX, a blend of κ-Car with a second biopolymer was proposed. A literature review suggested agar could be a suitable candidate. Agar is another polysaccharide extracted from red seaweeds and is used in food and pharmaceutical industries due to its gelling and film forming ability, biocompatibility and biodegradability[6] (Ouyang et al., 2018). Agar and κ-Car have closely related chemical structures. Both are based on galactopyranose dimers, such as alternating galactose and 3,6-anhydro-α-galactopyranose units connected by alternating α-1,3 and β-1,4 linkages. The important difference between κ-Car and agar is that the 3,6-anhydro-α-galactopyranose units are D-configured in κ-Car but in agar are L-configured (Usov, 2011). These two biopolymers form hydrogels by helix formation and aggregation of the polysaccharide chains through inter-molecular hydrogen bonds, but κ-Car requires presence of anions (usually potassium ions) to form a stable three-dimensional network (Schafer & Stevens, 1995).

[6] This was the expression used in that publication but without further definition.

Blends of κ-Car and agar hydrogels have been reported in development of dye-absorbent hydrogel composites (Duman, Polat, Diker, & Tunç, 2020), hydrogel films for food packaging (Rhim & Wang, 2013), and a drug loaded hydrogel (Liu, Lin, Li, & Liu, 2005). These studies revealed that addition of agar to κ-Car increased swelling ratio and improved mechanical properties of the hydrogel, followed by a desirable extended drug release.

This chapter describes incorporating an antibiotic model drug, gatifloxacin (GFX), into the κ-Car cryogel matrix with and without agar addition. It was hypothesized that a blend of κ-Car and agar in the drug carrier formulation would improve the physical characteristics and drug release profile compared with the κ-Car control.

6.2 Materials

Food-grade κ-Car powder (Gelcarin® GP 911) containing 3.8% potassium and 2.5% calcium cations and agar powder (Agar agar *Gracilaria* type 8925Q min 900) were kindly donated by Hawkins Watts Ltd. (Auckland). Authentic gatifloxacin (purity > 0.99%) (GFX) (log P = 1.81) was donated by the School of Pharmacy, University of Auckland. Mucin from porcine stomach (type III, bound sialic acid 0.5-1.5%) was purchased from Sigma Aldrich. Ultrapure water was used for preparation of hydrogels. All reagents were analytical grade.

6.3 Methods

6.3.1 Preparation of GFX-loaded cryogels

Six formulations were prepared (Table 13). The GFX κ-Car1 and GFX κ-Car2 formulations were made by addition of 1.5 and 2 g κ-Car to 90 mL of water heated to 85˚C with constant magnetic stirring until a transparent hydrosol was obtained. GFX solution was prepared by adding 120 mg of the drug powder in 10 mL of water and 100 µL HCl (0.01 M) to dissolve the drug. The drug solution was thoroughly mixed with the κ-Car hydrosol. Other formulations (GFX AGAR1 through GFX AGAR4) were comprised of the two biopolymers in arbitrary concentrations prepared by a parallel method (Liu et al., 2005).

The drug-loaded hydrosols were subsequently cast in cylindrical polyethylene syringe barrels (30 mm long x 14 mm diameter) as described in Chapter 4. The assemblies

were kept at ambient temperature for 1 hour then stored overnight at 4°C to create hydrogels. The hydrogels were extruded, placed vertically on polystyrene tray and freeze dried under the following conditions: shelf temperature, 2°C; temperature on refrigeration coils, -70°C; and vacuum 120 mbar in an AdVantage Pro freeze dryer, SP Scientific). The cryogels were stored in plastic bags and placed in a vacuum desiccator at room temperature.

Table 13. Composition of drug-loaded formulations

Formulation	κ-Car (g)	Agar (g)	Water (mL)	GFX (mg)
GFX κ-Car1	1.5	0	100	120
GFX κ-Car2	2.0	0	100	120
GFX AGAR1	1.5	0.2	100	120
GFX AGAR2	1.5	0.4	100	120
GFX AGAR3	2	0.1	100	120
GFX AGAR4	2	0.2	100	120

6.3.2 Characterisation

The GFX-loaded formulations were characterised for their physicochemical and drug release characteristics using the following methods:

6.3.2.1 Microstructure analysis by scanning electron microscopy

Surface and cryo-fractured cross-sectional images of the GFX-loaded nasal packs were obtained using a Schottky field emission scanning electron microscope (SU-70, Hitachi) as described in section 3.2.3 of Chapter 3.

6.3.2.2 Mechanical properties of cryogels

Texture profile analysis of hardness, springiness and cohesiveness was evaluated using a TA.XT plus texture analyser (Stable Micro System) as described by D. S. Jones et al. (1997) and Thirawong et al. (2007) following the fully procedures in section 3.2.3 of Chapter 3.

6.3.2.3 Porosity measurement

The porosity of GFX-loaded cryogels were determined by a solvent replacement method (Nanda et al., 2013) as described in section 3.2.3 of Chapter 3.

6.3.2.4 Swelling ratio determined by cryogel wet weight

The swelling ratio of GFX-loaded nasal cryogels inserts in phosphate buffered saline (pH 7.4) was determined at 35 ± 2˚C in water bath using a gravimetric method (Khurma et al., 2006) following the procedure described in Section 3.2.3 of Chapter 3.

6.3.2.5 pH

The pH of the GFX-loaded hydrosol formulations was measured at 40˚C using a pH meter as described in Chapter 4.

6.3.2.6 In vitro bioadhesion studies

Bioadhesion measurements to mucin were performed using the TA.XT analyser adapting the methods of Boateng et al. (2013) and Şenyiğit Zeynep et al. (2014) as described in Chapter 4.

6.3.2.7 Fourier transform infrared (FTIR) spectroscopy

To characterise the presence of specific chemical groups in the GFX-loaded cryogel formulation, FTIR spectra were obtained using a Nicolet iS10 FTIR spectrophotometer (Thermo Scientific) in attenuated total reflectance mode using a diamond crystal. Experimental details are described in section 4.2.2 of Chapter 4.

6.3.2.8 Total GFX content and in vitro drug release studies

The content of GFX within the GFX-loaded cryogel formulations was determined after soaking the cryogel formulations in 100 mL of PBS (pH 7.4) at 35˚C with overnight stirring in the not unreasonable expectation that the drug would completely dissolve. The solutions were centrifuged and filtered to remove the any remaining gel particles. The concentration of GFX in PBS was determined by LC-MS as described below.

In vitro GFX release from the cryogel formulations was studied in PBS buffer (pH 7.4) under sink conditions over 48 hours following the procedure described in section 4.2.2 of Chapter 4.

Authentic GFX was used as standard and drug free cryogel formulations were used as controls.

6.3.2.9 GFX determination by LC-MS

GFX determination by LC-MS used an Agilent 1260 Infinity Quaternary LC System (Agilent, USA) fitted with a Waters XSelect CSH C18 (2.1 x 100mm, 3µm) and a diode array detector connected to a 6420 triple quadrupole LC-MS system (G1978B). The mobile phases were water containing 0.1% (v/v) formic acid (A) and acetonitrile containing 0.1% (v/v) formic acid (B). The initial condition was 90:10 (A:B). From 0 to 3 min the ratio changed to 10:90 and from 4 to 5 min the 90:10 ratio was restored and maintained to 10 min. The injection volume was 1 µL and the retention time for GFX was 3.51 min (Figure 42).

The MS ionisation conditions were as follows: capillary and charging voltage of 2 kV, drying gas temperature of 250 °C, drying gas flow of 6 L/min. The positive electrospray ionisation mode was performed with multiple reaction monitoring for quantitative analysis.

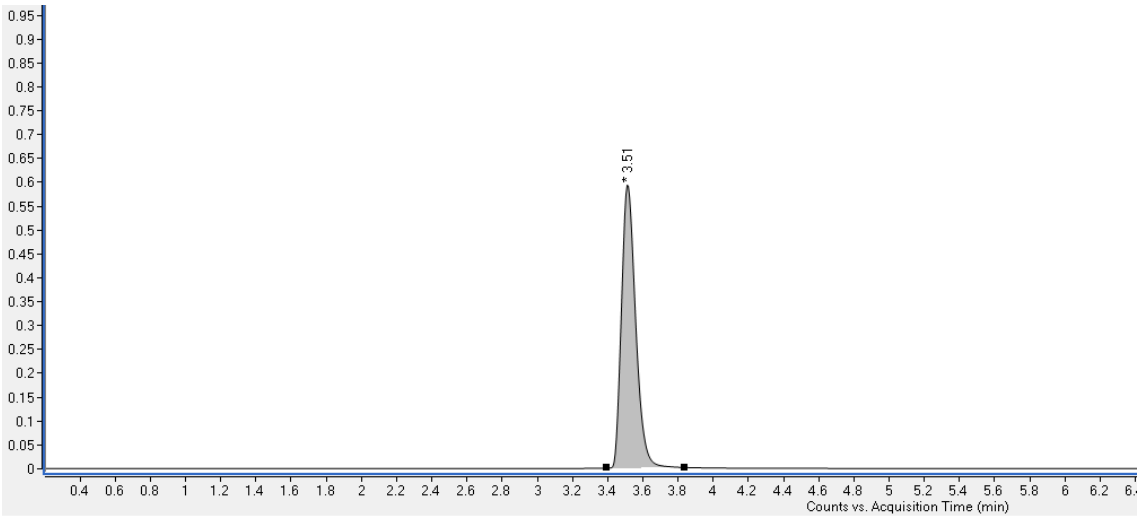

Figure 42. Representative chromatogram for GFX (retention time: 3.51 min)

A series of calibration standard solutions of 1 to 100 µg.mL^{-1} GFX were injected (1 µL) and a calibration curve was obtained based on the peak areas and concentrations of the standard solutions (Figure 43).

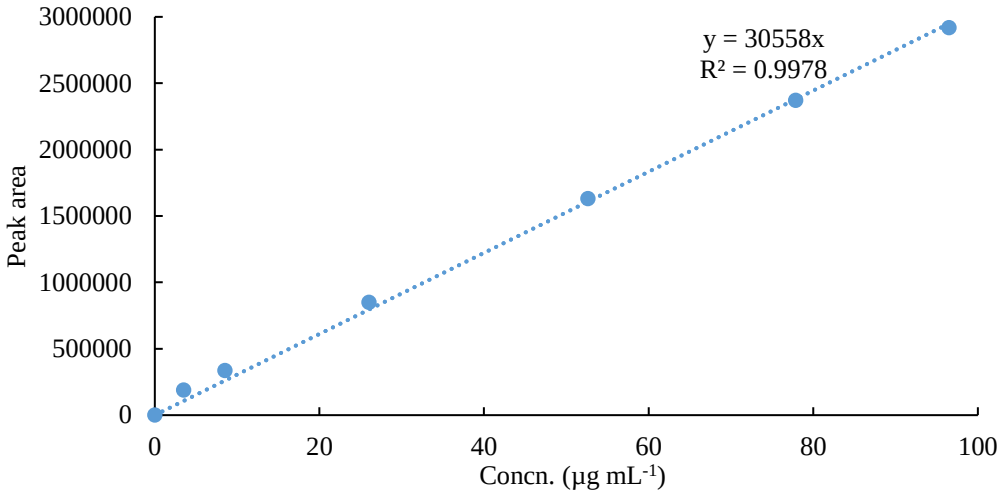

Figure 43. Calibration curve of GFX (Plot of peak areas versus concentrations)

6.3.2.10 Release kinetics

Release kinetics and thus the mechanism of GFX release from cryogels were studied and data fitted to the kinetic models proposed in Chapter 5.

6.3.2.11 Matrix erosion determined by cryogel dry weight

Erosion of GFX-loaded cryogels was determined as described in section 4.2.2 of Chapter 4.

6.3.2.12 Antimicrobial activity of GFX-loaded formulations

Antimicrobial activity of GFX-loaded formulations was performed using agar-disc diffusion assay against *Escherichia coli, Bacillus subtilis* and *Staphylococcus aureus*. In this method, the bacteria were inoculated in 5 mL of standard nutrient broth and incubated at 35˚C for 48 hours. Sterile plates of standard nutrient agar were used to culture all these bacteria. Blood agar was also used for *S. aureus*. The bacterial cultures were surface spread on agar plates by a standard method.

Thin disks (2 mm height) of each formulation (diameter 1.4 mm) were sterilized with ultraviolet light at 365 nm (UVP3UV ™ lamp, Analytic Jena) for 3 minutes on each side. The dry discs were then dipped in sterile deionized water to facilitate drug release and placed at the centre of triplicated inoculated agar plates and incubated

at 35˚C for 48 hours. Drug free formulations were the controls. The plates were subsequently observed and measured for inhibition zones around the discs.

6.4 Statistical analysis

Data were marshalled using Excel then analysed for one-way variance using the ANOVA routine in XLSTAT (Addinsoft) with Tukey's multiple range test.

6.5 Results and discussion

6.5.1 Macro and microstructure by inspection and scanning electron microscopy

The macrostructure of the GFX-loaded cryogel formulations were observed unaided and photographed (Figure 44). All formulations were visibly dry after freeze-drying and were pale yellow due to the yellowish colour of GFX. There were no longitudinal cracks on the surface of the GFX-loaded cryogels and all were much the same in appearance. All the four GFX AGAR formulations exhibited minor superficial wrinkles and rough, porous external surface (refer to GFX AGAR2 in Figure 44 b). The surface roughness by increase in agar concentration was only felt by rubbing the finger on the surface of cryogel and could not be detected by conventional photography. The surfaces of GFX κ-Car1 and GFX κ-Car2 were smooth without wrinkles seen by naked eyes (Refer to GFX κ-Car2 in Figure 44 a).

GFX AGAR3 and GFX AGAR4 showed the greatest diameter shrinkage, 11% of the original hydrogel diameter determined by syringe internal diameter. This shrinkage was consistent with the development of wrinkles. Diameter shrinkage in GFX AGAR1 and GFX AGAR2 was only 5% but the smooth GFX κ-Car formulations did not show any shrinkage.

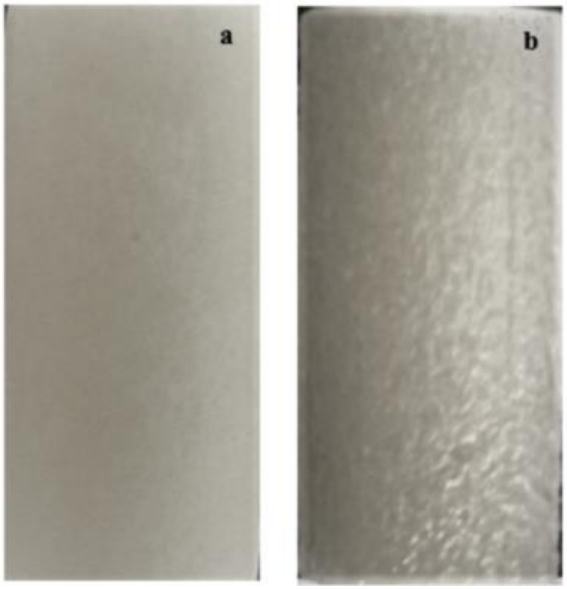

Figure 44. Smooth superficial surface of GFX κ-Car2 (a) and wrinkled superficial surface of GFX AGAR2 (b). This wrinkled surface was observed in all the GFX AGAR formulations.

In terms of macrostructure, the internal mid-sagittal and transverse views of the formulations showed slightly different morphologies. These sections in GFX κ-Car1 and 2 showed a spongy texture with a denser area at around the core of cylindrical GFX κ-Car1 and 2, and GFX AGAR2 (look at the centre of their midsagittal views in Figure 45 a) particularly in GFX AGAR2. The reason for formation of these texturally different regions is unknown, but it is likely to be caused by the kinetics of drying. However, the entire internal texture of GFX AGAR1, 3 and 4 formulations was uniformly spongy.

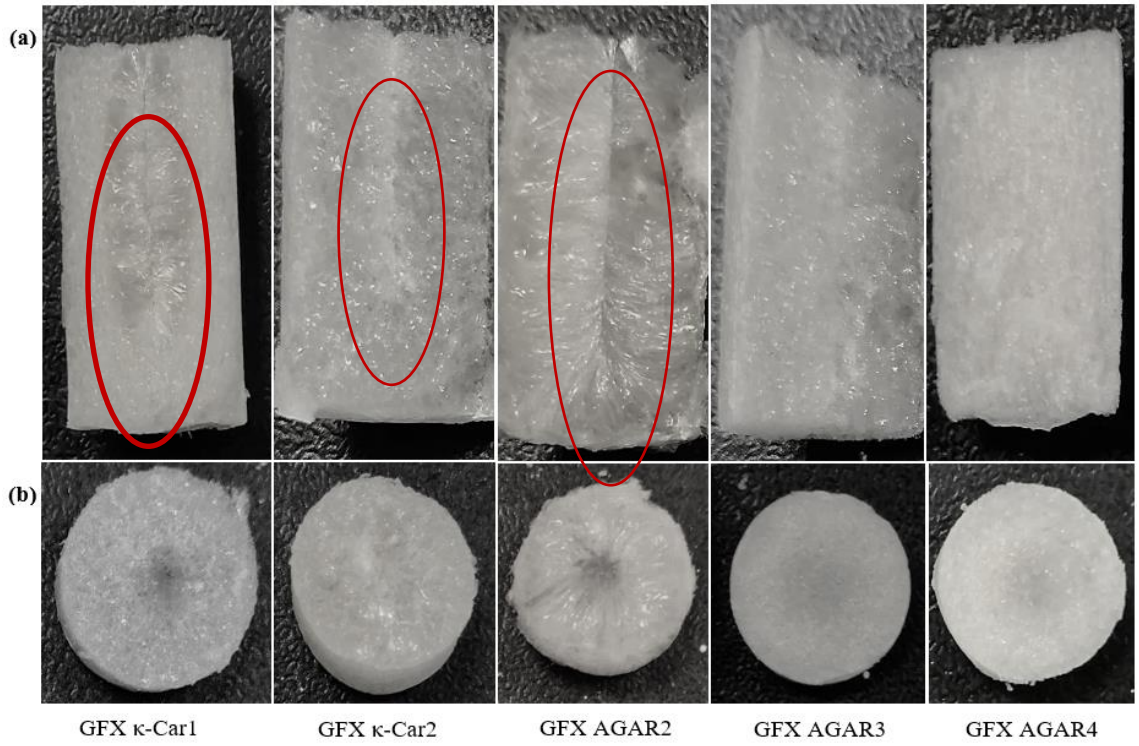

Figure 45. Macrographs of mid-sagittal (a) and transverse (b) views of GFX formulations. GFX AGAR1 (not shown) had very similar structure to GFX AGAR3.

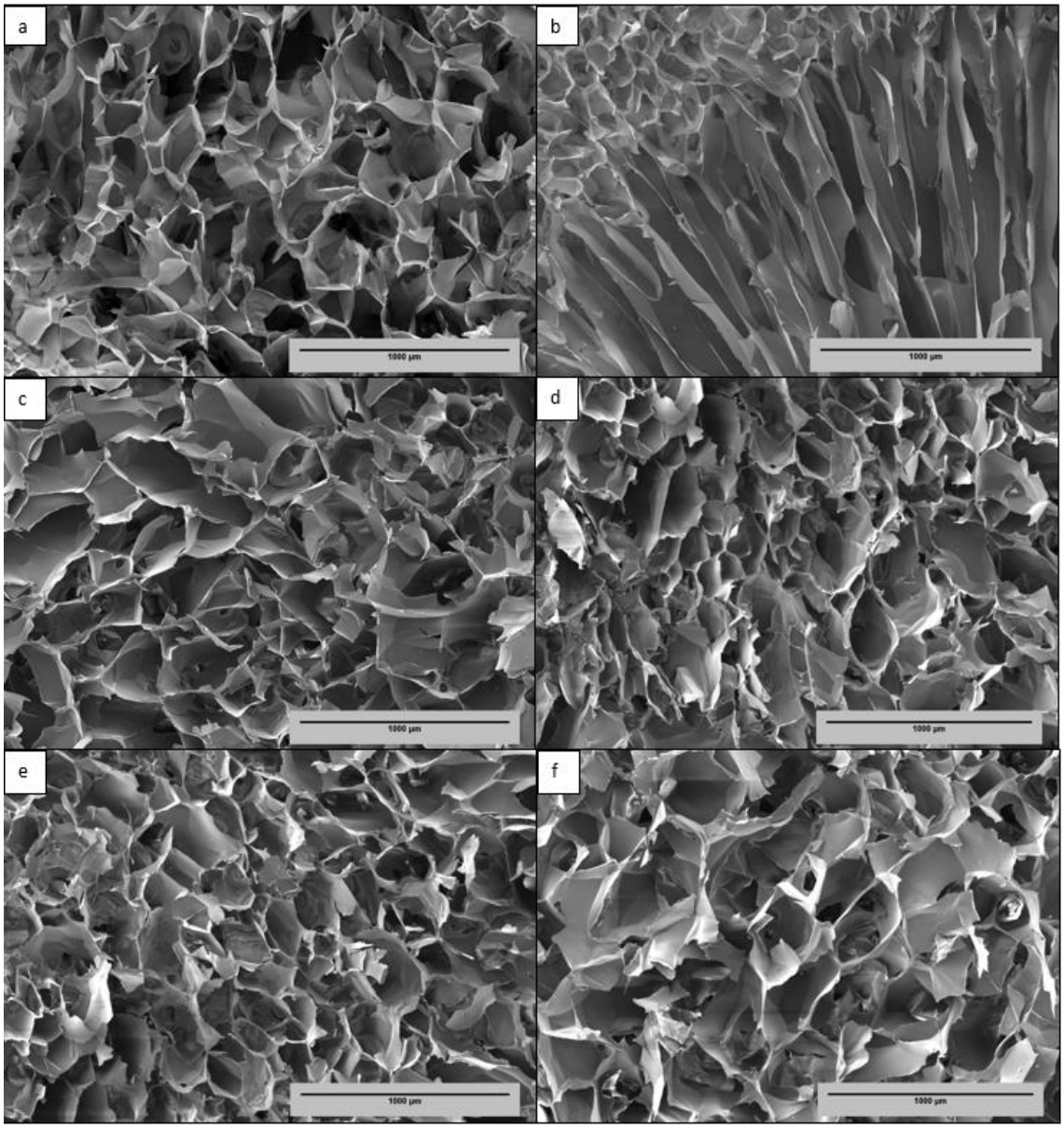

Figure 46. SEM images of cryo-fractured surface of a GFX k-Car1 (a), GFX k-Car2 (b), GFX AGAR1 (c), GFX AGAR2 (d) and GFX AGAR3 (e) and GFX AGAR4 (f). All images are identically scaled where the bar represents 1000 µm.

The internal microstructure of cryo-fractured GFX-loaded formulations external to the central axis are shown in Figure 46. A predominantly macropore range with broad pore size distribution was observed in all images. Drug-free κ-Car cryogels (in Chapter 3) showed a neatly ordered honeycomb structure with deep voids. Blending agar with κ-Car and addition of GFX prominently altered internal structures of GFX-loaded formulations to a denser spongy structure in random size and order. These porous architectures within the formulations were also reported by Duman et al. (2020) and provide absorption places for wound exudate.

6.5.2 Mechanical characteristics

Hardness, cohesiveness and springiness of the dry cryogel were measured using the TA.XT plus texture analyser. Table 14 indicated that GFX κ-Car1 (1.5% carrageenan) required 3.40 N whereas GFX κ-Car2 (2%) was at last twice as hard, showing the importance of polymer content. Blends of agar with κ-Car remarkably increased deformation resistance of the cryogel network, but the differences between GFX AGAR2, 3 and 4 formulations were statistically insignificant. This could be due to small absolute differences in their total polymer content (Table 13) but confounded by a difference in κ-Car content between AGAR2 and AGAR3/4. An increase in hardness of κ-Car and agar-blended cryogels with an increase in agar concentration was also reported by Zhao, Sun, Li, Dong, and Zhang (2020). It seems that high miscibility and blend compatibility of κ-Car and agar significantly increases hardness due to stronger interactions through hydrogen bonds between these two biopolymers (Rhim, 2012).

Table 14. Mechanical characteristics of GFX-loaded formulations. Different superscript letters within columns show significant Tukey differences ($p<0.0001$).

Formulation	Hardness (N)	Cohesiveness	Springiness (%)
GFX κ-Car1	3.40 ± 0.54^{a}	0.45 ± 0.02^{a}	81.45 ± 1.07^{a}
GFX κ-Car2	7.66 ± 0.96^{b}	0.39 ± 0.00^{b}	68.34 ± 1.02^{b}
GFX AGAR1	10.57 ± 0.43^{c}	0.38 ± 0.10^{c}	61.90 ± 1.68^{b}
GFX AGAR2	25.73 ± 1.55^{d}	0.36 ± 0.01^{d}	55.11 ± 2.28^{bc}
GFX AGAR3	25.51 ± 1.47^{d}	0.36 ± 0.01^{de}	55.76 ± 1.24^{bc}
GFX AGAR4	27.56 ± 0.84^{d}	0.32 ± 0.03^{e}	50.73 ± 2.29^{c}

Cohesiveness and springiness of the formulations decreased with increases in κ-Car concentrations with agar blends. In work on agar and κ-Car blends J. Zhao et al. (2020) showed an increase in κ-Car content improved springiness and cohesiveness, but an increase in agar content decreased these values. However, in this study, the total polymer concentration of the cryogels was fixed and the polymer ratios changed by 25% in each formulation. This conflict suggests that GFX can affect the cohesiveness and springiness of the formulations. A decrease in cohesiveness with an increase in polymer concentration has been reported by Sezer et al. (2008a) and Y. T. Tan, Peh,

and Al-Hanbali (2000) in development of chitosan film and carbopol [7] gel, respectively, but no literature information was found for κ-Car and agar blends.

An inverse but tending to flat relationship was found between hardness and springiness. The highest and lowest springiness values were respectively from GFX κ-Car1 (81.45%) and GFX AGAR4 (50.73%). However, the springiness values between the other formulations were not significantly different ($p > 0.05$).

6.5.3 Porosity measurement

The microstructure of GFX-loaded formulations (Figure 46) showed presence of numerous microscopic pores within the cryogel, presumably capable of absorbing wound exudate and subsequently releasing the drug.

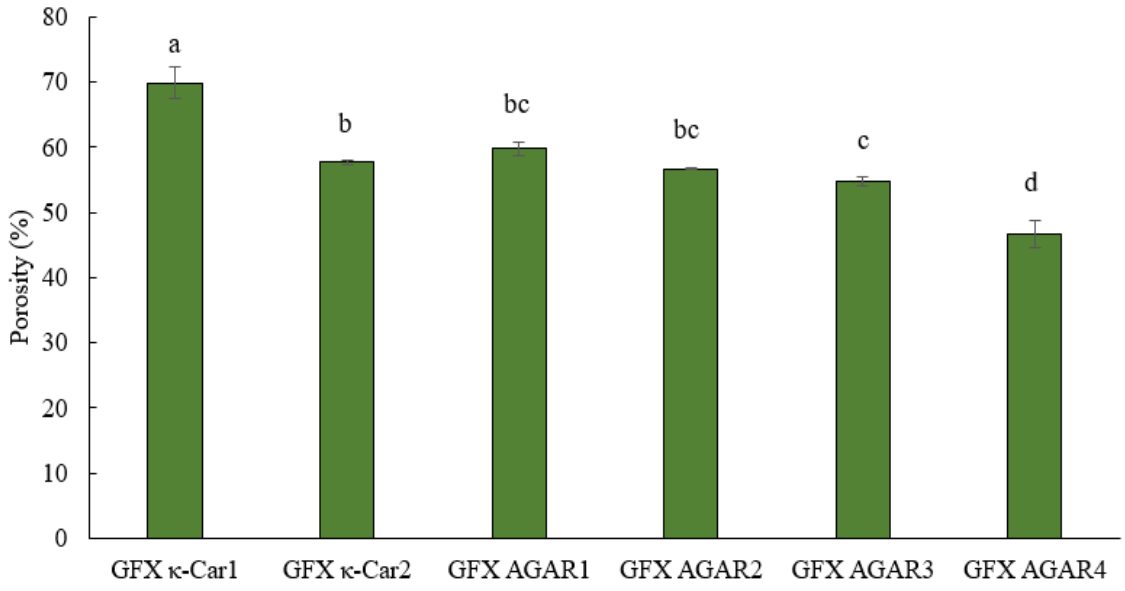

Figure 47. Porosity of GFX–loaded formulations. Data are means (n=3) ± SD. Means with different letters are significantly different (p<0.05).

Figure 47 shows the percent porosity of GFX-loaded formulations as determined by the cyclohexane method. There was an approximated inverse relationship between polymer concentration and porosity. GFX κ-Car1 with 1.5% polymer and GFX AGAR4 with 2.2% total polymer respectively had the highest (70%) and lowest (48%) porosities. All other formulations lay between these extremes, with varying

[7] Carbopol is a polyanionic carbomer used as thickener in making hydrogels

significant differences. Notably, porosity of GFX AGAR3 (0.1% agar) and GFX AGAR4 (0.2% agar) showed that doubling the agar concentration reduced porosity by 10%. A reduction in porosity by an increase in polymer concentration is apparently due to formation of more molecular entanglements between κ-Car and agar chains (J. Zhao et al., 2020), a denser structure and smaller hydrophilic pores that are unable to uptake the hydrophobic cyclohexane. However, hydrophilic wound exudate might penetrate with ease.

6.5.4 Swelling studies

Rapid swelling of the matrix of nasal pack is important because the swollen pack gently applies pressure on the wound site while absorbs the wound exudate to facilitate haemostasis. Also, the swelling of the pack fills the gap between the mucosa and the pack to make the drug accessible to the wound site. The formulations showed diverse swelling behaviour within the first 8 hours of swelling (Figure 48). Between 1 and 8 hours the most consistent high performer was GFX AGAR1. At all times GFX AGAR2 showed the least swelling ratio. What is the remarkable about these results is that doubling the agar concentration from 0.2 to 0.4% had such an adverse effect on swelling ratio of these two formulations.

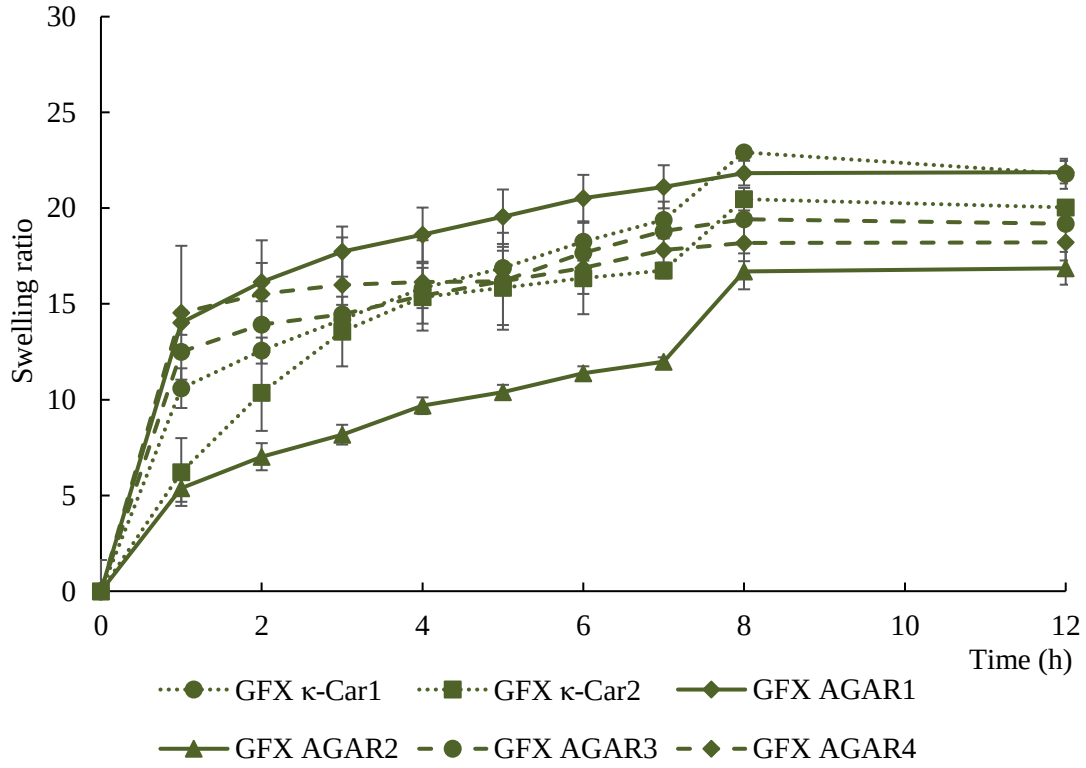

Figure 48. Swelling ratio kinetics of DEX loaded formulations at 35 ± 2˚C in PBS buffer. Values are means ± SD (n=3).

An abrupted swelling behaviour (sudden increase in swelling ratio) at time point of 7 hours was reported for GFX κ-Car1 and 2, and GFX AGAR2 that could be due to the swelling of the denser core area of these formulations (refer to Figure 45).

It was noted that all formulations exhibited signs of matrix erosion after 6 hours of swelling, but the weight gain due to water absorption exceeded weight loss from erosion. After 8 hours the swelling ratio became static possibly due to saturation of the matrix or an erosion rate matching the rate of swelling.

Swelling of the cryogels is attributable to penetration and diffusion of PBS through the hydrophilic polymer matrix and local relaxation of polymer segments. The rate of diffusion is limited by the rate of polymer relaxation and PBS penetration into the polymer matrix (Nanda et al., 2013). Addition of 0.2% agar to the κ-Car matrix facilitated diffusion of water into the polymer matrix, specifically in the first hour. Although κ-Car is more hydrophilic than agar (Gürkan Polat, Duman, & Tunç, 2020), the faster diffusion rate in agar containing formulations could be due to the presence of wrinkles on their external wall surface increasing the surface area, thus swelling of the matrix (Figure 44). However, the opposite effect was observed in GFX AGAR2

(0.4% agar) which could be because of the denser structure created by higher polymer concentration and more intramolecular bounds between κ-Car and agar (refer to the FTIR section of this chapter) making polymer relaxation and PBS penetration more difficult.

6.5.5 pH

The pH of the GFX-loaded hydrosols were in the range 5.85 to 6.75 (Table 15). The pH of the formulations increased when higher concentrations of κ-Car was used, or agar was added.

Table 15. pH of GFX-loaded formulations at 40˚C

Formulation	pH
GFX κ-Car1	5.8
GFX κ-Car2	6.7
GFX AGAR1	6.3
GFX AGAR2	6.4
GFX AGAR3	6.3
GFX AGAR4	6.4

The pH of these formulations is compatible with the olfactory mucosa in normal and CRS patients (pH 5.3 to 7.6), and it is not expected to irritate the intranasal membrane. Also, it is in the range of in situ nasal gels developed by Sherafudeen and Vasantha (2015) and Y. Wang et al. (2017).

6.5.6 Fourier transform infrared (FTIR) spectroscopy

The FTIR spectra of all the DF and GFX loaded formulations were collected and it was observed that both DF κ-Car formulations and both GFX κ-Car formulations showed the identical spectra. Also, DF AGAR cryogels in all the four concentrations of κ-Car and agar demonstrated identical spectra. The spectra of all the four GFX AGAR formulations were identical in terms of the peaks and their wave number. The FTIR spectra of formulations (Figure 49) were compared to understand the interactions between the two biopolymers of κ-Car and agar in the drug free (DF) cryogels: DF κ-Car2 and DF AGAR2 (Figure 49 a). Also, the interactions between the drug (GFX) and

the matrices were investigated by analysis of FTIR spectra of GFX, GFX κ-Car2, and GFX AGAR2 Figure 49 b and c).

In Figure 49 a, the peak at 850 cm^{-1} in the DF κ-Car2 cryogel is the of C–O–SO_3 stretching vibration in D-galactose-4-sulphate (Rochas, Lahaye, & Yaphe, 1986). The peak at 925 cm^{-1} is due to stretching vibration of C–O in polyhydroxy groups (Duman et al., 2020), the band at 1030 is vibration in the glycosidic linkage (C–O–C) of 3,6-anhydrogalactose, and the band 1149 and 1220 cm^{-1} are assigned for ester sulphate –S=O stretching (Croitoru et al., 2020). In addition, O–H bending vibration was located at 1647 cm^{-1}. The broad band in the region 2880 to 3000 cm^{-1} was assigned for C–H stretching vibration and the broad band in the 3140 to 3675 cm^{-1} region was related to the O–H stretching vibration (Duman et al., 2020). These peaks were also observed for DF AGAR2 meaning that the same bonds were present in this matrix due to the similar chemical structure of these two biopolymers.

The similarity of the drug-free κ-Car2 and drug-free AGAR2 is due to their very similar molecular chain structure (J. Zhao et al., 2020). A shift from higher frequency to lower frequency due to intermolecular interactions between κ-Car and agar combination was reported by Jumaidin, Sapuan, Jawaid, Ishak, and Sahari (2016), but was not observed in this study. Therefore, it is concluded that there was no chemical interaction between the κ-Car and agar and that these two compatible biopolymers produced a miscible polymer blend as proposed by Sarath, Shanks, and Thomas (2014).

The FTIR spectrum of pure GFX (Figure 49 b and c) showed main peaks at 820 cm^{-1} for C–H bending, 1273 cm^{-1} for –C=O stretching of –COOH (Patel, Chotai, & Nagda, 2012), 1320 cm^{-1} for C–N stretching and 1447 cm^{-1} for C–H bending of $–CH_3$. Also, the peaks on 1544 and 1630 cm^{-1} are assigned for aromatic stretching (Khurana, Arora, & Pawar, 2012).

Figure 49 b also compares the FTIR spectra of drug-free κ-Car and GFX κ-Car formulation to investigate chemical interactions of GFX and κ-Car. Inspection of these two spectra shows some changes in the GFX κ-Car spectrum indicating presence of GFX in the matrix. The small shift from 925 to 920 cm^{-1} can be due to formation of new hydrogen bonding after addition of GFX (stretching vibration of C–O) and the

shift from 1149 to 1159 cm^{-1} may indicate chemical interaction of ester sulphate group of κ-Car with GFX. In addition, a new peak at 1447 cm^{-1} corresponds to the C–H bending of $–CH_3$ in GFX and a shift from 1647 to 1630 cm^{-1} indicates the peak for aromatic stretching bonds of GFX at 1630 cm^{-1}.

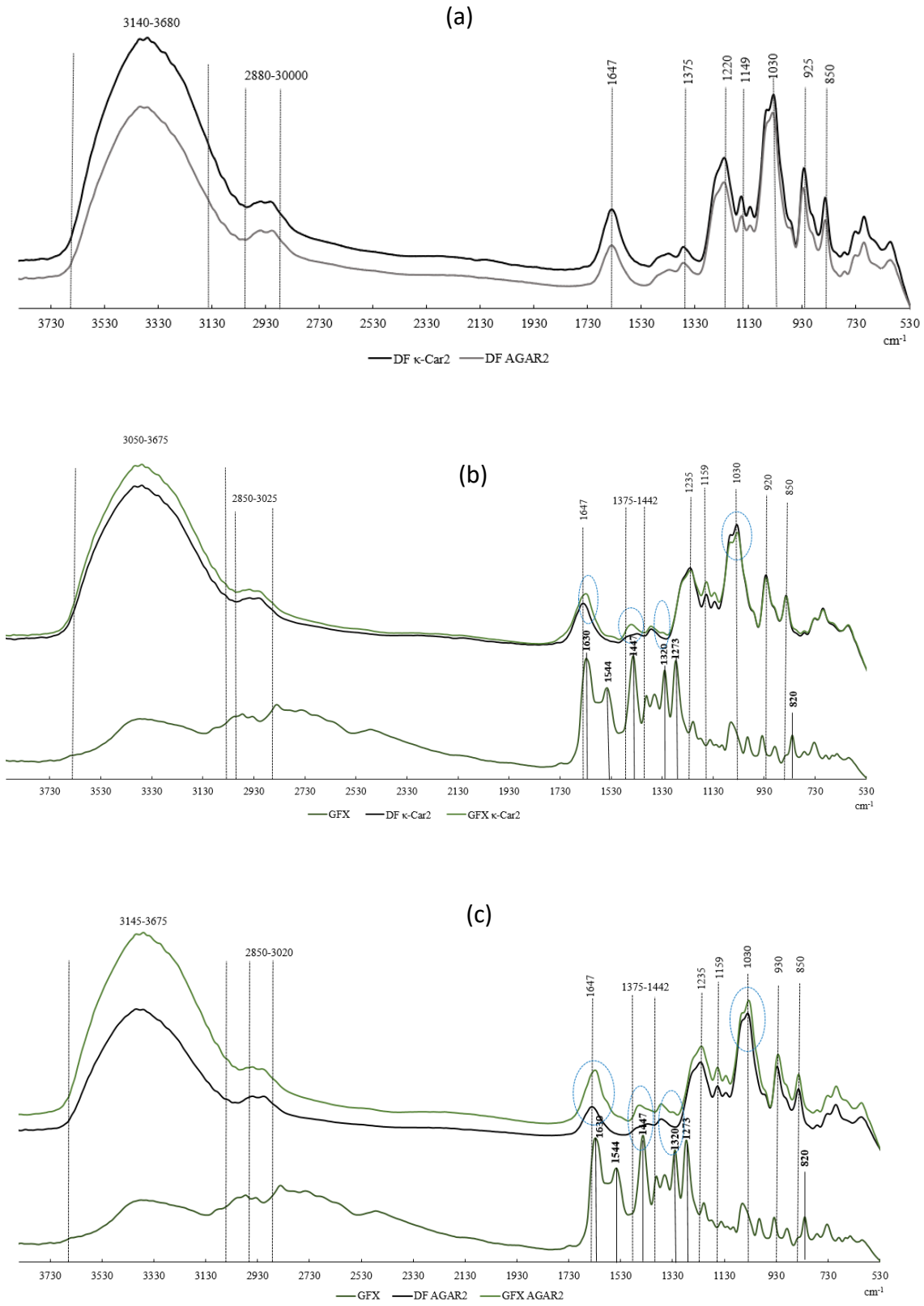

Figure 49. FTIR analysis of formulations. Graph (a) compares the FTIR spectra of drug free matrices containing κ-Car (DF κ-Car2) and κ-Car and agar (DF AGAR2). Graph (b) shows the FTIR spectra of the drug (GFX), DF κ-Car2 and its corresponding GFX loaded formulation. Graph (c) shows the spectra of the drug, drug free AGAR2 and its corresponding GFX–loaded formulation (GFX AGAR2).

The FTIR profile of GFX AGAR2 (Figure 49 c) was very similar to the GFX κ-Car spectrum indicating that agar in the highest concentration used in this study did not show noticeable chemical interaction that could be detected by FTIR. Therefore, it can be concluded that the two biopolymers (κ-Car and agar) physically interacted with GFX through hydrogen bonding.

6.5.7 Total GFX content and in vitro drug release studies

The total drug content of each nasal pack after complete dispersion in PBS was calculated (Table 16) based on the syringe dimensions of 14 mm diameter × 30 mm height (volume of 4.62 mL). Based on 120 mg of GFX in a nominal 100 mL (Table 12), the recoveries ranged between 77 and 117%. In theory all the drug should be 100% recovered, but the number of steps between mixing and determination by LC-MS will probably lead to random and systematic errors in recovery. (Interestingly, the determined GFX concentration reduced in rough proportion to the total polymer concentration (data not shown) suggesting the possibility of volume increases in the mixtures (Table 14) that would mean the cylindrical formulations with high polymer mixtures would contain less GFX.)

Table 16. Measured total GFX content of drug-loaded formulations

Formulation	Total GFX content (mg)
GFX κ-Car1	6.51 ± 0.04
GFX κ-Car2	5.77 ± 0.01
GFX AGAR1	5.49 ± 0.04
GFX AGAR2	5.48 ± 0.03
GFX AGAR3	4.72 ± 0.03
GFX AGAR4	4.30 ± 0.04

The release profile of GFX from the six formulations was monitored over 48 hours (Figure 50). In the first 3 hours, less than 25% of the drug was released but at a similar rate in all formulations. Although the period between 8 and 24 hours could not be monitored, because of university safety regulations, it is probable that the linking lines are a fair approximation of the true patterns. The greatest release was from GFX AGAR3 and the least from GFX AGAR4. After 24 hours, a constant release at similar

rate was observed in all the four formulations that included agar, but an abrupt increase in release for GFX κ-Car1 and 2 neither containing agar. All the formulations released the drug throughout the 48 hours allocated, but with GFX κ-Car 1 and 2 depleting more than 90% and the other four less than 80% of the total content within 48 hours.

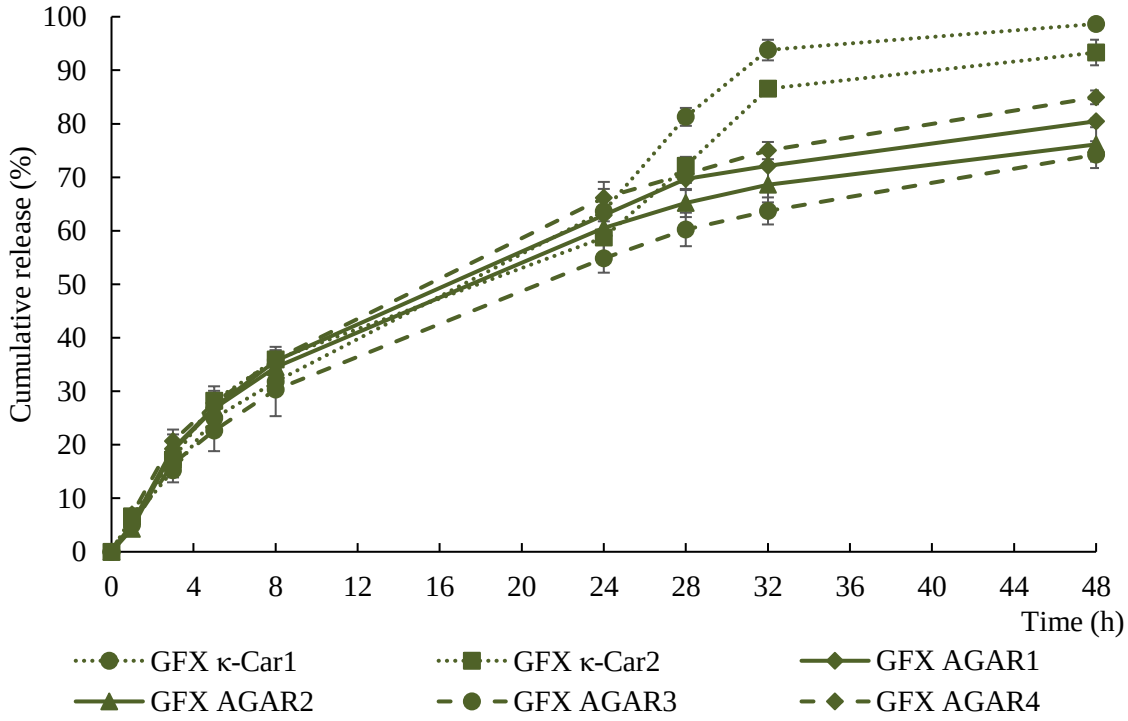

Figure 50. Cumulative release of GFX in drug loaded formulations, Data are means ± SD (n=3)

The unvarying release profile in the first 3 hours could be due to the release of the drug from the large external surface area of the formulations. As all the formulations had the same surface area, the similar release pattern was observed, regardless of the polymer composition. The slower release rate of the drug after 8 hours could be attributed to the slower diffusion of PBS into the smaller pores and internal area (due to the lower rate of polymer relaxation) and slower counter diffusion of the drug to the PBS (Jie Li et al., 2018).

The abrupt increase in GFX release of κ-Car formulations between 24 to 32 hours could be due release of the drug from the dense core of the matrices compared with the surrounding area. It could be explained that in 24 hours, the medium reached the core of the cylindrical matrix penetrated the small pores and abruptly diffused out the drug confined in this dense part. The consistent release of the drug from GFX

AGAR formulations could be explained by the consistent swelling rate and probably more uniform porous internal microstructure (Figure 46 c, d, e) that allowed steady diffusion of the PBS into the matrix and dissolution of the drug. Surprisingly, the axial dense area of the GFX AGAR2 (Figure 45) did not cause the abrupted release seen in both GFX κ-Car formulations.

Overall, Figure 50 showed the drug release was steady with only a hint of burst release in GFX κ-Car1 and 2. This suggested that GFX was evenly distributed into the structure and bound to the polymers of the matrix by hydrogen bonding as discussed in the earlier FTIR section (Pastor et al., 2015).

Mathematical models of in vitro drug release behaviours are used to define the drug release mechanism in a drug delivery system (Paolino et al., 2019). The in vitro drug release profile of GFX-loaded formulations were fitted into the equations of Zero-order, First order, Higuchi, Korsemeyer-Peppas and Hixon-Crowell models using KinetDS 3.0 software[8] (Mendyk et al., 2012) and regression values (R^2) were extracted (Table 17). The highest R^2 determines the suitable mathematical model that follows drug release kinetics (Gouda et al., 2017).

[8] The software is free open-source software and is available at http://sourceforge.net/projects/kinetds/.

Table 17. R2 values of GFX-loaded formulations fitted in mathematical drug release models. In Korsmeyer-Peppas model, n is the diffusion coefficient of the drug. The shaded values show the two top values for each model.

Formulation	Zero-order	First-order	Higuchi	Korsmeyer-Peppas		Hixon-Crowell
	R^2	R^2	R^2	R^2	n	R^2
GFX κ-Car1	0.936	0.771	0.822	0.989	0.740	0.854
GFX κ-Car2	0.938	0.743	0.904	0.979	0.670	0.835
GFX AGAR1	0.904	0.663	0.934	0.953	0.670	0.770
GFX AGAR2	0.896	0.624	0.923	0.930	0.690	0.743
GFX AGAR3	0.933	0.702	0.937	0.969	0.660	0.806
GFX AGAR4	0.920	0.711	0.961	0.973	0.620	0.804

The plotted experimental data of the six GFX-loaded formulations were best-fitted by a Korsmeyer-Peppas model followed by a Zero-order model. Korsmeyer-Peppas model describes simultaneous release mechanisms involved in a polymeric drug delivery system such as diffusion of dissolution medium into the matrix, swelling of the matrix and dissolution of the drug to the medium (Permanadewi, Kumoro, Wardhani, & Aryanti, 2019).

In this study, n values laid between 0.620 and 0.740, so the mechanism of release is non-Fickian and the transport is controlled by both rates of diffusion and erosion. P. I. Lee (1985) described that non-Fickian release of a water-soluble drug from a dry hydrogel matrix involves simultaneous water absorption and drug desorption through a swelling-controlled diffusion mechanism. As the water penetrates the glassy state drug-dispersed hydrogel matrix, the polymer swells, its glass transition temperature drops, and the dissolved drug diffuses out of the swollen rubbery region.

The Fickian mechanism indicates diffusion-controlled drug release, while the mechanism in GFX-loaded cryogels involves simultaneous diffusion and swelling. Perhaps easier to explain is a Zero-order model – the second best model – showing the initial and actual drug concentration in the formulation does not influence the release rate and the rate of drug release per time unit is constant (Lisik & Musiał, 2019). This model would require matrix erosion, which does occur, increasing the surface areas available for diffusion at the same time concentration in the hydrogel decreases.

6.5.8 Matrix erosion determined by cryogel dry weight

Erosion was monitored by mass loss as a function of time over 48 hours (Figure 51). In the first 8 hours of the experiment, all the formulations showed less than 28% erosion with the greatest weight loss in GFX κ-Car2 and the least in GFX AGAR2. Erosion was subsequently observed in all formulations with fastest rate in GFX κ-Car2 and slowest in GFX AGAR2, thus continuing the pattern of the first 8 hours. GFX κ-Car1 and 2, composed of the single polymer κ-Car, showed the highest overall erosion. In contrast, GFX AGAR1 and 2, composed of 1.5% κ-Car and highest agar content of 0.2 and 0.4%, showed the lowest overall erosion. These results suggested that although κ-Car was the dominant polymer and highly hydrophilic, addition of agar to the matrix markedly reduced the rate of erosion particularly in the first 8 hours.

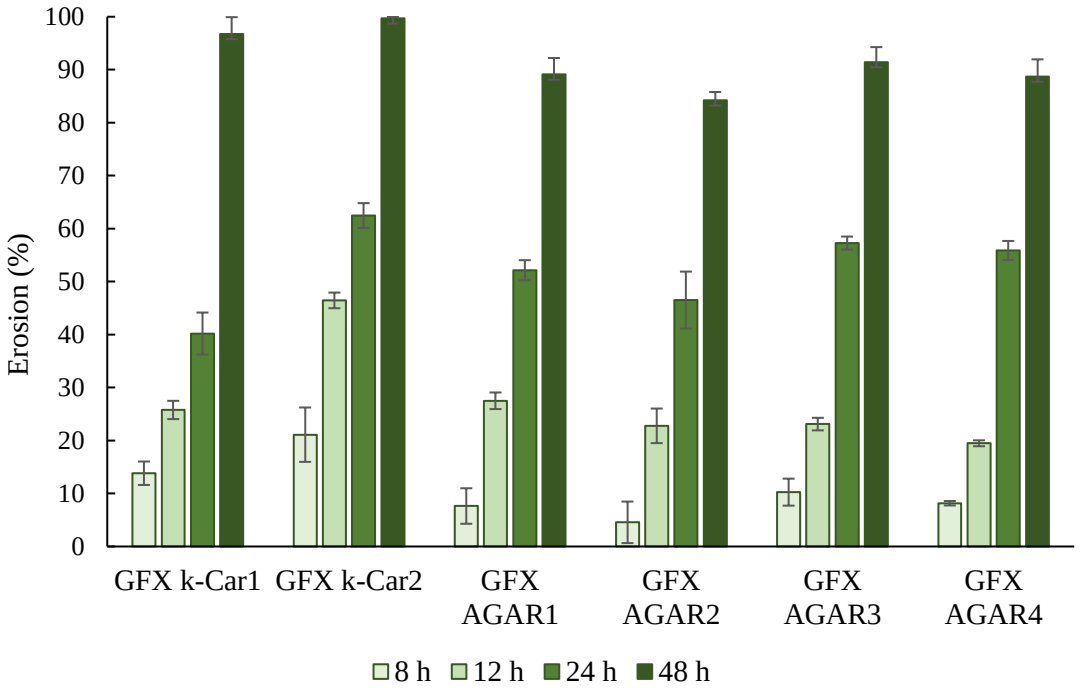

Figure 51. Erosion profile of GFX-loaded formulations in PBS medium (pH 7.4) at 35 ± 2˚C. Values are means ± SD (n=3)

Mechanical analysis of the formulations revealed that addition of agar increased the cryogel strength due to its contribution in helical structure of κ-Car and formation of intramolecular bonding between these two polymers as explained in the FTIR section of this chapter. This increase in strength may explain the relative stability of formulations containing agar.

6.5.9 GFX diffusion and Antibacterial activity of GFX-loaded formulations

Gatifloxacin is an 8-methoxy fluoroquinolone antibacterial agent with a broad spectrum of activity against many Gram-positive and Gram-negative pathogens. The antimicrobial activity arising from diffusion of GFX from hydrogels was tested by the inhibition zone technique. Figure 52 shows that in all the formulations, GFX could diffuse out of the matrix and prevent growth of the microorganism appearing as clear zones in the lawn growth around the formulation discs. The diameters of the clear zones were roughly the same for each formulation (Table 18) indicating that all the cryogel matrices could diffuse out the drug most likely in the manner.

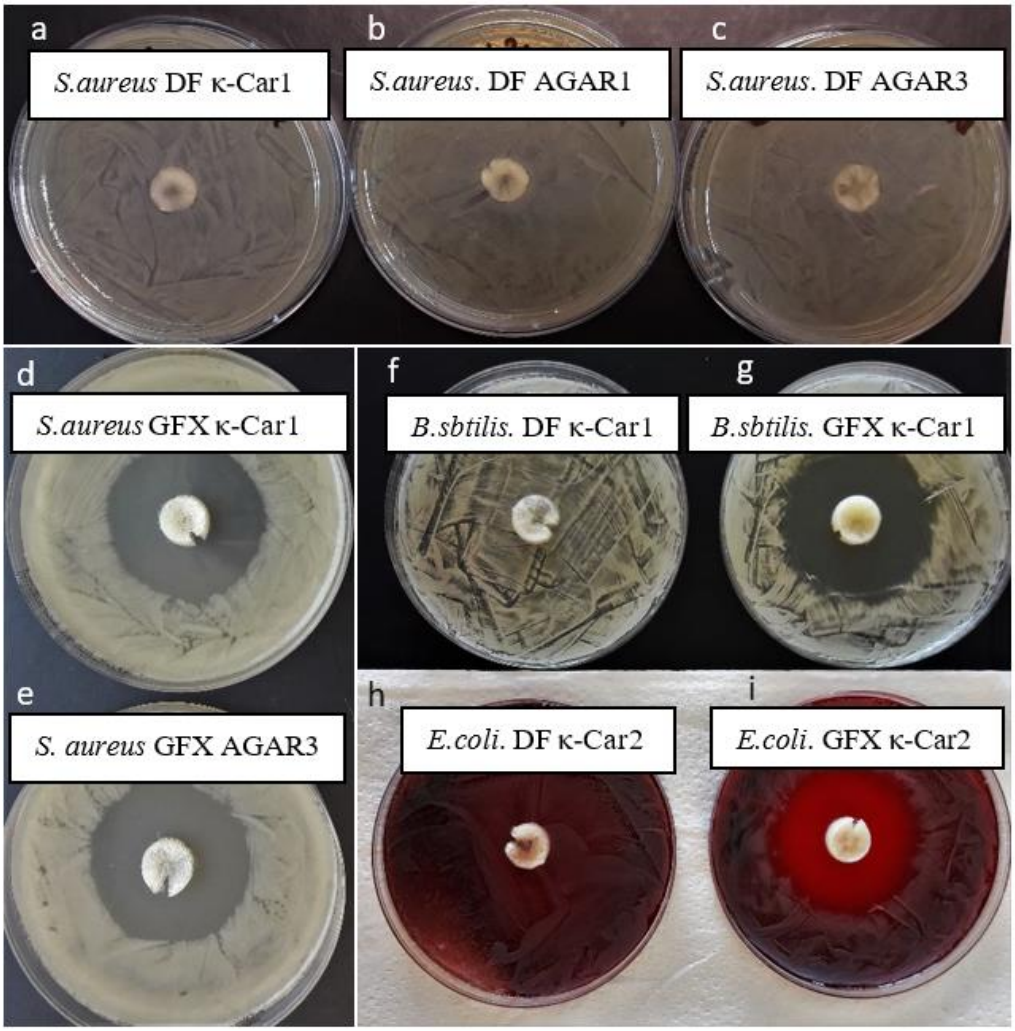

Figure 52. Diffusibility and antibacterial activity of GFX on selected strains of Gram positive (Bacillus subtilis and Staphylococcus aureus) and Gram negative (Echerichia coli) bacteria. Drug free (DF) formulations did not show antibacterial activity (a, b, c, f and h), while GFX-loaded formulations formed a clear inhibition zone around the discs (d, e, g, i).

A study on a blend of κ-Car and polyvinyl acetate hydrogels showed antibacterial activity of the blends on *Escherichia coli* due to the negatively charged SO_4^{2-} of κ -Car and bonding of κ-Car and polyvinyl acetate to DNA of the bacteria (Rasool et al., 2019) but in our study drug-free formulations did not show antimicrobial activity. Lack of inhibition zone around the drug free formulations indicated that the κ-Car and agar biopolymers do not have antibacterial activity on the tested microorganisms in the concentrations used in this study. Therefore, antimicrobial activity depends on GFX present in the cryogels and its release when hydrated.

Table 18. Diameter of inhibition zones in GFX-loaded formulations

Formulation	Diameter of zone of inhibition (mm)
GFX κ-Car1	5.2 ± 0.2
GFX κ-Car2	5.3 ± 0.1
GFX AGAR1	5.3 ± 0.2
GFX AGAR2	5.1 ± 0.3
GFX AGAR3	5.2 ± 0.2
GFX AGAR4	5.3 ± 0.2

6.6 Summary and conclusion

The aim of this chapter was modification of the κ-Car cryogel matrix developed in Chapter 3 to improve its physical structure and extend the controlled-release period of the drug. GFX was used as a drug model because of its water solubility and broad antibacterial activity against Gram-positive and Gram-negative bacteria. Agar was suggested due to its similar structure with κ-Car, water solubility and synergistic effect with κ-Car in formation of hydrogel.

The outcomes of this study indicated that all the formulations were able to swell and release GFX within the 48 hours timeframe, but their physical properties were affected by total concentration of the biopolymers and concentration of each biopolymer. Presence of agar in the formulation reduced the swelling degree, extended the release time of the drug and the release behaviour was more sustainable compared with the GFX κ-Car formulations.

Release data were best-fitted into Korsmeyer-Peppas and zero-order models, suggesting that a greater contribution of non-Fickian diffusion and involvement of both diffusion and erosion mechanisms in GFX release.

In principle, the present work confirms the feasibility and potential of κ-Car and agar blend hydrogel as suitable carriers for extended controlled release of GFX in pharmaceutical applications. If further GFX release extension required, addition of cross-linkers or blending with other bio and non-biopolymers can be suggested.

Chapter 7 General discussion

7.1 Thesis overview

Nasal packing is a well-established treatment for control of bleeding in both anterior and posterior epistaxis. An extensive range of packing materials are available which function by compression of the local vascular tissue to facilitate blood clotting and arrest bleeding. Nasal packs are also useful for filling the nasal cavity after intranasal operations such as septoplasty and endoscopic sinus surgery to provide support for the nasal structure and to reduce tissue adhesion.

A swift response to stop bleeding followed by minimising the risks of excessive inflammation and infection on the bleeding site are crucial steps in the healing process of intranasal wounds. Generally, current nasal packs stop bleeding, but not immediately, and there are several complications associated with their applications. In summary, non-erodible nasal packs can apply excessive pressure on the nasal mucosa and damage them; the regenerated tissue may grow into the pack and the mechanical pack removal may cause new wound events and thus re-bleeding. In contrast, erodible packs that by definition erode during the therapy period minimise pain on removal, if needed at all, but foreign body reactions associated with their compositions are concerning. They are also more expensive than non-erodible packs.

Therapeutic agents are sometimes required to enhance the outcomes of packing, for example: in cases of severe epistaxis, antifibrinolytic drugs are used to swiftly stop bleeding prior placement of the pack into the nasal cavity. In case of prolong packing prophylactic drugs such as anti-inflammatory and antibiotics are systemically or locally administrated to minimise inflammation and prevent infection. Systemic administration of these drugs as prophylactics is inherently flawed because they do not target the affected area and thus require high concentration of the drugs that can cause systemic toxicity.

Local regular administration of these drugs is an attractive alternative, but it is impossible when the nasal cavity is packed. Impregnation of nasal packs or stents with drugs prior insertion has been reported by some researchers (Sabarinath et al., 2017; Stefan et al., 2019) but the method was not satisfactory because the impregnated nasal pack tends to release the drug in uncontrolled and inconsistent ways resulting in erratic treatment outcomes. These findings have important

implications for development of drug-eluting nasal packs to locally deliver the prophylactic drugs in a desired controlled release manner. The pack may increase the residence time of the drug, improve drug absorption and its function. Therefore, development of drug-eluting nasal packs could be a solution for this problem.

The aim of this thesis was thus to formulate and develop several formulations of cost-effective erodible nasal packs for fast and extended release of the drugs once applied to the injured nasal cavity. The first formulation, the plain nasal pack, was designed with the view of it being used as a foundation model for intranasal drug delivery specifically for the treatment of epistaxis and associated complications (Chapter 3). The prototype was developed using κ-carrageenan hydrogel and freeze-drying technique to fabricate the basic nasal pack. This foundation nasal pack performed high fluid absorption capacity, swelling ability, sufficient mechanical strength to maintain its structure through insertion into nasal cavity and erode during the course of the treatment.

After identifying the feasibility of the developed cryogel formulation as the basic nasal pack, extension of the application to a drug eluting system was suggested. A second stage was designed to formulate a fast but controlled drug release system for the purpose of treating severe epistaxis. In this study tranexamic acid (TXA), an antifibrinolytic drug, was used to facilitate blood clotting by immediate release after placement into the nasal cavity (Chapter 4).

The third stage was designed to develop controlled extended-release formulations. As mentioned above, prophylactic drugs (anti-inflammatory and antibiotics) are generally prescribed when prolong packing is required. To improve effectiveness of the drug and reduce negative impacts of systemic delivery, local delivery of these drugs carried by the developed nasal pack formulation was suggested. Dexamethasone (DEX) and gatifloxacin (GFX) were used as the model drugs with the aim of local delivery following intranasal surgeries to reduce excessive inflammation, minimise chance of infection and promote wound healing (Chapters 5 and 6).

7.2 Interpretation of main thesis findings

Nasal packing is the second line of epistaxis treatment. Also, nasal packs are frequently used following some intranasal surgeries to facilitate wound healing and reduce postoperative complications. In Chapter 2 various types of nasal packs were reviewed highlighting the limitations of them and describing opportunities for development of improved or novel nasal packs. It was found that among the nasal packs present in the market, erodible nasal packs are preferred but their manufacturing costs and availability as well as some side effects arising from their composition limit their use. The review also described several attempts have been made in the past decade to load drugs into the nasal pack prior to nasal insertion to facilitate haemostasis and wound healing. However, there were undesirable erratic outcomes due to uncontrolled drug release and insufficient local drug absorption.

These studies signalled a demand for erodible drug-eluting nasal packs with the ability to perform their expected basic function plus releasing a drug in a kinetically useful way. Hence, in Chapter 3 a basic nasal pack was formulated using κ-carrageenan (κ-Car) hydrogel with three concentrations of κ-Car, followed by freeze drying. This basic nasal pack was intended to be the foundation pack for subsequent drug inclusion. The in vitro studies of rehydrated packs showed that the lowest κ-Car formulation had high porosity, swelling ratio and a degree of bioadhesion, good mechanical strength and a useful erosion rate. These properties deteriorated when higher biopolymer concentrations were used. From a practical perspective this effect, while worth noting, was peripheral to the project's aim so was not pursued to find causes. The successful formulation became the foundation for subsequent drug-loaded formulations and moreover as the base polymer for addition of other biopolymers as might be required.

Thus, a first drug-eluting nasal pack was formulated to rapidly release the loaded anti-fibrinolytic drug, TXA. The erodible nasal pack was formulated with the aim to deliver TXA for a very rapid cessation of bleeding in severe epistaxis or in patients with relevant blood disorders. The nasal pack acted as an all-in-one approach to arrest bleeding mechanically and therapeutically at the bleeding site. To improve some properties of the basic TXA-loaded formulations, two other biopolymers -locust bean gum and gelatine- were individually blended with κ-Car. Locust bean gum (LBG) was

used to improve bioadhesion of the hydrogel by formation of hydrogen bonds between the hydroxyl groups of the LBG and glycoprotein of mucin (Prajapati 2014). Also, gelatine (Gel) was used to improve bioadhesion (Y. Li, Meng, Liu, Narkar, & Lee, 2016) and accelerate erosion rate by increasing the hydrophilicity and reducing the mechanical stability of the hydrogel.

The outcomes of this study indicated that all the formulations typically released 100% of the drug in 4 hours. LBG substantially improved mechanical strength of the dry cryogel, did not change bioadhesion and drug release profile, but reduced erosion rate. In contrast, presence of Gel in the matrix increased the erosion rate due to fast secession of amide bonds and disintegration of the network, but the drug release rate slowed by 50% compared with the other formulations. When immediate treatment of epistaxis is required, the fast release formulation with high erosion rate is suitable, but in case of post-operative applications extended drug release and erosion is desired. In this study, the formulation made of κ-Car showed the best performance for rapid drug release and the formulation composed of κ-Car and LBG is appropriate for extended controlled release purpose. However, in vivo studies are required to investigate performance of the nasal packs in living organisms under real conditions.

Subsequently all the formulations developed for TXA – plus a formulation with higher concentration of κ-Car (2%) – were used as the matrices for loading the anti-inflammatory steroidal drug, dexamethasone (DEX). This drug is used to supress excessive inflammation of the mucosa post intranasal surgeries. With the same matrices' composition as TXA formulations, it was expected that the DEX-loaded formulations behave like TXA-loaded nasal packs releasing the drug and erode in the same manner. However, all the formulations actively released the drug for 33 hours following the Korsmeyer-Peppas release model, indicating that the type of drug extensively influences physical and chemical characteristics of the formulations and their drug release profiles. The slow rate of drug release was likely due to the lipophilicity of DEX compared with the hydrophilic TXA. Whatever the cause the kinetic outcomes for both drugs were unexpectedly useful.

The final formulation experiments were with an antibiotic-eluting nasal pack that also needed an extended drug release profile. In contrast to the role of TXA, rapid

haemostasis, an antibiotic would be acting as a prophylactic thus demanding slow and extended drug release kinetics. Gatifloxacin (GFX) was the model drug. κ-Car and its blends with agar was used as the drug carrier. Blends of these two biopolymers have been reported in development of absorbent hydrogels and drug delivery systems indicating their synergistic effect on gelation, reducing swelling ratio, improvement of mechanical stability, lowering erosion rate and subsequently extended drug release (Duman et al., 2020; Liu et al., 2005). Investigation of drug release profile in all the GFX-loaded formulations indicated that all the formulations were able to release the drug during the 48 hours period. However, only the GFX-loaded formulations containing single polymer of κ-Car fully released the drug within 48 hours. These formulations also showed an abrupt drug release after 24 hours indicating inconsistency in the release rate. The presence of agar and GFX in the formulation reduced flexibility and maximum swelling ratio of the formulations; however, a usefully steady drug release was observed over 48 hours in all formulations containing agar as well as complete hydrogel erosion in this period. The in vitro studies revealed that this formulation is suitable for extended controlled release of GFX and with some work on the chemical structure longer extension of drug release and matrix erosion can be obtained.

If the nasal pack is applied in post-operative intranasal surgeries, prolong packing of more than one week is required. To extend in situ life of the formulations and prevent multiple replacements of the nasal pack during the treatment period, mechanical stability must be improved. In addition, swelling, drug release and erosion rate of the formulations must be slowed down while ensuring sufficient drug concentration is consistently releasing and the pack is eroding. Alteration of the formulations can be achieved by changes in the ratio of the biopolymers used in this study. Although this study indicated that these blends delay swelling and erosion, but the ratio of the biopolymers was studied in a narrow range. As the function of polymer is concentration-dependent, expansion of the range to higher concentrations of up to 1% for LBG (Dunstan et al., 2001) and lower concentrations for gelatine (0.1 to 1.0%) is recommended. Alternatively, crosslinkers such as glutaraldehyde (Distantina, Rochmadi, Fahrurrozi, & Wiratni, 2013) and polyacrylamide (Deng et al., 2018) are reported to add strength to the mechanical structure of κ-Car but the ratio of the

biopolymer to the crosslinker must be optimised to fit the formulation for purpose. Combination of the biopolymer blending and addition of a crosslinker also can be suggested (Tytgat et al., 2019) on development of a formulation using κ-Car and gelatine.

It must be noted that in this research, it was attempted to perform in vitro studies in simulated living conditions, but the in vitro outcomes may not correlate with the results that will be obtained from future in vivo studies due to the limitations of this research.

These studies provided novel insights into the applications and functions of nasal packs in treatment of unmanageable epistaxis and minimising post-operative complications by using the absorbent bio-nasal pack as a drug delivery vector. According to these in vitro studies, the cryogel matrix erodes in less than 48 hours in the experimental conditions but the rate of release and erosion will be different in actual conditions.

Having summarised the main practical outcomes, it remains to discuss the results within the broad scope of epistaxis and intranasal post-operative treatments.

7.3 Implications for epistaxis and intranasal post-operative treatments

Epistaxis is a common problem estimating to occur in at least 60% of the world population and approximately 6% of this population require medical treatment (Akinpelu, Amusa, Eziyi, & Nwawolo, 2009; Kucik & Clenney, 2005). The prevalence of this incident is mainly in the children under 10 years of age and after the age of 50 years (Cho & Kim, 2012). In addition, the annual rate of intranasal surgeries such as septoplasty and endoscopic sinus surgeries (ESS) is high. It was reported that in England 20,000 septoplasty surgeries were performed in 2012 to 2013 (Alotaibi, Almutlaq, Alshammari, & Gadelkarim Ahmed, 2018) and 90,000 endoscopic sinus surgeries were performed between 2010 and 2019. The rate of these procedures is increasing worldwide due to trauma, hypertension, climate change and air pollution (Traboulsi et al., 2015). Nasal packs are extensively used in treatment of severe epistaxis and as post-operative intervention following intranasal surgeries. They are made of various materials and generally apply gentle pressure on the wound site to

cease bleeding. Also, as intranasal post-operative intervention, they provide support for the cartilaginous and bony structure of the nose and facilitate wound healing. According to some clinical studies, the outcomes of these procedures highly depend on the use of nasal pack, its type and duration of packing, however erratic results were observed comparing nasal packs in these studies showing inconsistency of outcomes.

In some cases, haemostatic drugs such as blood clotting agents or anti-inflammatory medicines, are prescribed in conjunction with nasal packing to facilitate haemostasis and enhance wound healing. Also, antibiotics are recommended to minimise infection in prolong packing. Although local administration of these drugs is more desirable than systemic administration, presence of a pack – erodible or non-erodible – in the nasal cavity makes the effective local drug delivery difficult to achieve. In the past decade, local administration of some drugs by impregnating the nasal pack has been attempted by some clinicians but the erratic outcomes of the procedures showed ineffectiveness of this method mainly due to uncontrolled drug availability and drug absorption.

A review of the present literature and demand for development of advanced drug delivery systems indicated the need for development of novel erodible nasal pack as a drug delivery vector. The focus of this research was development of an erodible basic nasal pack with the capability of loading drugs into its carrier matrix during its manufacturing process.

It was expected that the novel erodible nasal pack will be a cost-effective and suitable drug delivery device capable of hosting drugs during its manufacturing process and releasing it in desirable controlled manners, fast and slow-release purpose, to be locally absorbed in effective dose. The erodibility will eliminate mechanical removal and risk of re-bleeding associated with non-erodible packs and patients with severe epistaxis and intranasal surgeries will benefit from this drug delivery device.

Several biopolymers have been trialled in development of drug-eluting nasal packs. Chitosan, collagen, gelatine, hyaluronic acid and carboxymethyl cellulose are the biopolymers used in commercially available nasal packs. However, using seaweed polysaccharides to develop of intranasal drug delivery devices has been rare. Among

the limited studies, the most popular polysaccharides of this source are carrageenan, alginate, fucoidan and agar. I chose to work with κ-Car because it is FDA approved, used in food industry as gelling and thickening agent and in pharmaceutical industries in manufacturing of hydrogel films and erodible drug carriers. Also, it produces a hydrophilic firm hydrogel at room temperature even at low concentrations of κ-Car.

In pioneering work, Ganesan and Ratke (2014) synthesised a monolithic κ- Car aerogel by supercritical drying. The aerogel showed the expected low density, with high porosity and surface area and low shrinkage suggesting its suitability for hosting chemicals for various applications. Rege et al. (2018) later investigated the texture and mechanical characteristics of this aerogel and developed a constitutive predictive model of its mechanical behaviour. However, there were no indications of further uses of this aerogel in pharmaceutical applications have been found to date. Moreover in previous literature attention has focused on blends of κ-Car and other polymers to formulate films and beads (Y. Zhang & Zhang, 2012), and injectable hydrogels (Rasool et al., 2019). Applications of κ-Car as monolithic cryogel in drug delivery has not been exploited.

The Ganesan and Ratke aerogel appeared suitable for development of a drug-eluting nasal pack, however some other requirements for this application such as swelling, expansion, bioadhesion, mechanical properties (hardness, springiness, and cohesiveness) and erosion of the aerogels were not studied. Equally the feasibility of using standard freeze-drying as a simple, moderately fast and cost-effective method has not been investigated.

To address these gaps in the literature, this research investigated the feasibility of using the aerogel formulations developed by Ganesan and Ratke in formulation of a novel drug-eluting nasal device commonly known as nasal pack. As a starting point the formulation was reproduced and freeze drying was trialled. Following this, three drug models were loaded to fabricate fast and slow-release formulations. Also, combinations of κ-Car with three other biopolymers were studied to investigate effects of these biopolymers on pack properties.

Freeze drying was shown to be a suitable technique in cryogel formation. In terms of physical characteristics, all formulations showed macroscopically smooth external

surface, high surface area and porosity, and low shrinkage after drying. They also exhibited hydrophilicity with high swelling ratios and useful bioadhesion to mucosa. To my knowledge, there was no study that investigated these parameters in monolithic κ-Car cryogels.

It was observed that hydrophilicity of the polymers and the drugs influenced swelling ratios, drug release and erosion rates. In addition, the total polymer content of the formulations markedly affected porosity and swelling ratio of the nasal packs resulting in alteration of drug release profile and erosion.

This combination of findings shows important implications for development of an erodible intranasal drug delivery device using κ-Car and freeze-drying technology. The important behaviour parameters can be tuned by altering polymer formulation as required for each drug.

7.4 Study limitations and recommendations for future research

Although this research showed feasibility of formulating a drug-eluting nasal pack using κ-Car– individually or blended with other biopolymers– there were some unavoidable limitations. First, some experiments in Chapter 6 were interrupted by COVID19 lock downs in 2020 and the time constraint to submit the thesis by April 2021, did not allow further research on investigation of other biopolymers and use of cross-linkers to extend the release of GFX for a further period.

A second limitation was scarcity of literature in intranasal drug delivery devices, specifically hydrogel-based monolith nasal packs, therefore it was difficult to find prior literature to quantitatively compare my results with those of others. More positively this indicates the novelty of the idea and the formulations I developed.

In addition, there were some limitations in the methods used. In swelling ratio and erosion studies, the formulations were placed in stainless steel mesh containers to submerge in the medium and prevent floating. However, in drug release studies, the formulations were confined in a dialysis membrane to resemble the intranasal cavity and minimise passage of the polymer particles into the dissolution medium during the release period. The difference in method caused slight inconsistencies in rate of swelling and erosion with the rate of drug release. Swelling and erosion studies was

designed in this way because removal of the swollen gel from a dialysis membrane for weight checks at each time point would damage the remaining hydrogel and stop data collection.

The results obtained from this research confirm feasibility of formulating drug-eluting nasal packs using κ-Car. However, extensive studies are required to evaluate other aspects of the formulations in further in vitro studies. Also, to verify the in vitro results in vivo, ethically approved animal studies are recommended. These must be performed by painlessly inducing a wound in animal's nasal cavity or performing simulated sinus surgery under anaesthetic conditions. The non-medicated nasal packs should be included as controls.

It is further suggested to investigate formulating a dual drug-eluting nasal pack based on the basic formulation in this research. It can be a two-compartment device with TXA on the external surface for immediate effect and DEX or GFX in the central section to slowly release the drug. This might be achieved by coaxial extrusion.

7.5 Conclusion

With the increase in cases of epistaxis caused by trauma and hypertension and intranasal surgeries such as endoscopic sinus surgery and septoplasty there is a high demand for novel intranasal drug delivery devices to increase treatment efficacies of and patients' satisfaction. In this thesis, erodible drug-eluting nasal packs were developed by employing biopolymers popular in food and pharmaceutical applications coupled with freeze drying. Depending on the drugs' role in therapy the nasal packs were designed for fast or slow release. Mainly, the TXA-eluting nasal packs were developed to facilitate rapid formation of blood clots and subsequent haemostasis in severe epistaxis. DEX-eluting nasal packs were formulated to reduce inflammation and promote rapid wound healing and GFX-loaded formulations were designed to minimise infection when prolonged drug release is required. All these three nasal packs can be used as intranasal post-operative intervention depending on the possible complications that may occur.

These innovative, cost-effective, and patient-friendly drug-eluting nasal packs are a potential breakthrough in treatment of intranasal complications. The proposed nasal

packs will pave the way for a more customised approach to benefit patients who require treatments for conditions resulting from excessive epistaxis and intranasal surgery patients to minimise postoperative complications. The nasal packs could be customised in size, shape and type of therapeutic agent to suit specific end-user needs since they can be tailor-designed and capable of hosting and releasing various loaded therapeutics to enhance patient outcomes. This research is expected to have a positive impact on the use of abundant biopolymer hydrogels in development of intranasal drug delivery systems and sets a scene for future developmental opportunities.

References

Adams-S., M., A., & Keefe, D. M. (GRAS notice: No.GRN 000661). *FDA: Centre of Food Safety and Applied Nutrition*

Retrieved from https://www.ncbi.nlm.nih.gov/pmc/articles/PMC6722496/pdf/marinedrugs-17-00458.pdf

Adams, G. (2007). The Principles of Freeze-Drying. In J. G. Day & G. N. Stacey (Eds.), *Cryopreservation and Freeze-Drying Protocols* (pp. 15-38). Totowa, New Jersey: Humana Press.

Afjoul, H., Shamloo, A., & Kamali, A. (2020). Freeze-gelled alginate/gelatin scaffolds for wound healing applications: An in vitro, in vivo study. *Materials Science and Engineering C 113*, 1-10. https://doi.org/10.1016/j.msec.2020.110957

Akbari, A., & Yegani, R. (2012). Study on the impact of polymer concentration and coagulation bath temperature on the porosity of polyethylene membranes fabricated via TIPS method *Journal of Membrane and Separation Technology, 1*, 100-107. https://doi.org/10.6000/1929-6037.2012.01.02.4

Akinpelu, O. V., Amusa, Y. B., Eziyi, J. A., & Nwawolo, C. C. (2009). A retrospective analysis of aetiology and management of epistaxis in a south-western Nigerian teaching hospital. *West African Journal of Medicine, 28*(3), 165-168. https://doi.org/10.4314/wajm.v28i3.48443

Alagusundaram, M., Chengaiah, B., Gnanaprakash, K., Ramkanth, S., Madhusudhana Chetty, C., & Dhachinamoorthi, D. (2010). Nasal drug delivery system - an overview. . *International Journal of Research in Pharmaceutical Sciences,, 1*(4), 454-465.

Alavi, S., & Mortazavi, S. A. (2018). Freeze-dried k-Carrageenan/chitosan polyelectrolyte complex-based insert: A novel intranasal delivery system for sumatriptan succinate. *Iranian journal of pharmaceutical research, 17*(4), 1172-1181. https://doi.org/10.4314/wajm.v28i3.48443

Albu, S. (2012). Novel drug-delivery systems for patients with chronic rhinosinusitis. *Drug Design, development and Therapy 6*, 125-132. https://doi.org/10.2147/dddt.S25199

Ale, M. T., Mikkelsen, J. D., & Meyer, A. S. (2011). Important determinants for fucoidan bioactivity: A critical review of structure-function relations and extraction methods for fucose-containing sulfated polysaccharides from brown seaweeds. *Marine Drugs, 9*(10), 2106-2130. https://doi.org/10.3390/md9102106

Alotaibi, A. D., Almutlaq, B. A., Alshammari, F. N., & Gadelkarim Ahmed, H. (2018). The common clinical presentation of patients selected for septoplasty in Northern Saudi Arabia. *International Journal of Otolaryngology, 2018*, 1-8. https://doi.org/10.1155/2018/8536387

Alter, H. (2011). *Approach to the adult epistaxis*. Retrieved January 18, 2017, from https://www.uptodate.com/contents/approach-to-the-adult-with-epistaxis

Altuntaş, E., & Yener, G. (2017). Formulation and Evaluation of Thermoreversible In Situ Nasal Gels Containing Mometasone Furoate for Allergic Rhinitis. *AAPS PharmSciTech, 18*(7), 2673-2682. https://doi.org/10.1208/s12249-017-0747-8

Ansari, T. M., Raza, A., & Rehman, A.-u. (2005). Spectrophotometric determination of tranexamic acid in pharmaceutical bulk and dosage forms. *Analytical Sciences, 21*(9), 1133-1135. https://doi.org/10.2116/analsci.21.1133

Antisdel, J., Matijasec, J., Ting, J., & Sindwani, R. (2011). Microporous polysaccharide hemospheres do not increase synechiae after sinus surgery: Randomized controlled study. *American Journal of Rhinology and Allergy, 25*(4), 268-271. https://doi.org/10.2500/ajra.2011.25.3619

Arora, P., Sharma, S., & Garg, S. (2002). Permeability issues in nasal drug delivery. *Drug Discovery Today, 7*(18), 967-975. https://doi.org/10.1016/s1359-6446(02)02452-2

Athanasiadis, T., Beule, A. G., & Wormald, P. J. (2007). Effects of topical antifibrinolytics in endoscopic sinus surgery: A pilot randomized controlled trial. *American Journal of Rhinology, 21*(6), 737-742. https://doi.org/10.2500/ajr.2007.21.3097

Bacaita, E. S., Ciobanu, B. C., Popa, M., Agop, M., & Desbrieres, J. (2014). Phases in the temporal multiscale evolution of the drug release mechanism in IPN-type chitosan based hydrogels. *Physical Chemistry Chemical Physics, 16*(47), 25896-25905. https://doi.org/10.1039/C4CP03389B

Bachert, C., Pawankar, R., Zhang, L., Bunnag, C., Fokkens, W. J., Hamilos, D. L., . . . Blaiss, M. (2014). ICON: chronic rhinosinusitis. *World Allergy Organization Journal, 7*(1), 1-28. https://doi.org/10.1186/1939-4551-7-25

Bajpai, S. K., & Daheriya, P. (2014). Kappa-Carrageenan/PVA filmswith antibacterial properties: Optimization of preparation conditions and preliminary drug release studies. *Journal of Macromolecular Science, 51*(4), 286-295. https://doi.org/10.1080/10601325.2014.882687

Bajpai, S. K., Daheriya, P., Ahuja, S., & Gupta, K. (2016). Water absorption and antimicrobial behavior of physically cross linked poly (vinyl alcohol)/carrageenan films loaded with minocycline. *Designed Monomers and Polymers, 19*(7), 630-642. https://doi.org/10.1080/15685551.2016.1187444

Banglawala, S. M., Gill, M. S., Dhillion, N., Khan, J. S., Gupta, M. K., Psaltis, A., . . . Sommer, D. D. (2014). Nasal packing after septoplasty: Cardiopulmonary impact. *JAMA Otolaryngology–Head & Neck Surgery, 140*(3), 253-258. https://doi.org/10.1001/jamaoto.2013.6335

Barahona, T., Chandía, N. P., Encinas, M. V., Matsuhiro, B., & Zúñiga, E. A. (2011). Antioxidant capacity of sulfated polysaccharides from seaweeds. A kinetic approach. *Food Hydrocolloids, 25*(3), 529-535. https://doi.org/10.1016/j.foodhyd.2010.08.004

Basha, S. I., Ghosh, S., Vinothkumar, K., Ramesh, B., kumari, P. H. p., Mohan, K. V. M., & Sukumar, E. (2020). Fumaric acid incorporated Ag/agar-agar hybrid hydrogel: A multifunctional avenue to tackle wound healing. *Materials Science and Engineering C, 111*, 1-13. https://doi.org/10.1016/j.msec.2020.110743

Belgamwar, V. S., Patel, H. S., Joshi, A. S., Agrawal, A., Surana, S. J., & Tekade, A. R. (2011). Design and development of nasal mucoadhesive microspheres containing tramadol HCl for CNS targeting. *Drug Delivery, 18*(5), 353-360. https://doi.org/10.3109/10717544.2011.557787

BeMiller, J. N. (2019). In J. N. BeMiller (Ed.), *Carbohydrate Chemistry for Food Scientists* (pp. 293-301): Elsevier. https://doi.org/10.1016/B978-0-12-812069-9.00014-5

Berlucchi, M., Castelnuovo, P., Vincenzi, A., Morra, B., & Pasquini, E. (2009). Endoscopic outcomes of resorbable nasal packing after functional endoscopic sinus surgery: a multicenter prospective randomized controlled study. *European Archives of Oto-Rhino-Laryngology, 266*(6), 839-845. https://doi.org/10.1007/s00405-008-0841-3

Bertram, U., & Bodmeier, R. (2006). In situ gelling, bioadhesive nasal inserts for extended drug delivery: In vitro characterization of a new nasal dosage form. *European Journal of Pharmaceutical Sciences, 27*(1), 62-71. https://doi.org/https://doi.org/10.1016/j.ejps.2005.08.005

Bertrand, B., Eloy, P., Rombaux, P., Lamarque, C., Watelt, J. B., & Collet, S. (2005). Guidlines to the management of epistaxis. *B-ENT, Supplementary 1*, 27-43.

Bhattacharyya, N., Gopal, H. V., & Lee, K. H. (2004). Bacterial infection after endoscopic sinus surgery: a controlled prospective study. *Laryngoscope, 114*(4), 765-767. https://doi.org/10.1097/00005537-200404000-00032

Biggs, T. C., Nightingale, K., Patel, N. N., & Salib, R. J. (2013). Should prophylactic antibiotics be used routinely in epistaxis patients with nasal packs? *Annals of The Royal College of Surgeons of England, 95*(1), 40-42. https://doi.org/10.1308/003588413X13511609954734

Boateng, J. S., Pawar, H. V., & Tetteh, J. (2013). Polyox and carrageenan based composite film dressing containing anti-microbial and anti-inflammatory drugs for effective wound

healing. *International Journal of Pharmaceutics, 441*(1), 181-191. https://doi.org/10.1016/j.ijpharm.2012.11.045
Brown, Z. K., Fryer, P. J., Norton, I. T., & Bridson, R. H. (2010). Drying of agar gels using supercritical carbon dioxide. *Journal of Supercritical Fluids, 54*(1), 89-95. https://doi.org/10.1016/j.supflu.2010.03.008
Bruschi, M. (2015). *Strategies to Modify the Drug Release from Pharmaceutical Systems*. https://doi.org/10.1016/C2014-0-02342-8
Bugten, V., Nordgård, S., Skogvoll, E., & Steinsvåg, S. (2006). Effects of nonabsorbable packing in middle meatus after sinus surgery. *Laryngoscope, 116*(1), 83-88. https://doi.org/10.1097/01.mlg.0000184581.67185.6e
Buiret, G., Pavic, M., Pignat, J. C., & Pasquet, F. (2013). Gelatin-thrombin matrix: a new and simple way to manage recurrent epistaxis in hematology units. *Case reports in otolaryngology, 2013*, 1-2. https://doi.org/10.1155/2013/851270
Burduk, P. K., Wierzchowska, M., Grześkowiak, B., Kaźmierczak, W., & Wawrzyniak, K. (2016). Clinical outcome and patient satisfaction using biodegradable (NasoPore) and non-biodegradable packing, a double-blind, prospective, randomized study. *Brazilian Journal of Otorhinolaryngology, 83*(1), 23-28. https://doi.org/10.1016/j.bjorl.2016.01.001
Campo, V. L., Kawano, D. F., Silva, D. B. d., & Carvalho, I. (2009). Carrageenans: Biological properties, chemical modifications and structural analysis – A review. *Carbohydrate Polymers, 77*(2), 167-180. https://doi.org/10.1016/j.carbpol.2009.01.020
Catalano, P. J., & Roffman, E. J. (2003). Evaluation of middle meatal stenting after minimally invasive sinus techniques (mist). *Otolaryngology - Head and Neck Surgery, 128*(6), 875-881. https://doi.org/10.1016/S0194-5998(03)00469-8
Cazorla-Luna, R., Martín-Illana, A., Notario-Pérez, F., Bedoya, L.-M., Bermejo, P., Ruiz-Caro, R., & Veiga, M.-D. (2019). Dapivirine bioadhesive vaginal tablets based on natural polymers for the prevention of sexual transmission of HIV. *Polymers, 11*(3), 483-500.
Chang, E. H., Alandejani, T., Akbari, E., Ostry, A., & Javer, A. (2011). Double-blinded, randomized, controlled trial of medicated versus nonmedicated merocel sponges for functional endoscopic sinus surgery. *Journal of Otolaryngology- Head and Neck Surgery, 40 Suppl 1*, S14-19.
Chen, X., Yan, J., Yu, S., & Wang, P. (2018). Formulation and In vitro release kinetics of mucoadhesive blend gels containing matrine for buccal administration. *AAPS PharmSciTech, 19*(1), 470-480. https://doi.org/10.1208/s12249-017-0853-7
Cho, J. H., & Kim, Y. H. (2012). Epistaxis. In B. S. Gendeh (Ed.), *Otolarynology* (pp. 25-44): InTech.
Chronakis, I. S., Borgström, J., & Piculell, L. (1999). Conformation and association of kappa-carrageenan in the presence of locust bean gum in mixed NaI/CsI solutions from rheology and cryo-TEM. *International Journal of Biological Macromolecules, 25*(4), 317-328. https://doi.org/10.1016/s0141-8130(99)00050-1
Cielecka, I., Szustak, M., Gendaszewska-Darmach, E., Kalinowska, H., Ryngajłło, M., Maniukiewicz, W., & Bielecki, S. (2018). Novel Bionanocellulose/κ-Carrageenan Composites for Tissue Engineering. *Applied Sciences, 8*(8), 1352.
Coetzee, M. J. (2007). The use of topical crushed tranexamic acid tablets to control bleeding after dental surgery and from skin ulcers in haemophilia. *Haemophilia, 13*(4), 443-444. https://doi.org/10.1111/j.1365-2516.2007.01479.x
Cohen, S. M., & Ito, N. (2002). A Critical Review of the Toxicological Effects of Carrageenan and Processed Eucheuma Seaweed on the Gastrointestinal Tract. *Critical Reviews in Toxicology, 32*(5), 413-444. https://doi.org/10.1080/20024091064282
Côté, D. W., & Wright, E. D. (2010). Triamcinolone-impregnated nasal dressing following endoscopic sinus surgery: a randomized, double-blind, placebo-controlled study. *Laryngoscope, 120*(6), 1269-1273. https://doi.org/10.1002/lary.20905

Coughlan, C. A., & Bhandarkar, N. (2015). The role of antibiotics in endoscopic sinus surgery. *Current Opinion in Otolaryngology & Head and Neck Surgery, 23*(1), 47-52. https://doi.org/10.1097/moo.0000000000000122

Crisler, R., Johnston, N. A., Sivula, C., & Budelsky, C. L. (2020). Chapter 4 - Functional Anatomy and Physiology. In M. A. Suckow, F. C. Hankenson, R. P. Wilson, & P. L. Foley (Eds.), *The Laboratory Rat (Third Edition)* (pp. 91-132): Academic Press. https://doi.org/10.1016/B978-0-12-814338-4.00004-0

Croitoru, C., Pop, M. A., Bedo, T., Cosnita, M., Roata, I. C., & Hulka, I. (2020). Physically Crosslinked Poly (Vinyl Alcohol)/Kappa-Carrageenan Hydrogels: Structure and Applications. *Polymers, 12*(3), 560. https://doi.org/10.3390/polym12030560

Cumashi, A., Ushakova, N. A., Preobrazhenskaya, M. E., D'Incecco, A., Piccoli, A., Totani, L., . . . and on behalf of the Consorzio Interuniversitario Nazionale per la Bio-Oncologia , I. (2007). A comparative study of the anti-inflammatory, anticoagulant, antiangiogenic, and antiadhesive activities of nine different fucoidans from brown seaweeds. *Glycobiology, 17*(5), 541-552. https://doi.org/10.1093/glycob/cwm014

Cunha, L., & Grenha, A. (2016). Sulfated Seaweed Polysaccharides as Multifunctional Materials in Drug Delivery Applications. *Marine Drugs, 14*(3), 1-42. https://doi.org/10.3390/md14030042

Dahl, R., & Mygind, N. (1998). Anatomy, physiology and function of the nasal cavities in health and disease. *Adv Drug Deliv Rev, 29*(1-2), 3-12. https://doi.org/10.1016/s0169-409x(97)00058-6

Damodaran, S., Parkin, K. L., & Fennema, O. R. (2008). *Fennema's food chemistry* (5th ed.)

Davis, S., & Illum, L. (2003). Absorption Enhancers for Nasal Drug Delivery. *Clinical pharmacokinetics, 42*, 1107-1128. https://doi.org/10.2165/00003088-200342130-00003

Dawson, B., Gutteridge, I., Cervin, A., & Robinson, D. (2018). The effects of nasal lavage with betamethasone cream post-endoscopic sinus surgery: clinical trial. *The Journal of Laryngology and Otology, 132*(2), 143-149. https://doi.org/10.1017/s0022215117001827

Deng, Y., Huang, M., Sun, D., Hou, Y., Li, Y., Dong, T., . . . Yang, W. (2018). Dual Physically Cross-Linked κ-Carrageenan-Based Double Network Hydrogels with Superior Self-Healing Performance for Biomedical Application. *ACS Applied Materials & Interfaces, 10*(43), 37544-37554. https://doi.org/10.1021/acsami.8b15385

Deniz, M., Çiftçi, Z., Işık, A., Demirel, O. B., & Gültekin, E. (2014). The impact of different nasal packings on postoperative complications. *American Journal of Otolaryngology, 35*(5), 554-557. https://doi.org/10.1016/j.amjoto.2014.04.001

Derkach, S. R., Voron'ko, N. G., Kuchina, Y. A., Kolotova, D. S., Gordeeva, A. M., Faizullin, D. A., . . . Makshakova, O. N. (2018). Molecular structure and properties of κ-carrageenan-gelatin gels. *Carbohydrate Polymers, 197*, 66-74. https://doi.org/10.1016/j.carbpol.2018.05.063

Derkay, C. S., Hirsch, B. E., Johnson, J. T., & Wagner, R. L. (1989). Posterior nasal packing. Are intravenous antibiotics really necessary? *Archives of Otolaryngology-Head and Neck Surgery, 115*(4), 439-441. https://doi.org/10.1001/archotol.1989.01860280037013

Distantina, S., Rochmadi, R., Fahrurrozi, M., & Wiratni, W. (2013). Preparation and characterization of glutaraldehyde-crosslinked Kappa carrageenan hydrogel. *Modern Engineering Technology 17*(3), 57-66. https://doi.org/doi.org/10.4186/ej.2013.17.3.57

Djupesland, P. G. (2013). Nasal drug delivery devices: characteristics and performance in a clinical perspective-a review. *Drug Deliv Transl Res, 3*(1), 42-62. https://doi.org/10.1007/s13346-012-0108-9

Duan, X., & Mao, S. (2010). New strategies to improve the intranasal absorption of insulin. *Drug Discov Today, 15*(11-12), 416-427. https://doi.org/10.1016/j.drudis.2010.03.011

Dukovski, B. J., Plantić, I., Čunčić, I., Krtalić, I., Juretić, M., Pepić, I., . . . Hafner, A. (2017). Lipid/alginate nanoparticle-loaded in situ gelling system tailored for dexamethasone

nasal delivery. *International Journal of Pharmaceutics, 533*(2), 480-487. https://doi.org/https://doi.org/10.1016/j.ijpharm.2017.05.065

Duman, O., Polat, T. G., Diker, C. Ö., & Tunç, S. (2020). Agar/κ-carrageenan composite hydrogel adsorbent for the removal of Methylene Blue from water. *International Journal of Biological Macromolecules, 160*, 823-835. https://doi.org/https://doi.org/10.1016/j.ijbiomac.2020.05.191

Dunstan, D. E., Chen, Y., Liao, M. L., Salvatore, R., Boger, D. V., & Prica, M. (2001). Structure and rheology of the kappa-carrageenan/locust bean gum gels. *Food hydrocolloids., 15*(4/6), 475-484. https://doi.org/10.1016/s0268-005x(01)00054-6

Eiselt, P., Lee, K. Y., & Mooney, D. J. (1999). Rigidity of Two-Component Hydrogels Prepared from Alginate and Poly(ethylene glycol)−Diamines. *Macromolecules, 32*(17), 5561-5566. https://doi.org/10.1021/ma990514m

El Maraghy, A. A., Younis, M. A., Dawood, Y. M., & Mohammed, M. M. (2019). Comparative study between absorbable carboxymethyl cellulose and nonAbsorbable merocel nasal packs after sinonasal surgery. *The Egyptian Journal of Hospital Medicine, 76*(1). https://doi.org/10.12816/ejhm.2019.36896

England, R. J. A., Homer, J. J., Knight, L. C., & Ell, S. R. (1999). Nasal pH measurement: a reliable and repeatable parameter. *Clinical Otolaryngology & Allied Sciences, 24*(1), 67-68. https://doi.org/10.1046/j.1365-2273.1999.00223.x

Eouani, C., Piccerelle, P., Prinderre, P., Bourret, E., & Joachim, J. (2001). In-vitro comparative study of buccal mucoadhesive performance of different polymeric films. *European Journal of Pharmaceutics and Biopharmaceutics, 52*(1), 45-55. https://doi.org/10.1016/S0939-6411(01)00146-1

Eski, E., Guvenc, I. A., Hizal, E., & Yilmaz, I. (2014). Effects of nasal pack use on surgical success in septoplasty. *Kulak Burun Bogaz Ihtis Dreg, 24*(4), 206-210. https://doi.org/10.5606/kbbihtisas.2014.82160

Fairbanks, D. N. (1986). Complications of nasal packing. *Otolarynology, Head and Neck Surgery, 94*(3), 412-415. https://doi.org/10.1177/019459988609400337

Fan, L., Wang, L., Gao, S., Wu, P., Li, M., Xie, W., . . . Wang, W. (2011). Synthesis, characterization and properties of carboxymethyl kappa carrageenan. *Carbohydrate Polymers, 86*(3), 1167-1174. https://doi.org/10.1016/j.carbpol.2011.06.010

Fatakia, A., Winters, R., & Amedee, R. G. (2010). Epistaxis: A Common Problem. *Ochsner Journal, 10*(3), 176-178.

Fisher, A. N., Illum, L., Davis, S. S., & Schacht, E. H. (1992). Di-iodo-L-tyrosine-labelled dextrans as molecular size markers of nasal absorption in the rat. *J Pharm Pharmacol, 44*(7), 550-554. https://doi.org/10.1111/j.2042-7158.1992.tb05462.x

Fokkens, W. J., Lund, V. J., Mullol, J., Bachert, C., Alobid, I., Baroody, F., . . . Wormald, P. J. (2012). EPOS 2012: European position paper on rhinosinusitis and nasal polyps 2012. A summary for otorhinolaryngologists. *Rhinology, 50*(1), 1-12. https://doi.org/10.4193/Rhino50E2

Funami, T., Hiroe, M., Noda, S., Asai, I., Ikeda, S., & Nishinari, K. (2007). Influence of molecular structure imaged with atomic force microscopy on the rheological behavior of carrageenan aqueous systems in the presence or absence of cations. *Food Hydrocolloids, 21*(4), 617-629. https://doi.org/https://doi.org/10.1016/j.foodhyd.2006.07.013

Galgatte, U. C., Kumbhar, A. B., & Chaudhari, P. D. (2014). Development of in situ gel for nasal delivery: design, optimization, in vitro and in vivo evaluation. *Drug Delivery, 21*(1), 62-73. https://doi.org/10.3109/10717544.2013.849778

Gambhir, V. (2001). Axiom: Always Treat Nasal Packing with Antibiotics. *Emergency Medicine News, 23*(3), 44.

Ganesan, K., & Ratke, L. (2014). Facile preparation of monolithic [small kappa]-carrageenan aerogels. *Soft Matter, 10*(18), 3218-3224. https://doi.org/10.1039/C3SM52862F

Ganji, F., Vasheghani Farahani, S., & Vasheghani-Farahani, E. (2010). Theoretical Description of Hydrogel Swelling: A Review. *Iranian Polymer Journal, 19*, 375-398.

Garcia-Gonzalez, C. A., Alnaief, M., & Smirnova, I. (2011). Polysaccharide based aerogels promissing biodegradable carriers for drug delivery. *Carbohydrate Polymers, 86*. https://doi.org/10.1016/jcarbpol.2011.06.066

Garcia, C. E. R., Yamashita, F., Youssef, E. Y., Prudencio, S. H., & Shimokomaki, M. (2013). Effect of carrageenan addition on the yield and functional properties of charqui (Jerked Beef). *Brazilian Archives of Biology and Technology, 56*, 311-318.

Gholizadeh, H., Messerotti, E., Pozzoli, M., Cheng, S., Traini, D., Young, P., . . . Ong, H. X. (2019). Application of a Thermosensitive In Situ Gel of Chitosan-Based Nasal Spray Loaded with Tranexamic Acid for Localised Treatment of Nasal Wounds. *AAPS PharmSciTech, 20*(7), 299. https://doi.org/10.1208/s12249-019-1517-6

Ghori, M., Mahdi Aljeboury, M., Smith, A., & Conway, B. (2015). Nasal Drug Delivery Systems: An Overview. *American Journal of Pharmacological Sciences, 3*.

Gouda, R., Baishya, H., & Qing, Z. (2017). Application of Mathematical Models in Drug Release Kinetics of Carbidopa and Levodopa ER Tablets. *Journal of Developing Drugs, 6*(2). https://doi.org/10.4172/2329-6631.1000171

Grant, G. T., Morris, E. R., Rees, D. A., Smith, P. J. C., & Thom, D. (1973). Biological interactions between polysaccharides and divalent cations: The egg-box model. *FEBS Letters, 32*(1), 195-198. https://doi.org/10.1016/0014-5793(73)80770-7

Grenier, J., Duval, H., Barou, F., Lv, P., David, B., & Letourneur, D. (2019). Mechanisms of pore formation in hydrogel scaffolds textured by freeze-drying. *Acta Biomaterialia, 94*, 195-203. https://doi.org/https://doi.org/10.1016/j.actbio.2019.05.070

Grzeskowiak, B., Wierzchowska, M., Walorek, R., Seredyka-Burduk, M., Wawrzyniak, K., & Burduk, P. K. (2019). Steroid vs. antibiotic impregnated absorbable nasal packing for wound healing after endoscopic sinus surgery: a randomized, double blind, placebo-controlled study. *Brazilian journal of otorhinolaryngology, 85*(4), 473-480. https://doi.org/10.1016/j.bjorl.2018.04.002

Gupta, P., Vermani, K., & Garg, S. (2002). Hydrogels: from controlled release to pH-responsive drug delivery. *Drug Discovery Today, 7*(10), 569-579. https://doi.org/https://doi.org/10.1016/S1359-6446(02)02255-9

Gürkan Polat, T., Duman, O., & Tunç, S. (2020). Preparation and characterization of environmentally friendly agar/κ-carrageenan/montmorillonite nanocomposite hydrogels. *Colloids and Surfaces A: Physicochemical and Engineering Aspects, 602*, 124987. https://doi.org/https://doi.org/10.1016/j.colsurfa.2020.124987

Harikrishnan, V., Madhusudhan, S., & Santhiagu, A. (2015). Evaluation of a novel, natural locust bean gum as a sustained release and mucoadhesive component of tizanidine hydrochloride buccal tablets. *Asian Journal of Pharmaceutical and Clinical Research, 8*(6), 7-10.

Harris, A. S., Nilsson, I. M., G-.Wagner, Z., & Alkner, U. (1986). Intranasal Administration of Peptides: Nasal Deposition, Biological Response, and Absorption of Desmopressin. *Journal of Pharmaceutical Sciences, 75*(11), 1085-1088. https://doi.org/https://doi.org/10.1002/jps.2600751113

Hauser, L. J., Ir, D., Kingdom, T. T., Robertson, C. E., Frank, D. N., & Ramakrishnan, V. R. (2016). Investigation of bacterial repopulation after sinus surgery and perioperative antibiotics. *International Forum of Allergy & Rhinology, 6*(1), 34-40. https://doi.org/https://doi.org/10.1002/alr.21630

Hillier, K., & Rakkar, M. (2007). Alginic Acid. In S. J. Enna & D. B. Bylund (Eds.), *xPharm: The Comprehensive Pharmacology Reference* (pp. 1-3). New York: Elsevier. https://doi.org/10.1016/B978-008055232-3.61186-9

Huang, Y.-C., Chen, J.-K., Lam, U. I., & Chen, S.-Y. (2014). Preparing, characterizing, and evaluating chitosan/fucoidan nanoparticles as oral delivery carriers. *Journal of Polymer Research, 21*(5), 415. https://doi.org/10.1007/s10965-014-0415-6

Huang, Y. C., & Yang, Y. T. (2016). Effect of basic fibroblast growth factor released from chitosan–fucoidan nanoparticles on neurite extension. *Journal of Tissue Engineering and Regenerative Medicine, 10*(5), 418-427. https://doi.org/10.1002/term.1752

Illum, L. (2000). Transport of drugs from the nasal cavity to the central nervous system. *Eur J Pharm Sci, 11*(1), 1-18. https://doi.org/10.1016/s0928-0987(00)00087-7

Inagaki, M., Sakakura, Y., Itoh, H., Ukai, K., & Miyoshi, Y. (1985). Macromolecular permeability of the tight junction of the human nasal mucosa. *Rhinology, 23*(3), 213-221.

Jackman, A. H., & Fried, M. P. (2009). Complications of Nasal Surgery and Epistaxis Management. In D. W. Eisele & R. V. Smith (Eds.), *Complications in Head and Neck Surgery* (2nd ed., pp. 531-541). Philadelphia: Mosby. https://doi.org/10.1016/B978-141604220-4.50045-6

Jacob, A., Faddis, B. T., & Chole, R. A. (2002). MeroGel hyaluronic acid sinonasal implants: osteogenic implications. *The Laryngoscope, 112*(1), 37-42.

Jahadi Hosseini, S. H. R., Khalili, M. R., & Motallebi, M. (2014). Comparison between Topical and Oral Tranexamic Acid in Management of Traumatic Hyphema. *Iranian journal of medical sciences, 39*(2 Suppl), 178-183.

Jahanshahi, J., Hashemian, F., Pazira, S., Bakhshaei, M. H., Farahani, F., Abasi, R., & Poorolajal, J. (2014). Effect of topical tranexamic acid on bleeding and quality of surgical field during functional endoscopic sinus surgery in patients with chronic rhinosinusitis: a triple blind randomized clinical trial. *PLoS One, 9*(8), e104477. https://doi.org/10.1371/journal.pone.0104477

Johnson, K.-a., Muzzin, N., Toufanian, S., Slick, R. A., Lawlor, M. W., Seifried, B., . . . Hoare, T. (2020). Drug-impregnated, pressurized gas expanded liquid-processed alginate hydrogel scaffolds for accelerated burn wound healing. *Acta Biomaterialia, 112*, 101-111. https://doi.org/10.1016/j.actbio.2020.06.006

Jones, D. S., Woolfson, A. D., & Brown, A. F. (1997). Textural, viscoelastic and mucoadhesive properties of pharmaceutical gels composed of cellulose polymers. *International Journal of Pharmaceutics, 151*(2), 223-233. https://doi.org/10.1016/S0378-5173(97)04904-1

Jones, N. (2001). The nose and paranasal sinuses physiology and anatomy. *Advanced Drug Delivery Reviews, 51*(1), 5-19. https://doi.org/https://doi.org/10.1016/S0169-409X(01)00172-7

Jumaidin, R., Sapuan, S. M., Jawaid, M., Ishak, M. R., & Sahari, J. (2016). Characteristics of thermoplastic sugar palm Starch/Agar blend: Thermal, tensile, and physical properties. *International Journal of Biological Macromolecules, 89*, 575-581. https://doi.org/10.1016/j.ijbiomac.2016.05.028

Kaewpradub, P. D. D. S., Apipan, B. M. D., & Rummasak, D. M. D. (2011). Does Tranexamic Acid in an Irrigating Fluid Reduce Intraope rative Blood Loss in Orthognathic Surgery? A Double-Blind, Randomized Clinical Trial. *Journal of Oral and Maxillofacial Surgery, 69*(6), e186-e189. https://doi.org/10.1016/j.joms.2010.11.041

Kang, B., Kim, J.-R., Shin, J.-M., Park, I.-H., & Lee, H.-M. (2017). Efficacy and Safety of Guardcel Nasal Packing After Endoscopic Sinus Surgery: A Prospective, Single-Blind, Randomized Controlled Study. *Clinical and Experimental Otorhinolaryngology, 10*(3), 248-253. https://doi.org/10.21053/ceo.2016.01081

Keller, L.-A., Merkel, O., & Popp, A. (2021). Intranasal drug delivery: opportunities and toxicologic challenges during drug development. *Drug Delivery and Translational Research*. https://doi.org/10.1007/s13346-020-00891-5

Khalil, H. P. S. A., Tye, Y. Y., Saurabh, C. K., Leh, C. P., Lai, T. K., Chong, E. W. N., . . . Syakir, M. I. (2017). Biodegradable polymer films from seaweed polysaccharides: A review on cellulose as a reinforcement material. *Express Polymer Letters, 11*(4), 244-265. https://doi.org/10.3144/expresspolymlett.2017.26

Khalmuratova, R., Kim, D. W., & Jeon, S. Y. (2011). Effect of dexamethasone on wound healing of the septal mucosa in the rat. *American Journal of Rhinology and Allergy, 25*(3), 112-116. https://doi.org/10.2500/ajra.2011.25.3595

Khanna, A., & Sama, A. (2019). Managing Complications and Revisions in Sinus Surgery. *Current Otorhinolaryngology Reports, 7*(1), 79-86. https://doi.org/10.1007/s40136-019-00231-3

Khurana, G., Arora, S., & Pawar, P. K. (2012). Ocular insert for sustained delivery of gatifloxacin sesquihydrate: Preparation and evaluations. *Internatinal Journal of Pharmaceutical Investigation, 2*(2), 70-77. https://doi.org/10.4103/2230-973x.100040

Khurma, J. R., Rohindra, D. R., & Nand, A. V. (2006). Synthesis and Properties of Hydrogels Based on Chitosan and Poly(Vinyl Alcohol) Crosslinked by Genipin. *Journal of Macromolecular Science, Part A, 43*(4-5), 749-758. https://doi.org/10.1080/10601320600602829

Kianfar, F., Antonijevic, M.D., Chowdhry,B.Z., Boateng, J.S. (2011). Formulation Development of a Carrageenan Based Delivery System for Buccal Drug Delivery Using Ibuprofen as a Model Drug *Biomaterials and Nanobiotechnology, 2*, 582-595. https://doi.org/10.4236/jbnb.2011.225070

Kim, B.-G., Kim, J.-H., Kim, S.-W., Kim, S.-W., Jin, K.-S., Cho, J. H., . . . Park, S.-Y. (2013). Nasal pH in patients with chronic rhinosinusitis before and after endoscopic sinus surgery. *American journal of otolaryngology, 34*(5). https://doi.org/10.1016/j.amjoto.2013.04.015

Kouchak, M. (2014). In situ gelling systems for drug delivery. *Jundishapur journal of natural pharmaceutical products, 9*(3), e20126-e20126. https://doi.org/10.17795/jjnpp-20126

Kovacs, A. J., Adappa, N. D., & Kuan, E. C. (2021). Exhalation Delivery Systems for Application of Intranasal Corticosteroids. *Ear Nose Throat J, 100*(5), 309-313. https://doi.org/10.1177/0145561320980194

Kucik, C., J., & Clenney, T. (2005). Management of Epistaxis. *American Family Physician, 71*(2), 305-311.

Kumar, S., Singh, A., Prajapati, S., & Singh, V. (2012). Formulation and evaluation of once daily sustained release matrix tablet of aceclofenac using natural gums. *Journal of Drug Delivery & Therapeutics, 2*(1), 16-24. https://doi.org/10.22270/jddt.v2i1.57

Kuznetsova, T. A., Besednova, N. N., Mamaev, A. N., Momot, A. P., Shevchenko, N. M., & Zvyagintseva, T. N. (2003). Anticoagulant activity of fucoidan from brown algae Fucus evanescens of the Okhotsk Sea. *Bulletin of experimental biology and medicine, 136*(5), 471-473. https://doi.org/10.1023/b:bebm.0000017096.72246.1f

Lafci Fahrioglu, S., VanKampen, N., & Andaloro, C. (2020). *Anatomy, Head and Neck, Sinus Function and Development* (30422521): StatPearls Publishing, Treasure Island (FL). Retrieved from http://europepmc.org/abstract/MED/30422521

http://europepmc.org/books/NBK532926

https://www.ncbi.nlm.nih.gov/books/NBK532926

Lahaye, M. (2001). Chemistry and physico-chemistry of phycocolloids. *Cahiers de Biologie Marine, 42*, 137-157.

Lai, V. M. F., Wong, P. A.-L., & Lii, C.-Y. (2000). Effects of Cation Properties on Sol-gel Transition and Gel Properties of κ-carrageenan. *Journal of Food Science, 65*(8), 1332-1337. https://doi.org/10.1111/j.1365-2621.2000.tb10607.x

Lee, K. Y., Rowley, J. A., Eiselt, P., Moy, E. M., Bouhadir, K. H., & Mooney, D. J. (2000). Controlling Mechanical and Swelling Properties of Alginate Hydrogels Independently by Cross-Linker Type and Cross-Linking Density. *Macromolecules, 33*(11), 4291-4294. https://doi.org/10.1021/ma9921347

Lee, P. I. (1985). Kinetics of drug release from hydrogel matrices. *Journal of Controlled Release, 2*, 277-288. https://doi.org/https://doi.org/10.1016/0168-3659(85)90051-3

Lefnaoui, S., & Moulai-Mostefa, N. (2011). Formulation and in vitro evaluation of κ-carrageenan-pregelatinized starch-based mucoadhesive gels containing miconazole. *Starch - Stärke, 63*(8), 512-521. https://doi.org/10.1002/star.201000141

Li, C., Li, C., Liu, Z., Li, Q., Yan, X., Liu, Y., & Lu, W. (2014). Enhancement in bioavailability of ketorolac tromethamine via intranasal in situ hydrogel based on poloxamer 407 and carrageenan. *International Journal of Pharmaceutics, 474*(1), 123-133. https://doi.org/10.1016/j.ijpharm.2014.08.023

Li, J., & Mooney, D. J. (2016). Designing hydrogels for controlled drug delivery. *Nature Reviews Materials, 1*(12), 16071. https://doi.org/10.1038/natrevmats.2016.71
Li, J., Shen, S., Kong, F., Jiang, T., Tang, C., & Yin, C. (2018). Effects of pore size on: In vitro and in vivo anticancer efficacies of mesoporous silica nanoparticles. *RSC Advances, 8*, 24633-24640. https://doi.org/10.1039/C8RA03914C
Li, Y., Meng, H., Liu, Y., Narkar, A., & Lee, B. P. (2016). Gelatin Microgel Incorporated Poly(ethylene glycol)-Based Bioadhesive with Enhanced Adhesive Property and Bioactivity. *ACS Applied Materials & Interfaces, 8*(19), 11980-11989. https://doi.org/10.1021/acsami.6b01364
Liang, J., & Lane, A. P. (2013). Topical Drug Delivery for Chronic Rhinosinusitis. *Current otorhinolaryngology reports, 1*(1), 51-60. https://doi.org/10.1007/s40136-012-0003-4
Liang, J., Liu, H., Huang, X., Xiong, W., Zhao, H., Chua, S., & Li, Z. (2016). Using tranexamic acid soaked absorbable gelatin sponge following complex posterior lumbar spine surgery: A randomized control trial. *Clinical Neurology and Neurosurgery, 147*, 110-114. https://doi.org/10.1016/j.clineuro.2016.06.001
Lisik, A., & Musiał, W. (2019). Conductomeric Evaluation of the Release Kinetics of Active Substances from Pharmaceutical Preparations Containing Iron Ions. *Materials, 12*(5), 730-739. https://doi.org/10.3390/ma12050730
Liu, J., Lin, S., Li, L., & Liu, E. (2005). Release of theophylline from polymer blend hydrogels. *International Journal of Pharmaceutics, 298*(1), 117-125. https://doi.org/https://doi.org/10.1016/j.ijpharm.2005.04.006
Logan, J. K., & Pantle, H. (2016). Role of topical tranexamic acid in the management of idiopathic anterior epistaxis in adult patients in the emergency department. *American Journal of Health-System Pharmacy, 73*(21), 1755-1759. https://doi.org/10.2146/ajhp150829
Lokhande, G., Carrow, J. K., Thakur, T., Xavier, J. R., Parani, M., Bayless, K. J., & Gaharwar, A. K. (2018). Nanoengineered injectable hydrogels for wound healing application. *Acta Biomaterialia, 70*, 35-47. https://doi.org/10.1016/j.actbio.2018.01.045
Long, L.-Y., Weng, Y.-X., & Wang, Y.-Z. (2018). Cellulose Aerogels: Synthesis, Applications, and Prospects. *Polymers, 10*(6), 623. https://doi.org/10.3390/polym10060623
Luppi, B., Bigucci, F., Cerchiara, T., & Zecchi, V. (2010). Chitosan-based hydrogels for nasal drug delivery: from inserts to nanoparticles. *Expert Opinion on Drug Delivery, 7*(7), 811-828. https://doi.org/10.1517/17425247.2010.495981
Luthuli, S., Wu, S., Cheng, Y., Zheng, X., Wu, M., & Tong, H. (2019). Therapeutic Effects of Fucoidan: A Review on Recent Studies. *Marine Drugs, 17*(9). https://doi.org/10.3390/md17090487
Lynch, C. R., Kondiah, P. P. D., Choonara, Y. E., du Toit, L. C., Ally, N., & Pillay, V. (2020). Hydrogel Biomaterials for Application in Ocular Drug Delivery. *Frontiers in Bioengineering and Biotechnology, 8*(228). https://doi.org/10.3389/fbioe.2020.00228
MacArthur, F. J. D., & McGarry, G. W. (2017). The arterial supply of the nasal cavity. *European Archives of Oto-Rhino-Laryngology, 274*(2), 809-815. https://doi.org/10.1007/s00405-016-4281-1
Maccabee, M. S., Trune, D. R., & Hwang, P. H. (2003). Effects of topically applied biomaterials on paranasal sinus mucosal healing. *American Jurnal of Rhinology, 17*(4), 203-207.
Malyarenko, O. S., & Ermakova, S. P. (2017). Fucoidans: Anticancer Activity and Molecular Mechanisms of Action. In J. Venkatesan, S. Anil, & S.-K. Kim (Eds.), *Seaweed Polysaccharides* (pp. 175-203): Elsevier. https://doi.org/10.1016/B978-0-12-809816-5.00010-4
Manzocco, L., Valoppi, F., Calligaris, S., Andreatta, F., Spilimbergo, S., & Nicoli, M. C. (2017). Exploitation of κ-carrageenan aerogels as template for edible oleogel preparation. *Food Hydrocolloids, 71*, 68-75. https://doi.org/10.1016/j.foodhyd.2017.04.021
Marple, B. F., Smith, T. L., Han, J. K., Gould, A. R., Jampel, H. D., Stambaugh, J. W., & Mugglin, A. S. (2012). Advance II: a prospective, randomized study assessing safety and efficacy

of bioabsorbable steroid-releasing sinus implants. *Otolaryngology, Head and Neck Surgery, 146*(6), 1004-1011. https://doi.org/10.1177/0194599811435968

Martins, J. T., Cerqueira, M. A., Bourbon, A. I., Pinheiro, A. C., Souza, B. W. S., & Vicente, A. A. (2012). Synergistic effects between κ-carrageenan and locust bean gum on physicochemical properties of edible films made thereof. *Food Hydrocolloids, 29*(2), 280-289. https://doi.org/10.1016/j.foodhyd.2012.03.004

Marx, D., Williams, G., & Birkhoff, M. (2015). Intranasal Drug Administration — An Attractive Delivery Route for Some Drugs. In O. Vallisuta & S. Olimat (Eds.), *Drug discovery and development: From Molecules to Medicine*. https://doi.org/10.5772/59468

Massey, C. J. M. D., & Singh, A. M. D. (2017). Advances in Absorbable Biomaterials and Nasal Packing. *Otolaryngologic Clinics of North America, 50*(3), 545-563. https://doi.org/10.1016/j.otc.2017.01.006

McInnes, F. J., Thapa, P., Baillie, A. J., Welling, P. G., Watson, D. G., Gibson, I., . . . Stevens, H. N. E. (2005). In vivo evaluation of nicotine lyophilised nasal insert in sheep. *International Journal of Pharmaceutics, 304*(1), 72-82. https://doi.org/10.1016/j.ijpharm.2005.07.025

McMartin, C., Hutchinson, L. E., Hyde, R., & Peters, G. E. (1987). Analysis of structural requirements for the absorption of drugs and macromolecules from the nasal cavity. *J Pharm Sci, 76*(7), 535-540. https://doi.org/10.1002/jps.2600760709

Medtronic. (2012). *Medtronic*. Retrieved from http://www.merocel.com/what-is-merocel-material/index.htm

Menchicchi, B., Fuenzalida, J. P., Hensel, A., Swamy, M. J., David, L., Rochas, C., & Goycoolea, F. M. (2015). Biophysical Analysis of the Molecular Interactions between Polysaccharides and Mucin. *Biomacromolecules, 16*(3), 924-935. https://doi.org/10.1021/bm501832y

Mendyk, A., Jachowicz, R., Fijorek, K., Dorożyński, P., Kulinowski, P. P., & Polak, S. (2012). KinetDS: An Open Source Software for Dissolution Test Data Analysis. *Dissolution Technologies, 19*. https://doi.org/10.14227/DT190112P6

Merkus, F. W., Verhoef, J. C., Schipper, N. G., & Marttin, E. (1998). Nasal mucociliary clearance as a factor in nasal drug delivery. *Adv Drug Deliv Rev, 29*(1-2), 13-38. https://doi.org/10.1016/s0169-409x(97)00059-8

Mihaila, S. M., Gaharwar, A. K., Reis, R. L., Marques, A. P., Gomes, M. E., & Khademhosseini, A. (2013). Photocrosslinkable Kappa-Carrageenan Hydrogels for Tissue Engineering Applications. *Advanced Healthcare Materials, 2*(6), 895-907. https://doi.org/10.1002/adhm.201200317

Mohanty, D., Bakshi, D. R., Simharaju, N., Haque, M., & Sahoo, C. (2018). A Review on in situ Gel : A Novel Drug Delivery System

Morita, T., Yamamoto, A., Hashida, M., & Sezaki, H. (1991). Effect of absorption promoters on nasal and pulmonary absorption of drugs with various molecular weight was examined in rats. *Drug Delivery System, 6*(3), 207-211. https://doi.org/10.2745/dds.6.207

Murakami, K., Aoki, H., Nakamura, S., Nakamura, S., Takikawa, M., Hanzawa, M., . . . Ishihara, M. (2010). Hydrogel blends of chitin/chitosan, fucoidan and alginate as healing-impaired wound dressings. *Biomaterials, 31*(1), 83-90. https://doi.org/10.1016/j.biomaterials.2009.09.031

Murakami, K., Ishihara, M., Aoki, H., Nakamura, S., Nakamura, S., Yanagibayashi, S., . . . Sato, Y. (2010). Enhanced healing of mitomycin C-treated healing-impaired wounds in rats with hydrosheets composed of chitin/chitosan, fucoidan, and alginate as wound dressings. *Wound Repair and Regeneration, 18*(5), 478-485. https://doi.org/10.1111/j.1524-475X.2010.00606.x

Murray, S., Mendez, A., Hopkins, A., El-Hakim, H., Jeffery, C. C., & Côté, D. W. J. (2018). Management of persistent epistaxis using Floseal hemostatic matrix vs. traditional nasal packing: a prospective randomized control trial. *Journal of Otolaryngology - Head & Neck Surgery, 47*(1), 3-3. https://doi.org/10.1186/s40463-017-0248-5

Muthumanickam, A., B.Chengaiah, K.Gnanaprakash, Ramkanth, D. S., Chetty, C. M., & D.Dhachinamoorthi. (2010). Nasal drug delivery system - an overview. *International Journal of Research in Pharmaceutical Sciences, 1*.

Nair, A. V., Raman, M., & Doble, M. (2016). Cyclic β-(1→3) (1→6) glucan/carrageenan hydrogels for wound healing applications. *RSC Advances, 6*(100), 98545-98553. https://doi.org/10.1039/C6RA23386D

Nakagawa, K., Sowasod, N., Charinpanitkul, T., Soottitantawat, A., & Tanthapanichakoon, W. (2011). Encapsulation of Curcumin Loaded Oil Droplets By Cryotropic Gel Formation from O/W Emulsion. *Procedia Food Science, 1*, 1973-1979. https://doi.org/10.1016/j.profoo.2011.09.290

Nanda, S., Sood, N., Reddy, B., & Markandeywar, T. (2013). Preparation and Characterization of Poly(vinyl alcohol)-chondroitin Sulphate Hydrogel as Scaffolds for Articular Cartilage Regeneration. *Indian Journal of Materials Science, 2013*, 1-8. https://doi.org/10.1155/2013/516021

Ngwuluka, N. C., Choonara, Y. E., Kumar, P., du Toit, L. C., Modi, G., & Pillay, V. (2015). A Co-blended Locust Bean Gum and Polymethacrylate-NaCMC Matrix to Achieve Zero-Order Release via Hydro-Erosive Modulation. *An Official Journal of the American Association of Pharmaceutical Scientists, 16*(6), 1377-1389. https://doi.org/10.1208/s12249-015-0326-9

Nita, L. E., Ghilan, A., Rusu, A. G., Neamtu, I., & Chiriac, A. P. (2020). New Trends in Bio-Based Aerogels. *Pharmaceutics, 12*(5), 449.

Nižić, L., Ugrina, I., Špoljarić, D., Saršon, V., Kučuk, M. S., Pepić, I., & Hafner, A. (2019). Innovative sprayable in situ gelling fluticasone suspension: Development and optimization of nasal deposition. *Int J Pharm, 563*, 445-456. https://doi.org/10.1016/j.ijpharm.2019.04.015

Nuñez-Castruita, A., López-Serna, N., & Guzmán-López, S. (2012). Prenatal development of the maxillary sinus: a perspective for paranasal sinus surgery. *Otolaryngology--head and neck surgery : official journal of American Academy of Otolaryngology-Head and Neck Surgery, 146*(6), 997-1003. https://doi.org/10.1177/0194599811435883

Ottoline, A. C., Tomita, S., Marques, M., Felix, F., Ferraiolo, P. N., & Laurindo, R. S. (2013). Antibiotic prophylaxis in otolaryngologic surgery. *International archives of otorhinolaryngology,, 17*(1), 85-91. https://doi.org/10.7162/S1809-97772013000100015

Ouyang, Q.-Q., Hu, Z., Li, S.-D., Quan, W.-Y., Wen, L.-L., Yang, Z.-M., & Li, P.-W. (2018). Thermal degradation of agar: Mechanism and toxicity of products. *Food Chemistry, 264*, 277-283. https://doi.org/https://doi.org/10.1016/j.foodchem.2018.04.098

Panyukov, S. (2019). Loops in polymer networks. *Macromolecules, 52*(11), 4145-4153. https://doi.org/10.1021/acs.macromol.9b00782

Paolino, D., Tudose, A., Celia, C., Di Marzio, L., Cilurzo, F., & Mircioiu, C. (2019). Mathematical Models as Tools to Predict the ReleaseKinetic of Fluorescein from Lyotropic ColloidalLiquid Crystals. *Materials, 12*(693). https://doi.org/10.3390/ma12050693

Park, J. H., Choi, S. H., Park, S. J., Ku, S. K., Song, C. H., Lee, Y. J., . . . Cho, C. M. (2017). Promoting wound healing using low molecular weight fucoidan in a full-thickness dermal excision rat model. *Marine Drugs, 15*(4). https://doi.org/10.3390/md15040112

Paşcalău, V., Popescu, V., Popescu, G. L., Dudescu, M. C., Borodi, G., Dinescu, A., . . . Paul, M. (2012). The alginate/k-carrageenan ratio's influence on the properties of the cross-linked composite films. *Journal of Alloys and Compounds, 536*, S418-S423. https://doi.org/10.1016/j.jallcom.2011.12.026

Pastor, E., Reguera, E., Matveeva, E., & Garcia-Fuentes, M. (2015). Pore size is a critical parameter for obtaining sustained protein release from electrochemically synthesized mesoporous silicon microparticles. *PeerJ Life and Environment, 3*(e1277), 1-12. https://doi.org/10.7717/peerj.1277

Patel, U. L., Chotai, N. P., & Nagda, C. D. (2012). Design and evaluation of ocular drug delivery system for controlled delivery of gatifloxacin sesquehydrate: In vitro and in vivo

evaluation. *Pharmaceutical Development and Technology, 17*(1), 15-22. https://doi.org/10.3109/10837450.2010.502178

Pawar, V. K., Singh, Y., Sharma, K., Shrivastav, A., Sharma, A., Singh, A., . . . Chourasia, M. K. (2019). Improved chemotherapy against breast cancer through immunotherapeutic activity of fucoidan decorated electrostatically assembled nanoparticles bearing doxorubicin. *International Journal of Biological Macromolecules, 122*, 1100-1114. https://doi.org/10.1016/j.ijbiomac.2018.09.059

Permanadewi, I., Kumoro, A. C., Wardhani, D. H., & Aryanti, N. (2019). Modelling of controlled drug release in gastrointestinal tract simulation. *Journal of Physics: Conference Series, 1295*. https://doi.org/10.1088/1742-6596/1295/1/012063

Piluso, S., Lendlein, A., & Neffe, A. T. (2017). Enzymatic action as switch of bulk to surface degradation of clicked gelatin-based networks. *Polymers for Advanced Technologies, 28*(10), 1318-1324. https://doi.org/https://doi.org/10.1002/pat.3962

Pinkas, O., & Zilberman, M. (2014). Effect of hemostatic agents on properties of gelatin-alginate soft tissue adhesives. *Journal of Biomaterials Science: Polymer Edition, 25*(6), 555-573. https://doi.org/10.1080/09205063.2014.881681

Pires, A., Fortuna, A., Alves, G., & Falcão, A. (2009). Intranasal drug delivery: how, why and what for? *J Pharm Pharm Sci, 12*(3), 288-311. https://doi.org/10.18433/j3nc79

Plazzotta, S., Calligaris, S., & Manzocco, L. (2019). Structure of oleogels from κ-carrageenan templates as affected by supercritical-CO2-drying, freeze-drying and lettuce-filler addition. *Food Hydrocolloids, 96*, 1-10. https://doi.org/https://doi.org/10.1016/j.foodhyd.2019.05.008

Prajapati, V. D., Jani, G. K., Moradiya, N. G., Randeria, N. P., Maheriya, P. M., & Nagar, B. J. (2014). Locust bean gum in the development of sustained release mucoadhesive macromolecules of aceclofenac. *Carbohydrate Polymers, 113*, 138-148. https://doi.org/10.1016/j.carbpol.2014.06.061

Pundir, V., Pundir, J., Lancaster, G., Baer, S., Kirkland, P., Cornet, M., . . . Fokkens, W. J. (2016). Role of corticosteroids in Functional Endoscopic Sinus Surgery--a systematic review and meta-analysis. *Rhinology, 54*(1), 3-19. https://doi.org/10.4193/Rhin15.079

Pushpamalar, V., Langford, S. J., Ahmad, M., Hashim, K., & Lim, Y. Y. (2013). Preparation of carboxymethyl sago pulp hydrogel from sago waste by electron beam irradiation and swelling behavior in water and various pH media. *Journal of Applied Polymer Science, 128*(1), 451-459. https://doi.org/10.1002/app.38192

Rabin, C., & Siegel, S. (2012). Delivery Systems and Dosing for Antipsychotics. *Handbook of experimental pharmacology, 212*, 267-298. https://doi.org/10.1007/978-3-642-25761-2_11

Racheva, M., Julich-Gruner, K. K., Nöchel, U., Neffe, A. T., Wischke, C., & Lendlein, A. (2013). Influence of Drying Procedures on Network Formation and Properties of Hydrogels from Functionalized Gelatin. *Macromolecular Symposia, 334*(1), 24-32. https://doi.org/10.1002/masy.201300112

Ramalingam, N., Parida, P., Saxena, S., & Surianarayanan, G. (2018). Comparison of triamcinolone and mitomycin C nasal pack in functional endoscopic sinus surgery: a randomized, clinical trial. *The Egyptian Journal of Otolaryngology, 34*(4), 242-247. https://doi.org/10.4103/ejo.ejo_9_17

Rasool, A., Ata, S., Islam, A., & Khan, R. U. (2019). Fabrication of novel carrageenan based stimuli responsive injectable hydrogels for controlled release of cephradine. *RSC Advances, 9*(22), 12282-12290. https://doi.org/10.1039/C9RA02130B

Rege, A., Preibisch, I., Schestakow, M., Ganesan, K., Gurikov, P., Milow, B., . . . Itskov, M. (2018). Correlating Synthesis Parameters to Morphological Entities: Predictive Modeling of Biopolymer Aerogels. *Materials, 11*(9), 1670.

Rhim, J. W. (2012). Physical-mechanical properties of agar/κ-carrageenan blend film and derived clay nanocomposite film. *Journal of Food Science, 77*(12), N66-73. https://doi.org/10.1111/j.1750-3841.2012.02988.x

Rhim, J. W., & Wang, L. F. (2013). Mechanical and water barrier properties of agar/κ-carrageenan/konjac glucomannan ternary blend biohydrogel films. *Carbohydrate Polymers, 96*(1), 71-81. https://doi.org/10.1016/j.carbpol.2013.03.083

Riley, R. G., Smart, J. D., Tsibouklis, J., Dettmar, P. W., Hampson, F., Davis, J. A., . . . Wilber, W. R. (2001). An investigation of mucus/polymer rheological synergism using synthesised and characterised poly(acrylic acid)s. *International Journal of Pharmaceutics, 217*(1), 87-100. https://doi.org/https://doi.org/10.1016/S0378-5173(01)00592-0

Rind, E. M., Laghari, M. G., Memon, A. H., Mughal, U. R., Almani, F., Memon, N., . . . Maheshwari, M. L. (2009). Spectrophotometric determination of tranexamic acid using vanillin. *Yao xue xue bao = Acta pharmaceutica Sinica, 44*(2), 175-180.

Rochas, C., Lahaye, M., & Yaphe, W. (1986). Sulfate Content of Carrageenan and Agar Determined by Infrared Spectroscopy. *Botanica Marina, 29*, 335-340. https://doi.org/10.1515/botm.1986.29.4.335

Rode, M. P., Batti Angulski, A. B., Gomes, F. A., da Silva, M. M., Jeremias, T. d. S., de Carvalho, R. G., . . . Calloni, G. W. (2018). Carrageenan hydrogel as a scaffold for skin-derived multipotent stromal cells delivery. *Journal of Biomaterials Applications, 33*(3), 422-434. https://doi.org/10.1177/0885328218795569

Romeo, V. D., deMeireles, J. C., Gries, W. J., Xia, W. J., Sileno, A. P., Pimplaskar, H. K., & Behl, C. R. (1998). Optimization of systemic nasal drug delivery with pharmaceutical excipients. *Adv Drug Deliv Rev, 29*(1-2), 117-133. https://doi.org/10.1016/s0169-409x(97)00064-1

Rowe-Jones, J. M., Medcalf, M., Durham, S. R., Richards, D. H., & Mackay, I. S. (2005). Functional endoscopic sinus surgery: 5 year follow up and results of a prospective, randomised, stratified, double-blind, placebo controlled study of postoperative fluticasone propionate aqueous nasal spray. *Rhinology, 43*(1), 2-10.

Roy, D. S., & Rohera, B. D. (2002). Comparative evaluation of rate of hydration and matrix erosion of HEC and HPC and study of drug release from their matrices. *European Journal of Pharmaceutical Sciences, 16*(3), 193-199. https://doi.org/10.1016/S0928-0987(02)00103-3

Rudmik, L., Mace, J., & Mechor, B. (2012). Effect of a dexamethasone Sinu-Foam™ middle meatal spacer on endoscopic sinus surgery outcomes: a randomized, double-blind, placebo-controlled trial. *International Forum of Allergy and Rhinology, 2*(3), 248-251. https://doi.org/10.1002/alr.21011

Sabarinath, V., Harish, M. R., & Divakaran, S. (2017). Triamcinolone Impregnated Nasal Pack in Endoscopic Sinus Surgery: Our Experience. *Indian Journal of Otolaryngology, Head and Neck Surgery, 69*(1), 88-92. https://doi.org/10.1007/s12070-016-1041-x

Sachithanadam, M., & Joshi, S. C. (2014). High strain recovery with improved mechanical properties of gelatin–silica aerogel composites post-binding treatment. *Journal of Materials Science, 49*(1), 163-179. https://doi.org/10.1007/s10853-013-7690-1

Saha, D., & Bhattacharya, S. (2010). Hydrocolloids as thickening and gelling agents in food: a critical review. *Journal of Food Science and Technology, 47*(6), 587-597. https://doi.org/10.1007/s13197-010-0162-6

Saidi, M., Dabbaghi, A., & Rahmani, S. (2020). Swelling and drug delivery kinetics of click-synthesized hydrogels based on various combinations of PEG and star-shaped PCL: influence of network parameters on swelling and release behavior. *Polymer Bulletin, 77*(8), 3989-4010. https://doi.org/10.1007/s00289-019-02948-z

Salazar, C., Armenta, J. M., & Shulaev, V. (2012). An UPLC-ESI-MS/MS Assay Using 6-Aminoquinolyl-N-Hydroxysuccinimidyl Carbamate Derivatization for Targeted Amino Acid Analysis: Application to Screening of Arabidopsis thaliana Mutants. *Metabolites, 2*(3), 398-428.

Sánchez-Sánchez, M.-P., Martín-Illana, A., Ruiz-Caro, R., Bermejo, P., Abad, M.-J., Carro, R., . . . Veiga, M.-D. (2015). Chitosan and Kappa-Carrageenan Vaginal Acyclovir Formulations for Prevention of Genital Herpes. In Vitro and Ex Vivo Evaluation. *Marine Drugs, 13*(9), 5976-5992.

Sarath, C. C., Shanks, R. A., & Thomas, S. (2014). Polymer Blends. In S. Thomas, R. Shanks, & S. Chandrasekharakurup (Eds.), *Nanostructured Polymer Blends* (pp. 1-14). Oxford: William Andrew Publishing. https://doi.org/10.1016/B978-1-4557-3159-6.00001-8

Sawant, P. D., Luu, D., Ye, R., & Buchta, R. (2010). Drug release from hydroethanolic gels. Effect of drug's lipophilicity (logP), polymer-drug interactions and solvent lipophilicity. *International Journal of Pharmacy, 396*(1-2), 45-52. https://doi.org/10.1016/j.ijpharm.2010.06.008

Schafer, S. E., & Stevens, E. S. (1995). A reexamination of the double-helix model for agarose gels using optical rotation. *Biopolymers, 36*(1), 103-108. https://doi.org/https://doi.org/10.1002/bip.360360109

Segtnan, V. H., & Isaksson, T. (2004). Temperature, sample and time dependent structural characteristics of gelatine gels studied by near infrared spectroscopy. *Food Hydrocolloids, 18*(1), 1-11. https://doi.org/10.1016/S0268-005X(02)00096-6

Şenyiğit Zeynep, A., Karavana Sinem, Y., Eraç, B., Gürsel, Ö., Limoncu Mine, H., & Baloğlu, E. (2014). Evaluation of chitosan based vaginal bioadhesive gel formulations for antifungal drugs. *Acta Pharmaceutica*(2), 139. https://doi.org/10.2478/acph-2014-0013

Sezer, A. D., & Akbuğa, J. (2006). Fucosphere--new microsphere carriers for peptide and protein delivery: preparation and in vitro characterization. *Journal of Microencapsulation, 23*(5), 513-522. https://doi.org/10.1080/02652040600687563

Sezer, A. D., & Akbuğa, J. (2009). Comparison on in vitro characterization of fucospheres and chitosan microspheres encapsulated plasmid DNA (pGM-CSF): formulation design and release characteristics. *AAPS Pharmacy, Science and Technology, 10*(4), 1193-1199. https://doi.org/10.1208/s12249-009-9324-0

Sezer, A. D., Cevher, E., Hatipoğlu, F., Oğurtan, Z., Baş, A. L., & Akbuğa, J. (2008a). Preparation of fucoidan-chitosan hydrogel and its application as burn healing accelerator on rabbits. *Biological Pharmacy Bulletin, 31*(12), 2326-2333. https://doi.org/10.1248/bpb.31.2326

Sezer, A. D., Cevher, E., Hatipoğlu, F., Oğurtan, Z., Baş, A. L., & Akbuğa, J. (2008b). The use of fucosphere in the treatment of dermal burns in rabbits. *European Journal of Pharmaceutics and Biopharmaceutics, 69*(1), 189-198. https://doi.org/10.1016/j.ejpb.2007.09.004

Shaikh, R., Raj Singh, T. R., Garland, M. J., Woolfson, A. D., & Donnelly, R. F. (2011). Mucoadhesive drug delivery systems. *Journal of pharmacy & bioallied sciences, 3*(1), 89-100. https://doi.org/10.4103/0975-7406.76478

Shanmugarajan, T. S., Selvan, N. K., & Uppuluri, V. N. V. A. (2020). Development and Characterization of Squalene-Loaded Topical Agar-Based Emulgel Scaffold: Wound Healing Potential in Full-Thickness Burn Model. *International Journal of Lower Extremity Wounds*. https://doi.org/10.1177/1534734620921629

Shchipunov, Y. A., & Chesnokov, A. V. (2003). Carrageenan Gels in Skim Milk: Formation and Rheological Properties. *Colloid Journal, 65*(1), 105-113. https://doi.org/10.1023/A:1022335428512

Sherafudeen, S. P., & Vasantha, P. V. (2015). Development and evaluation of in situ nasal gel formulations of loratadine. *Research in pharmaceutical sciences, 10*(6), 466-476.

Shikani, A. H. (1996). Use of Antibiotics for Expansion of the Merocel® Packing following Endoscopic Sinus Surgery. *Ear, Nose & Throat Journal, 75*(8), 524-528. https://doi.org/10.1177/014556139607500811

Silva, S., Duarte, A., Mano, J. F., & Reis, R. L. (2013). Design and functionalization of chitin-based microsphere scaffolds. *Green Chemistry., 15*, 3252-3258. https://doi.org/10.1039/C3GC41060A

Silva, T. H., Alves, A., Popa, E. G., Reys, L. L., Gomes, M. E., Sousa, R. A., . . . Reis, R. L. (2012). Marine algae sulfated polysaccharides for tissue engineering and drug delivery approaches. *Biomatter, 2*(4), 278-289. https://doi.org/10.4161/biom.22947

Singh, A. K., Singh, A., & Madhav, N. V. S. (2012). Nasal cavity: A promising transmucosal platform for drug delivery and research approaches from nasal to brain targetting. *Journal of Drug Delivery and Theraputics, 2*(3), 22-33. https://doi.org/10.22270/jddt.v2i3.163

Singh, R. M., Kumar, A., & Pathak, K. (2013). Mucoadhesive in situ nasal gelling drug delivery systems for modulated drug delivery. *Expert Opin Drug Deliv, 10*(1), 115-130. https://doi.org/10.1517/17425247.2013.746659

Siu, J., Shrestha, K., Inthavong, K., Shang, Y., & Douglas, R. (2020). Particle deposition in the paranasal sinuses following endoscopic sinus surgery. *Computers in Biology and Medicine, 116*. https://doi.org/10.1016/j.compbiomed.2019.103573

Smith, & Nephew. (2015). RapidRhino Epistaxis Products. Austin, USA.

Soane, R. J., Hinchcliffe, M., Davis, S. S., & Illum, L. (2001). Clearance characteristics of chitosan based formulations in the sheep nasal cavity. *Int J Pharm, 217*(1-2), 183-191. https://doi.org/10.1016/s0378-5173(01)00602-0

Sobol, S. E. (2007). CHAPTER 8 - Management of Acute Sinusitis and Its Complications. In R. F. Wetmore & L. M. Bell (Eds.), *Pediatric Otolaryngology* (pp. 118-128). Philadelphia: Mosby. https://doi.org/10.1016/B978-0-323-04855-2.50013-7

Soler, Z. M., Mace, J., & Smith, T. L. (2008). Symptom-based presentation of chronic rhinosinusitis and symptom-specific outcomes after endoscopic sinus surgery. *American Journal of Rhinology, 22*(3), 297-301. https://doi.org/10.2500/ajr.2008.22.3172

Sonawane, R. O., & Patil, S. D. (2017). Gelatin–κ-carrageenan polyelectrolyte complex hydrogel compositions for the design and development of extended-release pellets. *International Journal of Polymeric Materials and Polymeric Biomaterials, 66*(16), 812-823. https://doi.org/10.1080/00914037.2016.1276060

Sosnik, A., & Seremeta, K. P. (2017). Polymeric Hydrogels as Technology Platform for Drug Delivery Applications. *Gels (Basel, Switzerland), 3*(3), 25. https://doi.org/10.3390/gels3030025

Sousa, J., Alvesbc, G., Oliveiraa, P., Fortuna, A., & Falcão, A. (2017). Intranasal delivery of ciprofloxacin to rats: A topical approach using a thermoreversible in situ gel. *European Journal of Pharmaceutical Sciences, 97*, 30-37. https://doi.org/10.1016/j.ejps.2016.10.033

Stefan, M., Rabie, N., Sobhy, T., & Maarouf, A. (2019). Effect of steroid-releasing sinus implants after endoscopic sinus surgery (ESS) on postoperative outcomes: A meta-analytical study. *The Egyptian Journal of Otolaryngology, 35*(3), 250-255. https://doi.org/10.4103/ejo.ejo_92_18

Stevens, W. W., Lee, R. J., Schleimer, R. P., & Cohen, N. A. (2015). Chronic rhinosinusitis pathogenesis. *Journal of Allergy and Clinical Immunology, 136*(6), 1442-1453. https://doi.org/10.1016/j.jaci.2015.10.009

Stuart, B. O. (1984). Deposition and clearance of inhaled particles. *Environ Health Perspect, 55*, 369-390. https://doi.org/10.1289/ehp.8455369

Summitmedical. (2017). *AnsorbNet nasl and sinus packing*. Retrieved from http://www.summitmedicalusa.com/products/ent/rhinology/nasal-packing-absorbent.php

Sun, Z., Song, C., Wang, C., Hu, Y., & Wu, J. (2020). Hydrogel-Based Controlled Drug Delivery for Cancer Treatment: A Review. *Molecular Pharmaceutics, 17*(2), 373-391. https://doi.org/10.1021/acs.molpharmaceut.9b01020

Suzuki, Y., Nishimura, Y., Tanihara, M., Suzuki, K., Nakamura, T., Shimizu, Y., . . . Kakimaru, Y. (1998). Evaluation of a novel alginate gel dressing: Cytotoxicity to fibroblasts in vitro and foreign-body reaction in pig skin in vivo. *Journal of Biomedical Materials Research, 39*(2), 317-322. https://doi.org/10.1002/(sici)1097-4636(199802)39:2<317::Aid-jbm20>3.0.Co;2-8

Szilágyi, B. Á., Mammadova, A., Gyarmati, B., & Szilágyi, A. (2020). Mucoadhesive interactions between synthetic polyaspartamides and porcine gastric mucin on the colloid size

scale. *Colloids and Surfaces B: Biointerfaces, 194*, 111219. https://doi.org/10.1016/j.colsurfb.2020.111219

Tan, W. S., Arulselvan, P., Ng, S.-F., Taib, C. N. M., Sarian, M. N., & Fakurazi, S. (2020). Healing Effect of Vicenin-2 (VCN-2) on Human Dermal Fibroblast (HDF) and Development VCN-2 Hydrocolloid Film Based on Alginate as Potential Wound Dressing. *BioMed Research International*, 1-15. https://doi.org/10.1155/2020/4730858

Tan, Y. T., Peh, K. K., & Al-Hanbali, O. (2000). Effect of Carbopol and polyvinylpyrrolidone on the mechanical, rheological, and release properties of bioadhesive polyethylene glycol gels. *AAPS Pharmacy, Science and Technology, 1*(3), 69-78. https://doi.org/10.1208/pt010324

Tanna, B., & Mishra, A. (2019). Nutraceutical Potential of Seaweed Polysaccharides: Structure, Bioactivity, Safety, and Toxicity. *Comprehensive Reviews in Food Science and Food Safety, 18*(3), 817-831. https://doi.org/10.1111/1541-4337.12441

Thangapandi, M., Ajith Kumar, T. T., Shanmugaasokan, L., & Devi, D. K. N. (2014). In vitro Antioxidant Properties of Fucoidan Fractions From Sargassum tenerrimum. *Pakistan journal of biological sciences, 17*, 402-407. https://doi.org/10.3923/pjbs.2014.402.407

Thirawong, N., Nunthanid, J., Puttipipatkhachorn, S., & Sriamornsak, P. (2007). Mucoadhesive properties of various pectins on gastrointestinal mucosa: An in vitro evaluation using texture analyzer. *European Journal of Pharmaceutics and Biopharmaceutics, 67*(1), 132-140. https://doi.org/10.1016/j.ejpb.2007.01.010

Thrimawithana, T. R., Young, S., Dunstan, D. E., & Alany, R. G. (2010). Texture and rheological characterization of kappa and iota carrageenan in the presence of counter ions. *Carbohydrate Polymers, 82*(1), 69-77. https://doi.org/https://doi.org/10.1016/j.carbpol.2010.04.024

Tian, G., Lu, Z., Miao, K., Ji, Z., Zhang, H., & Li, D. (2015). Formation Mechanism of Cracks During the Freeze Drying of Gelcast Ceramic Parts. *Journal of the American Ceramic Society, 98*(10), 3338-3345. https://doi.org/10.1111/jace.13761

Tibbelin, A., Aust, R., Bende, M., Holgersson, M., Petruson, B., Rundcrantz, H., & Ålander, U. (1995). Effect of Local Tranexamic Acid Gel in the Treatment of Epistaxis. *ORL, 57*(4), 207-209. https://doi.org/10.1159/000276741

Tom, L. W., Palasti, S., Potsic, W. P., Handler, S. D., & Wetmore, R. F. (1997). The effects of gelatin film stents in the middle meatus. *American journal of rhinology, 11*(3), 229-232.

Traboulsi, H., Alam, E., & Hadi, U. (2015). Changing Trends in the Management of Epistaxis. *International Journal of Otolaryngology, 2015*, 263987-263987. https://doi.org/10.1155/2015/263987

Trafton, A. (2012). *Loops in polymer networks* [MIT News]. Retrieved July 29, 2020, from http://news.mit.edu/2012/counting-loops-for-stronger-polymers-1105

Tyeb, S., Kumar, N., Kumar, A., & Verma, V. (2018). Flexible agar-sericin hydrogel film dressing for chronic wounds. *Carbohydrate Polymers, 200*, 572-582. https://doi.org/10.1016/j.carbpol.2018.08.030

Tytgat, L., Van Damme, L., Ortega Arevalo, M. d. P., Declercq, H., Thienpont, H., Otteveare, H., . . . Van Vlierberghe, S. (2019). Extrusion-based 3D printing of photo-crosslinkable gelatin and κ-carrageenan hydrogel blends for adipose tissue regeneration. *International Journal of Biological Macromolecules, 140*, 929-938. https://doi.org/10.1016/j.ijbiomac.2019.08.124

Uppuluri, V. N. V. A., & Shanmugarajan, T. S. (2019). Icariin-Loaded Polyvinyl Alcohol/Agar Hydrogel: Development, Characterization, and In Vivo Evaluation in a Full-Thickness Burn Model. *International Journal of Lower Extremity Wounds, 18*(3), 323-335. https://doi.org/10.1177/1534734619849982

Ushakova, N. A., Morozevich, G. E., Ustiuzhanina, N. E., Bilan, M. I., Usov, A. I., Nifant'ev, N. E., & Preobrazhenskaia, M. E. (2009). Anticoagulant activity of fucoidans from brown algae. *Biochemistry (Moscow) Supplement Series B: Biomedical Chemistry, 3*, 77-83.

Usov, A. I. (2011). Polysaccharides of the red algae. *Advanced Carbohydrate Chemistry and Biochemistry, 65*, 115-217. https://doi.org/10.1016/b978-0-12-385520-6.00004-2

Valentine, R. M., Wormald, P.-J. M. D., & Sindwani, R. M. D. F. F. (2009). Advances in Absorbable Biomaterials and Nasal Packing. *Otolaryngologic Clinics of North America, The, 42*(5), 813-828. https://doi.org/10.1016/j.otc.2009.07.009

Varshosaz, J., & Hajian, M. (2004). Characterization of Drug Release and Diffusion Mechanism Through Hydroxyethylmethacrylate/Methacrylic Acid pH-Sensitive Hydrogel. *Drug Delivery, 11*(1), 53-58. https://doi.org/10.1080/10717540490265298

Verbeken, D., Thas, O., & Dewettinck, K. (2004). Textural properties of gelled dairy desserts containing κ-carrageenan and starch. *Food Hydrocolloids, 18*(5), 817-823. https://doi.org/https://doi.org/10.1016/j.foodhyd.2003.12.007

Vigani, B., Rossi, S., Gentile, M., Sandri, G., Bonferoni, M. C., Cavalloro, V., . . . Ferrari, F. (2019). Development of a Mucoadhesive and an in Situ Gelling Formulation Based on κ-Carrageenan for Application on Oral Mucosa and Esophagus Walls. II. Loading of a Bioactive Hydroalcoholic Extract. *Marine Drugs, 17*(3), 153. https://doi.org/10.3390/md17030153

Vigani, B., Rossi, S., Sandri, G., Bonferoni, M. C., Caramella, C. M., & Ferrari, F. (2020). Recent Advances in the Development of In Situ Gelling Drug Delivery Systems for Non-Parenteral Administration Routes. *Pharmaceutics, 12*(9), 859. https://doi.org/10.3390/pharmaceutics12090859

Vijayaraghavan, C., Vasanthakumar, S., & Ramakrishnan, A. (2008). In vitro and in vivo evaluation of locust bean gum and chitosan combination as a carrier for buccal drug delivery. *Pharmazie, 63*(5), 342-347.

Wang, J., Cai, C., & Wang, S. (2014). Merocel versus Nasopore for Nasal Packing: A Meta-Analysis of Randomized Controlled Trials. *PLOS ONE, 9*(4), e93959. https://doi.org/10.1371/journal.pone.0093959

Wang, T. C., & Hsu, C. L. (2017). Nasal packing after functional sinus surgery. In B. Singh Gendeh (Ed.), *Paranasal sinuses* (pp. 80-90). https://doi.org/105772/66003

Wang, Y., Jiang, S., Wang, H., & Bie, H. (2017). A mucoadhesive, thermoreversible in situ nasal gel of geniposide for neurodegenerative diseases. *PLOS ONE, 12*(12), e0189478. https://doi.org/10.1371/journal.pone.0189478

Wang, Y. P., Wang, M. C., Chen, Y. C., Leu, Y. S., Lin, H. C., & Lee, K. S. (2011). The effects of Vaseline gauze strip, Merocel, and Nasopore on the formation of synechiae and excessive granulation tissue in the middle meatus and the incidence of major postoperative bleeding after endoscopic sinus surgery. *Journal of the Chinese Medical Association, 74*(1), 16-21. https://doi.org/10.1016/j.jcma.2010.09.001

Washington, N., Washington, C., & Wilson, C. (2000). *Physiological Pharmaceutics: Barriers to Drug Absorption* (1st ed.). London, UK: CRC Press. https://doi.org/10.1201/9780203483701

Watelet, J. B., Demetter, P., Claeys, C., Van Cauwenberge, P., Cuvelier, C., & Bachert, C. (2005). Neutrophil-derived metalloproteinase-9 predicts healing quality after sinus surgery. *Laryngoscope, 115*(1), 56-61. https://doi.org/10.1097/01.mlg.0000150674.30237.3f

Weber, R. K. (2009). Nasal packing and stenting. *GMS Current Topics in Otorhinolaryngology, Head and Neck Surgery, 8*, Doc02. https://doi.org/10.3205/cto000054

Weber, R. K., & Hosemann, W. (2015). Comprehensive review on endonasal endoscopic sinus surgery. *GMS Current Topics in Otorhinolaryngology- Head and Neck Surgery, 14*, 1-108.

Weber, R. K., Keerl, R., Hochapfel, F., Draf, W., & Toffel, P. H. (2001). Packing in endonasal surgery. *American Journal of Otolaryngology, 22*(5), 306-320. https://doi.org/10.1053/ajot.2001.26499

Weiner, M. L. (1991). Toxicological properties of carrageenan. *Agents and Actions, 32*(1-2), 46-51.

Welch, K. C., & Stankiewicz, J. A. (2009). A contemporary review of endoscopic sinus surgery: techniques, tools, and outcomes. *Laryngoscope, 119*(11), 2258-2268. https://doi.org/10.1002/lary.20618

Whitworth, k., Johnson, J., Wisniewski, S., & Schrader, M. (2020). Comparative Effectiveness of Topically Administered Tranexamic Acid Versus Topical Oxymetazoline Spray for Achieving Hemostasis in Epistaxis. *The Journal of Emergency Medicine, 58*(2), 211-216. https://doi.org/10.1016/j.jemermed.2019.11.038

Xu, G., Chen, H. B., Wen, W., & Li, Y. (2003). Clinical evaluation of local application of merogel after endoscopic sinus surgery. *Zhonghua er bi yan hou ke za zhi, 38*(2), 95-97.

Xu, J. J., Busato, G. M., McKnight, C., & Lee, J. M. (2016). Absorbable Steroid-Impregnated Spacer After Endoscopic Sinus Surgery to Reduce Synechiae Formation. *Annals of Otology, Rhinology and Laryngology, 125*(3), 195-198. https://doi.org/10.1177/0003489415606446

Yan, M., Zheng, D., Li, Y., Zheng, Q., Chen, J., & Yang, B. (2014). Biodegradable Nasal Packings for Endoscopic Sinonasal Surgery: A Systematic Review and Meta-Analysis. *PLoS ONE, 9*(12), e115458. https://doi.org/10.1371/journal.pone.0115458

Yokota, T., Nomura, K., Nagashima, M., & Kamimura, N. (2016). Fucoidan alleviates high-fat diet-induced dyslipidemia and atherosclerosis in ApoE(shl) mice deficient in apolipoprotein E expression. *Journal of Nutritional Biochemistry, 32*, 46-54. https://doi.org/10.1016/j.jnutbio.2016.01.011

Zahed, R., Moharamzadeh, P., AlizadehArasi, S., Ghasemi, A., & Saeedi, M. (2013). A new and rapid method for epistaxis treatment using injectable form of tranexamic acid topically: a randomized controlled trial☆. *American Journal of Emergency Medicine, 21*(9), 1389. https://doi.org/10.1016/j.ajem.2013.06.043

Zahed, R., Mousavi Jazayeri, M. H., Naderi, A., Naderpour, Z., & Saeedi, M. (2017). Topical tranexamic acid compared with anterior nasal apcking for treatment of epistaxis in patients taking antiplatelet drugs: randomised controlled trial. *Society for Academic Emergency Medicine*. https://doi.org/10.1111/acem.13345

Zhang, D., Zhang, Y., Xie, R., & Zhou, K. (2012). Freeze gelcasting of aqueous alumina suspensions for porous ceramics. *Ceramics International, 38*(7), 6063-6066. https://doi.org/10.1016/j.ceramint.2012.04.044

Zhang, X., & Cresswell, M. (2016). *Inorganic controlled release technology : materials and concepts for advanced drug formulation*. England: Butterworth-Heinemann.

Zhang, Y., Ye, L., Cui, M., Yang, B., Li, J., Sun, H., & Yao, F. (2015). Physically crosslinked poly(vinyl alcohol)-carrageenan composite hydrogels: Pore structure stability and cell adhesive ability. *RSC Advances, 5*(95), 78180-78191. https://doi.org/10.1039/c5ra11331h

Zhang, Y., & Zhang, Y. (2012). Preparation of kappa-carrageenan-chitosan polyelectrolyte gel beads. *Zhongguo Zhong Yao Za Zhi, 37*(4), 466-470.

Zhao, J., Sun, C., Li, H., Dong, X., & Zhang, X. (2020). Studies on the physicochemical properties, gelling behavior and drug release performance of agar/κ-carrageenan mixed hydrogels. *International Journal of Biological Macromolecules, 154*, 878-887. https://doi.org/10.1016/j.ijbiomac.2020.03.087

Zhao, X., Liu, L., An, T., Xian, M., Luckanagul, J. A., Su, Z., . . . Wang, Q. (2020). A hydrogen sulfide-releasing alginate dressing for effective wound healing. *Acta Biomaterialia, 104*, 85-94.

Zia, K. M., Tabasum, S., Nasif, M., Sultan, N., Aslam, N., Noreen, A., & Zuber, M. (2017). A review on synthesis, properties and applications of natural polymer based carrageenan blends and composites. *International Journal of Biological Macromolecules, 96*, 282-301. https://doi.org/10.1016/j.ijbiomac.2016.11.095